Interaction of Surfactants of Natural Origin with Phospholipid Membranes

Adam Grzywaczyk

Doctor of Philosophy Dissertation

Supervised by Professor Ewa Kaczorek

Auxiliary supervisor Dr. Eng. Wojciech Smułek

Institute of Chemical Technology and Engineering

Poznan University of Technology

Poland, 2025

Research conducted within this dissertation was supported by the National Science Centre in Poland, OPUS 20 project entitled *Is there a synergistic effect of plant surfactants and antibiotics against bacterial cells?*

Grant number: 2020/39/B/NZ9/03196

Grant Recipient: Professor Ewa Kaczorek

Acknowledgments

Tempora mutantur et nos mutamur in illis, as a Roman would say. However, the Western Empire fell 1,549 years ago, after lasting for approximately 1,483 years. Five years of doctoral studies sounds amusing when compared to such a long period, but I believe I have used this saying correctly. It is a period of ups and downs. There are moments when you feel like you have caught God by the feet, and others when you would rather hide at home and never leave. There are times when the research you are doing is worthy of a Nobel Prize, and others when you would throw your measurements and results in the bin. *Perfer et obdura; dolor hic tibi proderit.*

Without the people who accompanied me on this difficult journey, I would not have been able to cope. The order of thanks is not important; you have to start with someone, and you have to mention someone last.

I will start with my wife Anna, who has been and continues to be an incredible support to me. Thank you for being with me then and now. It wasn't easy, but we made it. *Amor vincit omnia.*

Thank you to Professor Ewa Kaczorek and Professor Wojciech Smułek (soon to be, which I wish for with all my heart). You are outstanding supervisors. Kind, patient, supportive. The kind everyone should have. *If I have seen further it is by standing on the shoulders of giants*.

Thank you to my partner in crime, Natalia Burlaga. With you, it was easy to overcome every challenge. There will probably be many more on our way, and may there be as many as possible, because we will manage anyway. *Fortes fortuna adiuvat.*

I would like to thank Oliwia Degórska, Agata and Jakub Zdarta, Aleksandra Makiej, Witold Stachowiak, Marta Wojcieszak, Amanda Pacholak, Jerzy Maciejewski, Ewa Dziurla, Aleksandra Rybak, Anna Parus, Marta Woźniak-Karczewska, Łukasz Ławniczak, Martin Reiser for every piece of advice, kind word, smile, and moment of conversation. *Homo doctus in se semper divitias habet.*

I would like to thank Zuzanna Styrna, Michał Kapczyński, Olimpia Wojciechowska, Paulina Laufer, the staff of the Department of Organic and Bioorganic Chemistry, the staff of the Institute of Chemical Technology and Engineering, the team and Prof. Philip Gale, the team and Prof. Andreas Zimmer. Working with you has been extremely inspiring. May there be more of it. *Concordia res parvae crescent.*

I would like to thank my parents, grandparents, parents-in-law and the whole family. Thank you for being there for me, even though it was not always easy for me to explain what I was working on or whether I was working at all. Every choice you made and every word you said led me to this moment. *Concordia domi, foris pax.*

I would also like to thank God for the end of the beginning of the journey called Science. It has lasted 25 years since I went to kindergarten, and I hope it will continue. *Nam etsi ambulavero in medio umbræ mortis, non timebo mala, quoniam tu mecum es.*

I dedicate this work to my daughter Jadwiga.

I love you,

Dad

Podziękowania

Tempora mutantur et nos mutamur in illis powiedziałby mieszkaniec Rzymu. Cesarstwo Zachodnie upadło jednak 1549 lat temu, po około 1483 latach trwania. 5 lat studiów doktoranckich brzmi przy tak długim okresie co najmniej zabawnie, niemniej uważam, że powiedzenie to zastosowałem poprawnie. Jest to okres wzlotów i upadków. Są momenty, gdzie czujesz jakbyś Pana Boga za nogi złapał i takie, że najchętniej schowałbyś się w domu i z niego nie wychodził. Jest czas, gdzie badania, które robisz są minimum na nagrodę Nobla i taki, że pomiary i wyniki wyrzuciłoby się do śmieci. *Perfer et obdura; dolor hic tibi proderit*.

Bez ludzi, którzy towarzyszyli mi na tej niełatwej drodze nie dałbym sobie rady. Kolejność podziękowań nie jest ważna, trzeba od kogoś zacząć i trzeba kogoś wymienić jako ostatniego.

Zacznę zatem od mojej żony Anny, która była i jest niebywałym dla mnie wsparciem. Dziękuję za to, że ze mną byłaś wtedy i jesteś teraz. Łatwo nie było, ale daliśmy radę. *Amor vincit omnia.*

Dziękuję Pani Profesor Ewie Kaczorek oraz Panu Profesorowi (już niedługo, czego ci z całego serca życzę) Wojciechowi Smułkowi. Jesteście promotorami wybitnymi. Życzliwymi, cierpliwymi, wspierającymi. Takimi, na których każdy powinien trafić. *If I have seen further, it is by standing on the shoulders of giants.*

Dziękuję mojej *partner in crime* Natalii Burlaga. Z tobą łatwo było przezwyciężyć każde wyzwanie. Będzie ich na naszej drodze jeszcze pewnie wiele, oby jak najwięcej, bo i tak damy sobie radę. *Fortes fortuna adiuvat.*

Dziękuję Oliwii Degórskiej, Agacie i Jakubowi Zdarta, Aleksandrze Makiej, Witoldowi Stachowiakowi, Marcie Wojcieszak, Amandzie Pacholak, Jerzemu Maciejewskiemu, Ewie Dziurli, Aleksandrze Rybak, Annie Parus, Marcie Woźniak-Karczewskiej, Łukaszowi Ławniczakowi, Martinowi Reiser za każde wskazówki, dobre słowo, każdy uśmiech, chwilę rozmowy. *Homo doctus in se semper divitias habet.*

Dziękuję Zuzannie Styrna, Michałowi Kapczyńskiemu, Olimpii Wojciechowskiej, Paulinie Laufer, pracownikom Zakładu Chemii Organicznej i Bioorganicznej, pracownikom Instytutu Technologii i Inżynierii Chemicznej, zespołowi i Prof. Philip Gale, zespołowi oraz Prof. Andreasowi Zimmer. Współpraca z wami była niezwykle inspirująca. Oby było jej jak najwięcej. *Concordia res parvae crescunt.*

Dziękuję Rodzicom, Dziadkom, Teściom, Przyjaciołom i całej rodzinie. Dziękuję, że jesteście i byliście ze mną, chociaż nie zawsze łatwo mi było wytłumaczyć nad czym pracuję i czy w ogóle pracuję. Każdy wasz wybór i każde słowo doprowadziło mnie do tej właśnie chwili. *Concordia domi, foris pax.*

Dziękuję też Bogu za koniec początku podróży zwanej Nauką. Trwała 25 lat, odkąd poszedłem do przedszkola i mam nadzieję, że będzie trwała dalej. *Nam etsi ambulavero in medio umbræ mortis, non timebo mala, quoniam tu mecum es.*

Niniejszą pracę dedykuje mojej córce Jadwidze.

Kocham Cię,

Tata

Table of content

Acknowledgments 3

Podziękowania 4

Abstract 7

Streszczenie 8

List of abbreviations 9

1. Literature review 10

Structure of the membrane and its functions 10

Permeability of microbial membranes 14

Natural surfactants as adjuvants that affect cell properties 16

Mechanisms of interaction of saponins with the membrane 19

Membrane model systems 23

2. Research gap & hypothesis 25

3. Aims of the dissertation 26

4. List of publications included in the dissertation 27

5. Summary of the results 28

P1. Nanofiltered saponin-rich extract of *Saponaria officinalis* – Adsorption and aggregation properties of particular fractions 28

P2. Study of interactions between saponin biosurfactant and model biological membranes: phospholipid monolayers and liposomes 32

P3. *Saponaria officinalis* saponins as a factor increasing permeability of *Candida* yeasts' biomembrane 36

P4. *Glycyrrhiza glabra* L. saponins modulate the biophysical properties of bacterial model membranes and affect their interactions with tobramycin 40

P5. Co-interaction of nitrofuran antibiotics and the saponin-rich extract on gram-negative bacteria and colon epithelial cells 43

6. Summarizing conclusions 46

References 48

Figures licensing 56

Other scientific achievements 57

Full texts of papers 64

Publication P1 65

P1 Supplementary Materials 77

Publication P2 81

Publication P3 96

P3 Supplementary Materials 107

Publication P4 129
P4 Supplementary Materials 140
Publication P5 144
P5 Supplementary material 156
Author's contribution 179
All authors' contributions 181

Abstract

In view of the growing threat posed by infections caused by multidrug-resistant microorganisms, it is necessary to seek new and effective strategies that will increase the effectiveness of antibiotic therapy through appropriate mechanisms. In this context, surfactants, especially compounds from the saponin group, are noteworthy. These natural compounds, thanks to their amphiphilic structure, undergo partial adsorption in the lipid bilayer. This effect, which depends on the lipid composition and the presence of other components, such as sterols, is responsible for modifying the fluidity of membranes and even creating gaps and pores in them, ultimately increasing the access of antibiotics to their targets or facilitating their accumulation in the cell.

Therefore, this dissertation discusses the influence of naturally occurring surfactants, i.e. saponins, on the properties of phospholipid membranes. Starting from a research gap concerning the mechanisms by which saponins modify membrane properties, a hypothesis was put forward that saponins modify the physicochemical properties of phospholipid membranes both in living cells and in model membrane systems, thus enabling them to act as adjuvants, increasing the effectiveness of medicinal substances. The scope of the work included: (A) extraction, filtration and characterisation of individual fractions of plant extracts, (B) studies of interactions with phospholipid monolayers and liposomal vesicles, (C) assessment of the effect of extracts on the properties of yeast and bacterial cells, and (D) assessment of the interaction of saponins with antibiotics and their effect on human cells.

Publication P1 concerned the separation of *Saponaria officinalis* extract using a two-stage nanofiltration process. It was demonstrated that the 0.5-3 kDa fraction is rich in saponins, forms micelles with sizes of several dozen nanometres and retains surface activity comparable to that of the raw extract. P2 investigated the interactions of saponins derived from *Glycyrrhiza glabra* with model membranes. In monolayers, film expansion and a decrease in the compressibility modulus were observed. In publication P3, studies were conducted on *Candida* yeast cells in the form of spheroplasts. It was confirmed that saponins from *S. officinalis* increase membrane permeability while changing the zeta potential to more negative values. In P4, it was shown that saponins from *G. glabra* liquefy phospholipid monolayers and, in combination with tobramycin, additionally modify the zeta potential of liposomes while maintaining their integrity. Publication P5 demonstrated the synergistic effect of saponins from *Sapindus mukorossi* with nitrofurantoin and furazolidone against *Pseudomonas* bacteria, without increasing cytotoxicity towards human colon epithelial cells.

The results obtained confirm that saponins interact with lipid membranes, modifying their packing and permeability, and also affect the action of the antibiotics studied. The study indicates two possible directions for practical applications of the results. Firstly, by using saponins as adjuvants to antibiotics in the treatment of infections caused by resistant microorganisms, and as a built-in component of membranes in lipid carriers used in controlled drug delivery systems. The conclusions from the individual studies confirm the hypothesis and provide an experimental basis for the further design of therapeutic systems using surfactants from the saponin group.

Streszczenie

Wobec narastającego zagrożenia wynikającego z zakażeń wywoływanych przez drobnoustroje wielolekooporne koniecznym jest poszukiwanie nowych i skutecznych strategii leczenia, które zwiększą skuteczność terapii antybiotykowej. W tym kontekście uwagę zwracają surfaktanty, szczególnie związki z grupy saponin. Dzięki budowie amfifilowej związki te ulegają częściowej adsorpcji w dwuwarstwie lipidowej. Efekt ten, zależny od składu lipidowego, a także obecności innych składników, np. steroli, odpowiada za modyfikację płynności błon, a nawet tworzenie w nich wyrw i porów. Potencjalnie zwiększa to dostęp antybiotyków do miejsc docelowych ułatwiając także ich akumulację w komórce.

Niniejsza rozprawa omawia wpływ surfaktantów pochodzenia naturalnego, tj. saponin, na właściwości błon fosfolipidowych. Wychodząc od luki badawczej dotyczącej mechanizmów poprzez które saponiny modyfikują właściwości błon, postawiono hipotezę, że saponiny modyfikują właściwości fizykochemiczne błon fosfolipidowych zarówno w żywych komórkach, jak i modelowych układach błonowych, dzięki czemu mogą pełnić funkcję adiuwantów, zwiększając skuteczność działania substancji leczniczych. Zakres pracy obejmował: (A) ekstrakcję, filtrację i charakterystykę poszczególnych frakcji ekstraktów roślinnych, (B) badania oddziaływań z monowarstwami fosfolipidowymi i pęcherzykami liposomalnymi, (C) ocenę wpływu ekstraktów na właściwości komórek drożdży i bakterii oraz (D) ocenę współdziałania saponin z antybiotykami i ich wpływu na komórki ludzkie.

Publikacja P1 dotyczyła rozdziału ekstraktu z *Saponaria officinalis* z wykorzystaniem dwustopniowego procesu nanofiltracji. Wykazano, że frakcja 0,5-3 kDa (E2) jest bogata w saponiny, tworzy micele o rozmiarach rzędu kilkudziesięciu nanometrów i zachowuje aktywność powierzchniową porównywalną z ekstraktem surowym. W P2 zbadano oddziaływania saponin pochodzących z *Glycyrrhiza glabra* z błonami modelowymi. Zaobserwowano rozszerzanie filmu i spadek modułu ściśliwości w układach monowarstwowych. W publikacji P3, przeprowadzono badania na komórkach drożdżaków *Candida* w formie sferoplastów. Potwierdzono, że saponiny z *S. officinalis* zwiększają przepuszczalność błony. W pracy P4 pokazano, że saponiny z *G. glabra* upłynniają monowarstwy fosfolipidowe i w połączeniu z tobramycyną dodatkowo modyfikują potencjał zeta liposomów, przy jednoczesnym zachowaniu ich integralności. W publikacji P5 wykazano synergiczne działanie saponin z *Sapindus mukorossi* z nitrofurantoiną oraz furazolidonem wobec bakterii z rodzaju *Pseudomonas* przy jednoczesnym braku zwiększenia cytotoksyczności wobec komórek ludzkiego nabłonka okrężnicy.

Uzyskane wyniki potwierdzają, że saponiny oddziałują z błonami lipidowymi modyfikując ich upakowanie i przepuszczalność, a także wpływają na działanie badanych antybiotyków. Praca wskazuje dwa możliwe kierunki praktycznych zastosowań wyników. Po pierwsze, poprzez wykorzystanie saponin jako adjuwantów antybiotyków w terapii zakażeń wywoływanych przez drobnoustroje oporne oraz jako wbudowany składnik błon w nośnikach lipidowych stosowanych w systemach kontrolowanego dostarczania leków. Wnioski z poszczególnych badań potwierdzają postawioną hipotezę i dostarczają eksperymentalnych podstaw do dalszego projektowania układów terapeutycznych wykorzystujących surfaktanty z grupy saponin.

List of abbreviations

API – Active Pharmaceutical Ingredient

CF – Carboxyfluorescein

CMC – Critical Micelle Concentration

Ctrl – Control sample

DLS – Dynamic Light Scattering

DOPG – 1,2-dioleoyl-sn-glycero-3-phosphoglycerol

DPPE – 1,2-dipalmitoyl-sn-glycero-3-phosphoethanolamine

E0-E4 – Subsequent determination of individual extract fractions

FZD – Furazolidone

GC-MS – Gas Chromatography-Mass Spectrometry

Glc – Glucose

GlcA – Glucuronic Acid

GgC – *Glycyrrhiza glabra* crude extract

GUV – Giant Unilamellar Vesicle

HPTS – 8-Hydroxypyrene-1,3,6-trisulfonic acid trisodium salt

IF – Impact Factor

LC-MS – Liquid Chromatography-Mass Spectrometry

LPS – Lipopolysaccharide

LUV – Large Unilamellar Vesicle

MLV – Multilamellar Vesicle

MVL – Multivesicular Liposome

NFT – Nitrofurantoin

OM – Outer Membranef

SoC – *Saponaria officinalis* crude extract,

SoP – *Saponaria officinalis* purified extract

SUV – Small Unilamellar Vesicle

Tbrm – Tobramycin

TEM – Transmission Electron Microscopy

1. Literature review

Structure of the membrane and its functions

Biomembranes are basic structural elements that establish cell boundaries and separate internal compartments. The membranes consist of a phospholipid bilayer structure with various proteins embedded or associated with it. According to the fluid mosaic model, biomembranes exist as two-dimensional dynamic fluids that allow both lipids and proteins to move freely within the membrane plane [1]. The specific structural design provides cells with both flexibility and selective permeability needed for various cellular operations [2]. The bilayer structure shows amphipathic properties because phospholipid head groups face the water environment while fatty acid tails remain distant from water. The specific arrangement of molecules creates a stable semi-permeable barrier that separates the cell interior from its external environment [3].

While both prokaryotic and eukaryotic cells possess phospholipid membranes, their structural and functional differences result in considerable variability in membrane composition [4]. There is no universally defined phospholipid profile for biological membranes. Instead, their lipid composition is tailored to the specific physiological requirements of each organism [4,5]. In addition to phospholipids, biological membranes may also contain glycolipids and sterols, particularly in eukaryotes. Carbohydrates covalently bound to lipids and proteins are also present, contributing to membrane structure and function [6]. For example, bacterial membranes consist of equal amounts of phospholipids and proteins, while variations in lipid composition influence membrane properties and protein interactions. Bacteria lack sterols, which is a characteristic feature that distinguishes them from eukaryotic cells [7]. However, they can obtain sterols from their host or environment, and these sterols can form membrane domains analogous to eukaryotic lipid rafts [8]. Moreover, certain genera, such as *Methylobacterium*, have been observed to incorporate hopanoids into their membranes. Hopanoids have a structural similarity to cholesterol and have been shown to modulate membrane fluidity and permeability [9].

The bacterial domain shows additional diversity through outer cell barrier variations, which distinguish Gram-positive from Gram-negative species. Gram-positive bacteria consist of a single phospholipid bilayer, which is surrounded by multiple layers of peptidoglycan cell wall. On the other hand, Gram-negative bacteria such as *Pseudomonas aeruginosa*, possesses

an envelope structure that includes an inner membrane, a thin peptidoglycan layer in the periplasmic space and an outer membrane (OM) [10]. The OM shows distinct lipid asymmetry - its inner leaflet contains mostly glycerophospholipids, while its outer leaflet contains lipopolysaccharides. The amphipathic molecules embedded into OM, including lipid A, core oligosaccharide and O-antigen polysaccharide components, maintain membrane stability while forming an effective permeability barrier [11,12]. In contrast, the plasma membrane of the single-celled fungi, such as *Candida* spp., an eukaryotic microorganism, is characterised by a lipid composition that is rich in phospholipids, significant levels of sphingolipids, and ergosterol as the primary sterol. Phospholipids constitute approximately 55-75% of the total membrane lipids, with phosphatidylcholine representing the most prevalent class [13]. Structural schemes of chosen biomembranes are presented in Fig. 1.

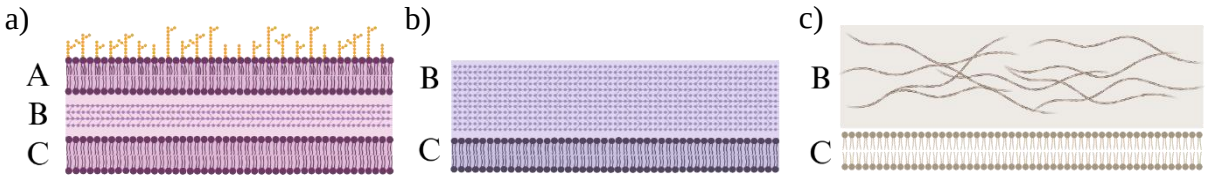

Fig. 1 Simplified graphical representation of biomembranes; a) bacteria Gram-negative, b) bacteria Gram-positive, c) fungal eukaryotic; A - outer membrane, B - cell wall, C - inner membrane

It is also important to note that phospholipids not only perform structural functions but also actively participate in cellular processes through the modulation of membrane curvature, signal transduction, and the formation of specialised lipid microdomains. These processes affect both membrane behavior and cellular responses (Table 1).

Table 1. Major classes of membrane lipids and their biological functions

Lipid	Occurrence	Functions	Ref.
Phosphatidylethanolamine	Eukaryotic and prokaryotic membranes	Induces negative membrane curvature, assists folding and insertion of inner-membrane proteins, preserves bilayer fluidity during cell division	[14,15]
Phosphatidylcholine	Predominantly eukaryotic membranes, and prokaryotic membranes	Forms cylindrical bilayer matrix, modulates membrane thickness and viscosity	[16,17]
Phosphatidylserine	Eukaryotic membranes	Protein binding, electrostatic association, and signaling events like blood clotting andapoptosis	[18]
Phosphatidylinositol	Eukaryotic membranes	Regulating vesicular trafficking, regulate ion channels, pumps, and transporters, modulate lipid distribution, regulate endocytic and exocytic processes	[19]
Phosphatidic Acid	Eukaryotic and prokaryotic membranes	Affects membrane structure and dynamics, regulating various cellular processes by influencing membrane tethering, enzymatic activities, and vesicular trafficking, acts as a signaling molecule	[20]
Phosphatidylglycerol	Prokaryotic membranes	Structural support and modulation of membrane fluidity, acting as a precursor for cardiolipin synthesis, and being a component of pulmonary surfactant	[21]
Cardiolipin	Prokaryotic and mitochondrial membranes	Essential for maintaining the integrity and structure of the mitochondrial membrane, involved in mitophagy process, interacts with and stabilises various proteins and complexes within the inner mitochondrial membrane	[22,23]
Sphingomyelin	Eukaryotic (animal) membranes	Primary sphingolipid in the outer leaflet of cell membranes, interacts with cholesterol to form lipid rafts	[24]
Ceramide	Eukaryotic membranes	Induce the formation and stabilisation of lipid rafts, promote the clustering of receptors within lipid rafts, facilitating and amplifying signaling events	[25]
Lysophosphatidylcholine	Eukaryotic membranes	Induces migration of lymphocytes and macrophages, increases pro-inflammatory cytokines, and plays a role in transporting fatty acids across the blood-brain barrier	[26-28]
Lysyl-phosphatidylglycerol	Prokaryotic membranes	Facilitates cell aggregation and biofilm formation, modifies the membrane's anionic charge, reducing the interaction between positively charged cationic antimicrobial peptides	[29-30]

Table 1. Major classes of membrane lipids and their biological functions (cont.)

Lipid	Occurrence	Functions	Ref.
Alanyl-phosphatidylglycerol	Prokaryotic membranes	Reduces the negative charge on their cell membranes, making them less susceptible to cationic antimicrobial peptides, maintains membrane integrity particularly in acidic environments	[31,32]
Plasmalogen	Eukaryotic and some anaerobic prokaryotic membranes	Enhances membrane fluidity, allowing for dynamic cellular processes like membrane fusion and vesicle trafficking, influences the transport of ions and molecules across membranes	[33,34]
Lipid A-modified lipopolysaccharide	Gram-negative bacterial outer membranes	Anchors the outer membrane to the inner membrane, contributing to the integrity of the bacterial cell, and contributes to the stability and flexibility of the outer membrane	[35,36]
Phosphatidylinositol 4,5-bisphosphat	Eukaryotic membranes	Involved in vesicle trafficking and endocytosis, playing a role in regulating membrane dynamics and protein trafficking, and modulates the activity of various ion channels	[37]
Ornithine Lipids	Prokaryotic membranes	Act as a surrogate for phospholipids under phosphate-limited conditions, modify bacterial surface properties, influencing antibiotic sensitivity, macrophage binding, and biofilm formation	[38]
Phosphatidylinositol Mannosides	Mycobacterial membranes	Major components of the mycobacterial cell wall and plasma membrane, involve in the binding of mycobacteria to host cells	[39,40]
Sulfoquinovosyl Diacyl-glycerol	Cyanobacterial and plant chloroplast membranes	Stabilisation and proper operation of photosystem II (key protein complex in thylakoid membranes), under phosphate-deficient conditions, SQDG converts the site of phospholipids in membranes	[41,42]
Monogalactosyldiacylglycerol	Plant chloroplast membranes	A major component of thylakoid membranes - the site of photosynthesis within chloroplasts	[43]
Cholesterol	Eukaryotic (animal) membranes	Modulates membrane fluidity and permeability, can contribute to the formation of lipid rafts	[44,45]
Ergosterol	Fungal membranes	Maintaining membrane structure, fluidity and permeability, plays a role in plasma membrane fusion,	[46,47]
Hopanoids	Bacterial membranes	Contribute to the structural integrity of bacterial membranes; can promote the formation of liquid-ordered phases, which is analogous to the role of sterols in eukaryotic membranes	[9,48]

The pivotal significance of biomembranes lies in serving as protective barriers and providing organisational support for various vital cellular operations. Biomembranes are capable of facilitating compartmentalisation of biochemical reactions by their capacity to establish distinct metabolic pathways in discrete environments [49]. They play a role in preserving cellular integrity by regulating the controlled passage of substances, thereby ensuring the maintenance of necessary concentration gradients for ions and molecules that are critical to cell metabolism and function (types of membrane transport are presented in Fig. 2). Furthermore, membranes enable energy conversion through processes like oxidative phosphorylation and photosynthesis by preserving essential proton gradients that lead to adenosine triphosphate production [50]. Moreover, biomembranes serve as essential components for cellular sensing and communication processes. The detection of extracellular signals, including hormones, neurotransmitters and environmental stimuli, triggers both intracellular signalling cascades and gene regulatory mechanisms. Cells use this ability to detect environmental changes while preserving internal equilibrium [51,52].

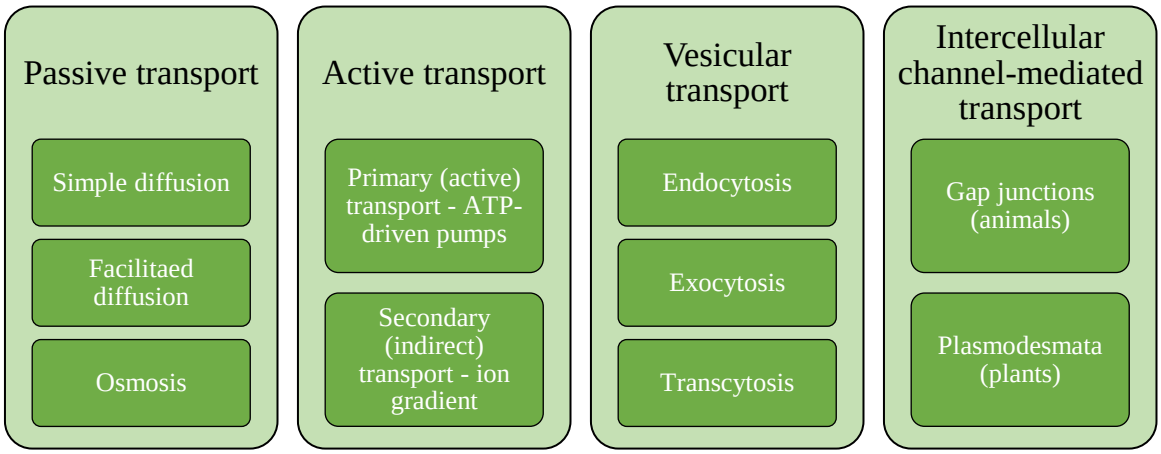

Fig. 2. Main types and sub-types of membrane transport, based on [53]

Permeability of microbial membranes

The ability of biological membranes to allow molecules to pass them through determines their permeability levels. The fundamental influence of membrane permeability shapes how cells interact with their environment and respond to environmental changes. Biomembranes require permeability as their fundamental property to perform their primary function of maintaining cellular homeostasis. The membrane enables controlled exchange of nutrients, signaling molecules, ions, and waste products between the cell interior and its external environment [54].

The permeability of biomembranes is linked to their fluidity, which is significantly influenced by lipid composition, especially the type, length, and saturation of fatty acid chains within phospholipids. Generally, membranes composed of longer and saturated fatty acid chains tend to be more rigid and orderly, resulting in decreased permeability. On the other hand, shorter, unsaturated, or branched fatty acids disrupt lipid packing, increasing fluidity and enhancing permeability [55,56]. Consequently, organisms such as bacteria have developed mechanisms to adjust their membrane fluidity through a process known as homeoviscous adaptation. Through this process, they dynamically alter lipid composition, including adjustments in fatty acid saturation and chain length, to maintain optimal permeability under changing environmental conditions, such as variations in temperature and exposure to membrane-damaging agents [57].

Within the membranes of prokaryotic cells, functional membrane microdomains play a critical role in regulating local permeability and cellular functionality. Compared to the surrounding membrane regions, these specialised areas are characterised by distinct lipid compositions and lower fluidity. Hence, they are similar to lipid rafts found in eukaryotic membranes. Enriched in specific lipids such as cardiolipin and hopanoids, and associated with particular proteins such as flotillins, these microdomains facilitate the localised anchoring of proteins, signaling molecules, and transport systems. This structural organisation allows precise regulation of permeability in specific membrane areas, which is crucial for efficient signaling, nutrient uptake, and targeted responses to environmental stresses [56,58-60].

In addition to fluidity, the specific lipid composition of the biomembrane significantly affects permeability by influencing bilayer packing, surface charge, and electrical potential. Variations in phospholipid head groups, fatty acid saturation, and chain length directly impact the structural arrangement of the membrane, thereby modulating its permeability to various substances [61]. For instance, Gram-positive bacteria can adapt to environmental stresses by converting negatively charged phosphatidylglycerol into neutral or positively charged lipid derivatives. This process has been shown to affect their membrane permeability and interactions with external molecules [61,62]. Furthermore, it has been demonstrated that specific structural modifications, such as cyclopropanation and branching of fatty acids, can enhance membrane stability and selectively modulate permeability. This is particularly evident under conditions of environmental stress or nutrient limitation [63,64].

Furthermore, membrane polarisation, defined by differences in electrical potential across the membrane, typically ranging from -40 to -80 mV in bacterial cells, directly impacts permeability, especially in the case of charged molecules. The electrochemical gradient created by this polarisation actively facilitates the selective uptake and transport of positively charged ions, nutrients, and other essential metabolites [65]. Moreover, bacterial organisms can modulate membrane surface charge through enzymatic lipid modifications, thereby altering interactions with external molecules, including antimicrobial peptides, ions, and environmental compounds. As a result, this impacts membrane permeability and cellular interactions [66-68].

Natural surfactants as adjuvants that affect cell properties

In addition to the functions outlined in the previous section, the bacterial membrane plays an important role in mediating resistance to antibiotics. This is achieved through structural adaptation, altered permeability, surface charge modulation, and the spatial reorganisation of membrane microdomains. As a result, the membrane functions as both a physical and functional barrier to antimicrobial therapy [69]. Research has demonstrated that altering membrane properties can restrict antibiotic access and facilitate the activity of efflux pumps, thereby contributing to the stability of biomembranes [56,70]. Therefore, developing strategies that target or circumvent these membrane-centric defense mechanisms is of the highest importance in the ongoing battle against multidrug-resistant bacteria.

In this context, natural surfactants (further stated as biosurfactants), which are amphiphilic molecules produced by microorganisms or plants, have proven to be effective adjuvants, capable of enhancing the action of antibiotics and reversing bacterial resistance [71-74]. These compounds possess a capacity to interact directly with the bacterial cell envelope, causing disruption of cell membrane integrity, disruption of biofilm structure, and impairment of cell membrane-related resistance mechanisms, such as efflux pumps [75-78]. By targeting the structural fundamentals that facilitate bacterial resilience, surfactants offer a multifaceted approach to restoring pathogens to antibiotic action.

Biosurfactants are a diverse group of compounds, both structurally and functionally, produced by various organisms, including bacteria (e.g., *Pseudomonas*, *Bacillus*, *Acinetobacter*), yeasts (e.g., *Candida*, *Starmerella*), filamentous fungi (e.g., *Aspergillus*, *Fusarium*), and plants (e.g., *Quillaja saponaria* Molina, *Sapindus mukorossi*, *Glycyrhizza glabra*) [78-87]. These substances can be classified based on their source and chemical

composition. Examples of such substances include glycolipids (such as rhamnolipids and sophorolipids), lipopeptides (including surfactin and polymyxins), phospholipids, fatty acids, intricate polymeric structures (e.g., lipopolysaccharide-protein conjugates or bioemulsifiers) [74]. Their amphiphilic nature facilitates interactions with both hydrophobic and hydrophilic phases, enabling extensive physicochemical interactions with biological membranes and drug molecules [72,88,89]. Moreover, numerous amphiphilic compounds of plant origin, such as saponins, also exhibit surfactant activity [90,91]. Saponins, like other natural and synthetic surfactants, due to their amphiphilic properties, interact with biological membranes and microbial biofilm. Hence, their classification in the functional class of natural surfactants and biosurfactants is justified, and in the dissertation, the two terms will be used interchangeably.

Biosurfactants confer a notable advantage for antibiotics that are hydrophilic or possess charged structures and encounter difficulties in penetrating lipid-rich bacterial membranes. Several classes of biosurfactants can affect biomembrane properties. For instance, rhamnolipids produced by *Pseudomonas aeruginosa* enhance membrane permeability and facilitate aminoglycoside uptake in resistant cells [92,93]. Similarly, sophorolipids (from *Starmerella bombicola)* and mannosylerythritol lipids (from *Ustilago maydis*) exhibit antimicrobial and antibiofilm properties by destabilizing bacterial membranes, thereby improving antibiotic access, particularly against Gram-negative pathogens and *Listeria monocytogenes* [94-96]. Lipopeptides such as surfactin further contribute to this effect by increasing membrane permeability and promoting antibiotic entry, which has been shown to significantly enhance the eradication of *Escherichia coli* and *Staphylococcus aureus* biofilms [97,98].

In addition to those of microbiological origins, certain plant-derived biosurfactants exhibit comparable characteristics. Among these, saponins, amphiphilic glycosides produced by a wide variety of plants, stand out for their ability to interact with and permeabilise bacterial membranes [99]. Saponins are classified as non-ionic surfactants due to their amphiphilic structure [90]. They exhibit the classic properties of surfactants, including the ability to reduce surface tension, micellisation, the formation of foam, and emulsification. Due to the aglycone structure, there are two primary classifications of saponins: steroidal and triterpene saponins. Steroidal saponins contain a four-ring sterol skeleton with 27 carbon atoms, while triterpene saponins contain a five-ring triterpene skeleton with 30 carbon atoms. Triterpene saponins exhibit a higher degree of prevalence in natural environments, particularly within the genera of dicotyledonous plants (e.g., *Fabaceae, Araliaceae, Caryophyllaceae families*). In contrast,

steroidal saponins are predominantly found in monocotyledons (e.g., *Liliaceae*, *Dioscoreaceae*, *Agavaceae*) [91].

As a consequence of the variation in aglycone structure (over a hundred known terpene and steroid skeletons) and the combination and arrangement of sugar units, the structural diversity of saponins is enormous (examples are presented in Fig. 3) [100]. This variability has been demonstrated to affect the physicochemical properties (e.g., solubility, critical micelle concentration (CMC) values) and biological activity of saponins [101]. For example, the cytotoxic and haemolytic properties of saponins depend on the presence of specific groups in the aglycone (e.g., the presence of an oleanolic acid as a side chain) and the length and branching of the sugar chain. This, in turn, affects the ability to interact with cell membranes [102].

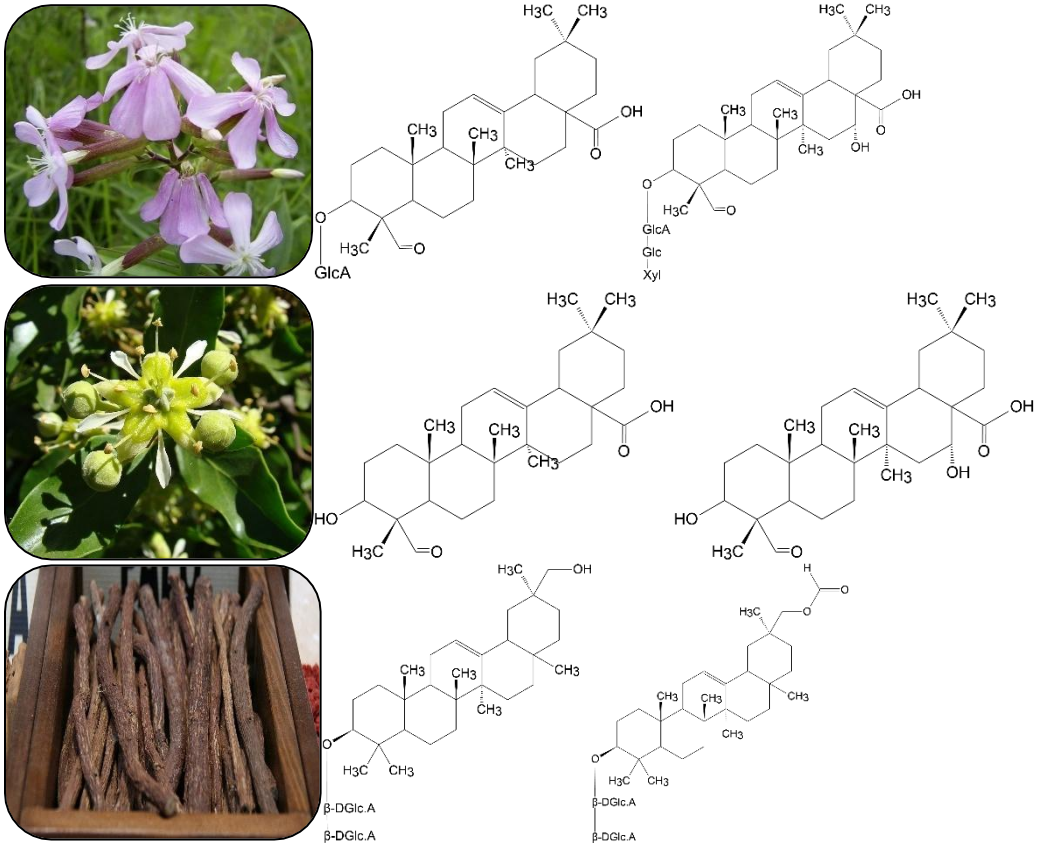

Fig 3. Saponin structures examples and their source, upper: *Saponaria officinalis* L., middle: *Quillaja saponaria* Molina, lower: *Glycyrrhiza glabra* L. roots. structures taken from [103-105]; glucuronic acid (GlcA), glucose (Glc), xylose (Xyl); pictures from the public domain

Mechanisms of interaction of saponins with the membrane

Due to their amphiphilic nature, saponins have been observed to integrate into lipid bilayers, causing changes in their organisation and permeability. In model systems, such as liposomes and lipid monolayers, it has been observed that saponins preferentially interact with sterol-containing domains [106]. In the context of cholesterol-containing bilayers, some saponins, such as digitonin, exhibit high affinity for cholesterol, resulting in the formation of complexes that induce the formation of pores in the membrane [107]. This, in turn, leads to the destabilisation of the membrane, the loss of membrane integrity, and an increase in membrane permeability [108]. The presence of membrane defects has been observed, manifesting themselves as specific pores with an estimated diameter of 40-50 Å [109]. This process has been shown to induce morphological changes in cell shape, including the transformation of erythrocytes from discocyte form to echinocyte or stomatocyte, which then undergo lysis of the cell [109]. For instance, haemolysis of erythrocytes is a classic effect of saponins, resulting from the perforation of their cholesterol-rich membranes. As demonstrated in the research conducted by Zheng et al. [110], the presence of saponins in model lipid membranes containing cholesterol has been shown to induce phase reorganisation, resulting in the precipitation of cholesterol from ordered domains. This process leads to the formation of non-selective pores, which facilitate the escape of the contents of liposomes.

On the other hand, in sterol-deprived membranes, the mechanism of action of saponins is different. These molecules can still intercalate between lipids, but primarily cause the bilayer to expand and relax. This results in a decrease in its cohesion and an increase in its fluidity, which also may increase permeability to a variety of molecules [85]. Recent research has provided further clarification on the distinct mechanisms by which saponins influence membranes lacking sterols. For instance, ginsenoside Rh2 has induced a positive curvature in lipid bilayers, promoting structural rearrangements such as the formation of small vesicular bubbles in cholesterol-free giant unilamellar vesicles. Such observations strongly suggest that Rh2 modifies membrane morphology independently of sterol interactions, pointing to alternative pathways of membrane perturbation [111]. Furthermore, other saponins, including α-chaconine and tomatine, have been shown to exhibit significant membranolytic activities in sterol-free membranes. The function of these saponins is thought to be the disruption of the bilayer integrity, potentially through pore formation, thereby facilitating enhanced membrane permeability and promoting molecular transport even in the absence of cholesterol [112]. These

results confirm the findings of Rojewska et al. [85], which demonstrated an interaction mechanism involving saponins extracted from *Saponaria officinalis* roots. At concentrations greater than their CMC, these saponins effectively integrate into POPE (2-oleoyl-1-palmitoyl-sn-glycero-3-phosphoethanolamine) monolayers. The resulting incorporation exerts a notable influence on membrane adsorption characteristics and permeability. It was proposed that while the hydrophobic parts of saponins integrate into the bilayer, their hydrophilic sugar moieties protrude outward, thereby altering surface properties and interactions with external molecules such as Congo red.

Collectively, these examples emphasise the amphiphilic nature of saponins, enabling their integration into phospholipid bilayers, disrupting lipid acyl chain orientations, and consequently modifying membrane fluidity and permeability [113,114]. Given the heterogeneity of these interactions and their ramifications for membrane integrity, a systematic summary of potential saponin-membrane interactions is imperative. This justification is reflected in the compilation presented in Table 2, which outlines and categorises these interactions comprehensively.

Table 2. Possible observed mechanisms of interaction of saponins with phospholipid membranes

Observed Effect	Type of Interaction	Consequences	Saponin(s)	Ref.
Insertion into cholesterol-containing monolayers	Saponins interact specifically with cholesterol-rich monolayers, causing an increase in lateral pressure.	Formation of tighter lipid packing and increased membrane rigidity.	α-Tomatine	[113, 115,116]
Insertion into pure phospholipid monolayers	Certain saponins insert into phospholipid monolayers without cholesterol, reducing surface tension.	Membrane destabilisation and surface activity increase.	*Saponaria officinalis* saponins, Digitonin, Avenacin A1	[85,114,117]
Insertion and aggregation in raft-like monolayers	Saponins insert into raft-like lipid domains, creating stripes and structural defects above their critical micelle concentration (CMC).	Altered domain integrity and potential membrane disruption.	Glycyrrhizin	[118]
Formation of cholesterol-saponin domains	Interaction of saponins with cholesterol leads to distinct domain formation within the lipid monolayers.	Enhanced formation of cholesterol-rich micro-domains.	α-Tomatine	[113,115]
Raft size modulation in cholesterol-containing monolayers	Saponins alter the size of lipid rafts depending on concentration, reducing domain size below CMC and causing defect formation above CMC.	Modified membrane organisation and integrity.	Glycyrrhizin	[118]
Binding to phospholipid bilayers	Saponins bind to phospholipid bilayers, decreasing the surface potential without cholesterol involvement.	Altered electrostatic properties and potential interactions.	Digitonin, Desglucodigitonin, α-Hederin	[113,119-121]
Binding to cholesterol-containing bilayers	Saponins form stable equimolecular complexes with cholesterol in bilayers, resulting in sustained membrane insertion.	Formation of stable cholesterol-saponin complexes influencing membrane stability.	α-Tomatine, α-Chaconine	[113,122]
Dynamic changes in membranes without cholesterol	Saponins generally increase lipid order and reduce lipid mobility in the absence of cholesterol.	Enhanced membrane rigidity and reduced fluidity.	Digitonin, Ginsenosides, Avenacin A1, α-Hederin	[113, 121,123]

21:2417562329

Table 2. Possible observed mechanisms of interaction of saponins with phospholipid membranes (cont).

Observed Effect	Type of Interaction	Consequences	Saponin(s)	Ref.
Dynamic changes in cholesterol-rich membranes	Saponins typically decrease lipid order in cholesterol-rich membranes, enhancing membrane fluidity and disorder.	Reduced membrane stability and increased permeability.	Digitonin, α-Hederin	[119,121]
Extraction of raft-associated proteins	Saponins facilitate extracting and solubilizing raft-associated proteins, such as alkaline phosphatase, from lipid membranes.	Disrupted lipid raft structures affecting membrane protein distribution.	Saponin mix	[124]
Expansion of ganglioside GM1 clusters	Certain saponins cause clustering and enlargement of ganglioside GM1-rich domains, altering the lateral membrane organisation.	Expanded lipid raft domains and modified membrane signaling.	Cofactor for acrosome reaction-inducing substance (steroidal saponin)	[125]
Formation of worm-like aggregates and curvature	Saponins induce the formation of elongated worm-like aggregates and membrane curvature, leading to domain budding and macroscopic pore formation.	Significant disruption of membrane integrity and leakage.	α-Hederin	[119,126]
Cholesterol-dependent toroidal pores	Certain saponins form cholesterol-dependent toroidal pores, causing selective ion permeability.	Ion-selective permeabilisation and controlled membrane disruption.	Avenacin A1	[113,117]
Cholesterol-independent membrane disruption	Specific saponins disrupt phospholipid membranes without requiring cholesterol, resulting in leakage.	Broad membrane permeability independent of cholesterol.	Bidesmosidic triterpenoid saponins	[127]
Stable protein-sized pore formation	Certain saponins form stable, approximately 1 nm wide pores in membranes, which are selective towards cations.	Selective permeability and sustained disruption.	Avicin D, Avicin G	[128]
Tubular budding induced by glycoalkaloids	Glycoalkaloids induce irreversible tubular structures and budding from sterol-rich lipid membranes.	Permanent structural reorganisation of membranes.	α-Tomatine and related glycoalkaloids	[113,129]

Membrane model systems

Many of the mechanistic insights (Table 2) have been elucidated using simplified model membrane systems, particularly two-dimensional monolayers and three-dimensional liposomal bilayers [85,113,119,126]. The use of such models allows precise control over membrane composition and structure, thereby enabling detailed observation of how saponins influence lipid organisation, surface packing, and permeability, under defined conditions. In monolayer systems, changes in lateral pressure, compressibility, or domain formation can be monitored after saponin adsorption. [85]. In contrast, three-dimensional models such as liposomes provide a closer structural analogue to biological membranes.

Liposomes are spherical vesicles consisting of one or more concentric phospholipid bilayers enclosing an aqueous core (Fig. 4) [130]. As 3D model membranes, they provide a physiologically relevant system for studying membrane interactions, including dynamic phenomena such as vesicle swelling, leakage, or bilayer destabilisation [119,126]. Importantly, their enclosed aqueous interior and amphiphilic membrane structure allow researchers to investigate how different compounds, including saponins and drug molecules, partition into or permeate through the lipid bilayer. Beyond their utility as models, liposomes are also well-established as drug delivery systems - they can encapsulate hydrophilic drugs within their core and lipophilic compounds in or between the bilayers, thereby enhancing drug stability, solubility, and biodistribution [131]. To utilise liposomes in research and drug delivery, robust preparation methods are employed to produce vesicles of the desired size and uniformity. Two common techniques are the rotary evaporation (thin-film hydration) method and the ethanol injection method [130].

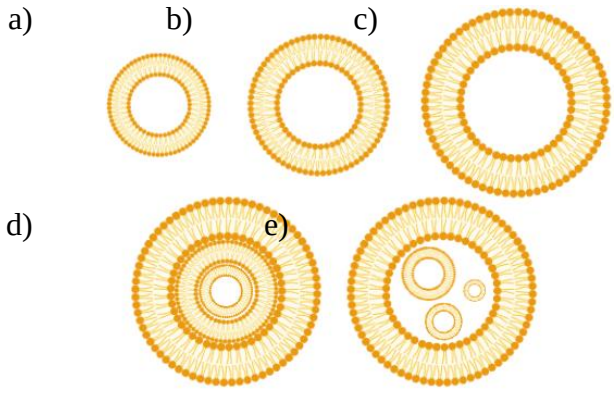

Fig 4. Graphical scheme of liposome types: a) small unilamellar vesicle (SUV; 30-100nm), b) large unilamellar vesicle (LUV; >100 nm), c) giant unilamellar vesicle (GUV; >1000nm), d) multilamellar vesicle (MLV), e) multivesicular liposome (MVL)

These membrane analogs enable the quantification of saponin-membrane interactions under well-defined conditions. Parameters such as vesicle size, number of bilayers, and lipid composition can be tailored to represent target membranes (e.g., bacterial vs. mammalian). By incorporating specific lipids (cholesterol, ergosterol, charged phospholipids, etc.), liposomes can mimic the key features of microbial or human cell membranes and observe how saponins interact. For example, cholesterol-containing liposomal membranes can simulate mammalian cell membranes, whereas sterol-free liposomes made of phosphatidylcholine or phosphatidylglycerol mimic bacterial inner membranes [85,118-121,123,126]. Using liposome models, researchers have been able to directly observe how saponins incorporate into and perturb phospholipid bilayers. Saponins tend to accumulate at the interface of the lipid bilayer, with their hydrophobic aglycone inserting among fatty acid tails and the hydrophilic sugar chains oriented toward the aqueous phase. However, the extent of insertion versus surface adsorption can depend on the membrane's composition [85,132]. Kinetic experiments with liposomes often show that saponin addition leads to leakage of encapsulated contents (such as fluorescent dyes or drug molecules), confirming that membrane permeability increases upon saponin treatment [119]. The use of liposomes thus allows researchers to bridge the gap between simplified planar models (like monolayers), complex curvature and real cell membranes.

The ability of saponins to increase membrane permeability and disrupt lipid packing translates into several practical applications in pharmaceutical formulation and therapy. One major implication is the use of saponins as penetration enhancers or adjuvants, where they are co-formulated with an Active Pharmaceutical Ingredient (API) to facilitate their transport across biological barriers. This suggests that saponins might serve not only as permeabilisers but also as natural solubilizing agents, forming mixed micellar structures with hydrophobic drugs, increasing the effective drug concentration available for absorption. Recent research demonstrated that saponin extracts from plants like *Quillaja saponaria* (*Quillaja* bark) and *Sapindus mukorossi* (soapnut) can improve the aqueous solubility of hydrophobic antibiotics such as Polymyxin B [86]. Hence, basic research using model membrane systems, such as liposomes, is invaluable for predicting saponin behavior in real biological membranes.

2. Research gap & hypothesis

The extant literature extensively discusses interactions between natural surfactants, particularly saponins, and biological membranes, highlighting their potential roles in various biological and pharmaceutical applications. However, there are still significant gaps in a deeper understanding of the physicochemical modifications induced by saponins on phospholipid membranes. Detailed examinations of these interactions, both in cellular contexts and using model membrane systems, remain insufficiently explored. Moreover, there is a shortage of in-depth analysis on how these membrane modifications directly influence or enhance the efficacy of pharmaceutical substances when saponins are used as adjuvants. The majority of existing studies have focused on two aspects: firstly, the general surface activities of the substances in question, and secondly, the broad antibacterial and antifungal effects of saponins. Therefore, there is still a lack of specific information on molecular mechanisms through which saponins interact with lipid bilayers, the structural changes they induce, and their implications for biological functions and pharmaceutical performance. This shortage of details represents a critical limitation that the current research seeks to address comprehensively. Thus, based on the identified research gaps, the following hypothesis has been stated:

Saponins modify the physicochemical properties of phospholipid membranes both in living cells and model membrane systems, thus may function as adjuvants, enhancing the effectiveness of active pharmaceutical substances.

3. Aims of the dissertation

The central objective of this dissertation was to investigate the interactions of natural surfactants - saponins, with phospholipid membranes. This study is crucial to understand their potential role in enhancing pharmaceutical applications, specifically their functionality as membrane-modifying adjuvants. The research employs both model membrane systems and living cells, utilising advanced techniques to explain the structural and functional alterations induced by saponins. The approach combines classical analytical methods with cutting-edge instrumental analysis and microbiological techniques. The specific objectives of this dissertation were:

- characterise the adsorption and aggregation properties of saponin-rich extracts (P1),
- determine the impact of purification processes on their physicochemical interactions with phospholipid membranes (P1, P2, P3),
- determine the saponin integration into phospholipid membranes using 2D monolayer and 3D liposome models (P2, P4),
- investigate the effects of saponins on fungal membrane integrity, particularly regarding *Candida* yeast biomembranes (P3),
- examine the biophysical consequences of saponin integration into bacterial membrane models and their interactions with non-surfactant antibiotics (P4),
- assess the cytotoxicity and collaborative interactions of saponins with antibiotics in bacterial and human cell models (P5).

4. List of publications included in the dissertation

The dissertation is based on research articles published in journals listed in the Journal Citation Reports. The referenced publications are as follows:

P1. **Adam Grzywaczyk**, Wojciech Smułek, Agnieszka Zgoła-Grześkowiak, Ewa Kaczorek*, Anna Zdziennicka, Bronisław Jańczuk *Nanofiltered saponin-rich extract of Saponaria officinalis – Adsorption and aggregation properties of particular fractions*. Colloids and Surfaces A: Physicochemical and Engineering Aspects 661 (2023) 130937 DOI: 10.1016/j.colsurfa.2023.130937

IF: 4.9 MNiSW: 70

P2. Monika Rojewska, Wojciech Smułek, **Adam Grzywaczyk**, Ewa Kaczorek, Krystyna Prochaska* *Study of interactions between saponin biosurfactant and model biological membranes: Phospholipid monolayers and liposomes.* Molecules 2023, 28, 1965. DOI: 0.3390/molecules28041965

IF: 4.2 MNiSW: 140

P3. **Adam Grzywaczyk*** Wojciech Smułek, Ewa Kaczorek *Saponaria officinalis saponins as a factor increasing permeability of Candida yeasts' biomembrane.* World Journal of Microbiology and Biotechnology (2024) 40:152. DOI: 10.1007/s11274-024-03961-9

IF: 4.0 MNiSW: 70

P4. **Adam Grzywaczyk*,** Monika Rojewska, Wojciech Smułek, Daniel A. McNaughton, Krystyna Prochaska, Philip A. Gale, Ewa Kaczorek *Glycyrrhiza glabra L. saponins modulate the biophysical properties of bacterial model membranes and affect their interactions with tobramycin.* Langmuir 2025, 41, 18, 11701–11710. DOI: 10.1021/acs.langmuir.5c00927

IF: 3.7 MNiSW: 100

P5. **Adam Grzywaczyk**, Wojciech Smułek, Anna Olejnik, Urszula Guzik, Agnieszka Nowak, Ewa Kaczorek* *Co-interaction of nitrofuran antibiotics and the saponin-rich extract on gram-negative bacteria and colon epithelial cells.* World Journal of Microbiology and Biotechnology (2023) 39:221. DOI: 10.1007/s11274-023-03669-2

IF: 4.0 MNiSW: 70

* Corresponding author

5. Summary of the results

P1. Nanofiltered saponin-rich extract of *Saponaria officinalis* – adsorption and aggregation properties of particular fractions

Adam Grzywaczyk, Wojciech Smułek, Agnieszka Zgoła-Grześkowiak, Ewa Kaczorek*, Anna Zdziennicka, Bronisław Jańczuk

Journal: Colloids and Surfaces A: Physicochemical and Engineering Aspects, 661 (2023) 130937

DOI: 10.1016/j.colsurfa.2023.130937 Impact Factor: 4.9 MNiSW: 70

This paper investigates the behaviour of complex plant-derived surfactants through the isolation of specific fractions from a crude saponin extract. The root extract of *Saponaria officinalis*, which is characterised by its high content of saponin biosurfactants, was separated based on molecular size. The aim was to determine how purification and molecular weight cut-offs affect the surfactant properties of the extract. By doing so, the study identifies a fraction enriched in active saponins and characterises its surface activity and aggregation behavior. It is necessary to understand these phenomena, taking into account the diversity of components present in plant extracts, including sugars and proteins, which may affect surface activity.

A methanolic extract of *S. officinalis* roots was prepared by Soxhlet extraction (yielding fraction E0), then sequentially nanofiltered to obtain fractions by molecular weight: The first step in the process is the separation of the 3 kDa permeate from the 3 kDa retentate. This was followed by the further splitting of the 3 kDa permeate into the 0.5 kDa permeate (E3) and the 0.5-3 kDa retentate (E2). This approach resulted in the concentration of the saponin content in the mid-range 0.5-3 kDa fraction (E2) (scheme in Fig. 5).

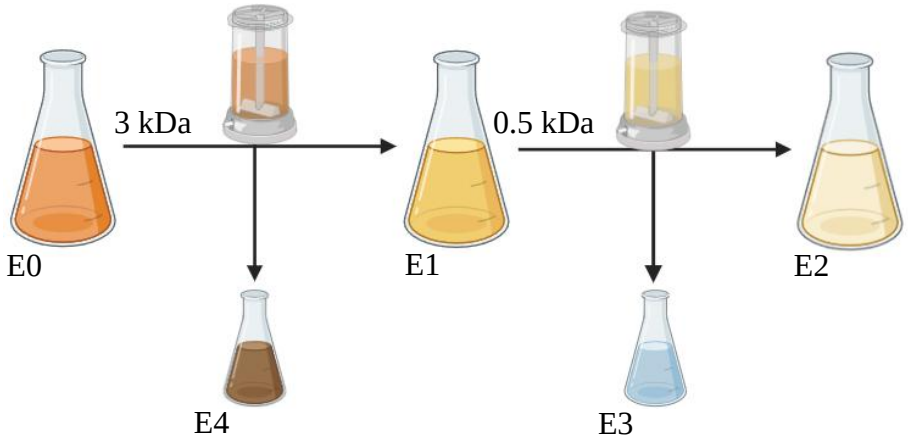

Fig. 5 A scheme of the extraction procedure; E0 - crude extract, E1 - permeate after 3 kDa filtration (<3 kDa), E2 - retentate after 0.5 kDa filtration (0.5-3kDa fraction), E3 - retentate after 0.5 kDa filtration (<0.5 kDa), E4 - retentate after 3 kDa filtration (>3 kDa).

The E2 fraction was enriched in saponins and showed clear surfactant activity, but it did not outperform the crude extract in minimum surface tension or in critical micelle concentration. LC-MS detected saponins in E1 and E2, while no saponins were found in E3. The E3 contained mainly small polar compounds such as sugars. Identified saponins were predominantly derivatives of hydroxygypsogenic acid and quillaic acid glycosylated mainly with hexoses (e.g., fructose, mannose, psicose) and pentoses (e.g., arabinose), as supported by GC-MS data. Surface tension measurements demonstrated that all fractions exhibited surface activity, although to different degrees. Across all tested fractions, the minimum values of surface tension were similar, and E2 did not reach a lower value than the others. In every case, the minimum value of surface tension stayed higher than for common synthetic surfactants such as sodium dodecyl sulfate and cetyltrimethylammonium bromide. The crude extract and E2 had the same critical micelle concentration 1.5 g L^{-1}. E1 and E4 had lower CMC values, 1.29 and 1.3 g L^{-1} respectively, and E3 possessed a higher CMC value, 2.33 g L^{-1}. This finding indicates that removing specific impurities led to differences in the critical micelle concentration between fractions. However, for E2 the concentration needed for micelle self-assembly was similar to that of the crude mixture. This observation may be attributed to the removal of synergistic amphiphiles present in E0, such as other surfactants or co-solutes. Nevertheless, E2 demonstrated a high degree of surface activity. Thermodynamic analysis (Gibbs free energy of adsorption and micellisation) indicated that micelle formation in all extract fractions is spontaneous. The standard free energy of micellisation for these plant extracts was found to be negative, signifying a greater tendency to aggregate than classical synthetic surfactants. Dynamic Light Scattering (DLS) analysis revealed clear differences in aggregate size between

fractions: the saponin-rich fraction E2 formed the smallest micelles, on the order of tens of nanometers (down to ~24 nm at higher concentrations). Conversely, the crude extract (E0) and other fractions yielded larger aggregates or micellar structures. For instance, E1 and E4 exhibited micelle hydrodynamic diameters ranging from approximately 37 to 120 nanometers, while E2's micelles demonstrated diameters of around 24 to 105 nanometers under comparable conditions (Fig. 6). The higher values may correspond to micelle aggregates.

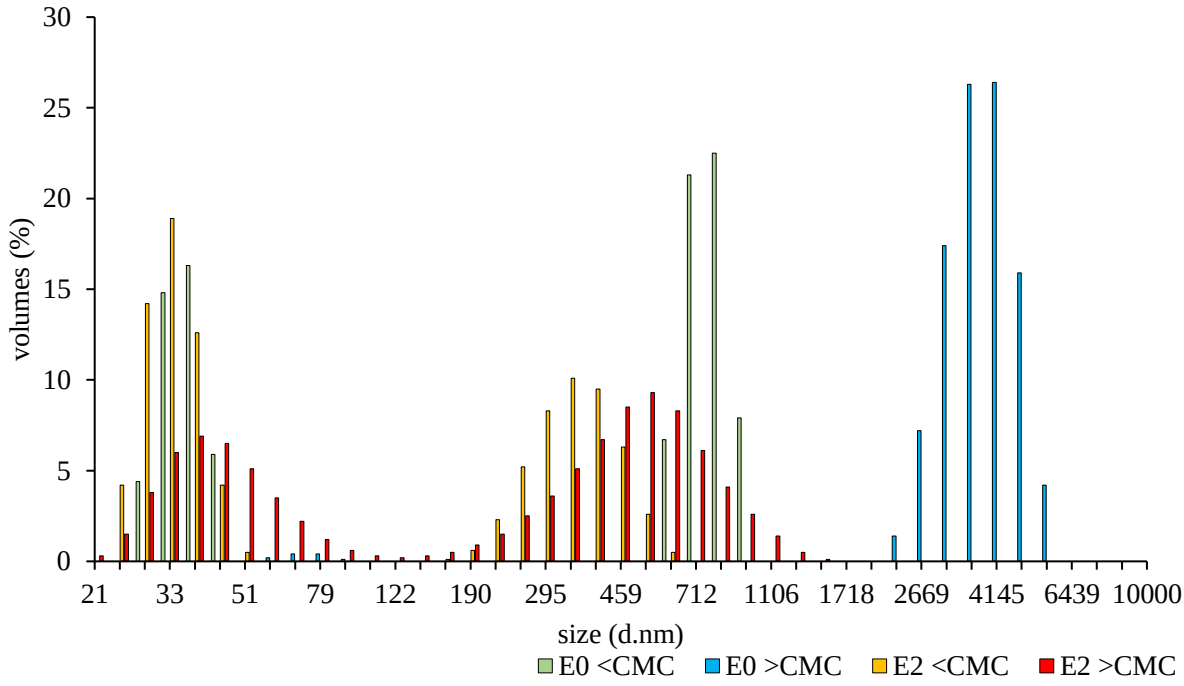

Fig. 6 Particle size distribution of the crude (E0) and saponin-rich (E2) fractions of the *Saponaria officinalis* extracts (x_v - volume fraction in %, d - hydrodynamic diameter in nm).

The application of nanofiltration to purify the extract resulted in two notable effects: a concentration of the active saponin compounds and an alteration in aggregation behaviour. The purified fraction, while highly effective, did not reduce surface tension to the same extent as the crude extract, suggesting that certain minor constituents of the crude extract may synergistically contribute to surface tension reduction or micelle formation. Nevertheless, the purified fraction's willingness to form uniformly smaller micelles is advantageous for applications requiring nanoscale aggregates. These findings confirm that the nanofiltration approach successfully isolated a bioactive fraction with predictable and enhanced properties, thereby providing a basis for the utilisation of *Saponaria*-derived saponins in formulated products.

Conclusions

The study demonstrated that two-step membrane filtration can obtain a *S. officinalis* root extract fraction highly enriched in saponins. Fraction E2 (0.5–3 kDa) was identified as the fraction containing the majority of them. The formation of micelles of nanometric size, smaller than those in other fractions, is advantageous for the creation of stable nano-emulsions or drug delivery micelles. The work demonstrated that established thermodynamic models can be applied to complex natural mixtures. It can be used to extract meaningful parameters like CMC and Gibbs free energy. The capacity of the purified saponin-rich extract to aggregate and reduce surface tension confirms its potential as a natural ingredient within the pharmaceutical, cosmetic, and food industries.

The primary accomplishment of this article was the detailed characterisation and fractionation of the saponin-rich extract from *S. officinalis*. We described its surface-active properties, directly linking them to the chemical composition of individual fractions. Crucially, we developed an optimised nanofiltration purification strategy to obtain highly enriched saponin fractions suitable for precise biomedical research and practical applications.

P2. Study of interactions between saponin biosurfactant and model biological membranes: phospholipid monolayers and liposomes

Authors: Monika Rojewska, Wojciech Smułek, **Adam Grzywaczyk**, Ewa Kaczorek, Krystyna Prochaska*

Journal: Molecules 28(4), 1965 (2023)

DOI: 10.3390/molecules28041965 Impact Factor: 4.2 MNiSW: 140

The detailed characterisation of saponin extract fractions presented in P1 laid the groundwork for examining their specific interactions with biological membranes. Therefore, in P2, we investigated fractions more deeply, using a simplified biomembrane model. Hence, this publication explores the interaction of plant extract containing saponins with simplified models of biological membranes, using both two-dimensional (monolayer) and three-dimensional (liposome) systems. The motivation for this study stems from the dual nature of saponins as membrane-active agents. It is well established that some saponins have biological activity (antimicrobial, antifungal, etc.), but the specifics of how they incorporate into or disrupt lipid membranes remain incompletely understood. The study examined biomembrane models to gain complementary insights into the membrane affinity and perturbation caused by saponins. In particular, a saponin-rich extract from licorice (*Glycyrrhiza glabra* L.) roots was selected. Moreover, crude extract and purified one (0.5-3 kDa fraction, method similar to one described in P1) was used. Licorice root saponins have a known amphiphilic structure and were hypothesised to integrate into lipid assemblies. The fundamental question concerns the capacity of saponins to permeate biological membranes and disrupt their lipid packing, and the potential influence of any non-saponin impurities present in the extract on this process. The scheme of procedure to verify this question is presented in Fig. 7.

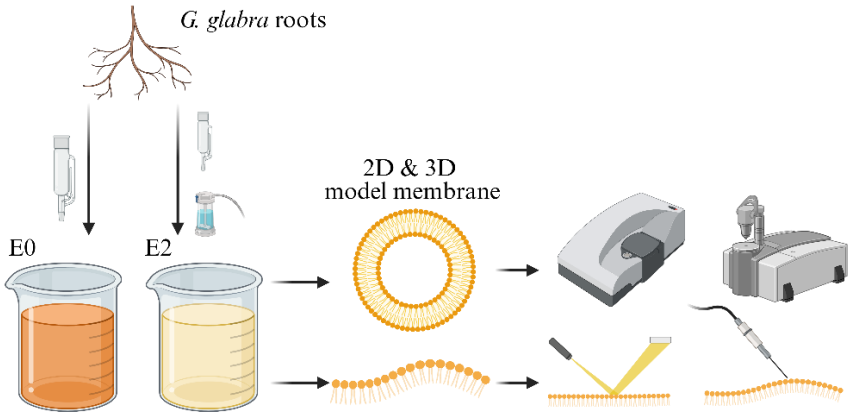

Fig. 7 A scheme of procedure in P2; E0 – crude extract, E2 – fraction 0,5-3kDa

The interactions of the licorice-derived saponins with model membranes revealed notable differences between the monolayer and bilayer systems, thus highlighting the value of the dual approach. In the DPPE (1,2-dipalmitoyl-sn-glycero-3-phosphorylethanolamine) monolayer experiments, the introduction of the saponin-rich extract resulted in measurable shifts in the π-A isotherms, indicating that saponin molecules penetrate the monolayer and expand the lipid film. Specifically, the insertion of saponins resulted in an augmentation of the molecular area per lipid at a given surface pressure, concomitant with a diminution in the monolayer's compressional modulus (elasticity). This signifies that the monolayer is more fluid and less tightly packed in the presence of saponins. However, the stability of monolayers was found to depend on the purity of the saponin extract. The presence of impurities in the extract resulted in a decrease in monolayer stability, which is evidenced by an increase in surface pressure drop over time. This indicates that non-saponin components may interfere with the packing of the DPPE to a greater extent, thereby hindering the optimal organisation of the saponins at the interface. On the other hand, a more purified saponin extract sample would be expected to integrate more uniformly, thus resulting in a more stable film. Brewster Angle Microscopy visualisation supported these findings by showing differences in domain morphology with and without the crude extract. Films affected by the crude extract have exhibited more heterogeneous textures (indicating phase separation due to impurities), whereas those with purified extract were more uniform.

In the liposome experiments, the saponins also interacted with the model bilayer, but the nature of the interaction was somewhat different. Measurements of the zeta potential exhibited an alteration in the surface charge of the liposomes upon the addition of extract fractions. The

negative zeta potential of the phospholipid vesicles (-46.94 ± 3.06 mV for control) noted a decline, approaching -51.40 ± 0.89 mV after being treated with crude extract. However, in the case of the purified fraction treatment, the zeta potential of DPPE liposomes increased up to -42.74 ± 1.77 mV. This suggests that the adsorption of saponin neutralised a proportion of the surface charge or introduced some positively charged groups at the interface. This observation provides further confirmation of the hypothesis that saponins coat the external surface of the liposome, with their sugar moieties potentially contributing to a more neutral surface character. The size of the liposomes remained essentially unchanged after purified extract treatment, with no signs of large aggregation or vesicle rupture. On the other hand, after crude extract treatment, there was a shift towards larger particles, up to 2000 nm, suggesting an aggregation of vesicles. There was no increase in polydispersity or the emergence of smaller vesicle fragments, which indicates that the saponins did not cause lysis or major structural breakdown of the bilayers. In contrast, the vesicles maintained their integrity, acquiring merely a layer of saponin, resulting in a decrease of the polydispersity index (from 0.8 ± 0.1 for a control to 0.5 ± 0.1 after treatment with purified fraction), which suggests a shift toward a monodisperse system.

It is important to note that the monolayer studies demonstrated a more pronounced perturbation. Due to the lack of a lipid reservoir in the monolayer that could accommodate saponin, expansion and instability caused by insertion occur. In contrast, the bilayer studies exhibited a more moderate effect, with the membrane demonstrating the capacity to incorporate saponin without compromising its structural integrity. This difference underscores the necessity for a cautious interpretation of results from model systems when extrapolating to real membranes. It is important to note that a compound that appears highly disruptive in monolayer or bilayer assays may only have moderate effects in living cells, which can adjust and reorganise.

Conclusions

The study provided insight into the interactions of saponins from *G. glabra* with model membranes. It demonstrated that saponins integrate into phospholipid assemblies, localise at the membrane interface, associate with lipid headgroup regions, and modify the biophysical properties of the membrane. However, the effect of saponins is context dependent. In a 2D lipid monolayer, saponins have been observed to induce disruption to lipid packing, with the potential to compromise membrane stability, particularly when the saponin preparation contains

heterogeneous components. In a 3D bilayer, the same saponins bind to the membrane surface, but the bilayer can accommodate them without sustaining damage. This indicates partial insertion, which leaves the membrane largely intact. This suggests that in biological systems, saponins may modulate membrane properties, such as fluidity and permeability, without unconditionally lysing cells at moderate concentrations. This is a valuable property in case of using them as drug delivery adjuvants. The study also highlights that extract purity is an important factor: purified saponins might have a different impact than crude extracts.

In this study, significant progress in understanding how saponins from *Glycyrrhiza glabra* L. interact with simplified biological membrane models has been made. We demonstrated differences and similarities in saponin integration between these two membrane models, emphasising that liposomes may represent a biological approximation. The results also confirmed that careful fractionation impacts the efficacy and specificity of biosurfactant-membrane interactions.

P3. *Saponaria officinalis* saponins as a factor increasing permeability of *Candida* yeasts' biomembrane

Authors: **Adam Grzywaczyk***, Wojciech Smułek, Ewa Kaczorek

Journal: World Journal of Microbiology and Biotechnology 40:152 (2024)

DOI: 10.1007/s11274-024-03961-9 Impact Factor: 4.0 MNiSW: 70

Building on the model membrane interactions explored in P2, we recognised the necessity to validate findings in a biologically relevant scenario. Consequently, in P3, we examined whether the membrane-modifying effects observed could enhance membrane permeability in actual fungal cells. Thus, the study investigates the effect of saponins on fungal cell membranes, with a specific focus on the opportunistic yeast from the *Candida* genus. Fungal infections pose significant health challenges, and *Candida* species possess robust cell envelope structures (including a cell wall) that protect them from antifungal agents. It has been established through previous research that saponins possess antifungal properties. However, these studies have generally focused on whole-cell outcomes, failing to identify the membrane as the primary site of action. The novel approach adopted in this study required the removal of the fungal cell wall, thereby creating spheroplasts of *Candida* (cells devoid of their cell wall, leaving only the plasma membrane) to expose the biomembrane to saponin-rich extract. This approach makes it possible to assess the interaction of saponins with the fungal cell membrane, thereby avoiding the potential confounding effects of the cell wall. Two species, *Candida albicans* (Polish Collection of Microorganisms no. 2566) and *Candida krusei* (Polish Collection of Microorganisms no. 2706), were selected as test organisms. The primary hypothesis set was that saponins from *S. officinalis* would integrate into the yeast plasma membrane and increase its permeability. As a result, this process could help explain the antifungal effects of saponins and suggest a role for them as adjuvants to conventional antifungals. The present study directly aligns with the dissertation's theme by examining a living cell membrane and evaluating the impact of natural surfactant on its integrity.

Saponin exposure increased the permeability of the *Candida* cell membrane. Specifically, treatment with a 10 $mg \cdot L^{-1}$ concentration of the *S. officinalis* saponin-rich extract (SoC) led to a notable increase in membrane permeability in *Candida albicans* spheroplasts by approximately 22% compared to untreated controls. Notably, *Candida krusei* showed even higher sensitivity, demonstrating a maximum permeability increase of 30.52% at 15 $mg \cdot L^{-1}$

SoC. Furthermore, the purified saponin fraction (SoP; process described in P1; fraction 0.5-3 kDa) was more effective than the crude extract, especially at the 10 mg·L^{-1} concentration (Table 3). Additionally, zeta potential measurements provided deeper insights into the interactions between saponins and fungal membranes. After saponin treatment, significant shifts toward more negative values were observed. Specifically, for *Candida albicans*, the zeta potential decreased markedly from approximately -9 mV (untreated) to about -17 mV and -25 mV after treatments with SoC and SoP, respectively. A comparable but slightly different pattern was observed for *Candida krusei*, where zeta potential values decreased from around -7 mV (untreated) to approximately -18 mV with SoP and -14 mV with SoC treatment (Table 3). These suggest strong interactions between the saponins and fungal biomembranes, possibly due to complex formation or binding to essential sterols like ergosterol, thereby altering membrane integrity and fluidity.

Table 3. *C. albicans and C. krusei* spheroplasts properties. SoC – *Saponaria officinalis* crude extract, SoP – *Saponaria officinalis* purified extract; green color indicates the increase of permeability (relative to the control sample), red color indicates a decrease of permeability (relative to the control sample)

	Treatment (mg L^{-1})		Zeta potential (mV)	Permeability; relative to the control sample (%)
C. albicans spheroplasts	SoC	5	-17.78±2.61	+12.31±10.69
		10	-17.62±0.96	+21.76±2.97
		15	-16.96±1.56	+16.74±4.79
	SoP	5	-24.85±2.77	-3.97±13.18
		10	-24.19±1.93	+26.10±7.22
		15	-25.19±2.16	+16.54±2.88
C. krusei spheroplasts	SoC	5	-4.68±0.31	-22.28±6.28
		10	-13.72±0.47	+10.11±13.25
		15	-14.40±0.82	+30.52±7.96
	SoP	5	-17.89±2.35	-22.49±13.18
		10	-18.43±2.02	+10.47±13.71
		15	-18.70±1.40	+4.82±7.1

Interestingly, despite permeability increases, immediate cell lysis was not uniformly observed at the tested concentrations, emphasizing a sub-lethal mechanism of membrane disruption. This could be therapeutically advantageous, facilitating enhanced drug penetration without immediate cell death, thus preventing rapid cellular responses or resistance development. Further clarity into the mode of action was provided through transmission electron microscopy (TEM) observations, revealing important morphological distinctions after treatment. At a lower concentration of 5 $mg \cdot L^{-1}$, SoC-treated spheroplasts showed minimal morphological change. In contrast, the SoP at the same concentration induced visible cell lysis, clearly evidenced by increased dye uptake in the TEM images.

Additionally, enzyme activity assays provide insight into the physiological and metabolic effects of saponin treatments. Remarkably, the metabolic activity of *C. albicans* spheroplasts increased significantly after treatment with 10 $mg \cdot L^{-1}$ SoP, possibly reflecting a stress-induced activation of some metabolic pathways. On the other hand, the same treatment resulted in decreased metabolic activity in *C. krusei*, indicating species-specific responses to saponin-induced membrane stress. These divergent metabolic responses suggest complex and varied adaptive strategies employed by different fungal species.

Conclusions

This study demonstrated that saponins from a natural source can directly increase the permeability of fungal cell membranes when the cell wall is removed, highlighting a possible membrane-targeted mode of action for saponins' antifungal effects. It established that the *S. officinalis* saponin-rich extract affects *Candida* membranes, causing biophysical changes: approximately a 20% rise in permeability and a shift in zeta potential values. The outcome is a proof-of-concept that saponins compromise fungal membrane integrity. From a practical perspective, this finding supports the idea of using saponins as adjuvants in antifungal therapy, potentially weakening the pathogen's membrane defenses and making antifungal drugs more effective or allowing for lower doses. Moreover, by successfully employing *Candida* spheroplasts as a model, the study introduced a useful experimental approach for examining membrane-specific effects of antimicrobial agents on fungi. Within the broader dissertation context, these results provide a crucial link between model membrane systems explored in

previous studies and practical, biological applications in live cells, directly validating the hypothesis that natural surfactants can modulate phospholipid membranes in biological contexts.

A key achievement here was demonstrating that *S. officinalis* saponins directly increase the permeability of *Candida* yeast cell membranes, particularly using purified fractions. Importantly, we demonstrated sub-lethal disruption mechanisms that are well-suited to adjuvant antifungal strategies. This provides robust biological evidence to support membrane-targeted antifungal therapy using naturally derived biosurfactants.

P4. *Glycyrrhiza glabra* L. saponins modulate the biophysical properties of bacterial model membranes and affect their interactions with tobramycin

Authors: Adam Grzywaczyk*, Monika Rojewska, Wojciech Smułek, Daniel A. McNaughton, Krystyna Prochaska, Philip A. Gale, Ewa Kaczorek

Journal: Langmuir 41(18), 11701-11710 (2025)

DOI: 10.1021/acs.langmuir.5c00927 Impact Factor: 3.7 MNiSW: 100

The positive findings from P2 and P3 led us to explore whether similar effects could be extended to bacterial membranes. Hence, in P4, another natural saponin source, *Glycyrrhiza glabra* (licorice), was chosen to evaluate its potential to alter bacterial membrane properties and enhance antibiotic interactions. Thus, this paper extends the investigation of saponin-membrane interactions to bacterial model membranes and examines how these interactions can potentiate antibiotic activity. The research focuses on tobramycin, a broad-spectrum aminoglycoside antibiotic that targets bacterial ribosomes but must pass the membrane to reach its site of action. The central idea explored is using saponins from *G. glabra* root (as in P2) as membrane-modulating adjuvants to improve antibiotic penetration or action. P2 has shown that saponins can insert into lipid membranes; here, the question becomes: can such insertion alter bacterial membrane properties in a way that makes antibiotics like tobramycin more effective? The model systems used are similar to those in P2 but tailored to mimic bacterial membranes: a 1,2-dioleoyl-sn-glycero-3-phosphoglycerol lipid monolayer and liposomes. By monitoring biophysical changes in the presence of saponins and tobramycin, the study aims to reveal any synergistic interactions at the membrane level that could correlate with improved antimicrobial outcomes.

Licorice saponins altered the biophysical properties of bacterial membrane models, creating conditions potentially favorable for antibiotic action. In monolayer experiments, insertion resulted in a decrease in the compressibility modulus, reducing it by approximately 25% to over 50%, depending on saponin concentration. This decrease indicated that the lipid monolayer became less rigid and more fluid, suggesting a disruption of the tightly packed lipid arrangement due to the amphiphilic nature of saponins. Notably, the most notable softening effect (around a 50% reduction) was observed at higher saponin concentrations (approx. 10 $mg \cdot L^{-1}$). Importantly, even at the highest tested concentrations, no complete collapse or rupture of the monolayer occurred, which means that the membrane-modulating effect of

saponins is significant but controlled, and at tested concentration, does not cause membrane damage. Surface pressure isotherms showed a clear shift towards larger molecular areas after the saponin treatment, indicating significant incorporation of saponin molecules into the lipid structure and resulting in the expansion of less compact monolayers. Higher saponin concentrations correlated with increased fluidisation and reduced collapse pressure, highlighting their potential to destabilise lipid arrangements and enhance membrane permeability. Notably, the combined presence of saponins and tobramycin altered the monolayer properties more significantly than either compound alone, evidenced by increased compressibility and elasticity. Relaxation experiments further demonstrated that combined treatments expanded the lipid film surface area, confirming the concept of synergistic modulation of the cell membrane.

Table 4. Treated and untreated liposome properties. Ctrl - untreated control; GgC - *G. glabra* crude saponin extract at 5 mg L^{-1}; Tbrm - tobramycin at 10 mg L^{-1}; GgC/Tbrm:- combination of GgC + tobramycin

Sample	PDI	Zeta potential (mV)
Ctrl	0.13±0.02	-50.0±2.5
GgC	0.15±0.02	-49.1±1.6
Tbrm	0.13±0.03	-22.1±0.3
GgC/Tbrm	0.13±0.04	-17.7±1.0

Liposome experiments provided additional insight into the interactions of saponins with antibiotics. Zeta potential calculations indicated charge alterations when saponins and tobramycin were combined. Specifically, liposomes treated with tobramycin alone exhibited a substantial reduction in negative charge, moving from -50 mV to -22 mV. When combined with licorice saponins, the zeta potential further shifted to -17.7 mV, suggesting enhanced interactions or a potential cooperative mechanism between saponins and tobramycin. This alteration could facilitate a closer approach or increased penetration of the positively charged antibiotic. DLS analyses revealed that liposome size distributions remained generally stable, with minimal size increase and moderate broadening in distribution, suggesting slight structural alterations without severe aggregation or vesicle rupture (Table 4). This stability was further validated by complementary membrane integrity assays, including the HPTS and

carboxyfluorescein release assays, which demonstrated negligible membrane disruption across all treatment conditions.

Conclusions

This research provided evidence that licorice root saponins can modify bacterial membrane properties to enhance antibiotic effectiveness. By reducing membrane rigidity and altering zeta potential without causing significant lysis, saponins may create conditions conducive to improved interactions between antibiotics and the bacterial cell envelope. These saponins, despite their pronounced membrane modulation, do not cause outright membrane rupture at tested concentrations, which is beneficial for controlled and reversible modulation. When combined with tobramycin, saponins alter antibiotic-membrane interactions, likely facilitating enhanced antibiotic binding or uptake. Such combinations could strategically enhance antibiotic efficacy, potentially overcoming certain resistance mechanisms by promoting drug penetration into bacterial cells.

The main achievement of this paper was the explanation of how saponins from *Glycyrrhiza glabra* modulate bacterial model membranes, enhancing membrane interactions with the antibiotic tobramycin. It has been verified that these interactions did not affect the membrane's integrity, but they did disrupt the packing and fluidity of the membrane to a degree that potentially enhances the effectiveness of the antibiotics.

P5. Co-interaction of nitrofuran antibiotics and the saponin-rich extract on gram-negative bacteria and colon epithelial cells

Authors: Adam Grzywaczyk, Wojciech Smułek, Anna Olejnik, Urszula Guzik, Agnieszka Nowak, Ewa Kaczorek*

Journal: World Journal of Microbiology and Biotechnology 39:221 (2023)

DOI: 10.1007/s11274-023-03669-2 Impact Factor: 4.0 MNiSW: 70

In P5, previously obtained results were tested on bacterial cells, with a particular focus on the practical synergy of saponins with nitrofuran antibiotics. This publication presents an applied microbiological study that builds on the prior mechanistic findings by testing the combined effect of natural saponins and antibiotics on living bacterial cells, as well as assessing safety on human cells. The goal was to determine if a saponin-rich extract (from *Sapindus mukorossi*, the soapnut) can act as an adjuvant to nitrofuran antibiotics, enhancing their antimicrobial efficacy against Gram-negative bacteria while not increasing toxicity to mammalian cells. Based on earlier parts of the dissertation, the hypothesis was formulated that saponins with nitrofuran antibiotics would produce a synergistic antibacterial effect greater than either alone. Additionally, since any adjuvant for antibiotics must be safe to human tissues, the impact of the combined treatment on human colon epithelial cells was evaluated (since colon cells could be exposed to antibiotics). This dual consideration of efficiency and safety makes the study comprehensive. This also serves as a practical validation of the membrane-centric mechanism proposed: if saponins truly modify membrane properties (as shown in P2 and P4), and may serve as an antibiotic adjuvant, we should observe improved antibiotic action and minimal harm to human cells at the same doses.

The combination of saponins from *S. mukorossi* with nitrofuran antibiotics produced a significant synergistic antibacterial effect against the tested Gram-negative bacterial strains: *Pseudomonas plecoglossicida* IsA, *Pseudomonas* sp. MChB, and *Pseudomonas* sp. OS4. When bacterial cultures were treated with nitrofurantoin (NFT) or furazolidone (FZD) in combination with saponin extract, bacterial metabolic activity dropped up to 50% compared to the control sample for *Pseudomonas plecoglossicida* IsA. This effect emphasises the potential for a reduction in the antibiotic dosage required to achieve the desired therapeutic outcomes. It is worth noting that the combination of saponins and nitrofuran antibiotics displayed negligible cytotoxicity towards human colon epithelial cells (CCD 841CoN), as demonstrated through

detailed viability assays. Human cells exposed to the combined saponin-antibiotic treatments maintained high viability, comparable to untreated control cells.

Table 5. Cell membrane permeability and cell surface properties of tested strains after exposure to antibiotics and/or *S. mukorossi* extract; changes in % relative to the control sample (100%). NFT – nitrofurantoin, FZD – furazolidone, Sap – saponins from *Sapindus mukorossi*

	Pseudomonas sp. OS.4	*P. plecoglossicida* IsA	*Pseudomonas* sp. MChB
Changes in cell permeability (%)			
NFT	-24.8±2.2	-30.8±2.3	-40.9±1.7
FZD	-38.5±1.8	1.2±3.3	-15.2±2.5
NFT + Sap	42.8±4.2	28.2±4.2	47.7±4.3
FZD + Sap	49.1±4.4	36.4±4.5	49.6±4.4
Sap	43.6±4.2	37.7±4.5	48.7±4.4
Changes in cell surface adhesivity (%)			
NFT	-20.8±2.6	-4.3±3.4	1.1±3.6
FZD	-4.0±3.1	-2.4±3.4	-8.3±3.3
NFT + Sap	<-96.9	-52.0±1.7	<-97.2
FZD + Sap	<-96.9	-79.0±0.7	-91.6±0.3
Sap	<-96.9	-65.3±1.2	-58.0±1.5
Changes in zeta potential (mV)			
NFT	0.3±0.5	2.6±0.5	0.9±0.7
FZD	0.6±0.5	3.5±0.4	-0.3±0.7
NFT + Sap	-26±1.8	-14.9±1.4	-17.8±1.6
FZD + Sap	-23.7±1.7	-12.6±1.2	-18.1±1.6
Sap	-7.6±0.9	-3.9±0.8	-3.1±0.9

Lipidomic analysis provided further insight into bacterial adaptive responses upon exposure to combined treatments. Membrane fatty acid profiles revealed notable shifts toward increased levels of branched-chain fatty acids in IsA and OS4 bacteria treated with the saponin-antibiotic combinations. Such fatty acid modifications are recognised as a bacterial stress response mechanism that aims at maintaining membrane integrity. This pronounced increase in branched-chain fatty acids indicates a membrane-targeted stress imposed by the treatments. Simultaneously, bacterial cell surface hydrophobicity exhibited decreases, resulting in a hydrophilic bacterial surface after saponin exposure. This change suggests that saponins adsorb to the bacterial surface, potentially forming a hydrophilic layer through their sugar moieties. Such structural modifications likely enhance antibiotic penetration by disrupting hydrophobic barriers typically found in bacterial outer membranes. Additionally, cell permeability assays employing Crystal Violet uptake demonstrated increases in membrane

permeability after saponin treatment, directly correlating with enhanced antibiotic effectiveness (Table 5). These permeability changes confirm the hypothesised mechanism of improved antibiotic access facilitated by saponins. Complementary zeta potential calculations further supported these findings by revealing decreases in bacterial surface charge upon saponin exposure.

Conclusions

The study demonstrates the potential for using *Sapindus mukorossi* saponins as adjuvants to enhance the efficacy of nitrofuran antibiotics against Gram-negative bacteria. The observed synergistic interactions decreased bacterial metabolisms, without inducing significant cytotoxicity in human colon epithelial cells. Saponins effectively modified bacterial membrane properties, including increased branched-chain fatty acids, enhanced membrane permeability, decreased surface hydrophobicity, and reduced surface charge, confirming their role in facilitating antibiotic action. These findings provide a foundation for the therapeutic application of natural saponins to improve antibiotic performance, potentially reducing the necessary antibiotic dosage and lowering the risk of antibiotic resistance.

The major achievement here was demonstrating antibacterial synergy between *Sapindus mukorossi* saponins and nitrofurantoin and furazolidone against Gram-negative bacteria. Remarkably, this effect was achieved without detectable toxicity to human colon epithelial cells, confirming both efficacy and safety. In addition, detailed investigations revealed changes in bacterial membrane composition and properties. These findings provide strong support for proposed mechanism, which suggests that saponins facilitate antibiotic entry and enhance therapeutic efficacy.

6. Summarizing conclusions

The research conducted within this dissertation provided comprehensive insight into the interaction of natural-origin surfactants, predominantly saponins, with biological and model phospholipid membranes. The first research included a complete analysis with separation of *Saponaria officinalis* extracts containing saponins. The analysis of fundamental adsorption and aggregation properties revealed essential information for understanding saponin interactions with biological membranes. The complete characterisation process provided the essential information needed for analyzing saponin interactions at the molecular level. The research conducted in P2 investigated the specific interactions between *Glyrhizza glabra* purified saponin fractions with biological model membranes, which consisted of phospholipid monolayers and liposomes. It demonstrated how saponins affect membrane structures, making them more permeable, thereby highlighting their potential application in targeted biomedical practices. Further investigation of biologically relevant systems demonstrated that *Saponaria officinalis* saponins caused an increase in *Candida* cell membrane permeability (P3). These results indicate that saponins work well as additional therapeutic agents in antifungal treatment. Consequently, in P4, saponins from *Glycyrrhiza glabra* exhibited the capacity to significantly modulate bacterial membrane biophysical properties. Importantly, the research confirmed enhanced interactions between bacterial membranes and the antibiotic tobramycin, thus identifying a practical approach to potentiating antibiotic activity against bacterial pathogens. P5 research proved the practical antibacterial potential of saponins when combined with nitrofuran antibiotics. *Sapindus mukorossi* saponins, together with nitrofurantoin or furazolidone, displayed substantial synergistic antibacterial properties against Gram-negative bacteria. The saponin combinations proved non-toxic to human cells, which demonstrates their potential therapeutic value as antibiotic enhancers for lowering medication amounts while combating antibiotic resistance.

The dissertation made a significant discovery regarding saponins, which were found to function as effective adjuvants, thereby enhancing the effectiveness of antibiotics through their ability to modify biological membranes. The combination of saponins with antibiotics resulted in synergy effects, thereby enhancing antimicrobial activity against Gram-negative bacteria. The significance of this discovery lies in the increasing prevalence of multidrug-resistant microorganisms, which necessitates the development of novel therapeutic strategies.

The presented dissertation:

- confirmed that saponins interact with model membranes (monolayers and liposomes), shifting packing and zeta potential, while membranes stayed intact at tested saponin concentrations,
- showed that *S. officinalis* saponins increase the permeability of *Candida* spheroplast membranes and shift zeta potential,
- found that *Glycyrrhiza glabra* saponins loosen DOPG monolayers and, together with tobramycin, further change surface charge without dye leakage from liposomes,
- demonstrated synergy between *Sapindus mukorossi* saponins and nitrofuran antibiotics on *Pseudomonas* strains, with no added toxicity to colon cells.

Moreover, the research findings demonstrated that saponins behave in a different manner when interacting with monolayer versus bilayer systems. It is therefore imperative that monolayer results are carefully evaluated in order to ascertain the complexity of biological bilayer systems. The bilayer models, notably liposomes, yielded applicable biological results by demonstrating the capacity of saponins to exist in moderate concentrations within membranes without inducing complete structural breakdown.

Future research should concentrate on two promising strategies involving the application of saponins. First, exploring their role as antibiotic adjuvants offers significant potential, particularly in combating multidrug-resistant microorganisms. To optimise dosage regimens and maximise therapeutic outcomes, it is essential to conduct detailed investigations into the mechanisms of synergy between saponins and various antibiotic classes. Alternatively, saponins could be used as adjuvants in lipid-based drug delivery systems, enhancing drug encapsulation efficiency and targeted delivery. This approach uses the membrane-modulating properties of saponins to potentially improve how well therapeutic agents are absorbed and how long they are released for. However, further comprehensive studies are necessary to fully understand their interactions within complex lipid carrier systems, assess long-term stability, and confirm efficacy and safety in clinical contexts. Ongoing research in both of these areas must be continued to fully uncover the therapeutic potential of saponins.

References

[1] G. L. Nicolson and G. Ferreira De Mattos, 'Fifty years of the fluid-mosaic model of biomembrane structure and organization and its importance in biomedicine with particular emphasis on membrane lipid replacement', *Biomedicines*, vol. 10, no. 7, p. 1711, Jul. 2022, doi: 10.3390/biomedicines10071711.

[2] K. Jacobson, et al., 'The lateral organization and mobility of plasma membrane components', *Cell*, vol. 177, no. 4, pp. 806-819, May 2019, doi: 10.1016/j.cell.2019.04.018.

[3] G. L. Nicolson and G. Ferreira De Mattos, 'A brief introduction to some aspects of the fluid-mosaic model of cell membrane structure and its importance in membrane lipid replacement', *Membranes*, vol. 11, no. 12, p. 947, Nov. 2021, doi: 10.3390/membranes11120947.

[4] W. Dowhan, 'Molecular basis for membrane phospholipid diversity: why are there so many lipids?', *Annu. Rev. Biochem.*, vol. 66, no. 1, pp. 199-232, Jun. 1997, doi: 10.1146/annurev.biochem.66.1.199.

[5] J. Hazel and E. Williams 'The role of alterations in membrane lipid composition in enabling physiological adaptation of organisms to their physical environment', *Prog. Lipid Res.*, vol. 29, no. 3, pp. 167-227, 1990, doi: 10.1016/0163-7827(90)90002-3.

[6] T. Osawa, K. Fujikawa, and K. Shimamoto, 'Structures, functions, and syntheses of glycero-glycophospholipids', *Front. Chem.*, vol. 12, Feb. 2024, doi: 10.3389/fchem.2024.1353688.

[7] H. Strahl and J. Errington, 'Bacterial membranes: structure, domains, and function', *Annu. Rev. Microbiol.*, vol. 71, no. 1, pp. 519-538, Sep. 2017, doi: 10.1146/annurev-micro-102215-095630.

[8] Z. Huang and E. London, 'Cholesterol lipids and cholesterol-containing lipid rafts in bacteria', *Chem. Phys. Lipids*, vol. 199, pp. 11-16, Sep. 2016, doi: 10.1016/j.chemphyslip.2016.03.002.

[9] J. P. Sáenz *et al.*, 'Hopanoids as functional analogues of cholesterol in bacterial membranes', *Proc. Natl. Acad. Sci.*, vol. 112, no. 38, pp. 11971-11976, Sep. 2015, doi: 10.1073/pnas.1515607112.

[10] T. J. Silhavy, *et al.*, 'The bacterial cell envelope', *Cold Spring Harb. Perspect. Biol.*, vol. 2, no. 5, pp. a000414-a000414, May 2010, doi: 10.1101/cshperspect.a000414.

[11] E. R. Rojas *et al.*, 'The outer membrane is an essential load-bearing element in Gram-negative bacteria', *Nature*, vol. 559, no. 7715, pp. 617-621, Jul. 2018, doi: 10.1038/s41586-018-0344-3.

[12] M. Kaur *et al.*, 'Insight into the outer membrane asymmetry of *P. aeruginosa* and the role of MlaA in modulating the lipidic composition, mechanical, biophysical, and functional membrane properties of the cell envelope', *Microbiol. Spectr.*, vol. 12, no. 11, Nov. 2024, doi: 10.1128/spectrum.01484-24.

[13] J. Löffler, *et al.*, 'Phospholipid and sterol analysis of plasma membranes of azole-resistant *Candida albicans* strains', *FEMS Microbiol. Lett.*, vol. 185, no. 1, pp. 59-63, Apr. 2000, doi: 10.1111/j.1574-6968.2000.tb09040.x.

[14] M. Bogdanov, *et al.*, 'Phospholipid-assisted refolding of an integral membrane protein', *J. Biol. Chem.*, vol. 274, no. 18, pp. 12339-12345, Apr. 1999, doi: 10.1074/jbc.274.18.12339.

[15] V. W. Rowlett *et al.*, 'Impact of membrane phospholipid alterations in escherichia coli on cellular function and bacterial stress adaptation', *J. Bacteriol.*, vol. 199, no. 13, Jul. 2017, doi: 10.1128/JB.00849-16.

[16] P. J. Wilderman, *et al.*, '*Pseudomonas aeruginosa* synthesizes phosphatidylcholine by use of the phosphatidylcholine synthase pathway', *J. Bacteriol.*, vol. 184, no. 17, pp. 4792-4799, Sep. 2002, doi: 10.1128/JB.184.17.4792-4799.2002.
[17] C. Sohlenkamp and O. Geiger, 'Bacterial membrane lipids: diversity in structures and pathways', *FEMS Microbiol. Rev.*, vol. 40, no. 1, pp. 133-159, Jan. 2016, doi: 10.1093/femsre/fuv008.
[18] P. A. Leventis and S. Grinstein, 'The distribution and function of phosphatidylserine in cellular membranes', *Annu. Rev. Biophys.*, vol. 39, no. 1, pp. 407-427, Apr. 2010, doi: 10.1146/annurev.biophys.093008.131234.
[19] T. Balla, 'Phosphoinositides: tiny lipids with giant impact on cell regulation', *Physiol. Rev.*, vol. 93, no. 3, pp. 1019-1137, Jul. 2013, doi: 10.1152/physrev.00028.2012.
[20] H. Zhou, *et al.*, 'Phosphatidic acid: from biophysical properties to diverse functions', *FEBS J.*, vol. 291, no. 9, pp. 1870-1885, May 2024, doi: 10.1111/febs.16809.
[21] I. Domonkos, *et al.*, 'Lipid-assisted protein-protein interactions that support photosynthetic and other cellular activities', *Prog. Lipid Res.*, vol. 47, no. 6, pp. 422-435, Nov. 2008, doi: 10.1016/j.plipres.2008.05.003.
[22] G. Paradies, *et al.*, 'Role of cardiolipin in mitochondrial function and dynamics in health and disease: molecular and pharmacological aspects', *Cells*, vol. 8, no. 7, p. 728, Jul. 2019, doi: 10.3390/cells8070728.
[23] M. Falabella, *et al.*, 'Cardiolipin, mitochondria, and neurological disease', *Trends Endocrinol. Metab.*, vol. 32, no. 4, pp. 224-237, Apr. 2021, doi: 10.1016/j.tem.2021.01.006.
[24] J. P. Slotte, 'Biological functions of sphingomyelins', *Prog. Lipid Res.*, vol. 52, no. 4, pp. 424-437, Oct. 2013, doi: 10.1016/j.plipres.2013.05.001.
[25] Y. Zhang, *et al.*, 'Ceramide-enriched membrane domains—structure and function', *Biochim. Biophys. Acta BBA - Biomembr.*, vol. 1788, no. 1, pp. 178-183, Jan. 2009, doi: 10.1016/j.bbamem.2008.07.030.
[26] R. D. Semba, 'Perspective: the potential role of circulating lysophosphatidylcholine in neuroprotection against Alzheimer disease', *Adv. Nutr.*, vol. 11, no. 4, pp. 760-772, Jul. 2020, doi: 10.1093/advances/nmaa024.
[27] S.-H. Law, *et al.*, 'An updated review of lysophosphatidylcholine metabolism in human diseases', *Int. J. Mol. Sci.*, vol. 20, no. 5, p. 1149, Mar. 2019, doi: 10.3390/ijms20051149.
[28] P. Liu *et al.*, 'The mechanisms of lysophosphatidylcholine in the development of diseases', *Life Sci.*, vol. 247, p. 117443, Apr. 2020, doi: 10.1016/j.lfs.2020.117443.
[29] S. Sugimoto *et al.*, 'Lysyl-phosphatidylglycerol promotes cell-to-cell interaction and biofilm formation of *Staphylococcus aureus* as a biofilm matrix component', Feb. 19, 2025. doi: 10.1101/2025.02.19.638968.
[30] A. Vásquez, *et al.*, 'Lysyl-phosphatidylglycerol: a lipid involved in the resistance of *Staphylococcus aureus* to antimicrobial peptide activity', *Antibiotics*, vol. 14, no. 4, p. 349, Mar. 2025, doi: 10.3390/antibiotics14040349.
[31] C. J. Slavetinsky, *et al.*, 'Alanyl-phosphatidylglycerol and lysyl-phosphatidylglycerol are translocated by the same MprF flippases and have similar capacities to protect against the antibiotic daptomycin in *Staphylococcus aureus*', *Antimicrob. Agents Chemother.*, vol. 56, no. 7, pp. 3492-3497, Jul. 2012, doi: 10.1128/AAC.00370-12.
[32] S. Hebecker *et al.*, 'Structures of two bacterial resistance factors mediating tRNA-dependent aminoacylation of phosphatidylglycerol with lysine or alanine', *Proc. Natl. Acad. Sci.*, vol. 112, no. 34, pp. 10691-10696, Aug. 2015, doi: 10.1073/pnas.1511167112.
[33] Md. S. Hossain, *et al.*, 'Plasmalogens, the vinyl ether-linked glycerophospholipids, enhance learning and memory by regulating brain-derived neurotrophic factor', *Front. Cell Dev. Biol.*, vol. 10, p. 828282, Feb. 2022, doi: 10.3389/fcell.2022.828282.

[34] J. Udagawa and K. Hino, 'Plasmalogen in the brain: effects on cognitive functions and behaviors attributable to its properties', *Brain Res. Bull.*, vol. 188, pp. 197-202, Oct. 2022, doi: 10.1016/j.brainresbull.2022.08.008.
[35] S. Saha, *et al.*, 'Lipid A heterogeneity and its role in the host interactions with pathogenic and commensal bacteria', *microLife*, vol. 3, p. uqac011, Nov. 2022, doi: 10.1093/femsml/uqac011.
[36] A. Steimle, *et al.*, 'Structure and function: Lipid A modifications in commensals and pathogens', *Int. J. Med. Microbiol.*, vol. 306, no. 5, pp. 290-301, Aug. 2016, doi: 10.1016/j.ijmm.2016.03.001.
[37] R. V. S. Rajala and R. E. Anderson, 'Focus on molecules: phosphatidylinositol-4,5-bisphosphate (PIP2)', *Exp. Eye Res.*, vol. 91, no. 3, pp. 324-325, Sep. 2010, doi: 10.1016/j.exer.2010.05.001.
[38] S. Kim, *et al.*, 'Bacterial ornithine lipid, a surrogate membrane lipid under phosphate-limiting conditions, plays important roles in bacterial persistence and interaction with host', *Environ. Microbiol.*, vol. 20, no. 11, pp. 3992-4008, Nov. 2018, doi: 10.1111/1462-2920.14430.
[39] Y. S. Morita, *et al.*, 'Biosynthesis of mycobacterial phosphatidylinositol mannosides', *Biochem. J.*, vol. 378, no. 2, pp. 589-597, Mar. 2004, doi: 10.1042/bj20031372.
[40] M. E. Guerin, *et al.*, 'Molecular basis of phosphatidyl-myo-inositol mannoside biosynthesis and regulation in mycobacteria', *J. Biol. Chem.*, vol. 285, no. 44, pp. 33577-33583, Oct. 2010, doi: 10.1074/jbc.R110.168328.
[41] Y. Sun *et al.*, 'Does sulfoquinovosyl diacylglycerol synthase OsSQD1 affect the composition of lipids in rice phosphate-deprived root?', *Int. J. Mol. Sci.*, vol. 24, no. 1, p. 114, Dec. 2022, doi: 10.3390/ijms24010114.
[42] Y. Nakajima *et al.*, 'Thylakoid membrane lipid sulfoquinovosyl-diacylglycerol (SQDG) is required for full functioning of photosystem II in *Thermosynechococcus elongatus*', *J. Biol. Chem.*, vol. 293, no. 38, pp. 14786-14797, Sep. 2018, doi: 10.1074/jbc.RA118.004304.
[43] Y. Nakamura, *et al.*, 'Chapter 13 Biosynthesis and function of monogalactosyldiacylglycerol (MGDG), the signature lipid of chloroplasts', in *The Chloroplast*, vol. 31, C. A. Rebeiz, *et al.*, in Advances in Photosynthesis and Respiration, vol. 31., Dordrecht: Springer Netherlands, 2010, pp. 185-202. doi: 10.1007/978-90-481-8531-3_13.
[44] T. Harder, *et al.*,'Lipid domain structure of the plasma membrane revealed by patching of membrane components', *J. Cell Biol.*, vol. 141, no. 4, pp. 929-942, May 1998, doi: 10.1083/jcb.141.4.929.
[45] S. Raffy and J. Teissié, 'Control of lipid membrane stability by cholesterol content', *Biophys. J.*, vol. 76, no. 4, pp. 2072-2080, Apr. 1999, doi: 10.1016/S0006-3495(99)77363-7.
[46] D. Eliaš, *et al.*, 'Ergosterol biosynthesis and regulation impact the antifungal resistance and virulence of *Candida* spp.', *Stresses*, vol. 4, no. 4, pp. 641-662, Oct. 2024, doi: 10.3390/stresses4040041.
[47] H. Jin, *et al.*,'Ergosterol promotes pheromone signaling and plasma membrane fusion in mating yeast', *J. Cell Biol.*, vol. 180, no. 4, pp. 813-826, Feb. 2008, doi: 10.1083/jcb.200705076.
[48] A. Mangiarotti, *et al.*, 'Hopanoids, like sterols, modulate dynamics, compaction, phase segregation and permeability of membranes', *Biochim. Biophys. Acta BBA - Biomembr.*, vol. 1861, no. 12, p. 183060, Dec. 2019, doi: 10.1016/j.bbamem.2019.183060.

[49] T. A. Leonard, *et al.*, 'The membrane surface as a platform that organizes cellular and biochemical processes', *Dev. Cell*, vol. 58, no. 15, pp. 1315-1332, Aug. 2023, doi: 10.1016/j.devcel.2023.06.001.
[50] A. M. Morelli, *et al.*, 'An update of the chemiosmotic theory as suggested by possible proton currents inside the coupling membrane', *Open Biol.*, vol. 9, no. 4, Apr. 2019, doi: 10.1098/rsob.180221.
[51] R. A. Gatenby, 'The role of cell membrane information reception, processing, and communication in the structure and function of multicellular tissue', *Int. J. Mol. Sci.*, vol. 20, no. 15, p. 3609, Jul. 2019, doi: 10.3390/ijms20153609.
[52] A. K. Jayaram *et al.*, 'Biomembranes in bioelectronic sensing', *Trends Biotechnol.*, vol. 40, no. 1, pp. 107-123, Jan. 2022, doi: 10.1016/j.tibtech.2021.06.001.
[53] W. Stillwell, 'Membrane transport', in 'An introduction to biological membranes', Elsevier, 2013, pp. 305-337. doi: 10.1016/B978-0-444-52153-8.00014-3.
[54] J. Ude, *et al.*, 'Outer membrane permeability: antimicrobials and diverse nutrients bypass porins in *Pseudomonas aeruginosa*', *Proc. Natl. Acad. Sci.*, vol. 118, no. 31, Aug. 2021, doi: 10.1073/pnas.2107644118.
[55] R. Koynova and M. Caffrey, 'Phases and phase transitions of the phosphatidylcholines', *Biochim. Biophys. Acta BBA - Rev. Biomembr.*, vol. 1376, no. 1, pp. 91-145, Jun. 1998, doi: 10.1016/S0304-4157(98)00006-9.
[56] J. R. Willdigg and J. D. Helmann, 'Mini review: bacterial membrane composition and its modulation in response to stress', *Front. Mol. Biosci.*, vol. 8, p. 634438, May 2021, doi: 10.3389/fmolb.2021.634438.
[57] R. Ernst, *et al.*, 'Homeoviscous adaptation and the regulation of membrane lipids', *J. Mol. Biol.*, vol. 428, no. 24, pp. 4776-4791, Dec. 2016, doi: 10.1016/j.jmb.2016.08.013.
[58] J. Schneider *et al.*, 'Spatio-temporal remodeling of functional membrane microdomains organizes the signaling networks of a bacterium', *PLOS Genet.*, vol. 11, no. 4, p. e1005140, Apr. 2015, doi: 10.1371/journal.pgen.1005140.
[59] D. Lopez, 'Molecular composition of functional microdomains in bacterial membranes', *Chem. Phys. Lipids*, vol. 192, pp. 3-11, Nov. 2015, doi: 10.1016/j.chemphyslip.2015.08.015.
[60] D. Lopez and G. Koch, 'Exploring functional membrane microdomains in bacteria: an overview', *Curr. Opin. Microbiol.*, vol. 36, pp. 76-84, Apr. 2017, doi: 10.1016/j.mib.2017.02.001.
[61] R. M. Epand, *et al.*, 'Molecular mechanisms of membrane targeting antibiotics', *Biochim. Biophys. Acta BBA - Biomembr.*, vol. 1858, no. 5, pp. 980-987, May 2016, doi: 10.1016/j.bbamem.2015.10.018.
[62] A. H. Nguyen, *et al.*, 'Bacterial cell membranes and their role in daptomycin resistance: A review', *Front. Mol. Biosci.*, vol. 9, p. 1035574, Nov. 2022, doi: 10.3389/fmolb.2022.1035574.
[63] D. Poger and A. E. Mark, 'A ring to rule them all: the effect of cyclopropane fatty acids on the fluidity of lipid bilayers', *J. Phys. Chem. B*, vol. 119, no. 17, pp. 5487-5495, Apr. 2015, doi: 10.1021/acs.jpcb.5b00958.
[64] N. V. Berezhnoy, *et al.*, 'Transient complexity of *E. coli* lipidome is explained by fatty acyl synthesis and cyclopropanation', *Metabolites*, vol. 12, no. 9, p. 784, Aug. 2022, doi: 10.3390/metabo12090784.
[65] D. Saxena, *et al.*, 'Tackling the outer membrane: facilitating compound entry into Gram-negative bacterial pathogens', *Npj Antimicrob. Resist.*, vol. 1, no. 1, p. 17, Dec. 2023, doi: 10.1038/s44259-023-00016-1.
[66] R. M. Epand and R. F. Epand, 'Bacterial membrane lipids in the action of antimicrobial agents', *J. Pept. Sci.*, vol. 17, no. 5, pp. 298-305, May 2011, doi: 10.1002/psc.1319.

[67] P. W. Simcock *et al.*, 'Membrane binding of antimicrobial peptides is modulated by lipid charge modification', *J. Chem. Theory Comput.*, vol. 17, no. 2, pp. 1218-1228, Feb. 2021, doi: 10.1021/acs.jctc.0c01025.
[68] V. Rogga and I. Kosalec, 'Untying the anchor for the lipopolysaccharide: lipid A structural modification systems offer diagnostic and therapeutic options to tackle polymyxin resistance', *Arch. Ind. Hyg. Toxicol.*, vol. 74, no. 3, pp. 145-166, Sep. 2023, doi: 10.2478/aiht-2023-74-3717.
[69] J. M. Munita and C. A. Arias, 'Mechanisms of antibiotic resistance', *Microbiol. Spectr.*, vol. 4, no. 2, p. 4.2.15, Mar. 2016, doi: 10.1128/microbiolspec.VMBF-0016-2015.
[70] J. M. Blair, *et al.*, 'Multidrug efflux pumps in Gram-negative bacteria and their role in antibiotic resistance', *Future Microbiol.*, vol. 9, no. 10, pp. 1165-1177, Oct. 2014, doi: 10.2217/fmb.14.66.
[71] P. Puyol McKenna, *et al.*, 'Microbial biosurfactants: antimicrobial activity and potential biomedical and therapeutic exploits', *Pharmaceuticals*, vol. 17, no. 1, p. 138, Jan. 2024, doi: 10.3390/ph17010138.
[72] M. Choudhary, *et al.*,'Natural biosurfactant as antimicrobial agent: strategy to action against fungal and bacterial activities', *Cell Biochem. Biophys.*, vol. 80, no. 1, pp. 245-259, Mar. 2022, doi: 10.1007/s12013-021-01045-1.
[73] K. G. O. Bezerra, *et al.*, 'Plant-derived biosurfactants: extraction, characteristics and properties for application in cosmetics', *Biocatal. Agric. Biotechnol.*, vol. 34, p. 102036, Jul. 2021, doi: 10.1016/j.bcab.2021.102036.
[74] S. De, *et al.*,'A review on natural surfactants', *RSC Adv.*, vol. 5, no. 81, pp. 65757-65767, 2015, doi: 10.1039/C5RA11101C.
[75] K. Sambanthamoorthy, *et al.*,'Antimicrobial and antibiofilm potential of biosurfactants isolated from lactobacilli against multi-drug-resistant pathogens', *BMC Microbiol.*, vol. 14, no. 1, p. 197, Dec. 2014, doi: 10.1186/1471-2180-14-197.
[76] M. Stavri, *et al.*, 'Bacterial efflux pump inhibitors from natural sources', *J. Antimicrob. Chemother.*, vol. 59, no. 6, pp. 1247-1260, Jun. 2007, doi: 10.1093/jac/dkl460.
[77] N. J. Santos Araújo *et al.*, 'Evaluation of the antibacterial activity of hecogenin acetate and its inhibitory potential of NorA and MepA efflux pumps from *Staphylococcus aureus*', *Microb. Pathog.*, vol. 174, p. 105925, Jan. 2023, doi: 10.1016/j.micpath.2022.105925.
[78] M. A. Díaz De Rienzo, *et al.*, '*Pseudomonas aeruginosa* biofilm disruption using microbial surfactants', *J. Appl. Microbiol.*, vol. 120, no. 4, pp. 868-876, Apr. 2016, doi: 10.1111/jam.13049.
[79] Y. Al-Wahaibi, *et al.*,'Biosurfactant production by *Bacillus subtilis* B30 and its application in enhancing oil recovery', *Colloids Surf. B Biointerfaces*, vol. 114, pp. 324-333, Feb. 2014, doi: 10.1016/j.colsurfb.2013.09.022.
[80] S. Mujumdar, *et al.*, 'Production, characterization, and applications of bioemulsifiers (BE) and biosurfactants (BS) produced by *Acinetobacter* spp.: A review', *J. Basic Microbiol.*, vol. 59, no. 3, pp. 277-287, Mar. 2019, doi: 10.1002/jobm.201800364.
[81] T. De O Caretta, *et al.*,'Antimicrobial activity of sophorolipids produced by *Starmerella bombicola* against phytopathogens from cherry tomato', *J. Sci. Food Agric.*, vol. 102, no. 3, pp. 1245-1254, Feb. 2022, doi: 10.1002/jsfa.11462.
[82] A. Khanna, *et al.*,'Biosurfactant from *Candida*: sources, classification, and emerging applications', *Arch. Microbiol.*, vol. 205, no. 4, p. 149, Apr. 2023, doi: 10.1007/s00203-023-03495-y.
[83] M. A. Al-hazmi, *et al.*, 'Statistical optimization of biosurfactant production from *Aspergillus niger* SA1 fermentation process and mathematical modeling', *J. Microbiol. Biotechnol.*, vol. 33, no. 9, pp. 1238-1249, Sep. 2023, doi: 10.4014/jmb.2303.03005.

[84] S. Gupta, *et al.*, 'Biodegradation of naphthalene using biosurfactant producing fusarium proliferatum WC416 isolated from refinery effluent', *Appl. Biochem. Biotechnol.*, vol. 196, no. 5, pp. 2549-2565, May 2024, doi: 10.1007/s12010-023-04364-6.
[85] M. Rojewska, *et al.*,'Combined effect of nitrofurantoin and plant surfactant on bacteria phospholipid membrane', *Molecules*, vol. 25, no. 11, p. 2527, May 2020, doi: 10.3390/molecules25112527.
[86] W. Smułek, *et al.*,'*Quillaja* and *Sapindus* saponins influence on effect on solubilization of Polymyxin B peptide antibiotic in aqueous solutions', *J. Mol. Liq.*, vol. 395, p. 123944, Feb. 2024, doi: 10.1016/j.molliq.2023.123944.
[87] S. Sakamoto, *et al.*,'Investigation of interfacial behavior of glycyrrhizin with a lipid raft model via a Langmuir monolayer study', *Biochim. Biophys. Acta BBA - Biomembr.*, vol. 1828, no. 4, pp. 1271-1283, Apr. 2013, doi: 10.1016/j.bbamem.2013.01.006.
[88] F. J. Aranda, *et al.*, 'Recent advances on the interaction of glycolipid and lipopeptide biosurfactants with model and biological membranes', *Curr. Opin. Colloid Interface Sci.*, vol. 68, p. 101748, Dec. 2023, doi: 10.1016/j.cocis.2023.101748.
[89] D. E. Otzen, 'Biosurfactants and surfactants interacting with membranes and proteins: Same but different?', *Biochim. Biophys. Acta BBA - Biomembr.*, vol. 1859, no. 4, pp. 639-649, Apr. 2017, doi: 10.1016/j.bbamem.2016.09.024.
[90] I. Góral and K. Wojciechowski, 'Surface activity and foaming properties of saponin-rich plants extracts', *Adv. Colloid Interface Sci.*, vol. 279, p. 102145, May 2020, doi: 10.1016/j.cis.2020.102145.
[91] S. Rai, *et al.*, 'Plant-derived saponins: a review of their surfactant properties and applications', *Sci*, vol. 3, no. 4, p. 44, Nov. 2021, doi: 10.3390/sci3040044.
[92] R. M. Maier and G. Soberón-Chávez, '*Pseudomonas aeruginosa* rhamnolipids: biosynthesis and potential applications', *Appl. Microbiol. Biotechnol.*, vol. 54, no. 5, pp. 625-633, Nov. 2000, doi: 10.1007/s002530000443.
[93] J. Chen, *et al.*, 'Potential applications of biosurfactant rhamnolipids in agriculture and biomedicine', *Appl. Microbiol. Biotechnol.*, vol. 101, no. 23-24, pp. 8309-8319, Dec. 2017, doi: 10.1007/s00253-017-8554-4.
[94] I. C. C. D. Fontoura *et al.*, 'Antibacterial activity of sophorolipids from *Candida bombicola* against human pathogens', *Braz. Arch. Biol. Technol.*, vol. 63, p. e20180568, 2020, doi: 10.1590/1678-4324-2020180568.
[95] K. Joshi-Navare and A. Prabhune, 'A biosurfactant-sophorolipid acts in synergy with antibiotics to enhance their efficiency', *BioMed Res. Int.*, vol. 2013, pp. 1-8, 2013, doi: 10.1155/2013/512495.
[96] X. Liu *et al.*, 'Antibacterial efficacy and mechanism of mannosylerythritol Lipids-A on *Listeria monocytogenes*', *Molecules*, vol. 25, no. 20, p. 4857, Oct. 2020, doi: 10.3390/molecules25204857.
[97] F. Rivardo, 'Synergistic effect of lipopeptide biosurfactant with antibiotics against *Escherichia coli* CFT073 biofilm', *Int. J. Antimicrob. Agents*, 2011.
[98] K. Englerová *et al.*, '*Bacillus amyloliquefaciens*–derived lipopeptide biosurfactants inhibit biofilm formation and expression of biofilm-related genes of *Staphylococcus aureus*', *Antibiotics*, vol. 10, no. 10, p. 1252, Oct. 2021, doi: 10.3390/antibiotics10101252.
[99] W. Smułek and E. Kaczorek, 'Factors influencing the bioavailability of organic molecules to bacterial cells–a mini-review', *Molecules*, vol. 27, no. 19, p. 6579, Oct. 2022, doi: 10.3390/molecules27196579.
[100] P. Savarino, *et al.*, 'Mass spectrometry analysis of saponins', *Mass Spectrom. Rev.*, vol. 42, no. 3, pp. 954-983, May 2023, doi: 10.1002/mas.21728.
[101] P. D. Cárdenas, *et al.*,'Evolution of structural diversity of triterpenoids', *Front. Plant Sci.*, vol. 10, p. 1523, Dec. 2019, doi: 10.3389/fpls.2019.01523.

[102] I. I. Tatli Cankaya and E. I. Somuncuoglu, 'Potential and prophylactic use of plants containing saponin-type compounds as antibiofilm agents against respiratory tract infections', *Evid. Based Complement. Alternat. Med.*, vol. 2021, pp. 1-14, Jul. 2021, doi: 10.1155/2021/6814215.
[103] W. Smułek *et al.*, '*Saponaria officinalis* L. extract: surface active properties and impact on environmental bacterial strains', *Colloids Surf. B Biointerfaces*, vol. 150, pp. 209-215, Feb. 2017, doi: 10.1016/j.colsurfb.2016.11.035.
[104] C. Schmid, *et al.*, 'Saponins from european licorice roots (*Glycyrrhiza glabra*)', *J. Nat. Prod.*, vol. 81, no. 8, pp. 1734-1744, Aug. 2018, doi: 10.1021/acs.jnatprod.8b00022.
[105] J. D. Fleck *et al.*, 'Saponins from *Quillaja saponaria* and *Quillaja brasiliensis*: particular chemical characteristics and biological activities', *Molecules*, vol. 24, no. 1, p. 171, Jan. 2019, doi: 10.3390/molecules24010171.
[106] N. Frenkel, *et al.*,'Mechanistic investigation of interactions between steroidal saponin digitonin and cell membrane models', *J. Phys. Chem. B*, vol. 118, no. 50, pp. 14632-14639, Dec. 2014, doi: 10.1021/jp5074939.
[107] B. Korchowiec, *et al.*, 'The role of cholesterol in membrane activity of digitonin: Experimental and theoretical model studies', *J. Mol. Liq.*, vol. 323, p. 114598, Feb. 2021, doi: 10.1016/j.molliq.2020.114598.
[108] A. Shakeel, *et al.*, 'Saponins, the unexplored secondary metabolites in plant defense: opportunities in integrated pest management', *Plants*, vol. 14, no. 6, p. 861, Mar. 2025, doi: 10.3390/plants14060861.
[109] B. Paarvanova, *et al.*, 'Hemolysis by saponin is accelerated at hypertonic conditions', *Molecules*, vol. 28, no. 20, p. 7096, Oct. 2023, doi: 10.3390/molecules28207096.
[110] X. Zheng and G. Gallot, 'Dynamics of cell membrane permeabilization by saponins using terahertz attenuated total reflection', *Biophys. J.*, vol. 119, no. 4, pp. 749-755, Aug. 2020, doi: 10.1016/j.bpj.2020.05.040.
[111] S. L. Verstraeten *et al.*, 'The activity of the saponin ginsenoside Rh2 is enhanced by the interaction with membrane sphingomyelin but depressed by cholesterol', *Sci. Rep.*, vol. 9, no. 1, p. 7285, May 2019, doi: 10.1038/s41598-019-43674-w.
[112] C. Dawid *et al.*, 'Comparative assessment of purified saponins as permeabilization agents during respirometry', *Biochim. Biophys. Acta BBA - Bioenerg.*, vol. 1861, no. 10, p. 148251, Oct. 2020, doi: 10.1016/j.bbabio.2020.148251.
[113] J. H. Lorent, *et al.*, 'The amphiphilic nature of saponins and their effects on artificial and biological membranes and potential consequences for red blood and cancer cells', *Org Biomol Chem*, vol. 12, no. 44, pp. 8803-8822, 2014, doi: 10.1039/C4OB01652A.
[114] B. Korchowiec, *et al.*, 'Impact of two different saponins on the organization of model lipid membranes', *Biochim. Biophys. Acta BBA - Biomembr.*, vol. 1848, no. 10, pp. 1963-1973, Oct. 2015, doi: 10.1016/j.bbamem.2015.06.007.
[115] K. J. Stine, *et al.*, 'Interaction of the glycoalkaloid tomatine with DMPC and sterol monolayers studied by surface pressure measurements and Brewster angle microscopy', *J. Phys. Chem. B*, vol. 110, no. 44, pp. 22220-22229, Nov. 2006, doi: 10.1021/jp056139j.
[116] B. W. Walker, *et al.*, 'Comparison of the interaction of tomatine with mixed monolayers containing phospholipid, egg sphingomyelin, and sterols', *Biochim. Biophys. Acta BBA - Biomembr.*, vol. 1778, no. 10, pp. 2244-2257, Oct. 2008, doi: 10.1016/j.bbamem.2008.06.004.
[117] C. N. Armah *et al.*, 'The membrane-permeabilizing effect of avenacin a-1 involves the reorganization of bilayer cholesterol', *Biophys. J.*, vol. 76, no. 1, pp. 281-290, Jan. 1999, doi: 10.1016/S0006-3495(99)77196-1.

[118] S. Sakamoto, *et al.*, 'Investigation of interfacial behavior of glycyrrhizin with a lipid raft model via a Langmuir monolayer study', *Biochim. Biophys. Acta BBA - Biomembr.*, vol. 1828, no. 4, pp. 1271-1283, Apr. 2013, doi: 10.1016/j.bbamem.2013.01.006.
[119] J. Lorent, *et al.*,'Induction of highly curved structures in relation to membrane permeabilization and budding by the triterpenoid saponins, α- and δ-hederin', *J. Biol. Chem.*, vol. 288, no. 20, pp. 14000-14017, May 2013, doi: 10.1074/jbc.M112.407635.
[120] M. Nishikawa, *et al.*, 'Interaction of digitonin and its analogs with membrane cholesterol', *J. Biochem. (Tokyo)*, vol. 96, no. 4, pp. 1231-1239, Oct. 1984, doi: 10.1093/oxfordjournals.jbchem.a134941.
[121] T. Akiyama, *et al.*, 'Saponin-cholesterol interaction in the multibilayers of egg yolk lecithin as studied by deuterium nuclear magnetic resonance: digitonin and its analoguest' *Biochemistry*, 1980 Apr 29;19(9):1904-11. doi: 10.1021/bi00550a027
[122] E. A. J. Keukens *et al.*, 'Molecular basis of glycoalkaloid induced membrane disruption', *Biochim. Biophys. Acta BBA - Biomembr.*, vol. 1240, no. 2, pp. 216-228, Dec. 1995, doi: 10.1016/0005-2736(95)00186-7.
[123] K. Fukuda, *et al.*,'Specific interaction of arabinose residue in ginsenoside with egg phosphatidylcholine vesicles', *Biochim. Biophys. Acta BBA - Biomembr.*, vol. 900, no. 2, pp. 267-274, Jun. 1987, doi: 10.1016/0005-2736(87)90341-5.
[124] D. P. Cerneus, *et al.*, 'Detergent insolubility of alkaline phosphatase during biosynthetic transport and endocytosis. Role of cholesterol.', *J. Biol. Chem.*, vol. 268, no. 5, pp. 3150-3155, Feb. 1993, doi: 10.1016/S0021-9258(18)53671-1.
[125] M. Naruse *et al.*, 'Acrosome reaction-related steroidal saponin, Co-ARIS, from the starfish induces structural changes in microdomains', *Dev. Biol.*, vol. 347, no. 1, pp. 147-153, Nov. 2010, doi: 10.1016/j.ydbio.2010.08.019.
[126] J. Lorent, *et al.*, 'Domain formation and permeabilization induced by the saponin α-hederin and its aglycone hederagenin in a cholesterol-containing bilayer', *Langmuir*, vol. 30, no. 16, pp. 4556-4569, Apr. 2014, doi: 10.1021/la4049902.
[127] M. Hu, *et al.*,'Cholesterol-independent membrane disruption caused by triterpenoid saponins', *Biochim. Biophys. Acta BBA - Lipids Lipid Metab.*, vol. 1299, no. 2, pp. 252-258, Jan. 1996, doi: 10.1016/0005-2760(95)00214-6.
[128] X. X. Li, *et al.*, 'Proapoptotic triterpene electrophiles (avicins) form channels in membranes: cholesterol dependence', *Biophys. J.*, vol. 88, no. 4, pp. 2577-2584, Apr. 2005, doi: 10.1529/biophysj.104.049403.
[129] P. M. Elias, *et al.*,'Membrane sterol heterogeneity. Freeze-fracture detection with saponins and filipin.', *J. Histochem. Cytochem.*, vol. 27, no. 9, pp. 1247-1260, Sep. 1979, doi: 10.1177/27.9.479568.
[130] L. Šturm and N. Poklar Ulrih, 'Basic methods for preparation of liposomes and studying their interactions with different compounds, with the emphasis on polyphenols', *Int. J. Mol. Sci.*, vol. 22, no. 12, p. 6547, Jun. 2021, doi: 10.3390/ijms22126547.
[131] M. S. Gatto, *et al.*, 'Targeted liposomal drug delivery: overview of the current applications and challenges', *Life*, vol. 14, no. 6, p. 672, May 2024, doi: 10.3390/life14060672.
[132] J. Li and V. Monje-Galvan, 'Effect of glycone diversity on the interaction of triterpenoid saponins and lipid bilayers', *ACS Appl. Bio Mater.*, vol. 7, no. 2, pp. 553-563, Feb. 2024, doi: 10.1021/acsabm.2c00928.

Figures licensing

Fig 1, 4, 5, 7.: were prepared using BioRender app under Academic Lab License, as of 29 July 2025 19:48 https://www.biorender.com/academic-license

Fig 3.: Photograph of a soapberry inflorescence under CC BY-SA 3.0 license, https://commons.wikimedia.org/w/index.php?curid=84449; Photo of a soapberry inflorescence by Dick Culbert from Gibsons, B.C., Canada - Quillaja saponaria, CC BY 2.0, https://commons.wikimedia.org/w/index.php?curid=34451728 ; Photo of Liquorice root by Tamorlan - Own work, CC BY 3.0, https://commons.wikimedia.org/w/index.php?curid=9394622

Other scientific achievements

Total IF: 85.715 Total MNiSW points: 1650, Citation count: 280 (ResearchGate), 308(Google Scholar), 263 (Scopus), 239 (Web of Science), as of the date of 25.09.2025

Other publications not included in the dissertation

1. Marcin Cybulski, Olga Michalak, **Adam Grzywaczyk**, Piotr Krzeczyński, Michał Zieliński, Wojciech Smułek, *Exploration of sapogenins as promising lead compounds in the development of novel antimicrobial agents*, Chemistry & Biodiversity 2025, vol. 22, in press, e01569-1-e01569-12.

2. Agnieszka Rybarczyk, Malwina Nowak, Patrycja Frąckowiak, **Adam Grzywaczyk**, Wojciech Smułek, Jakub Zdarta, *Increasing the potential of enzymatic environmental reactions by applying Tesla valve*, Translational Chemistry – An Interface Journal, 2025, 1 (1), 1-9.

3. Marta Wojcieszak, Khrystyna Illienko, Jacek Różański, **Adam Grzywaczyk**, Ewa Kaczorek, Katarzyna Materna, *Evaluation of nonionic surfactant-based emulgels as a prospective approach for skincare products*, Journal of Molecular Liquids, 2025, vol. 431, 127702-1–127702-12.

4. Żaneta Polańska, Zuzanna Pietralik-Molińska, **Adam Grzywaczyk**, Wojciech Smułek, Ewa Banachowicz, Ewa Kaczorek, Maciej Kozak, *BPS2025 - Saponin-induced lipid membrane disruption: A potential strategy to combat antibiotic resistance*, Biophysical Journal - 2025, vol. 124, iss. 3, suppl. 1.

5. Anna Syguda, Marta Wojcieszak, Sylwia Zięba, Adam Mizera, Andrzej Łapiński, Jacek Różański, Alicja Putowska, Agnieszka Marcinkowska, **Adam Grzywaczyk**, Ewa Kaczorek, Katarzyna Materna, *Surface-active amidequats with an alkoxymethyl substituent: synthesis, analysis, and preliminary evaluation as potential emulsifiers and substitutes for conventional surfactants*, Langmuir, 2025, vol. 41, iss. 16, 10085–10098.

6. Agnieszka Rybarczyk, Wojciech Smułek, **Adam Grzywaczyk**, Ewa Kaczorek, Teofil Jesionowski, Long D. Nghiem, Jakub Zdarta, *3D printed polylactide scaffolding for laccase immobilization to improve enzyme stability and estrogen removal from wastewater*, Bioresource Technology, 2023, vol. 381, 129144-1–129144-9.

7. **Adam Grzywaczyk**, Wojciech Smułek, Ewa Kaczorek, Anna Zdziennicka, Bronisław Jańczuk, Thermodynamic *consideration of the solid saponin extract drop–air System*, Molecules, 2023, vol. 28, iss. 13, 4943-1–4943-16.

8. **Adam Grzywaczyk**, Wojciech Smułek, Grzegorz Smułek, Mariusz Ślachciński, Ewa Kaczorek, *Application of natural surfactants for improving the leaching of zinc and copper from different soils*, Environmental Technology & Innovation, 2021, vol. 24, 101926-1–101926-10.

9. Katarzyna Jankowska, **Adam Grzywaczyk**, Adam Piasecki, Ewa Kijeńska-Gawrońska, Luong N. Nguyen, Jakub Zdarta, Long D. Nghiem, Manuel Pinelo, Teofil Jesionowski, *Electrospun biosystems made of nylon 6 and laccase and its application in dyes removal*, Environmental Technology & Innovation, 2021, vol. 21, 101332-1–101332-14.

10. Katarzyna Jankowska, Jakub Zdarta, **Adam Grzywaczyk**, Oliwia Degórska, Ewa Kijeńska-Gawrońska, Manuel Pinelo, Teofil Jesionowski, *Horseradish peroxidase immobilised onto electrospun fibres and its application in decolourisation of dyes from model sea water,* Process Biochemistry, 2021, vol. 102, 10–21.

11. **Adam Grzywaczyk**, Agata Zdarta, Katarzyna Jankowska, Andrzej Biadasz, Jakub Zdarta, Teofil Jesionowski, Ewa Kaczorek, Wojciech Smułek, *New Biocomposite Electrospun Fiber/Alginate Hydrogel for Probiotic Bacteria Immobilization,* Materials, 2021, vol. 14, no. 14, 386-1–386-11.

12. Katarzyna Jankowska, Jakub Zdarta, **Adam Grzywaczyk**, Ewa Kijeńska-Gawrońska, Andrzej Biadasz, Teofil Jesionowski, *Electrospun poly(methyl methacrylate)/polyaniline fibres as a support for laccase immobilisation and use in dye decolourisation,* Environmental Research, 2020, vol. 184, 109332-1–109332-10.

13. Wojciech Smułek, Agata Zdarta, **Adam Grzywaczyk**, Urszula Guzik, Katarzyna Siwińska-Ciesielczyk, Filip Ciesielczyk, Beata Strzemiecka, Teofil Jesionowski, Adam Voelkel, Ewa Kaczorek, *Evaluation of the physico-chemical properties of hydrocarbons-exposed bacterial biomass,* Colloids and Surfaces B: Biointerfaces, 2020, vol. 196, 111310-1–111310-10.

Chapters in scientific monographs

1. *Zrównoważone zagospodarowanie odpadowej biomasy jako surowiec do syntezy polihydroksyalkanianów,* Michał Kapczyński, **Adam Grzywaczyk**, Natalia Burlaga, Ewa Kaczorek, II Ogólnopolska Konferencja Naukowa PUTChemikon: materiały konferencyjne red. Piotr Paweł Michałowski, Poznań, Polska: Wydawnictwo Politechniki Poznańskiej, 2024 - 153-155.

2. *Fungal enzymes in organic pollutants bioremediation***, Adam Grzywaczyk**, Wojciech Smułek, Jakub Zdarta, Ewa Kaczorek, Industrial Applications of Microbial Enzymes red. Pankaj Bhatt - Boca Raton, United States: Taylor & Francis Group, 2022 - 101-132.

3. *Saponiny w systemach kontrolowanego dostarczania leku*, **Adam Grzywaczyk**, Antonina Bulińska, Wojciech Smułek, Ewa Kaczorek, BioOrg 2022 - IV Ogólnopolskie Sympozjum Chemii Bioorganicznej, Organicznej i Biomateriałów: materiały konferencyjne - Poznań, Polska: Politechnika Poznańska. Wydział Technologii Chemicznej, 2022 - 87-89.

4. *Materiał elektroprzędzony PMMA/PANI jako nowatorski nośnik w immobilizacji enzymów*, **Adam Grzywaczyk**, Katarzyna Jankowska, Karolina Kaźmierczak, Ewa Kijeńska-Gawrońska, Jakub Zdarta, Teofil Jesionowski, BioOrg 2019 - III Ogólnopolskie Sympozjum Chemii Bioorganicznej, Organicznej i Biomateriałów 07.12.2019: materiały konferencyjne red. Wojciech Smułek (WTCH): Politechnika Poznańska. Wydział Technologii Chemicznej, 2019 - 363-365.

Patent applications

1. PAT 2514 *Układ nanocząstek lipidowych oraz sposób jego wytwarzania* **Adam Grzywaczyk**, Wojciech Smułek, Ewa Kaczorek

2. PAT 2513 *Układ do dostarczania mikroorganizmów probiotycznych stabilizowany za pomocą nanocząstek lipidowych* Natalia Burlaga, **Adam Grzywaczyk**, Amanda Pacholak, Ewa Kaczorek

Projects management & leadership

Impact of cytostatic drugs present in the environment on Gram-negative bacteria: mechanisms of adaptation and implications for microbial resistance
2025-01 – 2028-01
Registration number: 2024/53/N/NZ9/02287
Source of funding: National Science Centre, Preludium 23
Role in the project: Principal Investigator, Project manager

Innovative Biocomposite Product Using Industrial Hemp Fibers for High-Value Sustainable Applications
2025-03 – 2025-05
Registration number: 12450235
Source of funding: INDUSAC program funded from the European Union's Horizon Europe Program under grant agreement No 101070297
Role in the project: Team Leader

***Purifae* - a modular bioreactor for microalgae culture made of biopolymer using incremental techniques**
2024-05 – 2025-05
Registration number: KN/SP/601543/2024
Source of funding: Ministry of Science and Higher Education, Studenckie koła naukowe tworzą innowacje programm
Role in the project: Project leader, investigator

Effect of pharmacologically active substances on the development of resistance mechanisms of environmental microorganisms
2024-04 – 2024-11
Registration number: 0912/SBAD/2404
Source of funding: Poznan University of Technology
Role in the project: Project manager, investigator

Other projects

A comprehensive approach to 3D printing - from application to environmental impact
2025-04 – 2025-11
Registration number: 0912/SBAD/2513
Source of funding: Poznan University of Technology
Role in the project: Investigator

Is there a synergistic effect of plant surfactants and antibiotics against bacterial cells?
2022-01 – 2025-11
Registration number: 2020/37/B/NZ9/03196, Opus 20
Source of funding: National Science Centre
Role in the project: Investigator

Microbial removal of environmental pollutants by single strain and microbial consortia
2023-04 – 2023-11
Registration number: 0912/SBAD/2311
Source of funding: Poznan University of Technology
Role in the project: Investigator

Impact of natural and anthropogenic bioactive compounds on human and environmental microbiota
2022-04 – 2022-11
Registration number: 0912/SBAD/2211
Source of funding: Poznan University of Technology
Role in the project: Investigator

Biotechnological methods in the assessment of the properties of pharmaceuticals and new biomedical materials
2021-04 – 2021-11
Registration number: 0912/SBAD/2115
Source of funding: Poznan University of Technology
Role in the project: Investigator

Prizes and awards

Eu TalentON Alumni Award

1st Place – EU Sparks for Climate Hackathon (European Commission) (2024)

1st Place – EuTalentON Mission "A Soil Deal for Europe" (2024)

1st Place – Pitch Final Contest, Deep4Agri Deep Tech Innovators Program (2024)

1st Place – BASF Drive Innovation Competition (2024)

Santander Grant for Outstanding Doctoral Students (2023)

Scholarship Recipient, Poznan University of Technology (2022/23)

Elevation of Doctoral Scholarship for Outstanding Performance (2022/23)

Awardee, INPUTDoc STER Mobility Grant (2022/23)

Conference presentations in person

1. *Surfaktanty pochodzenia naturalnego jako odpowiedź na rosnącą antybiotykooporność mikroorganizmów,* **Adam Grzywaczyk**, Żaneta Polańska, Monika Rojewska, Wojciech Smułek, Maciej Kozak, Krystyna Prochaska, Ewa Kaczorek, XI Kongres Technologii Chemicznej. Materiały konferencyjne red. Robert Frankowski - Poznań, Polska: Politechnika Poznańska. Wydział Technologii Chemicznej, 2024 - s. 37 **Oral presentation**

2. *Phospholipid biomembrane treated with saponins – how to increase the effectiveness of antibiotics?,* **Adam Grzywaczyk**, Wojciech Smułek, Andreas Zimmer, Daniel McNaughton, Philip A. Gale, Ewa Kaczorek, EBSA-2023 congress book - Stockholm, Sweden: Swedish Society for Biochemistry, Biophysics and Molecular Biology (SFBBM), 2023 - s. 3 **Poster**

3. *Assessment of saponin content and properties in the extract obtained from Trigonella foenum L.,* **Adam Grzywaczyk**, Wojciech Smułek, Ewa Kaczorek, EYEC Monograph: 10th European Young Engineers Conference - Warsaw, Poland: Warsaw University of Technology, 2022 - s. 75 **Oral presentation**

4. *Purified extract of Saponaria officinalis as a factor affecting the cell membranes of yeast cells,* **Adam Grzywaczyk**, Wojciech Smułek, Ewa Kaczorek, 23rd International Syposium on Surfactants in Solution 2022, September 11-16, 2022, Lublin, Poland: book of abstracts - Lublin, Polska, 2022 - s. 45 **Oral presentation**

5. *Saponin as a tool to increase an efectiveness of antibiotics,* **Adam Grzywaczyk**, Wojciech Smułek, Anna Olejnik, Ewa Kaczorek, FEMS Conference on Microbiology, 30 June-2 July 2022, Serbia: electronic abstract book, 2022 - s. 480 **Poster**

6. *Saponiny w systemach kontrolowanego dostarczania leku,* **Adam Grzywaczyk**, Antonina Bulińska, Wojciech Smułek, Ewa Kaczorek, BioOrg 2022 - IV Ogólnopolskie Sympozjum Chemii Bioorganicznej, Organicznej i Biomateriałów: materiały konferencyjne - Poznań, Polska: Politechnika Poznańska. Wydział Technologii Chemicznej, 2022 - s. 87-89 **Poster**

7. *The use of phospholipid monolayer as a model biomembrane*, **Adam Grzywaczyk**, Science: Polish Perspectives, 7-8 May 2021, Zurich (online): book of abstracts, 2021 - s. 37 **Poster**

8. *Wykorzystanie nowatorskich technik membranowych w izolacji saponin - związków bioaktywnych o znaczeniu farmaceutycznym,* **Adam Grzywaczyk**, Wojciech Smułek, Jakub Zdarta, Ewa Kaczorek, XIV Kopernikańskie Seminarium Doktoranckie red. Anna Kmieciak, Sylwia Grabska-Zielińska, Henryk Szramowski - Toruń, Polska: Uniwersytet Mikołaja Kopernika w Toruniu, 2021 - s. 27 **Oral presentation**

9. *Wykorzystanie surfaktantów pochodzenia naturalnego w farmakologii,* **Adam Grzywaczyk**, Wojciech Smułek, Ewa Kaczorek, II Pomorskie Studenckie Sympozjum Chemiczne 20-21 marca 2021: książka abstraktów red. Mateusz Adam Baluk, 2021 - s. 95 **Poster**

10. *Rearrangement of bacterial biomembrane exposed to antibiotics,* **Adam Grzywaczyk**, Olga Ciura, Wojciech Smułek, E-Zjazd Zimowy Sekcji Studenckiej Polskiego Towarzystwa

Chemicznego - książka abstraktów red. Daria Jaworska: Polskie Towarzystwo Chemiczne, 2020 - s. 40 **Oral presentation**

11. *Materiał elektroprzędzony PMMA/PANI jako nowatorski nośnik w immobilizacji enzymów,* **Adam Grzywaczyk**, Katarzyna Jankowska, Karolina Kaźmierczak, Ewa Kijeńska-Gawrońska, Jakub Zdarta, Teofil Jesionowski, BioOrg 2019 - III Ogólnopolskie Sympozjum Chemii Bioorganicznej, Organicznej i Biomateriałów 07.12.2019: materiały konferencyjne red. Wojciech Smułek: Politechnika Poznańska. Wydział Technologii Chemicznej, 2019 - s. 363-365 **Poster**

Other conferences

1. *Purifae – a sustainable, additive-manufactured bioreactor for enhanced microalgae biomass production,* Olimpia Wojciechowska, Zuzanna Styrna, **Adam Grzywaczyk**, Wojciech Smułek, FAO Global Agrifood Biotechnologies Conference "Biotechnologies for a Sustainable Future: Driving Agrifood Systems Transformation", June 16-18, 2025, Rome, Italy. Book of abstracts to be published **Poster**

2. Purifae – modular bioreactor for microalgae cultivation fabricated with additive manufacturing techniques, Zuzanna Styrna, Olimpia Wojciechowska, **Adam Grzywaczyk**, Wojciech Smułek, 1st International Congress on Algae Biotechnology April 9-11, 2025, Lisbon, Portugal. **Poster**

3. *Microbial enzymatic adaptations for biotransformations of selected API,* Aleksandra Rybak, **Adam Grzywaczyk**, Amanda Pacholak, Agata Zdarta, Ewa Kaczorek 6th Symposium on Biotransformations for Pharmaceutical and Cosmetic Industry, June 17-21, 2024, Kraków, Poland. Book of abstracts - Kraków, Polska: Instytut Katalizy i Fizykochemii Powierzchni PAN im. Jerzego Habera w Krakowie, 2024 - s. 104-105 **Poster**

4. *Surfaktanty pochodzenia naturalnego a aktywność metaboliczna antybiotyków,* Amanda Pacholak, **Adam Grzywaczyk**, Natalia Burlaga, Aleksandra Makiej, Agata Zdarta, Wojciech Smułek, Ewa Kaczorek, XI Kongres Technologii Chemicznej. Materiały konferencyjne red. Robert Frankowski - Poznań, Polska: Politechnika Poznańska. Wydział Technologii Chemicznej, 2024 - s. 138 **Oral presentation**

5. *Sustainable management of waste biomass through biotransformation into polyhydroxyalkanoates,* Michał Kapczyński, Natalia Burlaga, **Adam Grzywaczyk**, Oliwia Rożnowska, Ewa Kaczorek, 6th Symposium on Biotransformations for Pharmaceutical and Cosmetic Industry, June 17-21, 2024, Kraków, Poland. Book of abstracts - Kraków, Polska:

Instytut Katalizy i Fizykochemii Powierzchni PAN im. Jerzego Habera w Krakowie, 2024 - s. 100-101 **Poster**

6. *Właściwości mikroorganizmów środowiskowych uczestniczących w biodegradacji ksenobiotyków,* Amanda Pacholak, Natalia Burlaga, **Adam Grzywaczyk**, Aleksandra Makiej, Agata Zdarta, Wojciech Smułek, Ewa Kaczorek, XI Kongres Technologii Chemicznej. Materiały konferencyjne red. Robert Frankowski - Poznań, Polska: Politechnika Poznańska. Wydział Technologii Chemicznej, 2024 - s. 134 **Oral presentation**

7. *Zrównoważone zagospodarowanie odpadowej biomasy jako surowiec do syntezy polihydroksyalkanianów,* Michał Kapczyński, **Adam Grzywaczyk**, Natalia Burlaga, Ewa Kaczorek, II Ogólnopolska Konferencja Naukowa PUTChemikon: materiały konferencyjne red. Piotr Paweł Michałowski - Poznań, Polska: Wydawnictwo Politechniki Poznańskiej, 2024 - s. 153-155 **Poster**

8. *Bioavailability of antibiotics modified with plant surfactants*, Wojciech Smułek, Natalia Burlaga, **Adam Grzywaczyk**, Aleksandra Makiej, Amanda Pacholak, Agata Zdarta, Ewa Kaczorek, 2nd French-Polish Chemistry Congress, Montpellier, 28-31 August 2023 - Montpellier, France: University of Montpellier, 2023 - s. 621-61 **Oral presentation**

9. *Study of interactions between phospholipids and antibiotics by Langmuir monolayer technique,* Oliwia Machrowicz, Monika Rojewska, Wojciech Smułek, **Adam Grzywaczyk**, Ewa Kaczorek, Krystyna Prochaska, NanoTech Poland 2021. Book of abstracts, 9th-11th June 2021, Poznań, Poland, 2021 - s. 163 **Poster**

10. *Improving of horseradish peroxidase activity by immobilization onto Nylon 6 electrospun fibers,* Katarzyna Jankowska, Jakub Zdarta, Adam Grzywaczyk, Manuel Pinelo, Teofil Jesionowski, National Scientific Conference „1st Summer Scientific On-line School": The Book of Abstracts: Wydawnictwo Fundacji Promovendi, 2020 - s. 171 **Oral presentation**

Other

A Co-founder of MiCo Scientific sp. z o. o. – Poznan University of Technology spin-off company

A member of Polish Chemical Society, Polish Microbiological Society, Polish Biophysical Society, PUT Chemistry Student Research Group

Full texts of papers

Publication P1

Colloids and Surfaces A: Physicochemical and Engineering Aspects 661 (2023) 130937

Contents lists available at ScienceDirect

Colloids and Surfaces A: Physicochemical and Engineering Aspects

journal homepage: www.elsevier.com/locate/colsurfa

Nanofiltered saponin-rich extract of *Saponaria officinalis* – Adsorption and aggregation properties of particular fractions

Adam Grzywaczyk [a], Wojciech Smułek [a], Agnieszka Zgoła-Grześkowiak [b], Ewa Kaczorek [a,*], Anna Zdziennicka [c], Bronisław Jańczuk [c]

[a] Institute of Chemical Technology and Engineering, Poznań University of Technology, Berdychowo 4, 60-965 Poznań, Poland
[b] Institute of Chemistry and Technical Electrochemistry, Poznań University of Technology, Berdychowo 4, 60-965 Poznań, Poland
[c] Department of Interfacial Phenomena, Institute of Chemical Sciences, Faculty of Chemistry, Maria Curie-Skłodowska University in Lublin, Maria Curie-Skłodowska Sq. 3, 20-031 Lublin, Poland

HIGHLIGHTS

- Szyszkowski equation is useful for multicomponent solution.
- E0, E1, E2, E3 and E4 have bigger tendency to aggregate than classical surfactants.
- Minimal surface tension of E0, E1, E2, E3, E4 solution is larger than classical surfactants.
- Tendency of saponins to micellization is smaller after nanofiltration process.

GRAPHICAL ABSTRACT

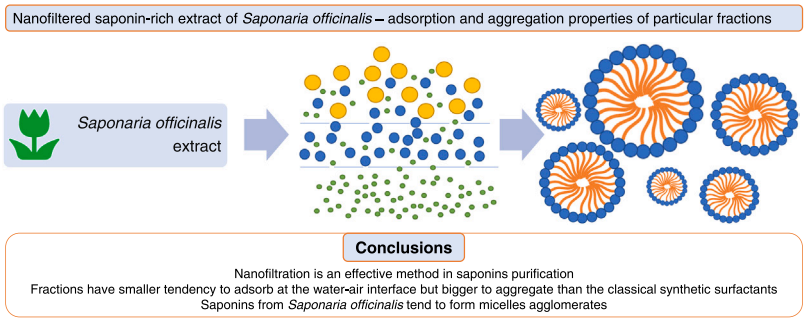

ARTICLE INFO

Keywords:
Saponin
Extract
Micelles
Nanofiltration
Surface activity

ABSTRACT

Plant extracts containing saponins combine high emulsifying properties with antibacterial activity, which makes them valuable adjuvants in pharmaceutical and food products. Saponins are natural surfactants present in various plant species, including *Saponaria officinalis*. Due to the variety of chemical structures and diversity of saponins in plant extracts, their surface-active properties are complex and differ from those of chemically pure surfactants. Hence, the aim of the study was to determine the correlation between the composition of *S. officinalis* extracts and their surface properties. The first stage of the study was characterization of the composition of the extracts studied by liquid chromatography coupled with mass spectrometry. Then the surface tension of the aqueous solutions of these extracts was measured, which permitted determination of their adsorption and aggregation parameters. The results have pointed out the differences between the properties of the studied extracts and those of pure surfactants of known molecular structure. The constants in the Szyszkowski equation allowed determination of the maximal excess concentration of a given extract at the water-air interface and the value of the Gibbs free energy of adsorption. The mentioned parameters were also determined from the Gibbs adsorption isotherm equation and the Langmuir equation modified by de Boer. The results obtained by these methods were found to be comparable with those determined from the Szyszkowski equation. What is more, it was found that the adsorption parameters correlated with the micelle sizes formed by the components of the tested *S. officinalis*

* Corresponding author.
E-mail address: ewa.kaczorek@put.poznan.pl (E. Kaczorek).

https://doi.org/10.1016/j.colsurfa.2023.130937
Received 17 October 2022; Received in revised form 3 January 2023; Accepted 6 January 2023
Available online 10 January 2023

extracts. All these valuable data help devise the informed use of extracts containing saponins in many branches of science and economy.

1. Introduction

Substances with surface active properties can be found in many different plant species as well as in the animal and even human organisms [3,7,25,33]. They play a very important role as components of many different industrial and household products and in a wide range of processes [1,3,10,21]. Among the surfactants of natural origin, saponins occupy an important position in terms of their practical applications [28]. Saponins are used, among others, in the production of food and cosmetics, animal feed and plant protection agents [8,16,27]. They can be also applied in the environmental protection as additives reacting with the soil pollutants and can be useful for the degradation of synthetic toxic surfactants [11]. The use of saponins in the medicine and pharmacy is not excluded [9,13]. Development of their applications requires a deep knowledge of their physicochemical properties. Among them, the tendency to be adsorbed at the water-air interface and to form micelles in the bulk phase is very important. Unfortunately, it is not easy to determine the tendency of saponins to adsorption at the water-air interface and to form micelles as they are mixtures of various types of chemical compounds, which are the secondary metabolites of plant cells.

The composition of saponins depends on their plant origin [24]. An additional difficulty in the analysis of the adsorption and aggregation properties of saponins is determination of their molar mass. For these reasons it is difficult to find unambiguous data about the adsorption and aggregation properties of saponins. If a characterization of the surfactant properties of saponins is given, it is in terms of micellar or emulsifying properties without any deeper analysis or mathematical description of interfacial phenomena [17,18]. These surfactant properties are most often determined based on the isotherm of the surface tension of their aqueous solutions. For the aqueous solutions of single surfactants or their mixtures, of a known molar mass and molecular dimensions based on the surface tension isotherms, it is easy to determine the concentration of surfactants in the surface monolayer at the water-air interface, orientation of surfactant molecules and the surface area occupied by one molecule in this monolayer as well as the critical micelle concentration (CMC). Thus, it is easy to determine the adsorption and aggregation tendency by solving the known thermodynamic equations. As is commonly known, these equations have been derived on the basis of the activity of the surfactants in the bulk phase. In many cases they are solved against the free Gibbs energy of adsorption and aggregation at the assumption of ideal behavior of the surfactants and/or their mixtures in aqueous solution. In such case the activity of the surfactants is equal to its mole fraction. To determine the mole fraction of a given compound in the solution its molar concentration or weight in a given volume of solution must be known. Unfortunately, it is more complicated to determine the mole fraction of a given component of the mixture in the case of the aqueous solutions of multicomponent mixtures in which concentrations of single compounds are unknown. The multicomponent mixtures can include not only the surface active compounds. It is possible that to determine, for example, the Gibbs excess concentration in the surface layer of the multicomponent mixtures and/or to analyse of the Szyszkowski equation, the isotherm of the surface tension of aqueous solution of this mixture expressed as a function of the mixture weight in a given volume of the solution can be used. However to determine the tendency to adsorb at the water-air interface and to aggregate in the aqueous solution of the multicomponents mixture the molar fraction or mole concentration of particular component of the mixture should be known or the equations described this tendency should be modified. For this purpose in the previous studies, the properties of a crude extract of saponins from *Saponaria officinalis* [20] were analysed among others, by using the modified Gibbs isotherm equation in which weight was used instead of mole concentration. Thus the aim of the current studies was to determine the total adsorption of saponins and the possibility of their aggregation in the presence of additives based on the thermodynamic relationships modified by us, as well as to evaluate the possibility of using nanofiltration in the saponin purification process. The thermodynamic relationships included the Gibbs isotherm, Szyszkowski and Szyszkowski-Langmuir (often called Frumkin) equations. In these equations instead of the mole concentration, the weight of a given mixture in 1 L was applied. In the case of Gibbs isotherm equation, the usefulness of a mixture weight was proved based on the Gibbs-Duhem equation.

Hence, the aim of the study was to explain the correlation between *S. officinalis* extracts composition and their surface activity. In our studies, the extract obtained from *Saponaria officinalis* was applied. It was subjected to a process of nanofiltration, as a result of which the E0, E1, E2, E3 and E4 extract fractions various compounds of different molar masses were obtained. Two membranes with the porosity of 500 Da and 3000 Da were used. The middle fraction, E2, should contain the largest amount of saponins (the saponins content was in the range of ~ 2.5 kDa-~ 0.5 kDa).

2. Materials and methods

2.1. Materials

Dried and cut roots of *Saponaria officinalis* L. were purchased as a herbal material from Flos, Poland. The methanol (HPLC grade) and other chemicals used in the experiments were from Merck, Germany. The deionized water (18.2 MΩ·cm) was obtained using Sartorius Stedim (Germany) Mili-Q water purification unit. Millipore® membrane filters of cut-off 3.0 kDa and Amicon® separation compartment were purchased from Merck Millipore, Germany. Membrane filters of cut-off 0.5 kDa was bought from Starlitech, USA.

2.2. Extracts preparation

The process of isolation and separation of different fractions of *S. officinalis* extracts is illustrated in Fig. 1. Firstly, the plant material was placed in a Soxhlet glass extractor (Chempur, Poland) and the extraction process was conducted for 6 h using methanol (10 mL per 1 g of dry roots) as an extractant. Then the solvent was evaporated using a rotary vacuum evaporator (Büchi AG, Switzerland). The obtained dry crude extract (E0 fraction) was dissolved in deionized water (1 g in 100 mL). In the next step, a separation with a 3.0 kDa membrane was performed; the permeate was marked as E1 and the retentate as E4. Then, the E1 fraction was separated using a 0.5 kDa membrane; the permeate was labelled as E3 and the retentate as E2. The term 'saponins' can be used to determine both, the plant extract or one specific group of compounds. Throughout this paper, the term saponins is used to describe a plant extract.

2.3. Qualitative analysis

The *Saponaria officinalis* L. extract purified on a membrane was analysed by LC-MS/MS. The Ultimate 3000 HPLC system from Dionex (Sunnyvale, CA, USA) coupled with the QTRAP 4000 mass spectrometer from AB-Sciex (Foster City, CA, USA) were used. The samples were injected onto a Kinetex Evo C18 column (150 mm × 2.1 mm I.D.; 2.6 μm) from Phenomenex (Torrance, CA, USA). The mobile phase (0.1% formic acid in water and acetonitrile (ACN)) was used at a flow

rate of 0.3 mL min^{-1} in the following gradient: 0 min 10 % ACN, 5 min 15% ACN, 10 min 20 % ACN, 12 min 70 % ACN, 15 min 90% ACN, 20 min 90% ACN. The eluate from the column was directed to the ESI source operating in negative ionization mode. The source and mass spectrometer parameters were as follows: source temperature 500 °C, nebulizer gas nitrogen at 45 psi, curtain gas nitrogen at 20 psi, declustering potential − 50 V, collision gas nitrogen at 10 psi. Mass spectra were recorded in the 300–2500 *m/z* range. For selected ions, chromatograms and their fragmentations were recorded in the enhanced ion product mode.

For the analysis of glycone part of saponins, the GC/MS was used. At first, the derivatization of 50 μg of dehydrated samples with 200 μL of BSTFA (Merck, Germany) was made. The samples were incubated for 1 h at 65 ℃. After that, hexane was added and the mixture was centrifuged for 5 min to get rid of any solid residue. The liquid phase was collected and then subjected to GC/MS analysis.

The GC–MS system used was a Pegasus 4D GCxGC-TOF MS from LECO (Leco Corp., USA). Data acquisition and analysis were performed using standard software supplied by the manufacturer. Substances were separated on a BPX5 capillary column (30 m × 0.25 mm ID, 0.25 μm film thickness) (Trajan Scientific and Medical, Australia). Temperature program: 65 ℃ held for 2 min, 6 ℃ min^{-1} up to 230 ℃, held for 5 min, and 6 ℃ min^{-1} up to 300 ℃, held for 5 min. The temperatures of the injection port and transfer line were set at 280 ℃ and 250 ℃, respectively. Splitless injection mode and helium with a flow rate of 1.00 mL min^{-1} as carrier gas were used.

2.4. Surface tension

The surface tensions of the deionized water solutions of *S. officinalis* extracts were measured by the du Nuoy platinum ring method using a K20 tensiometer (Krüss, Germany). All of the measurements were conducted at 22 ± 1 °C.

2.5. Particle and micelles size

To measure the hydrodynamic diameters (dH) of the particles, micelles and aggregates in the extracts solutions a Zetasizer Nano-ZS (Malvern Instruments Ltd., United Kingdom), working on the basis of a non-invasive backscattering method, was applied. The measurements were carried out at 22 ± 1 °C for solutions of extracts' concentrations: 0.3 ×CMC, 1.0 ×CMC, and 3 ×CMC.

2.6. Statistical analysis

All experiments and measurements were conducted in triplicate. For further calculations arithmetic means and standard deviations were used. The calculations were conducted in MATLAB software.

3. Results and discussion

3.1. Analysis of the qualitative composition of the Saponaria officinalis fraction

The cleaned-up extracts from *Saponaria officinalis* L. were analysed using the LC-MS/MS system. No saponins were detected in extract E3, but they were found in the other two extracts (E1 and E2). Both these clearer extracts showed cleaner spectra than that obtained for the extract not subjected to cleaning (extract E0). However, there was no considerable difference between extracts E1 and E2, both contained the same saponins. The saponins identified in these two extracts are collected in Table 1. The aglycones found in the samples are characteristic of *Saponaria officinalis* L. as described in previous studies, including gypsogenin, hydroxygypsogenic acid, quillaic acid, hederagenin, hydroxyhederagenin, and phytolaccagenic acid, whose characteristic ions were detected at *m/z* 176, 501, 485, 471, 487, and 515, respectively [4,12,15,26]. From among sugars, mainly hexoses and their uronic acids were detected for which losses of 162 and 176 Da were found. Other characteristic losses were also observed in the mass spectra, i.e. 132 Da (pentose), 44 Da (CO_2 from the carboxylic group), or 18 Da (water). Among the detected saponins, there were two of the most intensive signals: hydroxygypsogenic acid- HexA-Pen-Pen-dHex detected as [M-H]- ion at *m/z* 1087 and quillaic acid- Hex-HexA detected as [M-H]- ion at *m/z* 823 (Fig. S1) Chromatograms and mass spectra of these compounds are presented in Fig. S2, and their characteristic ions are given in Table 2.

The GC-MS analysis performed does not allow a complete analysis of the composition of both fractions of extracts because of the type of detector and the molecular weight of the saponins. However, it enabled an analysis of the sugar components that may be included in the saponin

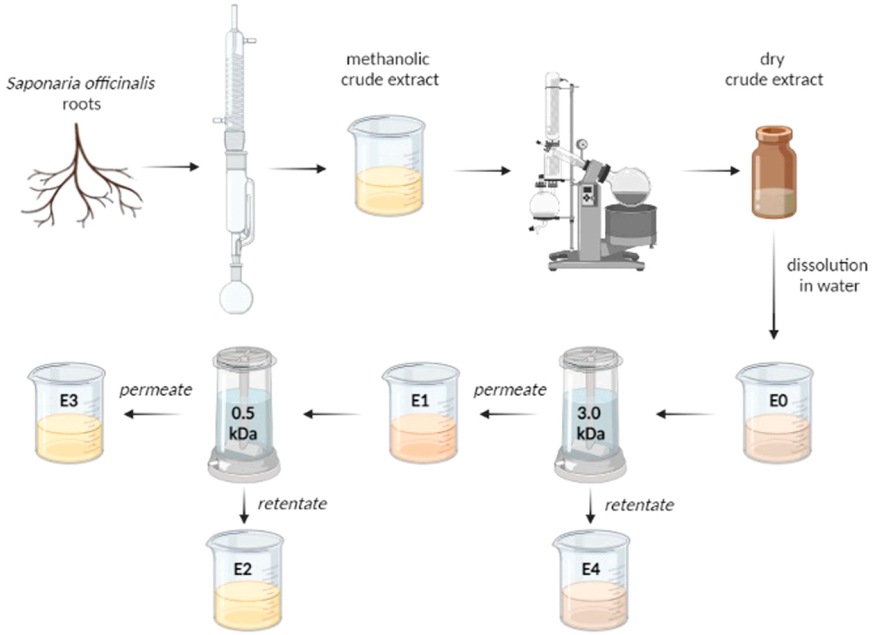

Fig. 1. A scheme of isolation and membrane separation of *Saponaria officinalis* extracts used in the study.

Table 1
Structures of saponins found in the *Saponaria officinalis* L. extract.

Aglycone	Sugar units	Mass fragments, *m/z*	Retention time (s)
Gypsogenin	Hex-HexA	807 [M-H]⁻, 645 [M-H-162]⁻, 601 [M-H-162–44]⁻, 583 [M-H-162–44–18]⁻, 469 [M-H-162–176]⁻, 451 [M-H-162–176–18]⁻	12.70
Gypsogenin	HexA	645 [M-H]⁻, 469 [M-H-176]⁻	13.75
Hydroxygypsogenic acid	HexA-Pen-Pen-dHex	1087 [M-H]⁻, 911 [M-H-176]⁻, 677 [M-H-410]⁻, 501 [M-H-176–410]⁻	12.77
Hydroxygypsogenic acid	Hex-HexA	839 [M-H]⁻, 677 [M-H-162]⁻, 501 [M-H-162–176]⁻	12.56
Hydroxygypsogenic acid	Hex	663 [M-H]⁻, 501 [M-H-162]⁻, 483 [M-H-162–18]⁻	13.10
Quillaic acid	Hex-HexA	823 [M-H]⁻, 661 [M-H-162]⁻, 617 [M-H-162–44]⁻, 599 [M-H-162–44–18]⁻, 485 [M-H-162–176]⁻, 467 [M-H-162–176–18]⁻	12.89
Quillaic acid	HexA	661 [M-H]⁻, 485 [M-H-176]⁻	13.27
Quillaic acid	HexA	661 [M-H]⁻, 485 [M-H-176]⁻, 467 [M-H-176–18]⁻	13.78
Hederagenin	Hex-HexA	809 [M-H]⁻, 647 [M-H-162]⁻, 603 [M-H-162–44]⁻, 585 [M-H-162–44–18]⁻, 471 [M-H-162–176]⁻	13.04
Hederagenin	Pen-HexA	779 [M-H]⁻, 647 [M-H-132]⁻, 471 [M-H-132–176]⁻	13.18
Hederagenin	HexA	647 [M-H]⁻, 471 [M-H-176]⁻	13.34
Hederagenin	HexA	647 [M-H]⁻, 471 [M-H-176]⁻, 453 [M-H-176–18]⁻	14.06
Hydroxyhederagenin	Hex-HexA	825 [M-H]⁻, 663 [M-H-162]⁻, 619 [M-H-162–44]⁻, 601 [M-H-162–44–18]⁻, 487 [M-H-162–176]⁻	12.75
Hydroxyhederagenin	HexA	663 [M-H]⁻, 487 [M-H-176]⁻	13.50
Hydroxyhederagenin	HexA	663 [M-H]⁻, 487 [M-H-176]⁻, 469 [M-H-176–18]⁻	13.83
Phytolaccagenic acid	HexA	691 [M-H]⁻, 515 [M-H-176]⁻	13.44
Phytolaccagenic acid	HexA	691 [M-H]⁻, 515 [M-H-176]⁻	13.61

molecules present in the extracted fractions. On the basis of the LC-MS analysis, the compounds with a high signal to noise ratio (S/N) and those present in both fractions were selected. They originated from pentose group: L-(-)-Arabitol and from hexose group: D-(-)-Fructopyranose, α-D-(+)-Mannopyranose, α -D-(-)-Tagatopyranose, D-Psicose, these compounds may be included in the saponins and are labelled as Pen - pentoses or Hex - hexoses, in Table 1. These are only the suggested chemical compounds. The similarities in the structures of the above-mentioned compounds, as well as the fact that the studied systems are plant extracts, make it extremely difficult to find the exact answer to the question of what sugar parts attach to specific aglycone parts. Attention should be paid to the high content of sugar alcohols, which, like saponins, may arise as a result of metabolic changes taking place in plant cells [2,39]. These are for example D-(-)-Ribofuranose or D-(-)-Fructofuranose, D-Pinitol, D-Mannitol.

3.2. Surface tension

The shape of the surface tension isotherms of the aqueous solutions of various types of surfactants and the minimum attainable values of the surface tension of these solutions provide information on the adsorption activity of a given compound. The minimum values of the surface tension of the aqueous solutions of extracts E0, E1, E2, E3 and E4 do not differ much from each other and are much higher than the minimum values of aqueous solutions of the classic non-ionic, anionic and cationic surfactants (Figs. 2 and 3) [36]. Since, as mentioned above, individual extract fractions contain many compounds, composed of both small and large molecules, it is difficult to present the changes of the surface tension of the investigated solutions as a function of the molar concentration. Therefore, in order to compare the isotherms of the surface tension of the aqueous solution of extract fractions with the isotherms of the aqueous solutions of the representatives classic surfactants, the isotherms of the extract fraction E0, nonionic Triton X-165 (TX165), anionic sodium dodecyl sulphate (SDS) and cationic hexadecyltrimethylammonium bromide (CTAB) as a function of the logarithm of their masses in 1 L are presented in Fig. 2 as an example. The comparison of the surface tension isotherms of aqueous solutions of the synthetic surfactants with those obtained for the solution of saponins may be useful for prediction of the properties of saponins mixtures with the classical surfactants. This seems to be important for the practical application of the saponins.

Fig. 2 shows that the shape of the surface tension isotherm of the aqueous solution of extract E0 fraction is similar to that of the nonionic TX165 solution. However, the values of the surface tension of the

Table 2
Carbohydrates and their derivatives found in the *Saponaria officinalis* L. extract.

Name	R.T. (s)	S/N	Sample
Allyl(methoxy)dimethylsilane	361.9	2564.4	E0
Allyl(methoxy)dimethylsilane	361.9	6138.8	E2
(Z)-Hex-3-enyl (E)− 2-methylbut-2-enoate	374.3	1000.1	E2
4-Dimethylsilyloxytridecane	378.6	3241.9	E0
4-Dimethylsilyloxytridecane	378.6	6421.2	E2
Glycerol, tris(trimethylsilyl) ether	741.6	1619.4	E2
Glycerol, tris(trimethylsilyl) ether	742.8	4126.5	E0
meso-Erythritol, tetrakis(trimethylsilyl) ether	1040.7	600.13	E0
1,5-Anhydro-D-sorbitol, tetrakis(trimethylsilyl) ether	1270.8	731.79	E0
L-(-)-Arabitol, pentakis(trimethylsilyl) ether	1281.1	1152	E2
L-(-)-Arabitol, pentakis(trimethylsilyl) ether	1281.4	1848.3	E0
Dihydroxyacetone dimer, tetra(trimethylsilyl)-	1318.5	512.41	E2
D-(-)-Tagatofuranose, pentakis(trimethylsilyl) ether (isomer 2)	1344.7	691.72	E0
D-(-)-Ribofuranose, tetrakis(trimethylsilyl) ether (isomer 1)	1347.4	924.23	E2
D-(-)-Fructofuranose, pentakis(trimethylsilyl) ether (isomer 1)	1373.3	1510.3	E0
D-(-)-Tagatofuranose, pentakis(trimethylsilyl) ether (isomer 1)	1381.2	5077.3	E2
D-(-)-Fructofuranose, pentakis(trimethylsilyl) ether (isomer 1)	1382.2	2052.9	E0
2,2,4,4,6,6-Hexamethylcyclotrisilazane	1384.4	1787	E0
α -D-(-)-Tagatopyranose, pentakis(trimethylsilyl) ether	1392.5	4217	E2
Ribitol, 1,2,3,4,5-pentakis-O-(trimethylsilyl)-	1397.2	534.25	E2
D-(+)-Talofuranose, pentakis(trimethylsilyl) ether (isomer 2)	1417.5	770.57	E2
à-D-(-)-Tagatopyranose, pentakis(trimethylsilyl) ether	1420.9	518.86	E2
D-(-)-Fructofuranose, pentakis(trimethylsilyl) ether (isomer 1)	1428.3	1650.3	E2
D-Pinitol, pentakis(trimethylsilyl) ether	1431.3	787.34	E0
D-Pinitol, pentakis(trimethylsilyl) ether	1433.6	784.17	E2
D-(-)-Fructopyranose, pentakis(trimethylsilyl) ether (isomer 2)	1443.4	501.17	E2
α -D-(-)-Tagatopyranose, pentakis(trimethylsilyl) ether	1453.8	18,522	E0
α-D-(+)-Mannopyranose, pentakis(trimethylsilyl) ether	1465.1	614.52	E0
D-Psicose, pentakis(trimethylsilyl) ether	1469.6	4333.3	E2
D-(+)-Galactopyranose, pentakis(trimethylsilyl) ether (isomer 2)	1474.3	4952.9	E2
Acrylic acid, 2,3-bis[(trimethylsilyl)oxy]-, trimethylsilyl ester	1480.1	933.97	E2
D-Mannitol, 1,2,3,4,5,6-hexakis-O-(trimethylsilyl)-	1492.4	725.18	E0
D-Mannitol, 1,2,3,4,5,6-hexakis-O-(trimethylsilyl)-	1495.3	2072.7	E2
D-Mannitol, 1,2,3,4,5,6-hexakis-O-(trimethylsilyl)-	1499.2	733	E0
D-Sorbitol. hexakis(trimethylsilyl) ether	1500.8	612.83	E2
α-D-Glucopyranose, 1,2,3,4,6-pentakis-O-(trimethylsilyl)-	1555	696.77	E0
D-Gluconic acid, 2,3,4,5,6-pentakis-O-(trimethylsilyl)-, trimethylsilyl ester	1569.5	729.61	E2

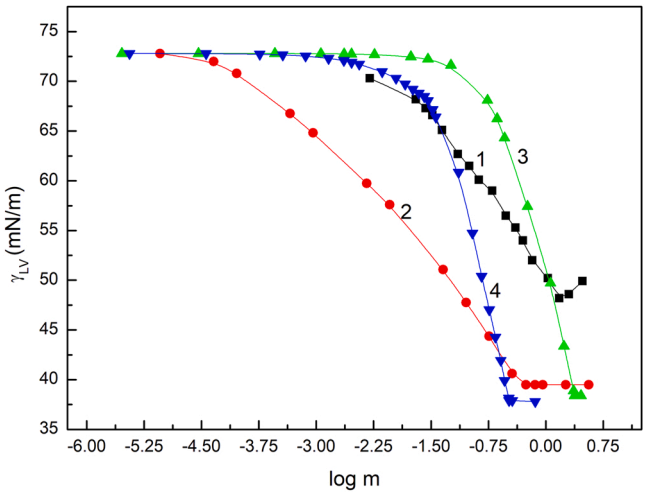

Fig. 2. A plot of the surface tension (γ_{LV}) of aqueous solutions of the E0 fraction (curve 1), TX165 (curve 2), SDS (curve 3) and CTAB (curve 4) vs. the logarithm of their molecular weight (m) (m – the numerical value corresponding to the weight in g L^{-1}).

aqueous E0 solution, at a given concentration, are between those for the cationic CTAB and anionic SDS solutions. Indeed, as mentioned above, the minimum surface tension value of the E0 solution is much higher than that of the TX165, SDS and CTAB solutions. It is worth noting that the concentration corresponding to the critical micelle concentration (CMC) for E0 is similar to the CMC of SDS.

A question arises why there are so great differences in the values of the minimum surface tension between the aqueous fractionate solutions and those of classic synthetic surfactants.

The surface tension of the aqueous surfactant solutions depends on the surface tension of water and all solution components as well as the contribution of various types of intermolecular interactions to the surface tension of water and surfactants. For the first time, [15] has noted that for a better understanding of interface phenomena, not only the measured surface tension of a liquid or solution and the indirectly determined surface tension of solids are important, but also the contribution of particular types of intermolecular interactions to this tension. Taking this into account, from the practical point of view, the surface tension of liquids and solids can be treated as the sum of the dispersive and non-dispersive components. In turn, van Oss et al. in their studies [29–32] divided the surface tension of the solid into the Lifshitz-van der Waals (LW) and acid-base (AB) components. The LW component results from dispersion, dipole-dipole and induced dipole-dipole intermolecular interactions. However, they have estimated that the contribution of the dipole-dipole and dipole-induced dipole interactions in the condensed phases to the surface tension is smaller than 2% [29–32]. Thus the LW component in the van Oss et al. approach to the surface tension is equal to the dispersion component in the Fowkes theory [6]. The acid-base component of the solid and liquid surface tension is practically associated with the hydrogen bonds formation. As a matter of fact, in the van Oss et al. concept, the electrostatic interactions are not taken into account. In turn, van Oss and Constanzo [32] have reported that the surface tension of surfactants depends on their molecules orientation toward the air phase. If the molecules are oriented with the tail to the air, the surface tension of surfactants is called the tail surfactant surface tension but if the surfactants molecule are oriented with the head to the air, the surfactant surface tension is called the head surface tension.

Taking into account the tail surface tensions of TX165, SDS and CTAB and assuming that their molecules in the monolayer at the water-air interface are oriented with the tail toward the air and that the monolayer is saturated, the minimal surface tension of the aqueous solutions of the surfactants should be about 22, 25 and 27 mN m^{-1} [19]. In practice, the minimal values of the surface tension of TX165, SDS and CTAB aqueous solutions are considerably higher than these values [36]. Moreover, the LW component of surface tension of these surfactant solutions does not depend on the concentration and is close to the LW component of the water surface tension (26.85 mN m^{-1}) [37]. This indicates that the addition of the classical synthetic surfactants to water and their adsorption at the water-air interface reduce only the AB component of the water surface tension resulting from the hydrogen bonds interactions.

The earlier studies of the sugar surfactants showed that their surface tension at the orientation of these surfactants molecules with the hydrophilic groups toward the air (the so-called the head surface tension) was greater than 40 mN m^{-1} [38] and was determined by the Lifshitz-van der Waals and hydrogen bonds intermolecular interactions. However, the contribution of the LW component to the sugar head surface tension was significantly greater than that of the AB one. As the compounds present in the given fraction of a extract have different types of sugar units, it should be expected that their surface tension is greater than 40 mN m^{-1} and the contribution of AB component to this tension is considerably smaller than that of the LW one. This is probably the reason for the higher minimal values of the surface tension of particular fractions of the extract than those for the classic synthetic surfactants.

In order to be able to analyse the adsorption properties of the studied extract fractions in the whole range of their concentration in the bulk phase, it is important to describe the surface tension isotherms with an appropriate mathematical or thermodynamic equation. It has been proved that the obtained surface tension isotherms can be described by the exponential function of the second order (Fig. 3). This function has the form:

$$\gamma_{LV} = y_0 + A_1 \exp\left(\frac{-\mathrm{m}}{\mathrm{t_1}}\right) + A_2 \exp\left(\frac{-\mathrm{m}}{t_2}\right) \quad (1)$$

where γ_{LV} is the surface tension of the aqueous solution of the extract fraction, m is the weight of the extract in g L^{-1} and y_0, A_1, A_2, t_1 and t_2 are the constants.

Unfortunately, so far it has been difficult to give the exact dependencies of the constants in Eq. (1) on the physicochemical properties of the solution components. However, it seems likely that these constants are related to the components and parameters of the surface tension of the compounds present in the solution. The LW components of this tension can be associated with y_0 constant. The values of y_0 (Table 3) for particular fractions of the extract are insignificantly lower than the minimal values of their aqueous solution surface tension. On the other hand, the values of y_0 are only insignificantly different from those of the sugar surfactants head surface tension [38]. It is possible that the A_1, A_2, t_1 and t_2 constants in Eq. (1) are related to the formation and breaking of hydrogen bonds. In other words, they depend on the electron-acceptor and electron-donor parameters of the surface tension of surfactants.

Our earlier studies have proved that the surface tension isotherms of the aqueous solutions not only of individual surfactants but also of their mixtures can be successfully described by the Szyszkowski equation. For the aqueous solution of individual surfactants this equation takes the form [22]:

$$\gamma_{\mathrm{W}} - \gamma_{LV} = RT\Gamma^{\max} \ln\left(\frac{\mathrm{C}}{a} + 1\right) \quad (2)$$

where γ_{W} is the water surface tension, $\Gamma^{\max}$ is the surfactant maximal Gibbs surface excess concentration at the water-air interface, R is the gas constant, T is the absolute temperature, C is the surfactant concentration in mole L^{-1} and a is the constant depending on the Gibbs free energy of adsorption.

Eq. (2) has been successfully used for description of the surface tension isotherms of the aqueous solutions of single surfactants and their mixtures if the concentration of the surfactants and/or their mixture at

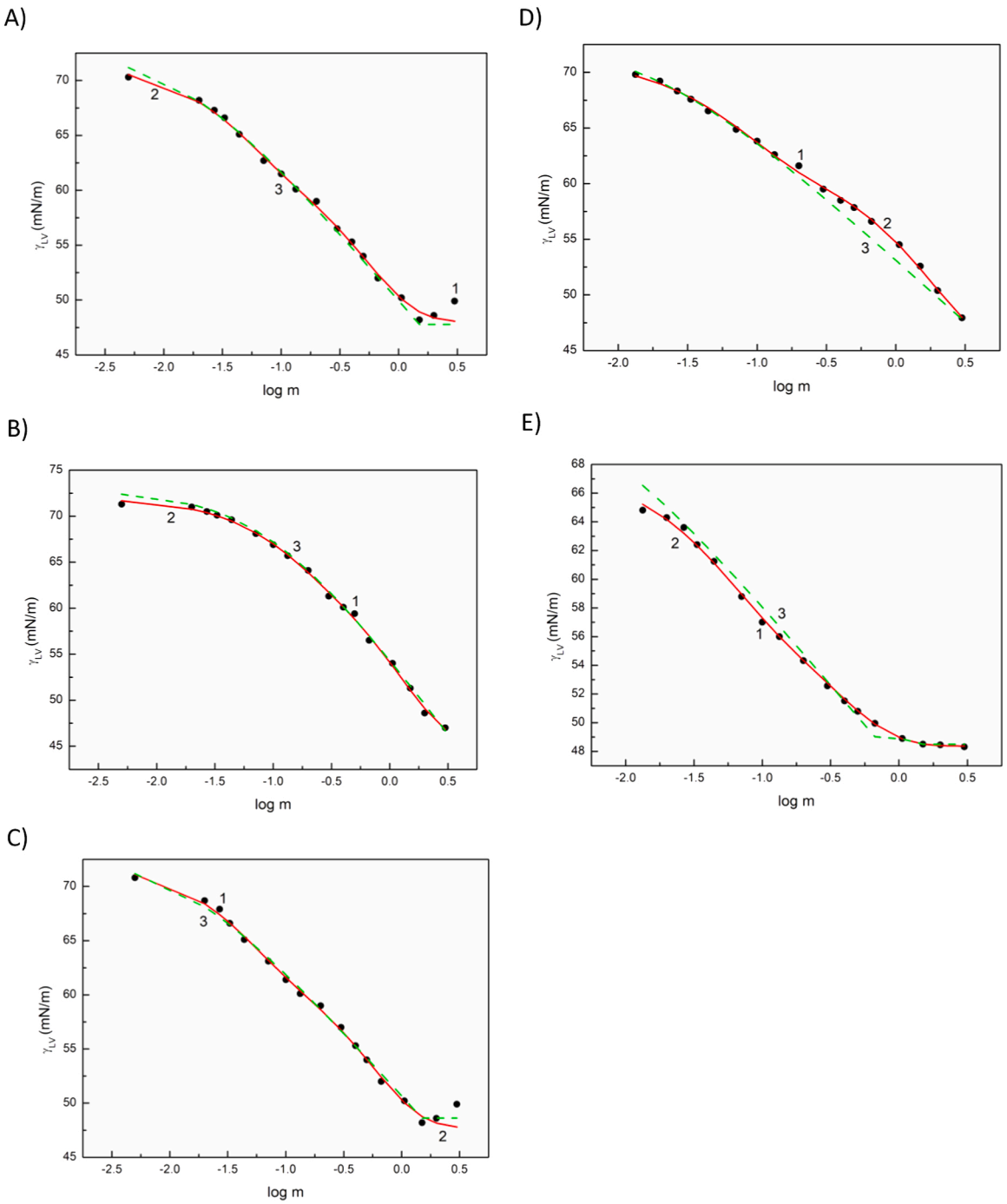

Fig. 3. A plot of the surface tension (γ_{LV}) of aqueous solutions of the fractions E0 (A), E1 (B), E2 (C), E3 (D), E4 (E) vs. the logarithm of their molecular weight (m) (m – the numerical value corresponding to the weight in g L^{-1}). Points 1 correspond to the measured values, curves 2 and 3 correspond to the values calculated from Eqs. (1) and (2), respectively.

which they were present in the solution in the monomeric form was taken into account in this equation [19]. In the case of the surfactants mixtures at the constant composition, the sum of the concentrations of the mixture components in the bulk phase and the maximal Gibbs surface excess concentration of the mixture were used for the isotherm surface tension determination from the Szyszkowski equation [36].

For the calculation of the isotherm of the surface tension of particular fractions of the extract, it is impossible to use the Szyszkowski equation in the form of Eq. (2) because we do not know the molar concentration of a given fraction of the extract. However, in Eq. (2) $\frac{m}{M_s}$ can be used instead of C, where $M_s = \sum_{i=j}^{i=1} \alpha_i M_i$ (α_i is the mole fraction of $i-th$ component in the mixture, j is the number of components and M_i is the molar weight of $i-th$ component). In such a case Eq. (2) takes the form:

$$\gamma_W - \gamma_{LV} = RT\Gamma^{max} \ln\left(\frac{m}{aM_s} + 1\right) \quad (3)$$

It proved that using Eq. (3) it is possible to describe the surface tension isotherm of the aqueous solution of all studied fractions of the extract (Fig. 3). In fact, Eq. (3) can be solved against γ_{LV} numerically by fitting the $\Gamma^{max}$and aM_s values. The Γ^{max} (Table 3) and aM_s values obtained in such a way depend on the type of the extract fraction.

As follows from the surface tension isotherms for the aqueous

Table 3
The values of the constants in Eq. (1) (y_0, A_1, A_2, t_1 and t_2), maximal Gibbs surface excess concentration (Γ^{max}), minimal area occupied by one molecule (A_{min}), critical micelle concentration (CMC) as well as the standard Gibbs free energy of adsorption (ΔG^0_{ads}) and micellization (ΔG^0_{mic}).

Magnitude		E0	E1	E2	E3	E4
Constant in Eq. (1)	y_0	48.03047	44.96415	47.73447	44.51936	48.36917
	A_1	15.17956	6.63508	15.46142	17.6059	10.27968
	t_1	0.52856	0.13625	0.55549	1.84268	0.35042
	A_2	8.33042	20.39518	9.01503	9.1269	9.11056
	t_2	0.04599	1.25044	0.0448	0.07721	0.0494
Γ^{max} ($\times 10^{-6}$ mol m^{-2})	Eq. (7)	2.01	2.70	2.00	1.92	1.76
	Eq. (3)	2.20	3.00	2.10	2.00	2.00
aM_s		0.0143	0.0865	0.0134	0.0179	0.0051
A_{min} (Å^2)	Γ^{max} from Eq. (7)	82.6	61.5	83.0	86.5	94.4
	Γ^{max} from Eq. (3)	75.5	55.3	79.1	83.0	83.0
Eq. (9)						
ΔG^0_{ads} (kJ mol^{-1})	Eq. (10)	-32.55[a] -36.80[b]	-30.91[a] -35.61[b]	-32.86[a] -37.23[b]	-31.32[a] -35.63[b]	-32.58[a] -36.94[b]
	Eq. (11)	-35.27[a] -39.63[b]	-30.88[a] -35.25[b]	-35.43[a] -39.79[b]	-34.72[a] -39.08[b]	-37.78[a] -42.14[b]
minimal ΔG^0_{ads} (kJ mol^{-1})	Eq. (10)	-32.70[a] -37.06[b]	-33.95[a] -38.32[b]	-33.03[a] -37.44[b]	-31.68[a] -36.05[b]	-32.86[a] -37.22[b]
ΔG^0_{ads} (kJ mol^{-1})	Eq. (12)	-35.31[a] -39.68[b]	-33.85[a] -38.21[b]	-35.37[a] -39.74[b]	-35.80[a] -40.16[b]	-38.18[a] -42.54[b]
CMC (g L^{-1})		1.50	1.29	1.50	2.33	1.30
ΔG^0_{mic} (kJ mol^{-1})	Eq. (12)	-23.92[a] -28.29[b]	-24.29[a] -28.65[b]	-23.92[a] -28.29[b]	-22.85[a] -27.21[b]	-24.27[a] -28.63[b]

[a] corresponds to the calculation made for the molecular weight $M_S = 500$ g.
[b] corresponds to the calculation made for the molecular weight $M_S = 3000$ g.

solution of particular fractions of the extract, the aggregation process may take place. Most probably the CMCs of the extracts E0, E1, E2, E3 and E4 are 1.5, 1.29, 1.5, 2.33 and 1.3 g L^{-1}, respectively. From among these CMC values, the value for E3 is the least certain. For comparison of the CMC values obtained for different fractions of the extract with those of TX165, SDS and CTAB, the CMC values of the latter were calculated in g L^{-1} to be close to 0.493, 2.365 and 0.334 g L^{-1}, respectively. Thus, the CMC values of the particular extract fractions are smaller only than the CMC value of the anionic SDS [35].

3.3. Concentration at the water-air interface

The concentration of the surfactants in the monolayer at the water-air interface can be determined, among others, using the Gibbs isotherm and Frumkin equations [22].

However, it should be remembered that using the Gibbs isotherm equation the excess concentration of a given compound in the surface layer relative to its concentration in the bulk phase is determined. In the case of surfactants at their low concentration in the bulk phase, the concentration of surfactants in the surface layer is considerable higher than that in the bulk phase and can be treated as a total concentration.

For the multicomponent surfactant mixtures in which the concentration of the surfactants without one component is constant and the coefficient of the surfactants activity is equal to unity, the Gibbs isotherm equation takes the form [22]:

$$\Gamma_i = -\frac{C_i}{RT}\left(\frac{\partial \gamma_{LV}}{\partial C_i}\right)_{C_{j\neq i},T} = -\frac{1}{2.303RT}\left(\frac{\partial \gamma_{LV}}{\partial \log C_i}\right)_{C_{j\neq i},T} \quad (4)$$

where Γ_i is the Gibbs surface excess concentration of the i-th component of the mixture, C_i is the concentration of the i-th opponent in the bulk phase.

In the case of the ionic surfactants, the constant kRT is used in. Eq. (4) instead of RT. Assuming that the activity of water is equal to unity, then for the aqueous solution of the multicomponent surfactants mixture at a constant composition and the variable total mixture concentration, the Gibbs-Duhem equation for the surface region has the form:

$$Ad\gamma + \sum_{i=j}^{i=1} n_i d\mu_i = 0 \quad (5)$$

where A is the area of the interface, n_i is the number of moles of the i-th component in the solution, j is the number of the components in the mixture and μ_i is the chemical potential of the i-th component in the interface region.

In fact, in the equilibrium state, the chemical potential of all components in the surface layer is equal to their chemical potential in the bulk phase. If the concentration of all components of the solution in the bulk phase is considerably smaller than the number of water moles in 1 L, it can be assumed that:

$$a_i = X_i = \frac{C\alpha_i}{\omega} = \frac{m\alpha_i}{M_S\omega} \quad (6)$$

where a_i is the activity of the i-th component in the bulk phase, X_i is the mole fraction of the i-th component in the bulk phase, C is the total concentration of the surfactants mixture in the bulk phase in mol L^{-1}, m is the weight of the surfactants mixture in g in 1 L of solution, α_i is the mole fraction of the i-th component in the surfactants mixture in the bulk phase and ω is the number of the water moles in 1 L.

Putting Eq. (6) into Eq. (5) we obtain:

$$\Gamma = -\frac{m}{RT}\left(\frac{\partial \gamma_{LV}}{\partial m}\right)_T = -\frac{1}{2.303RT}\left(\frac{\partial \gamma_{LV}}{\partial \log m}\right)_T \quad (7)$$

The Γ values calculated from Eq. (7) depend on the type of the extract fraction (Fig. 4). For the calculation of Γ from Eq. (7), kRT cannot be used instead of RT because in the studied mixtures the amount of acid compounds is small. In such a case the values of k should be very close to unity and are difficult to establish precisely. It is interesting that in some cases the maximal Gibbs surface excess concentration of the extract fraction calculated based on Eq. (7) is comparable to that deduced from the Szyszkowski equation. The surface tension isotherms of the studied

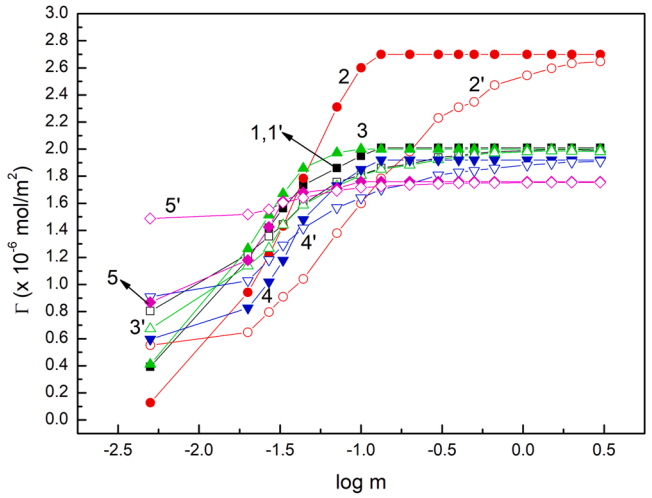

Fig. 4. The plot of the surface excess concentration (Γ) for the fractions E0 (curves 1, 1′), E1 (curves 2, 2′), E2 (curves 3, 3′), E3 (curves 4, 4′) and E4 (curves 5, 5′) vs. the logarithm of their weight (m) (m – the numerical value corresponding to the weight in g L^{-1}). Curves 1 – 5 correspond to the values calculated from Eq. (7), curves 1′ – 5′ to those calculated from Eq. (8).

mixtures can be also determined from the Szyszkowski-Langmuir equation, which can be expressed in the following form:

$$\gamma_W - \gamma_{LV} = \pi = -RT\Gamma^{max}\ln\left(1 - \frac{\Gamma}{\Gamma^{max}}\right) \tag{8}$$

where: γ_W is the water surface tension.

However, it should be noted that Eq. (8) is also known as the Frumkin equation [22].

Taking into account the Γ^{max} values obtained from Eq. (7) the Γ values were calculated from Eq. (8) (Fig. 4). It proved that the shape of Γ isotherms obtained from Eq. (8) is different than that of the isotherms determined using Eq. (7). The differences between the Gibbs and Frumkin isotherms of Γ depend on the type of the extract fraction. Taking into account the complexity of the studied systems, it is currently difficult to establish the reasons for these differences.

As mentioned above, it is difficult to determine the exact Γ values due to the presence of anionic compounds in the particular fractions of the extract. It can be only concluded that the real values of the surface excess concentration of the investigated fractions of the extract at the water-air interface are in the range from Γ/2 to Γ. The Γ^{max} values obtained for the extract fractions E0, E2 and E3 are comparable to those for the saponins. It probably results from the fact that these fractions contain the compounds whose adsorption properties are close to those of saponins. Unfortunately, it is difficult to establish which compounds have the same adsorption properties as saponins. On the other hand, the Γ^{max} values for the fractions E0, E2 and E3 are insignificantly smaller than the value of Γ^{max} for TX165 [35]. However, the Γ^{max} value for E1 is insignificantly smaller than the maximal values of the Gibbs surface excess concentration of ionic SDS and CTAB. The smallest value of Γ^{max} was obtained for E4 (Table 3).

On the basis of the Γ^{max} value it is possible to determine the minimal average value of the area occupied by one molecule of a given extract fraction (A_{min}) in the monolayer at the water-air interface using the simple expression:

$$A_{min} = \frac{1}{\Gamma^{max} N} \tag{9}$$

where: N is the Avogadro number.

It appeared that the calculated values of A_{min} for all extract fractions are higher than the contactable area of sugar units [38]. However, it is very difficult to establish the orientation of the compound molecules present in a given extract fraction in the mixed monolayer at the water-air interface based on this comparison.

3.4. Standard Gibbs free energy of adsorption and micellization

The standard Gibbs free energy of adsorption (ΔG^0_{ads}) and micellization (ΔG^0_{mic}) are the measures of the tendency of the surfactants to get adsorbed at the interfaces and to form the colloidal aggregates in the bulk phase, called micelles. A number of methods have been reported for determination of ΔG^0_{ads} and ΔG^0_{mic}. If we have the isotherm of the surfactants Gibbs surface excess concentration at the water-air interface in their concentration range in the bulk phase from zero to a concentration even higher than CMC, the standard Gibbs surface free energy of adsorption can be determined using the Langmuir equation modified by de Boer [5,22]. This equation has the form [22]:

$$\frac{A^0}{A - A^0}\exp\frac{A^0}{A - A^0} = \frac{C}{\omega}\exp\left(\frac{-\Delta G^0_{ads}}{RT}\right) \tag{10}$$

where A^0 is the limiting area occupied by one surfactant molecule and A is the area occupied by one surfactant molecule in the monolayer at the interface corresponding to a given mole concentration C, respectively.

To solve Eq. (10) the knowledge of A^0, A and C is needed. As a matter of fact, A can be calculated from Eq. (9) which applies not only for A_{min} determination. However, to establish the A^0 value for the particular fraction of the extract, which is the multicomponent mixture, none of the known concepts can be used. Taking into account the composition of the particular fraction of the extract, it seems reasonable that the A^0 value should be close to the contactable area of the sugar unit (35 $Å^2$) [38]. This results from the fact that the molecules of the most compounds present in the extract fraction contain the groups whose size is close to that of the sugar unit. In the case of diluted solutions, the value of A^0 has an insignificant impact on the ΔG^0_{ads} value calculated from Eq. (10). Another problem to solve Eq. (10) against ΔG^0_{ads} is to establish the C value of the extract fraction. As two membranes with the porosity of 500 and 3000 Da were used in the fractionation process of the extract, the molecular weight was assumed to be equal to 500 and 3000 g, respectively for the C calculations.

Using the A^0 and C values determined in the above mentioned ways and the A values determined based on the Gibbs isotherm of the excess

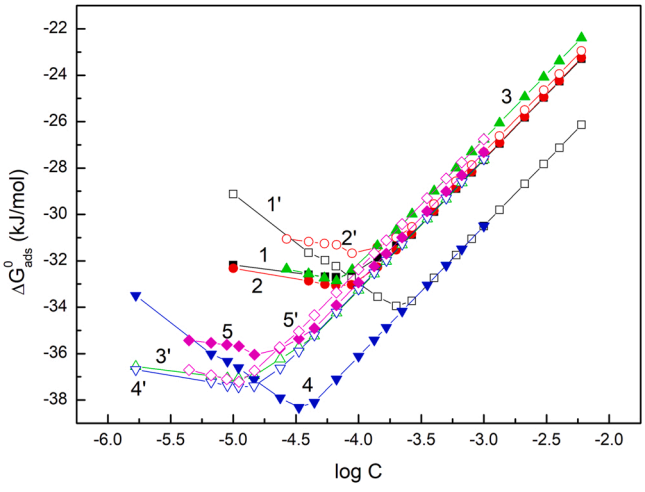

Fig. 5. The plot of the standard Gibbs free energy of adsorption (ΔG^0_{ads}) for the fractions E0 (curves 1, 1′), E1 (curves 2, 2′), E2 (curves 3, 3′), E3 (curves 4, 4′) and E4 (curves 5, 5′) calculated from Eq. (10) vs. the logarithm of their molar concentration (C). Curves 1 – 5 correspond to the molar concentration calculated for the molecular weight equal to 500 g and curves 1′ – 5′ to molecular weight equal to 3000 g, respectively.

concentration of particular extract fraction in Eq. (10), two ΔG^0_{ads} values were calculated for E0, E1, E2, E3 and E4 (Table 3) (Fig. 5). It proved that the absolute values of ΔG^0_{ads} for all types of extract fractions are smaller than that for TX165, SDS and CTAB (Table 3) [36]. These values of ΔG^0_{ads} depend on the type of the extract fraction.

Of course, the question arises whether the values of molecular weight used for the calculation of the standard Gibbs free energy of adsorption give its reasonable values for the particular components of the extract fraction. According to the experimental procedure, the maximal molecular weight of the compounds cannot be higher than 3000 g. However, the minimal molecular weight is not equal to 500 g. On the other hand, the molecular weight of more than 90% compounds present in the studied solutions is higher than 250 g. If in the calculation of ΔG^0_{ads} the compounds of molecular weight of 250 g are used instead of those of 500 g, then the obtained values differed by less than 2 kJ mol^{-1}. Thus, for all fractions from the *Saponaria* extract, the calculations of ΔG^0_{ads} were made assuming that the molecular weight of compounds was equal to 500 or 3000 g which corresponds numerically to the porosity of the membranes.

It seems to be interesting to calculate the ΔG^0_{ads} values based on the constant established solving the Szyszkowski equation against the surface tension of the aqueous solution of extract fractions.

Dividing aM_s by 500 or 3000, two values of a were obtained for each fraction of the extract and then the G^0_{ads} values were calculated from the following equation [22]:

$$a = \omega \exp \frac{\Delta G^0_{ads}}{RT} \tag{11}$$

In many cases, the values of ΔG^0_{ads} calculated from Eq. (11) are close to those obtained from Eq. (10). This indicates that using the Szyszkowski equation both the maximal Gibbs surface excess concentration as well as the standard Gibbs free energy of adsorption of such complicated systems can be determined. In fact, the ΔG^0_{ads} values calculated from Eq. (11) are higher than that for TX165 and smaller than those for SDS and CTAB [36] (Table 3).

According to Zdziennicka and Jańczuk [34] the ΔG^0_{ads} values are correlated with the standard Gibbs free energy of micellization (ΔG^0_{mic}) by the following expression:

$$\Delta G^0_{ads} = RT \ln \frac{\mathrm{CMC}}{\omega} - \frac{\gamma_{W-\gamma^{\min}_{LV}}}{\Gamma^{\max}} \tag{12}$$

where $RT \ln \frac{\mathrm{CMC}}{\omega}$ is equal to ΔG^0_{mic}.

For the calculations of ΔG^0_{ads} from this equation, the values of $\Gamma^{\max}$ determined from Eq. (7) and $\gamma^{\min}_{LV}$ as well as CMC obtained based on the surface tension isotherms (Figs. 2 and 3) were taken into account. The values of ΔG^0_{ads} calculated from Eq. (12) are slightly smaller than those calculated from Eqs. (10) and (11). However, they are higher than ΔG^0_{ads} values for TX165 and smaller than those for SDS and CTAB. (Table 3) [36].

In turn, the ΔG^0_{mic} calculated from Eq. (12) is comparable to that of TX165, being smaller than the values for SDS and CTAB, and depends on the type of the extract fraction (Table 3) [36].

3.5. Particle size distribution

The final stage of the research was the determination of micelle size of particular extract fractions. The particle size distribution analysis was performed using the previously obtained information on the CMC of individual fractions, to provide additional information about the hydrodynamic diameter of micelles, depending on the concentration. Tests were carried out using a concentration three times lower than CMC - 0.3 × CMC, at CMC – 1.0 × CMC, and three times higher than CMC – 3.0 × CMC. The results are shown in Fig. 6. For each fraction the particle

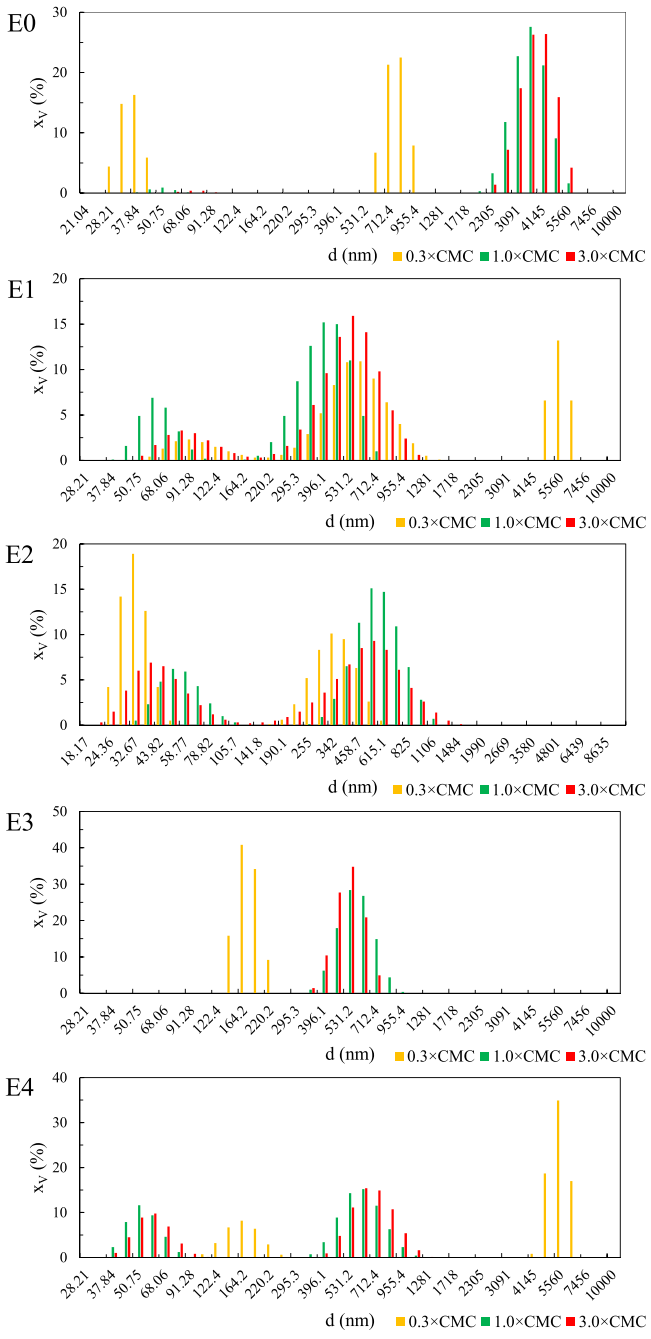

Fig. 6. Particle size distribution of the individual fractions of the *Saponaria officinalis* extracts (x_v – volume fraction in %, d – hydrodynamic diameter in nm).

size calculated for the concentrations of 1.0 × CMC and 3.0 × CMC were the same. For the fractions E0, E3 and E4 the particles' hydrodynamic diameters for the concentration of 1.0 × CMC and 3.0 ×CMC differed from that calculated for 0.3 ×CMC. However, there is a significant difference in the micelle size distribution between the E0 fraction - crude extract, and the fractions obtained after nanofiltration. As mentioned above, an extract is a mixture of many compounds, ranging from proteins, through lipids and waxes, to sugars. The E0 fraction is the crude extract and thus differences may arise. It is, therefore, worth noting that depending on the degree of purification of the extract and its concentration, the hydrodynamic diameter of particles is different. For the fractions E1 and E4, the size of the micelles ranges from approx. 37–120 nm, and for E2 from 24 nm to 105 nm. According to [14], these

values corresponded to typical micelle size range from 5 to 100 nm. On the other hand, the volume fractions signals appearing on each spectra between 220 nm and 1000 nm may correspond to the aggregated forms of micelles. As observed by [23], agglomerates of *Sapindus mukorossi* saponin micelles were also present in aqueous solution having particle size ranging from 132 to 235 nm, 390–990 nm, and 5155–8520 nm, which corresponds to the value obtained in our research. It is worth noting the lack of such signals for the fraction E3. In the case of the crude extract, the percentage of particles with a size from 37 nm to 91 nm is very limited. Particles with a size from 2300 nm to 5560 nm have the largest share, which suggests almost no disaggregated micelles.

4. Conclusions

Based on the carried out experiments and the analysis of the obtained results many conclusions can be drawn. The chromatographic-mass spectrometry analysis indicated the presence of saponins, the derivatives of gypsogenin, hydroxygypsogenic acid, quillaic acid, hederagenin, hydroxyhederagenin, and phytolaccagenic acid in the *S. officinalis* extract and showed great enrichment in their content in the fraction between 500 Da and 3000 Da.

The surface tension isotherms of the aqueous solution of different extracts' fractions can be described by the exponential function of the second order and the constants of this function are related to the components and parameters of the compounds present in the extract fraction.

It was observed that the saponins have non-ionic nature which is in accordance with the suggestions following from other research works.

The standard Gibbs free energy of micellization indicates that plant extracts have the greater tendency to aggregate than the classical synthetic surfactants. The thermodynamic equations used for the determination of Gibbs surface excess concentration isotherms as well as the standard Gibbs free energy of adsorption and micellization for the aqueous solution of individual surfactants and their mixtures can be customized to so complicated solution as the aqueous solution of fraction of extract. What is more, the saponin-rich fraction of the extract formed nanometric micelles and agglomerates, which were of smaller size then those formed in the other extract fractions.

The presented analyses constitute an appropriate basis for further planned research, as they confirm the effectiveness of extract purification, present the qualitative analysis as well as the CMC values that will support the application of bioactive *S. officinalis* extract in pharmaceutical, cosmetic and food products.

Ethical approval

This article does not contain any studies with human participants or animals performed by any of the authors.

CRediT authorship contribution statement

Adam Grzywaczyk: Methodology, Formal analysis, Investigation, Writing – original draft, Visualization. **Wojciech Smułek:** Conceptualization, Formal analysis Data curation, Writing – original draft, Supervision. **Agnieszka Zgoła-Grześkowiak:** Methodology, Investigation. **Ewa Kaczorek:** Conceptualization, Data curation Supervision, Writing – review & editing, Project administration, Funding acquisition. **Anna Zdziennicka:** Writing – original draft, Writing – review & editing, Visualization, Investigation, Formal analysis. **Bronisław Jańczuk:** Conceptualization, Validation, Formal analysis, Data curation, Writing – original draft, Writing – review & editing, Visualization.

Declaration of Competing Interest

The authors declare that they have no known competing financial interests or personal relationships that could have appeared to influence the work reported in this paper.

Data availability

The raw/processed data are available after e-mail contact with the corresponding author.

Acknowledgements

This research was funded in whole by National Science Centre, Poland, grant number: 2020/39/B/NZ9/03196.

Appendix A. Supporting information

Supplementary data associated with this article can be found in the online version at doi:10.1016/j.colsurfa.2023.130937.

References

[1] A.M. Benhur, S. Pingali, S. Amin, Application of biosurfactants and biopolymers in sustainable cosmetic formulation design, J. Cosmet. Sci. 71 (2020) 455–480.
[2] R.L. Bieleski, Sugar alcohols, in: F.A. Loewus, W. Tanner (Eds.), Plant Carbohydrates I, Springer Berlin Heidelberg, Berlin, Heidelberg, 1982, pp. 158–192, https://doi.org/10.1007/978-3-642-68275-9_5.
[3] T.R. Bjerk, P. Severino, S. Jain, C. Marques, A.M. Silva, T. Pashirova, E.B. Souto, Biosurfactants: properties and applications in drug delivery, biotechnology and ecotoxicology, Bioengineering 8 (2021) 115, https://doi.org/10.3390/bioengineering8080115.
[4] A. Budan, D. Bellenot, I. Freuze, L. Gillmann, P. Chicoteau, P. Richomme, D. Guilet, Potential of extracts from *Saponaria officinalis* and *Calendula officinalis* to modulate in vitro rumen fermentation with respect to their content in saponins, Biosci., Biotechnol., Biochem. 78 (2014) 288–295, https://doi.org/10.1080/09168451.2014.882742.
[5] H. De Boer, The Dynamical Character of Adsorption, Oxford University, Oxford, UK, 1953.
[6] F.M. Fowkes, Attractive forces at interfaces, Ind. Eng. Chem. 56 (1964) 40–52, https://doi.org/10.1021/ie50660a008.
[7] E. Fujimatu, T. Ishikawa, J. Kitajima, Aromatic compound glucosides, alkyl glucoside and glucide from the fruit of anise, Phytochemistry 63 (2003) 609–616, https://doi.org/10.1016/S0031-9422(03)00179-1.
[8] M. Hussain, B. Debnath, M. Qasim, B.S. Bamisile, W. Islam, M.S. Hameed, L. Wang, D. Qiu, Role of saponins in plant defense against specialist herbivores, Molecules 24 (2019) 2067, https://doi.org/10.3390/molecules24112067.
[9] M.-H. Jung, S.-J. Jung, T. Kim, Saponin and chitosan-based oral vaccine against viral haemorrhagic septicaemia virus (VHSV) provides protective immunity in olive flounder (Paralichthys olivaceus), Fish. Shellfish Immunol. 126 (2022) 336–346, https://doi.org/10.1016/j.fsi.2022.05.044.
[10] A.P. Karlapudi, T.C. Venkateswarulu, J. Tammineedi, L. Kanumuri, B.K. Ravuru, V. ramu Dirisala, V.P. Kodali, Role of biosurfactants in bioremediation of oil pollution-a review, Petroleum 4 (2018) 241–249, https://doi.org/10.1016/j.petlm.2018.03.007.
[11] T. Kobayashi, H. Kaminaga, R.R. Navarro, Y. Iimura, Application of aqueous saponin on the remediation of polycyclic aromatic hydrocarbons-contaminated soil, J. Environ. Sci. Health Part A 47 (2012) 1138–1145, https://doi.org/10.1080/10934529.2012.668106.
[12] Y. Lu, D. Van, L. Deibert, G. Bishop, J. Balsevich, Antiproliferative quillaic acid and gypsogenin saponins from Saponaria officinalis L. roots, Phytochemistry 113 (2015) 108–120, https://doi.org/10.1016/j.phytochem.2014.11.021.
[13] S. Man, W. Gao, Y. Zhang, L. Huang, C. Liu, Chemical study and medical application of saponins as anti-cancer agents, Fitoterapia 81 (2010) 703–714, https://doi.org/10.1016/j.fitote.2010.06.004.
[14] M. Milovanovic, A. Arsenijevic, J. Milovanovic, T. Kanjevac, N. Arsenijevic, Nanoparticles in antiviral therapy, in: in: Antimicrobial Nanoarchitectonics, Elsevier, 2017, pp. 383–410, https://doi.org/10.1016/B978-0-323-52733-0.00014-8.
[15] B. Moniuszko-Szajwaj, Ł. Pecio, M. Kowalczyk, A.M. Simonet, F.A. Macias, M. Szumacher-Strabel, A. Cieślak, W. Oleszek, A. Stochmal, New triterpenoid saponins from the roots of *Saponaria officinalis* (1934578×1300801), Nat. Prod. Commun. 8 (2013), https://doi.org/10.1177/1934578×1300801207.
[16] Z. Nizioł-Łukaszewska, T. Bujak, Saponins as natural raw materials for increasing the safety of bodywash cosmetic use, J. Surfactants Deterg. 21 (2018) 767–776, https://doi.org/10.1002/jsde.12168.
[17] A. Pradhan, S. Bhuyan, K. Chhetri, S. Mandal, A. Bhattacharyya, Saponins from Albizia procera extract: surfactant activity and preliminary analysis, Colloids Surf. A Physicochem. Eng. Asp. 643 (2022), 128778, https://doi.org/10.1016/j.colsurfa.2022.128778.
[18] T.H. Randriamamonjy, J.F. Ontiveros, M.T. Andrianjafy, P. Samiez, A. Berlioz-Barbier, V. Nardello-Rataj, J.-M. Aubry, V. Ramanandraibe, M. Lemaire, Comparative study on the amphiphilicity, emulsifying and foaming properties of

saponins extracted from Furcraea foetida, Colloids Surf. A Physicochem. Eng. Asp. 653 (2022), 129923, https://doi.org/10.1016/j.colsurfa.2022.129923.
[19] E. Rekiel, A. Zdziennicka, K. Szymczyk, B. Jańczuk, Thermodynamic analysis of the adsorption and micellization activity of the mixtures of rhamnolipid and surfactin with Triton X-165, Molecules 27 (2022) 3600, https://doi.org/10.3390/molecules27113600.
[20] E. Rekiel, W. Smułek, A. Zdziennicka, E. Kaczorek, B. Jańczuk, Wetting properties of Saponaria officinalis saponins, Colloids Surf. A Physicochem. Eng. Asp. 584 (2020), 123980, https://doi.org/10.1016/j.colsurfa.2019.123980.
[21] L. Rodrigues, I.M. Banat, J. Teixeira, R. Oliveira, Biosurfactants: potential applications in medicine, J. Antimicrob. Chemother. 57 (2006) 609–618, https://doi.org/10.1093/jac/dkl024.
[22] M.J. Rosen. Surfactants and Interfacial Phenomena, third ed., Wiley-Interscience, Hoboken, N.J, 2004.
[23] K. Samal, C. Das, K. Mohanty, Eco-friendly biosurfactant saponin for the solubilization of cationic and anionic dyes in aqueous system, Dyes Pigments 140 (2017) 100–108, https://doi.org/10.1016/j.dyepig.2017.01.031.
[24] T.B. Schreiner, G. Colucci, A. Santamaria-Echart, I.P. Fernandes, M.M. Dias, S. P. Pinho, M.F. Barreiro, Evaluation of saponin-rich extracts as natural alternative emulsifiers: a comparative study with pure Quillaja Bark saponin, Colloids Surf. A Physicochem. Eng. Asp. 623 (2021), 126748, https://doi.org/10.1016/j.colsurfa.2021.126748.
[25] L. Servillo, A. Giovane, M.L. Balestrieri, A. Bata-Csere, D. Cautela, D. Castaldo, Betaines in fruits of *Citrus* genus plants, J. Agric. Food Chem. 59 (2011) 9410–9416, https://doi.org/10.1021/jf2014815.
[26] W. Smułek, A. Zdarta, A. Pacholak, A. Zgoła-Grześkowiak, Ł. Marczak, M. Jarzębski, E. Kaczorek, Saponaria officinalis L. extract: surface active properties and impact on environmental bacterial strains, Colloids Surf. B Biointerfaces 150 (2017) 209–215, https://doi.org/10.1016/j.colsurfb.2016.11.035.
[27] Y. Tamura, M. Miyakoshi, M. Yamamoto, Application of saponin-containing plants in foods and cosmetics, in: H. Sakagami (Ed.), Alternative Medicine, InTech, 2012, https://doi.org/10.5772/53333.
[28] I.M. Tucker, A. Burley, R.E. Petkova, S.L. Hosking, J.P. Webster, P.X. Li, K. Ma, J. Doutch, J. Penfold, R.K. Thomas, Self-assembly of Quillaja saponin mixtures with different conventional synthetic surfactants, Colloids Surf. A Physicochem. Eng. Asp. 633 (2022), 127854, https://doi.org/10.1016/j.colsurfa.2021.127854.
[29] C.J. van Oss. Interfacial Forces in Aqueous Media, M. Dekker, New York, 1994.
[30] C.J. van Oss, R.J. Good, Surface tension and the solubility of polymers and biopolymers: the role of polar and apolar interfacial free energies, J. Macromol. Sci. Part A Chem. 26 (1989) 1183–1203, https://doi.org/10.1080/00222338908052041.
[31] C.J. van Oss, M.K. Chaudhury, R.J. Good, Monopolar surfaces, Adv. Colloid Interface Sci. 28 (1987) 35–64, https://doi.org/10.1016/0001-8686(87)80008-8.
[32] C.J. Van Oss, P.M. Costanzo, Adhesion of anionic surfactants to polymer surfaces and low-energy materials, J. Adhes. Sci. Technol. 6 (1992) 477–487, https://doi.org/10.1163/156856192×00809.
[33] J.-P. Vincken, L. Heng, A. de Groot, H. Gruppen, Saponins, classification and occurrence in the plant kingdom, Phytochemistry 68 (2007) 275–297, https://doi.org/10.1016/j.phytochem.2006.10.008.
[34] A. Zdziennicka, B. Jańczuk, Thermodynamic parameters of some biosurfactants and surfactants adsorption at water-air interface, J. Mol. Liq. 243 (2017) 236–244, https://doi.org/10.1016/j.molliq.2017.08.042.
[35] A. Zdziennicka, K. Szymczyk, J. Krawczyk, B. Jańczuk, Critical micelle concentration of some surfactants and thermodynamic parameters of their micellization, Fluid Phase Equilib. 322–323 (2012) 126–134, https://doi.org/10.1016/j.fluid.2012.03.018.
[36] A. Zdziennicka, K. Szymczyk, J. Krawczyk, B. Jańczuk, Activity and thermodynamic parameters of some surfactants adsorption at the water–air interface, Fluid Phase Equilib. 318 (2012) 25–33, https://doi.org/10.1016/j.fluid.2012.01.014.
[37] A. Zdziennicka, K. Szymczyk, J. Krawczyk, B. Jańczuk, Components and parameters of solid/surfactant layer surface tension, Colloids Surf. A Physicochem. Eng. Asp. 522 (2017) 461–469, https://doi.org/10.1016/j.colsurfa.2017.03.036.
[38] A. Zdziennicka, J. Krawczyk, K. Szymczyk, B. Jańczuk, Macroscopic and microscopic properties of some surfactants and biosurfactants, IJMS 19 (2018) 1934, https://doi.org/10.3390/ijms19071934.
[39] Y. Zhang, Enhancement of ginseng saponin production in suspension cultures of Panax notoginseng: manipulation of medium sucrose, J. Biotechnol. 51 (1996) 49–56, https://doi.org/10.1016/0168-1656(96)01560-X.

P1 Supplementary Materials

Supplementary Information

Nanofiltered saponin-rich extract of *Saponaria officinalis* – adsorption and aggregation properties of particular fractions

Submitted to

Colloids and Surfaces A: Physicochemical and Engineering Aspects

by

Adam Grzywaczyk[a], Wojciech Smułek[a], Agnieszka Zgoła-Grześkowiak[b], Ewa Kaczorek[a*], Anna Zdziennicka[c] and Bronisław Jańczuk[c]

[a]*Institute of Chemical Technology and Engineering, Poznań University of Technology, Berdychowo 4, 60-965 Poznań, Poland*

[b]*Institute of Chemistry and Technical Electrochemistry, Poznań University of Technology, Berdychowo 4, 60-965 Poznań, Poland*

[c]*Department of Interfacial Phenomena, Institute of Chemical Sciences, Faculty of Chemistry, Maria Curie-Skłodowska University in Lublin, Maria Curie-Skłodowska Sq. 3, 20-031 Lublin, Poland*

*Corresponding author:

e-mail: ewa.kaczorek@put.poznan.pl, tel. +48 (61) 6652601

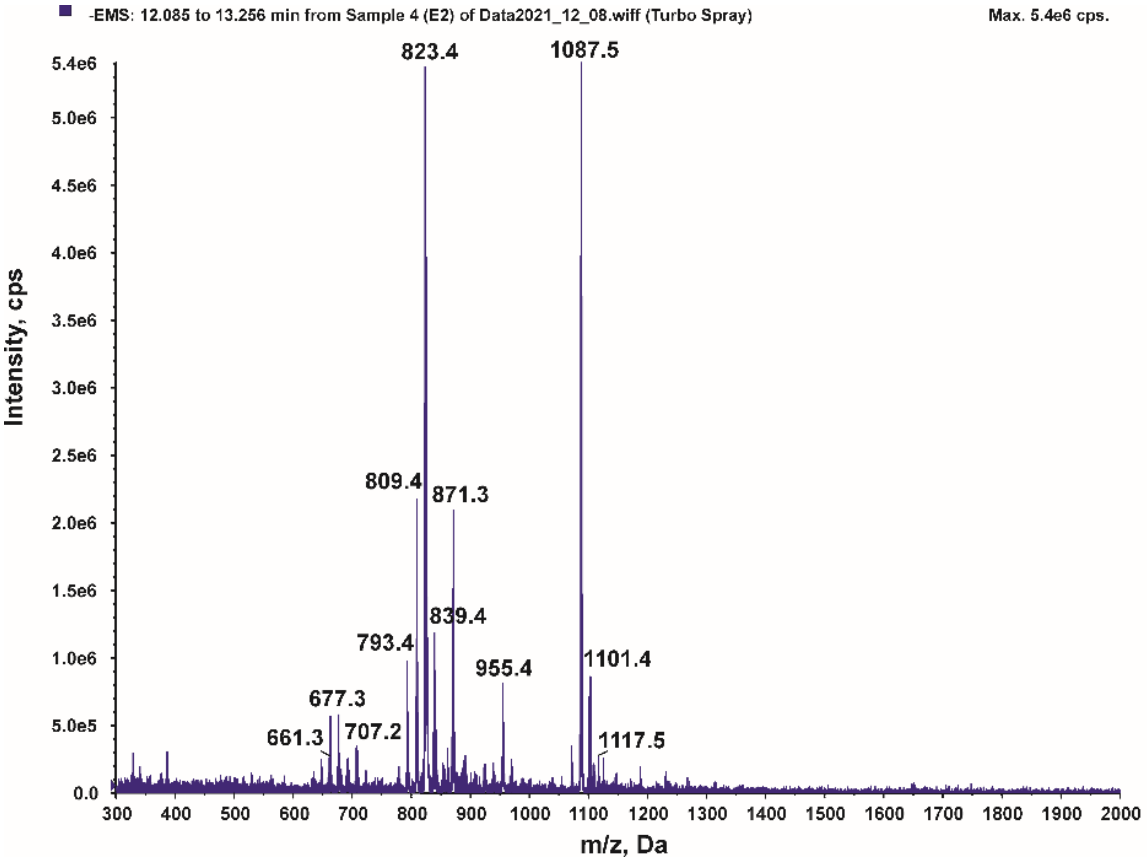

Fig S1. Mass spectra of purified (E2) fraction of *Saponaria officinalis*

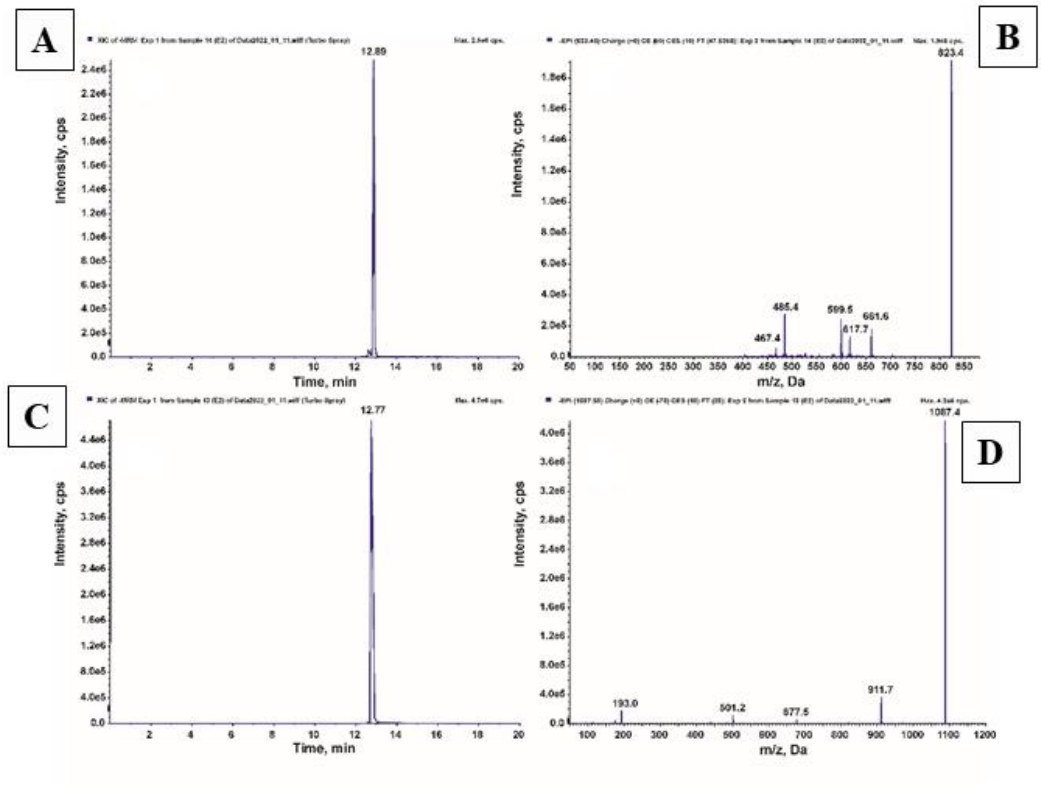

Fig. S2 Chromatograms (A,C) and mass spectra (B,D) of hydroxygypsogenic acid- HexA-Pen-Pen-dHex (A,B) and quillaic acid- Hex-HexA (C,D).

Publication P2

molecules

MDPI

Article

Study of Interactions between Saponin Biosurfactant and Model Biological Membranes: Phospholipid Monolayers and Liposomes

Monika Rojewska, Wojciech Smułek, Adam Grzywaczyk, Ewa Kaczorek and Krystyna Prochaska *

Institute of Chemical Technology and Engineering, Poznan University of Technology, Berdychowo 4, 60-965 Poznań, Poland

* Correspondence: krystyna.prochaska@put.poznan.pl; Tel.: +48-61-6653601; Fax: +48-61-6653749

Abstract: The aim of this study was to determine the effect of saponins-rich plant extract on two model biological membranes: phospholipid monolayers and liposomes. The Langmuir monolayer technique was used to study the interactions of model phospholipid membranes with saponins. The π-A isotherms were determined for DPPE (1,2-dipalmitoyl-sn-glycero-3-phosphoethanolamine) monolayer with the addition of various concentrations of licorice saponins extracts and subjected to qualitative as well as quantitative analysis. Additionally, relaxation studies of the obtained monolayers were carried out and morphological changes were examined using Brewster angle microscopy. Moreover, changes in the structure of phospholipid vesicles treated with solutions of saponins-rich plant extracts were assessed using the FTIR technique. The size and zeta potential of the liposomes were estimated based on DLS methods. The obtained results indicated that the saponins interact with the phospholipid membrane formed by DPPE molecules and that the stability of the mixed DPPE/saponins monolayer strongly depends on the presence of impurities in saponins. Furthermore, it was found that the plant extract rich in saponins biosurfactant interacts mainly with the hydrophilic part of liposomes.

Keywords: adsorption; BAM; DLS; extracts of saponins; FTIR technique; *Glycyrhiza glabra*; impurities; Langmuir monolayer; liposomes; π-A isotherm; relaxation of monolayer

Citation: Rojewska, M.; Smułek, W.; Grzywaczyk, A.; Kaczorek, E.; Prochaska, K. Study of Interactions between Saponin Biosurfactant and Model Biological Membranes: Phospholipid Monolayers and Liposomes. *Molecules* **2023**, *28*, 1965. https://doi.org/10.3390/molecules28041965

Academic Editor: Vasyl M. Haramus

Received: 31 January 2023
Revised: 15 February 2023
Accepted: 16 February 2023
Published: 18 February 2023

1. Introduction

Biosurfactants from the group of saponins have gained significant interest during recent years due to their various biological, therapeutic, and pharmaceutical effects [1–3]. Saponins are natural, surface-active glycosides which include a single or several hydrophilic glycoside molecules linked to a lipophilic triterpene molecule. Medicinal plants are the main source used for the preparation and extraction of various modern drugs and pharmaceutical agents, including saponins [4]. Among such plants, licorice is one of the oldest and most widely used herbs, containing more than 20 triterpenoids and 300 flavonoids [5]. Many studies have shown that the active compounds isolated from licorice exhibit anti-cancer, anti-viral, anti-inflammatory, and immunoregulatory effects, as well as several other actions which contribute to the regeneration and protection of the nervous, respiratory, digestive, endocrine, and cardiovascular systems [6]. The notable antibacterial properties of licorice have been emphasized in particular because many studies have reported that aqueous [7], ethanol, and supercritical fluid licorice extracts efficiently inhibit the activity of Gram-positive and -negative bacteria, such as *Staphylococcus aureus* [8], *Escherichia coli*, *Pseudomonas aeruginosa*, *Candida albicans* [9], and *Bacillus subtilis* [10].

Due to such valuable biological properties, the interest in saponins as a bionatural material is growing. Their application in antibacterial therapy is considered in order to

facilitate the transport of antibiotics through the biological membrane of bacteria [11,12]. For this reason, the first step to ensure a proper design of saponins–antibiotic mixtures is to elucidate the mechanism of interactions between saponins and bacterial membrane components, such as phospholipids. However, understanding how saponins interact with components of the membrane at the molecular level is a challenging task. Therefore, many studies have been conducted to determine the effects of saponins on the biomimetic systems [12–15]. These experiments allow to analyze the interactions between the components of a model membrane and biologically active substances using various physicochemical methods.

Biomimetic studies are commonly used as screening tests in laboratory practice during the first stages of an experiment focused on biologically active compounds (potential drugs) and constitute an important step in drug design research [16,17].

Liposomes are spherical, closed structures which consist of a lipid bilayer. The unique structure of these vesicles allows for encapsulation of different substances, both hydrophilic and hydrophobic, in order to deliver them to specific tissues or cells. Due to their flexibility, variety of ingredients, ease of functionalization, tunability of the number of layers/sizes, biocompatibility, and biodegradability, liposomes are widely used in medicine and cosmetics as good carriers for biologically active substances. Their efficiency as a carrier of drugs depends on their physicochemical parameters, such as composition, size, polydispersity, their zeta potential, and the capability of drug loading [18,19]. A structural unit of liposomes (a bilayer) can be considered as a set of two monolayers in which the polar parts of molecules are directed outwards. Hence, the Langmuir monolayer at the air–water interface may be applied to investigate the molecular packing and the interactions between molecules in the mixed vesicle systems [20].

The Langmuir monolayer technique is a very sensitive method used to investigate the interactions of bioactive substances with components of biological membranes [12,21–24]. A lipid monolayer at the air/water interface represents a promising model surface to study interactions with components dissolved in the adjacent water phase, such as saponins. The monolayer film is formed by spreading organic compounds (e.g., lipids, phospholipids, or glycolipids) on the aqueous subphase. The lipid layer is built by molecules which are specifically oriented at the air/water surface due to their amphiphilic character. The monolayer is compressed by Teflon barriers and the change in surface pressure vs. the monomolecular layer area is monitored. The surface pressure is recorded by a Wilhelmy plate connected to a pressure sensor. The monolayer compressed to the surface pressure of 30 mN/m represents a biological membrane under natural conditions [25,26].

The main aim of this study was to evaluate the ability of naturally occurring triterpenoid saponins to interact and cross a phospholipid membrane which consisted of DPPE (1,2-dipalmitoyl-sn-glycero-3-phosphoethanolamine) molecules. The experiments were prepared for two biomimetic systems: for a monolayer (2D structure) using the Langmuir technique and for liposomes (3D structure). The saponins used in our research were obtained by methanol extraction from *Glycyrhiza glabra* roots. Their chemical structure was previously defined by Schmid et al. [27]. During an attempt to associate the molecular structure with interfacial behavior, it should be kept in mind that the extracts can differ in terms of the saponins content and composition. We expected that impurities, such as residual plant substances, may be present and affect the interfacial properties. Therefore, we have studied two fractions of extracts: a crude extract (GgC) and a purified extract (GgP).

2. Results

2.1. Interactions with the Monolayer Membrane

2.1.1. The Surface Pressure-Area and Surface Potential-Area Isotherms

The Langmuir technique is a unique method used to prepare monomolecular insoluble films of biological substances on aqueous phases, whereby intermolecular interactions as well as their influence on the molecular alignment can be easily determined. In our experiments, the DPPE solution was initially spread on the surface of the subphases. Then, a saponins solution was injected into the subphase one minute prior to the start of compression. Saponins solution (1 g/mL) was added in an appropriate volume in order to achieve the following final subphase concentrations: 1 mg/L, 5 mg/L, and 10 mg/L. For such prepared system, the changes in the surface pressure of the monolayer (π) from the mean molecular area at the air/buffer interface (A) were recorded during film compression. The obtained isotherms are shown in Figure 1. Simultaneously, the surface potential–area per molecule (ΔV–A) isotherms were registered (Figure 1), and the morphology of the mixed monolayer was visualized using a BAM microscope.

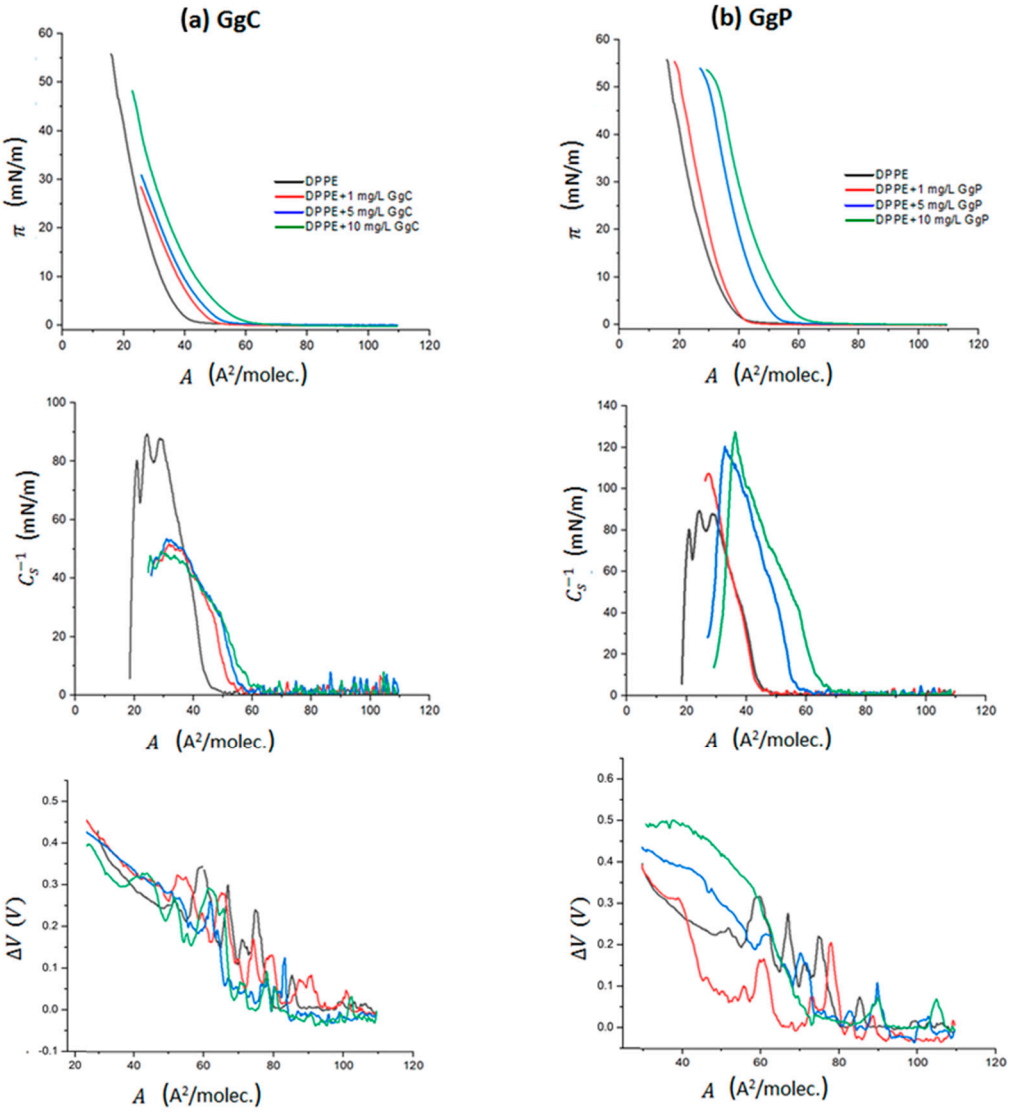

Figure 1. Surface pressure–area per molecule (π–A) isotherms, compression modulus-area per molecule (C_s^{-1}–A) graphs and surface potential- area per molecule (ΔV–A) for the analysed systems: DPPE and various concentrations of the crude saponins extract GgC (**a**) and purified extract GgP (**b**).

Figure 1 illustrates the π–A isotherms obtained for DPPE with two different extracts of saponins, crude (GgC) and purified (GgP). According to the literature [28], the obtained surface pressure–area isotherm of the DPPE monolayer on a D–PBS buffer is almost identical with the π–A isotherm for DPPE on water. For all analyzed systems, π–A isotherms are shifted towards higher values of the surface area A per molecule in the mixed DPPE/saponins monolayer with respect to the isotherm obtained for the DPPE monolayer. The "isotherm lift-off" occurs at different area per molecule values, $A_{lift\text{-}off}$, depending on the concentration. The obtained values of the $A_{lift\text{-}off}$ parameter, based on the π–A isotherms, are presented in Table 1. The observed shift of the π–A isotherm increases with the increase of saponins concentration in the subphase. For the system with the addition of the highest concentration (10 mg/L) of the GgC extract, we observed an increase in surface pressure at the $A_{lift\text{-}off}$ surface of approximately 61 Å²/molec, while for the lowest extract concentration $A_{lift\text{-}off}$ is equal to approximately 50 Å²/molec. Moreover, a more stable monolayer is formed in the presence of a higher concentration (10 mg/L). This film can be compressed to a higher surface pressure, which corresponds to the similar area of molecule at the interface ($A_{collapse}$) for both high and low concentrations. In the case of purified extract, such an effect is not clearly visible, and the created mixed monolayers are characterized by higher $A_{lift\text{-}off}$ values than those estimated for the GgC extract. As the concentration of the saponins extract increases, the values of $A_{lift\text{-}off}$ also increase from approximately 43 to 65 Å²/molec. This effect also indicates a stronger interaction of the molecules in the GgP extract with phospholipids at the interface. Based on the observed effect of a stronger expansion of the film it can be assumed that the content of saponins in the purified extract is definitely higher, as saponins molecules are more strongly incorporated into the lipid film. However, the collapse of the monolayer occurs at lower surface pressure in the presence of a higher concentration of the GgP extract. Detailed information regarding the parameters of the π–A isotherms is given in Table 1.

Table 1. Characteristic parameters of π–A isotherms: $A_{lift\text{-}off}$—lift-off area of surface pressure. $A_{collapse}$—area corresponding to the monolayer collapse, $\pi_{collapse}$—collapse pressure [mN/m], max. C_s^{-1}—maximum value of the compression modulus [mN/m] (refers to A_{max} or π_{max}).

	$A_{lift\text{-}off}$ (Å²/molec.)	$A_{collapse}$ (Å²/molec.)	$\pi_{collapse}$ (mN/m)	A_{max} (Å²/molec.)	π_{max} (mN/m)	$C_s^{-1}{}_{max}$ (mN/m)
DPPE	42.4	17.1	56.8	24.2	37.5	89.3
DPPE/ 1 mg/L GgC	50.2	24.2	28.1	31.6	18.9	51.2
DPPE/ 5 mg/L GgC	56.8	24.9	30.7	30.8	22.5	53.4
DPPE/ 10 mg/L GgC	61.2	21.8	48.3	29.2	24.3	49.3
DPPE/ 1 mg/L GgP	43.5	18.8	55.3	27.6	28.6	107.3
DPPE/ 5mg/L GgP	57.2	28.6	53.9	32.8	40.7	120.3
DPPE/ 10 mg/L GgP	64.9	29.8	53.3	36.3	40.6	127.3

The estimated values of $\pi_{collapse}$ for the DPPE monolayer in the presence of the GgP extract oscillate in the range of 53–55 mN/m. Thus, the mixed monolayer formed in the presence of the GgP extract is characterized by similar stability to that of the pure DPPE film. The opposite effect is observed for the GgC extract. The addition of the GgC extract to the subphase caused the collapse of the monolayer which corresponds to the surface pressure in the range 28–48 mN/m, which is notably lower compared to the DPPE film. Therefore, it can be assumed that the presence of impurities strongly affects the stability of the formed mixed monolayers.

The compression modulus values, C_s^{-1} = f(A), were directly calculated based on the π–A isotherm. The modulus is defined as follows [29]:

$$C_s^{-1} = -A \cdot \left(d\pi/dA\right)_T \quad (1)$$

The C_s^{-1} values provide information regarding the physical state of monolayers strictly associated with the ordering and packing of molecules at the air–water interface. The value of C_s^{-1} is assumed as zero for pure air-water interface and increases with the presence of surfactants at the interface. A higher compression modulus value corresponds to a less compressible membrane. According to the Davies and Rideal classification [29], the gas state (G) is in the range of 0–12.5 mN/m, the liquid-expanded (LE) state is characterized by the C_s^{-1} modulus values between 12.5 and 50 mN/m, while the liquid-condensed (LC) state in in the range between 100 and 250 mN/m. The C_s^{-1} values above 250 mN/m refer to a solid state (S) of the monolayer. The maximum values of C_s^{-1} correspond to the most compressed state of the monolayer that is manifested as the "highest peak" point of the $C_s^{-1} = f(A)$ function (Figure 1). Based on these maximum C_s^{-1} values (Table 1), it can be established that all mixed monolayers formed in the presence of the GgC extract are mainly in a liquid-expanded (LE) state. On the other hand, it can be observed that the π–A curves of DPPE/GgP systems exhibit a lower slope, which is more characteristic for higher monolayer compressibility than that of the DPPE/GgC systems. In consequence, this effect is reflected by the obtained values of the compressibility modulus, which are in the range of approximately 107 mN/m to 127 mN/m for the DPPE/GgP system. As a result, the compression molecules of DPPE and saponins from the purified extract lead to the formation of films in the LC state. Interestingly, a disparate result was observed for the DPPE film in the presence of both extracts. It can be observed that the degree of impurity strongly affects the surface properties of the phospholipid monolayer. The addition of the GgC extract causes the formation of a more fluidized phospholipid monolayer (characterized by a lower C_s^{-1} value than a pure DPPE monolayer), while the addition of the GcP extract leads to a more condensed structure in reference to the DPPE film.

The surface potential ΔV of a monolayer is defined as the difference in the potential between a clean water surface and a monolayer-covered surface [30]. This quantity depends on both the packing density and the orientation of the molecules [31]. The set of surface potential changes versus area (ΔV–A) for particular systems is presented in Figure 1.

For the analyzed systems, a change in the ΔV value was obtained in different ranges, which proves the reorientation of molecules at the interface during compression of the mixed film DPPE/saponins extract. For the DPPE/GgC system, when the monolayer was compressed to a molecular area A of approximately 65 Å²/molec., slight changes in potential were recorded. Only after exceeding this value, a rapid increase in the surface potential value was visible, which corresponds to a rapid increase in surface pressure on the π-A isotherm (Figure 1). This indicates that the molecules are reoriented perpendicular to the surface at the interface and form an increasingly ordered structure at the interface. For the DPPE/GgP system, a more diversified course of ΔV–A curves relative to each other was obtained. The influence of saponins concentration on the course of the surface potential curve is particularly visible. However, in the case of the purified extract GgP, the influence of saponins concentration on the course of the potential curve is much more pronounced.

The greatest increase in the change of the potential value was obtained for the system with the highest saponins concentration, i.e., 10 mg/L. It can be assumed that a higher concentration of surfactant molecules at the interface reduces the available surface area and forces the molecules to strongly reorient to each other during film compression to ensure the best and most favorable packing. This also proves the presence of strong interactions between DPPE molecules and saponins.

2.1.2. Brewster Angle Microscopy Images

Brewster angle microscopy (BAM) images demonstrate the phase behavior of the Langmuir monolayers mimicking single leaflets of cell membranes. During the compression of the mixed monolayer, a visual analysis of the formed films has been performed.

The effect of the GgC concentration on the model membrane structure has been investigated. Figure 2 presents the BAM images of the studied systems at different surface pressure. The obtained BAM images for the DPPE monolayer indicate that the packing of the monolayer increases during the lipid film compression and then a homogeneous film is created. A continuous and densely packed film is reached at approximately 49 mN/m. The observed effect is consistent with the results presented in the literature [28]. It has been shown that the hydrogens in the DPPE ammonium group can form hydrogen bonds with neighboring DPPE headgroups. Therefore, molecules can easily interact with each other to form domains and consequently create a stable DPPE monolayer.

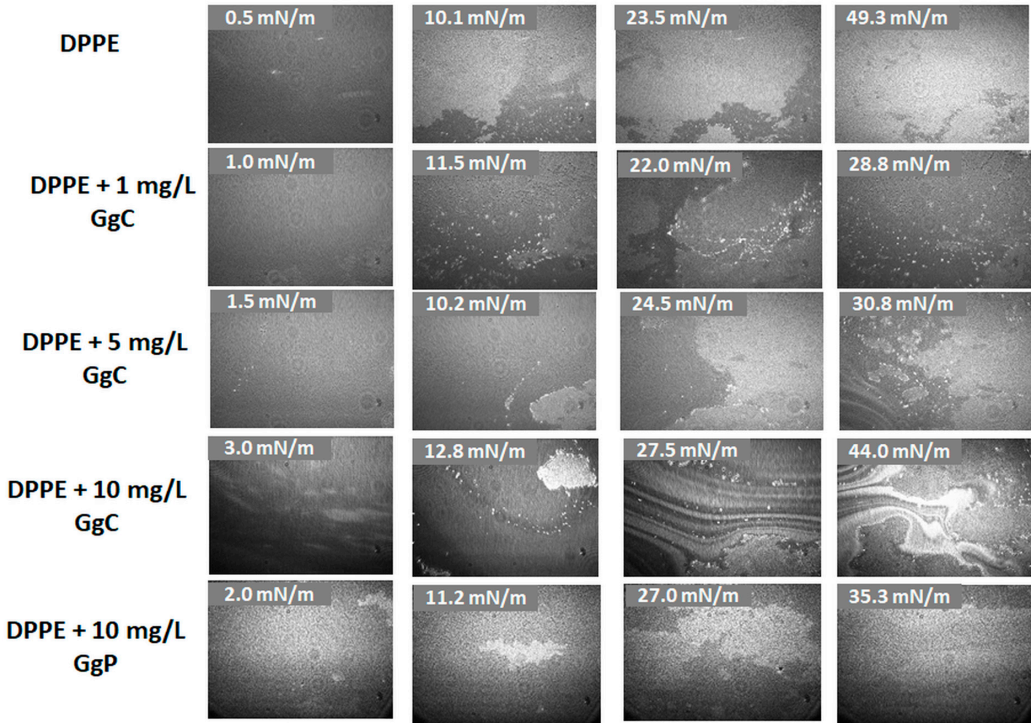

Figure 2. BAM images of DPPE, DPPE/GgC and DPPE/GgP monolayers at selected values of surface pressure, π.

BAM images indicated significant differences in the morphology of the clean DPPE and DPPE film after addition of the extract. Compressing a DPPE film with 1 mg/L of GgC to a surface pressure of approximately 11 mN/m results in the formation of domains that rise up at the lipids films (bright spots). The application of higher concentrations of the crude extract leads to the formation of large aggregates which interact with the lipid homogenous film and cause its disintegration. A two-phase heterogeneous structure was formed for a strongly compressed DPPE/GgC film (approximately 43 mN/m) at the concentration of 10 mg/L (Figure 2) and multi-layer ribbon-like structures were obtained afterwards. However, such a strong differentiation in the surface morphology cannot be observed for the DPPE/GgP system at the same concentration. Therefore, it can be assumed that the formed multilayer structures are mainly the result of the interaction between surface-active impurities present in the GgC extract and phospholipids.

2.1.3. Relaxation/Penetration Studies

The effect of saponins on monolayers was studied by measuring the surface pressure relaxation. The DPPE solution dissolved in chloroform was deposited onto the phosphate buffer and compressed to the initial surface pressure (π = 30 mN/m). Then, the subphase (phosphate buffer) was exchanged for the corresponding extract by a peristaltic pump.

Figure 3 shows the relaxation curves for the DPPE monolayers with various concentrations of the extracts. The relaxation experiment consisted of maintaining the molecular area (A) at a constant level and recording the surface pressure (π) as a function of time. When an extract was introduced into the subphase, a change in surface pressure value was observed in the monolayer ($\pi(t)$). If the value of ($\pi(t)$) is greater than the π_0 ($\pi(t)/\pi_0 > 1$), an increase in the area per molecule caused by the embedded saponins molecule in the phospholipid monolayer is indicated. Otherwise, if $\pi(t)/\pi_0 < 1$, there is a surface pressure loss in the monolayer. Hence, it can be assumed that the phospholipid molecules desorb from the monolayer and dissolve in the subphase. The π/π_0 parameter was therefore a measure of the monolayer stability. The obtained results clearly show that the process of incorporation of saponins molecules into the model membrane strongly depends on the concentration of the biosurfactant solution. Generally, it was observed that the increase of the saponins concentration in the subphase results in a more rapid incorporation of saponins into the monolayer. In case of both analyzed extracts, the relative value of the surface pressure was above 1, which means that saponins molecules slowly diffuse from the subphase to the phase boundary and are incorporated into the structure of the lipid film. A stronger effect of the interaction of the DPPE monolayer with the extract particles was observed for the GgP solution compared to GgC. The differences are clear in the case of a comparison of extract solutions at 50 mg/L. After 3500 s, the surface pressure of mixed monolayer increased by approximately 10% in the presence GgC solution, while in the case of the GgP system the increase was equal to approximately 50% (see Figure 3).

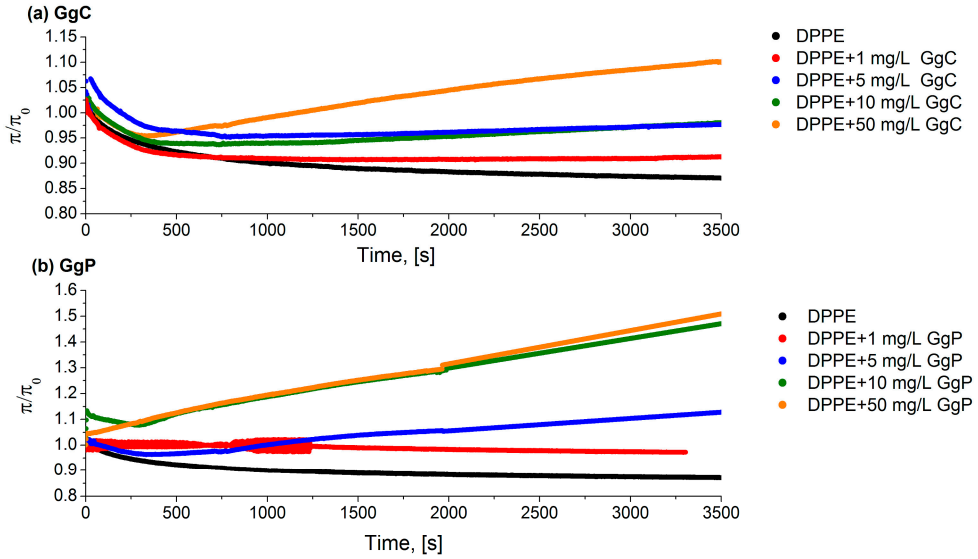

Figure 3. Relative surface pressure-time curves for a various concentration of saponins extracts (**a**) GgC, (**b**) GgP pumped underneath of DPPE monolayer.

On the basis of the obtained relaxation curves (Figure 3), it was found that the diffusion rate of molecules to the interface increased with the increase of the concentration of saponins in the system. The diffusivity of the system can be determined on the basis of the obtained slope of the relaxation curve. The greater slope, the stronger the diffusion of molecules from the subphase to the interface. On the other hand, for the GgC systems, it can also be observed that the lack of saponins' incorporation may result from the insufficient potential of the saponins molecules to expand the structure of the packed DPPE film. The DPPE monolayer at a surface pressure of 30 mN/m is characterized by C_s^{-1} value of approximately 90 mN/m, which corresponds to a film in the condensed liquid phase (LC). The formation of the DPPE film in the condensed liquid phase means an ordered film was

formed, in the case of which strong hydrophobic interactions occur between the hydrocarbon chains in the phospholipid molecules and contribute to a tightly packed monolayer. The formation of such a film may constitute a physical barrier that a small amount of saponins molecules are unable to overcome. Thus, they incorporate into the structure of the membrane, which leads to its emulsification. As presented in Figure 3, only a sufficiently high concentration of saponins can enhance the expansion of the compact structure and lead to its disturbance, thus facilitating the transport of other substances, such as drugs. Based on the obtained relaxation curves, it was found that the value of the surface pressure for the DPPE monolayer decreases over time, with a decline in the value of π/π_0 observed at the beginning of the relaxation process. Thus, the formed monomolecular DPPE film is not stable in the initial phase of the measurement, and the decreasing surface pressure values indicate the loss of adsorbed DPPE molecules from the buffer/air interface to the subphase. The addition of a low concentration of saponins extract to the system results in the formation of a mixed monolayer characterized by greater stability.

Nevertheless, it should be emphasized that the increase of the surfactant concentration in the subphase favors stronger penetration of saponins into the lipid structure of the membrane. Therefore, their excessive concentration may lead to changes in the turgor of cells. This applies not only to the membranes of bacteria, but also the membranes of other organelles in the body. Nowotarska et al. [32] also showed the effect of saponins (i.e., digitonin, tribulosin, dioscin, and escin) on the surface properties of the lipid monolayer of DMPC (dipalmitoyl phosphatidylcholine) enriched with cholesterol. The authors found that saponins strongly interact with the phospholipid film and the additional presence of cholesterol in the DMPC monolayer causes the formation of pores in the film and promotes the adsorption of saponins molecules to the lipid monolayer.

2.2. Interaction with a Spherical Model Membrane

In the next stage of the research, in order to approximate the model more closely to the real system, i.e., the living cell, tests were carried out with spherical systems, i.e., with liposomes. The results indicating the effect of saponins on surface properties of liposomes are presented in Figure 4. The hydrodynamic diameter of untreated liposomes is in the range of 342–615.1 nm with the largest share for 458.7 nm with $x_V = 37.2\%$. The addition of 10 mg/mL of GgC induced a shift towards larger particles, from 955.4 nm to 1990 nm. Hydrodynamic diameters, which are equal to 1484 nm with $x_V = 29.8\%$ and 1281 nm with $x_V = 28.5\%$, contribute to the total share to the greatest extent. Moreover, the increase of zeta potential of liposomes from −47 to almost −51.5 mV can be noticed (Table 2), with no noticeable effect on PDI. On the other hand, the purified extract did not cause a significant diameter shift toward larger particles when compared to liposomes exposed to GgC, but the stabilization of obtained suspension can be noticed, as the PDI declined to 0.537. On the other hand, the zeta potential increased to −42.74 mV.

Table 2. Zeta potential and Polydispersity Index (PDI) of samples, Ctrl—control sample of DPPE liposomes, GgC—liposomes with *G. glabra* crude extract, GgP—liposomes with *G. glabra* purified extract.

Sample	Zeta Potential ζ (mV)	PDI (-)
Control	−46.94 ± 3.06 [a]	0.800 ± 0.141 [a′]
GgC	−51.40 ± 0.89 [b]	0.797 ± 0.143 [a′]
GgP	−42.74 ± 1.77 [c]	0.537 ± 0.153 [a′]

Values marked with the same letter do not differ significantly ($p > 0.05$).

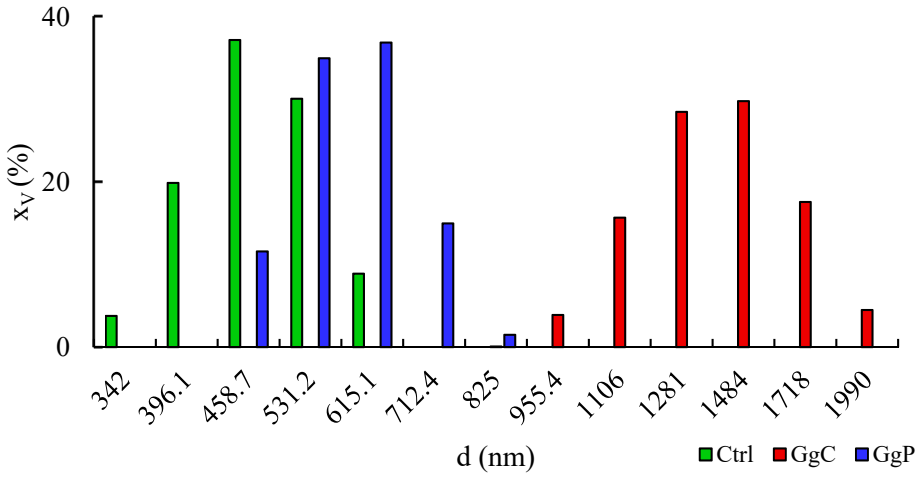

Figure 4. Particle size distribution of liposomes untreated and treated with extracts (x_v—volume fraction in %, d—hydrodynamic diameter); Ctrl—control sample of DPPE liposomes, GgC—liposomes with *G. glabra* crude extract, GgP—liposomes with *G. glabra* purified extract.

The zeta potential of a model biomembrane in the spherical form is mostly affected by the headgroups of phospholipids, the charges of which are responsible for the distribution of counter ions [2]. The value of zeta potential obtained for DPPE is typical for liposomes with an ethanolamine headgroup. As observed by Taetz et al., DOPE modified with hyaluronic acid and unmodified was in the range from +50 to +60 mV for pH 6.5 [3]. However, there are suggestions that the charge (positive or negative) of zeta potential may simply not be predicted based on the composition of headgroups i.e., it depends on ionic media and phase state [2,4]. Thus, the change in zeta potential value may indicate the disorders in charge distribution on the surface of liposomes. The presence of particles may disrupt the surface charge distribution as saponins are non-ionic surfactants.

Considering the size distribution, and polydispersity index results, the higher hydrodynamic diameter of particles treated with GgC and GgP may be noticed. As Rahnfeld et al. stated, the electrostatic interaction and hydration repulsive forces prevent the aggregation of negatively charged liposomes [5]. Hence, the size of particles may not be correlated with aggregation of liposomes but rather with a tear of liposome structures and joining into bigger vesicles with saponins during their incorporation. The effect of extract purification on the recorded results should also be noted. The shift in particle size toward larger values for the sample with GgC may be due to the greater influence of polymeric compounds (e.g., polysaccharides) on aggregate formation, also with DPPE. Similarly, in the case of zeta potential, it can be seen that the control sample and the sample with GgP exhibit more similar values than the one with liposomes from GgC.

This shows that not only the presence of saponins, but also the proportion of macromolecular compounds are important factors which affect the surface-active properties of natural surfactants.

Further important indications were provided by the analysis of infrared spectra of liposome samples, which are presented in Figure 5. Among the outstanding signals, one should point out those at approximately 1730 cm^{-1} originating from the stretching vibrations of the carbonyl group. Significant differences between the spectra can be seen at approximately 1240 cm^{-1} and 1090 cm^{-1}, which most likely originate from the P=O bond vibrations of the phosphate group of phospholipids. Changes in these regions may indicate that the compounds present in the GgC and GgP extracts interact mainly with the hydrophilic parts of the phospholipid molecules. Since there are no significant changes in

signals from the hydrocarbon chain, it can be assumed that the compounds present in the extracts, including saponins, do not penetrate deeper into the liposome membrane.

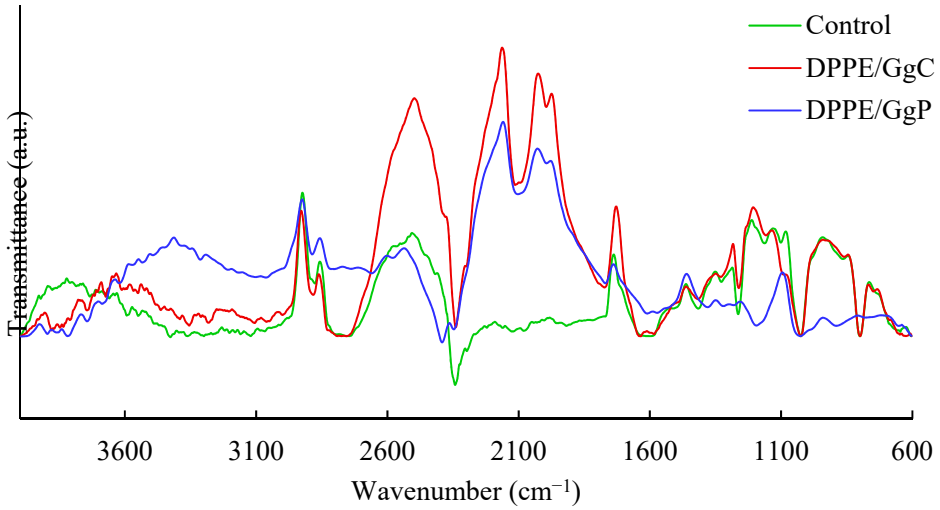

Figure 5. FTIR spectra of DPPE/GgC and DPPE/GgP.

3. Discussion

Model biological membranes prepared using the Langmuir technique are used to mimic real membrane conditions and represent a useful tool for characterizing membrane component interactions with active substances present in saponins extract at the molecular level. Through the use of a model membrane, the effects of licorice concentrations and its impurities on the surface properties of a lipid DPPE film were investigated. For all analyzed systems, it was established that interactions between saponins and phospholipids occur. This is evidenced by the incorporation of molecules into the structure of the film, which is confirmed by the obtained test results, e.g., shift of the π–A isotherm towards higher surface values as well as an increase in surface pressure during the DPPE relaxation process. Undoubtedly, it has been shown that the surface properties are influenced by the concentration of saponins and the purity of the applied extract. Stronger interaction effects were observed for the purified extract. Moreover, purified extracts GgP introduced into the DPPE monolayer cause the formation of mixed films characterized by greater condensation and packing, as evidenced by the estimated values of maximum compressibility. The obtained results also showed significant interference of saponins in the morphology of the model lipid membrane.

In addition, differences between purified and crude extracts were also found in terms of their interaction with liposomal systems. Changes in particle size distribution and zeta potential show that GgC may contain macromolecular compounds that form relatively large agglomerates. In addition, changes in the infrared spectra may suggest that the interaction of extract components with phospholipids mainly involves their hydrophilic parts, i.e., phosphate groups.

In summary, it can be concluded that the GgP extract exhibited better surface activities in reference to the two-dimensional lipid monolayer. The exclusion of other surface-active compounds present in the extract by filtration promoted the increase of interactions of saponins with lipid molecules. Moreover, filtration of the extract reduces the amount of other surface-active compounds which could be competitive with saponins during adsorption at the interface. The stronger surface-active properties of GgP compared to GgC directly indicate the importance of the extract purification process. The exclusion of large-molecular compounds above 3kDa and small-molecular compounds below 0.5 kDa clearly improved the homogeneity of the plant surfactant composition. Moreover, it can

be concluded that the percentage of saponins, as the key group of compounds responsible for the surface properties of the purified extract fraction, increased significantly in GgC.

4. Materials and Methods

Chemicals

Extract from *Glycyrhizza glabra* roots from FLOS (Mokrsko, Poland) was obtained by methanol extraction in a Soxhlet apparatus. Then, the extract was subjected to two nanofiltration processes, first using a 3-kDa (Merckmilipore, Darmstadt, Germany) membrane, then, the second, with the use of a 0.5-kDa membrane (TriSep, Sterlitech, Auburn, WA, USA). The process was conducted using Amicon Stirred Cell with a total volume of 200 mL (Merkmilipore). As a result, two fractions of extracts were used during the research, crude extract marked as GgC and purified extract (with molecules size between 3 kDa and 0.5 kDa), GgP.

In the presented studies, 1,2-dipalmitoyl-*sn*-glycero-3-phosphoethanolamine (DPPE, 99%; from Avanti Polar Lipids (Alabaster, AL, USA)) was used as the film and liposome forming substance. Chloroform of high-purity Uvasol (Merck, Warszawa, Poland) was used to prepare the Langmuir monolayer. Dulbecco's Phosphate Buffered Saline (Sigma Aldrich, Poznań wielkopolskie, Poland) was applied as a solvent to prepare saponins solution or as a subphase.

Deuterium oxide was purchased from Merck KGaA (Darmstadt, Germany)

4.1. Research Regarding Monolayer Membranes

π–A isotherms

The subphase was placed in a Teflon trough (KSV Nima, Helsinki, Finland) with a surface area of 238 cm^2. During the measurements, the temperature was kept constant at 25.0 ± 0.1 °C with a Julabo circulator. Before each measurement, the subphase was cleaned to the surface pressure below π = 0.35 mN/m reached in maximum compression.

First, the DPPC solution (with c = 1 mg/mL) was spread on the buffer surface with a Hamilton microsyringe (25 µL), and chloroform was allowed to evaporate for 15 min. One minute before the compression of the monolayer was started, the appropriate concentration of saponins solution was injected into the well and stirred. The monolayer was compressed by symmetrical movement of the barriers with a velocity of 10 mm/min.

The surface pressure π (mN/m) was measured as the function of the area per DPPE molecule A ($Å^2$/molec.).

Surface potential measurements

The surface potential (ΔV) was measured simultaneously with surface pressure using surface potential sensor. The non-destructive, non-contact vibrating capacitor method was applied (SPOT; KSV Nima). The instrument worked with two electrodes: the first immersed in the subphase and the vibrating electrode located just above the water surface. The surface potential was measured with the sensitivity of ±1 mV.

Brewster angle microscopy

Brewster angle microscopy (MicroBAM; KSV Nima) was used to visualize the monolayer morphology. The images were captured during the monolayer compression. A black glass plate was placed under the subphase to absorb the refracted beam. The resolution of the image was equal to approximately 6 microns $pixel^{-1}$.

Relaxation measurements

The relaxation of the DPPE film was observed when additional molecules were introduced into the monolayer using a peristaltic pump (MINIPULS 3, Gilson, Middleton, WI, USA). After formation of the DPPE monolayer, the subphase (DPBS buffer) was replaced with a new solution which contained various concentrations of saponins. A detailed description of the measurement has been provided in our previous publication [12]. The relaxation experiments were performed for the pure DPPE monolayer and mixed systems: DPPE/saponins. The DPPE film was initially compressed to a desired surface pressure of 30 mN/m and after that the solution of saponins was pumped underneath the film

to the subphase. The observed changes in surface pressure were recorded over time. The obtained results were presented as π/π_0, which is the ratio of the actual surface pressure in time t to the surface pressure at the moment of injection at a constant molecular area between barriers. The temperature of the experiments (25 °C) was kept constant and controlled during measurements by a Julabo F-12 circulator (Cole-Parmer, Wertheim-Mondfel, Germany).

4.2. Research Regarding Spherical Membranes

Liposomes preparation

Liposomes were prepared as described by Costa et al. [33]. Briefly, DPPE was dissolved in chloroform, followed by evaporation of the organic solvent in a nitrogen stream to obtain a thin phospholipid film. Then, 5 mg/mL of the extract in H_2O PBS buffer was used for hydronation of the obtained film, to achieve a final concentration of liposomes equal to 2.5%. Then, the solution was subjected to 10 freeze-thaw cycles as a form of homogenization of the systems. For FTIR measurements, H_2O was replaced by D_2O.

FTIR

Fourier-transform infrared spectroscopy–attenuated total reflectance (FTIR–ATR) was used to analyze the possible wavelength shift as a result of interaction between saponins and phospholipids. In this method, infrared radiation with a vibration frequency close to that of the particles' bonds is used. Because of that, radiation which penetrates the tested sample is absorbed selectively and increases the vibration amplitude of the functional groups. This allows the characteristic absorption spectrum to be obtained. Measurements was conducted for liposomes suspended in D_2O/PBS using Vertex 70 (Bruker, Billerica, MA, USA).

Zeta & Size

The hydrodynamic diameter of the particles was measured by using the dynamic light scattering method. Zeta potential was calculated using the Smoluchowski equation based on electrophoretic light scattering results. Both analyses were conducted Zetasizer Nano ZS (Malvern Panalytical, Malvern, UK). Measurements were performed at a stable pH equal to 7.4.

5. Conclusions

Studies carried out using the Langmuir technique as well as the experiments with liposomes allow to conclude that the tested plant extracts rich in saponins interact with phospholipids present in model biological membranes. However, the strength of these interactions is determined by both the concentration of saponins and the purity of the extract used. The addition of the purified extract to the phospholipid forms a mixed monolayer. It has been proven that the presence of saponins affects the structure and morphology of the model phospholipid membrane, both in the case of flat membrane and spherical liposomes. The results may suggest that the effects of natural surfactants on membranes are mainly caused by their interaction with the hydrophilic part of liposomes.

Author Contributions: Conceptualization, W.S., M.R., A.G., K.P. and E.K.; methodology, investigation, M.R., W.S. and A.G.; writing—original draft preparation, M.R., A.G. and W.S.; writing—review and editing, K.P. and E.K.; supervision, K.P. and E.K.; project administration and funding acquisition, E.K. All authors have read and agreed to the published version of the manuscript.

Funding: This research was funded by the National Science Center, Poland, grant number 2020/39/B/NZ9/03196.

Institutional Review Board Statement: Not applicable

Informed Consent Statement: Not applicable

Data Availability Statement: All data are available from the authors on request.

Conflicts of Interest: The authors declare no conflict of interest.

Sample Availability: Samples of the saponins-rich plant extracts are available from the authors.

References

1. Kregiel, D.; Berlowska, J.; Witonska, I.; Antolak, H.; Proestos, C.; Babic, M.; Babic, L.; Zhang, B. Saponin-Based, Biological-Active Surfactants from Plants. In *Application and Characterization of Surfactants*; Reza Najjar, R., Ed.; Intech Open: Rijeka, Croatia, 2017 https://doi.org/10.5772/68062. https://www.intechopen.com/chapters/54735.
2. Liao , Y.; Li, Z.; Zhou, Q.; Sheng, M.; Qu, Q.; Shi, Y.; Yanga, J.; Lv, L.; Dai, X.; Shi, X. Saponin surfactants used in drug delivery systems: A new application for natural medicine components, *Int. J. Pharm.* **2021**, *603*, 120709. https://doi.org/10.1016/j.ijpharm.2021.120709.
3. Liwa, A.C.; Barton, E.N.; Cole, W.C.; Nwokocha, C.R. Chapter 15—Bioactive Plant Molecules, Sources and Mechanism of Action in the Treatment of Cardiovascular Disease. In *Pharmacognosy Fundamentals, Applications and Strategies*; Academic Press: Boston, MA, USA, 2017; pp. 15–336.
4. Vincken, J.-P. ; Heng, L.; de Groot, A. ; Gruppen, H. Saponins, classification and occurrence in the plant kingdom, *Phytochemistry* **2007**, *68*, 275–297. https://doi.org/10.1016/j.phytochem.2006.10.008.
5. Yang, R.; Wang, L.; Yuan, B.; Liu, Y. The Pharmacological Activities of Licorice, *Planta Med*. **2015**, *81*, 1654–69. https://doi.org/10.1055/s-0035-1557893.
6. Pastorino, G.; Cornara, L.; Soares, S.; Rodrigues, F.; Beatriz, M.; Oliveira, M. Liquorice (Glycyrrhiza glabra): A phytochemical and pharmacological review, *Phytother Res.* **2018**, *32*, 2323–2339. https://doi.org/10.1002/ptr.6178.
7. Al-Turki, A.I.; El-Ziney, M.G.; Abdel-Salam, A.M. Chemical and anti-bacterial characterization of aqueous extracts of oregano, marjoram, sage and licorice and their application in milk and labneh. *J. Food Agric Environ.* **2008**, *6*, 39–44.
8. Zhou, T.Z.; Deng, X.M.; Qiu, J.Z. Antimicrobial activity of licochalcone E against Staphylococcus aureus and its impact on the production of staphylococcal alpha-toxin. *J. Microbiol. Biotechnol.* **2012**, *22*, 800–805. https://doi.org/10.4014/jmb.1112.12020.
9. Messier, C.; Grenier, D. Effect of licorice compounds licochalcone A, glabridin and glycyrrhizic acid on growth and virulence properties of Candida albicans. *Mycoses* **2011**, *54*, e801–e806. https://doi.org/10.1111/j.1439-0507.2011.02028.x.
10. Wang, L.; Yang, R.; Yuan, B.; Liu, Y.; Liu, C. The antiviral and antimicrobial activities of licorice, a widely-used Chinese herb, *Acta Pharm Sin B.* **2015**, *5*, 310–315.. https://doi.org/10.1016/j.apsb.2015.05.005.
11. Güçlü-Ustündağ, O.; Mazza, G. Saponins: Properties, applications and processing, *Crit. Rev. Food Sci. Nutr*. **2007**, *47*, 231–58. https://doi.org/10.1080/10408390600698197.
12. Rojewska, M.; Smułek, W.; Prochaska, K.; Kaczorek, E. Combined Effect of Nitrofurantoin and Plant Surfactant on Bacteria Phospholipid Membrane, *Molecules* **2020**, *25*, 2527. https://doi.org/10.3390/molecules25112527.
13. de Groot, C.; Müller-Goymann, C.C. Saponin Interactions with Model Membrane Systems—Langmuir Monolayer Studies, Hemolysis and Formation of ISCOMs, *Planta Med.* **2016**, *82*, 1496–1512. https://doi.org/10.1055/s-0042-118387.
14. Orczyk, M.; Wojciechowski, K. Comparison of the effect of two Quillaja bark saponin extracts on DPPC and DPPC/cholesterol Langmuir monolayers, *Colloids Surf. B* **2015**, *136*, 291–299. https://doi.org/10.1016/j.colsurfb.2015.09.018.
15. Korchowiec, B.; Gorczyca, M.; Wojszko, K.; Janikowska, M.; Henry, M.; Rogalska, E. Impact of two different saponins on the organization of model lipid membranes, *Biochim Biophys Acta* **2015**, *1848*, 1963–1973. https://doi.org/10.1016/j.bbamem.2015.06.007.
16. Stępnik, K. Biomimetic Chromatographic Studies Combined with the Computational Approach to Investigate the Ability of Triterpenoid Saponins of Plant Origin to Cross the Blood-Brain Barrier, *Int. J. Mol. Sci.* **2021**, *22*, 3573. https://doi.org/10.3390/ijms22073573.
17. Geisler, R.; Dargel, C.; Hellweg, T. The biosurfactant β-aescin: A review on the physico-chemical properties and its interaction with lipid model membranes and Langmuir monolayers. *Molecules* **2019**, *25*, 117. https://doi.org/10.3390/molecules25010117.
18. Aguilar-Pérez, K.; Avilés-Castrillo, J.; Medina, D.I.; Parra-Saldivar, R.; Iqbal, H. Insight into Nanoliposomes as Smart Nanocarriers for Greening the Twenty-First century Biomedical Settings. *Front. Bioeng. Biotechnol.* **2021**, *8*, 1441. https://doi.org/10.3389/fbioe.2020.579536.
19. Ajeeshkumar, K.K.; Aneesh, P.A.; Raju, N.; Suseela, M.; Ravishankar, C.N.; Benjakul, S. Advancements in liposome technology: Preparation techniques and applications in food, functional foods, and bioactive delivery: A review, *Compr. Rev. Food Sci. Food Saf.* **2021**, *20*, 1280–1306, doi.org/10.1111/1541-4337.12725.
20. Szcześ, A.; Jurak, M.; Chibowski, E. Stability of binary model membranes—Prediction of the liposome stability by the Langmuir monolayer study, *J. Colloid Interface Sci.* **2012**, *372*, 212–216. https://doi.org/10.1016/j.jcis.2012.01.035.
21. Rojewska, M.; Smułek, W.; Kaczorek, E.; Prochaska, K. Langmuir Monolayer Techniques for the Investigation of Model Bacterial Membranes and Antibiotic Biodegradation Mechanisms, *Membranes* **2021**, *11*, 707. https://doi.org/10.3390/membranes11090707.
22. Elderdfi, M.; Sikorski, A.F. Langmuir-monolayer methodologies for characterizing protein-lipid interactions, *Chem. Phys. Lipids* **2018**, *212*, 61–72. https://doi.org/10.1016/j.chemphyslip.2018.
23. Dopierała, K.; Weiss, M.; Krajewska, M.; Błońska, J. Towards understanding the binding affinity of lipid drug carriers to serum albumin, *Chem. Phys. Lipids* **2022**, *250*, 105271. https://doi.org/10.1016/j.chemphyslip.2022.105271.

24. Otzen, D.E. Biosurfactants and surfactants interacting with membranes and proteins: Same but different? *Biochim. Biophys. Acta Biomembr.* **2017**, *1859*, 639–649. https://doi.org/10.1016/j.bbamem.2016.09.024.
25. Brown, R.E.; Brockman, H.L. Using monomolecular films to characterize lipid lateral interactions. *Methods Mol. Biol.* **2007**, *398*, 41–58. https://doi.org/10.1007/978-1-59745-513-8_5.
26. Przykaza, K.; Woźniak, K.; Jurak, M.; Wiącek, A.E.; Mroczka, R. Properties of the Langmuir and Langmuir–Blodgett monolayers of cholesterol-cyclosporine A on water and polymer support. *Adsorption* **2019**, *25*, 923–936. https://doi.org/10.1007/s10450-019-00117-2.
27. Schmid, C.; Dawid, C.; Peter, V.; Hofmann, T. Saponins from European Licorice Roots (Glycyrrhiza glabra), *J. Nat. Prod.* **2018**, *81*, 1734–1744. https://doi.org/10.1021/acs.jnatprod.8b00022.
28. Chen, X.; Huang, Z.; Hua,W.; Castada, H.; Allen, H.C. Reorganization and Caging of DPPC, DPPE, DPPG, and DPPS Monolayers Caused by Dimethylsulfoxide Observed Using Brewster Angle Microscopy, *Langmuir* **2010**, *26*, 18902–18908. c10.1021/la102842a.
29. Davies, J.T.; Rideal,K. *Interfacial Phenomena*, 2nd ed.; Academic Press: New York, NY, USA, 1963; p. 265.
30. Dynarowicz–Łątka, P.; Dhanabalan, A.; Oliveira, O.N. Jr. Modern physicochemical research on Langmuir monolayers. *Adv. Colloid Interface Sci.* **2001**, 91, 221–293. https://doi.org/10.1016/S0001-868600034-2.
31. Jurak, M.; Szafran, K.; Cea, P.; Martin, S. Analysis of Molecular Interactions between Components in Phospholipid-Immunosuppressant-Antioxidant Mixed Langmuir Films. *Langmuir* **2021**, *37*, 5601–5616. https://doi.org/10.1021/acs.langmuir.1c00434.
32. Nowotarska, S.; Nowotarski, K.; Friedman, M.; Situ, C. Effect of Structure on the Interactions between Five Natural Antimicrobial Compounds and Phospholipids of Bacterial Cell Membrane on Model Monolayers. *Molecules* **2014**, *19*, 7497–7515. https://doi.org/10.3390/molecules19067497.
33. Costa, A.P.; Xu, X.; Khan, M.; Burgess, D.J. Liposome Formation Using a Coaxial Turbulent Jet in Co-Flow. *Pharmaceutical Research* **2016**, *33*, 404–416. https://doi.org/10.1007/s11095-015-1798-8.

Publication P3

World Journal of Microbiology and Biotechnology (2024) 40:152
https://doi.org/10.1007/s11274-024-03961-9

RESEARCH

Saponaria officinalis saponins as a factor increasing permeability of *Candida* yeasts' biomembrane

Adam Grzywaczyk[1] · Wojciech Smułek[1] · Ewa Kaczorek[1]

Received: 12 June 2023 / Accepted: 18 March 2024

Abstract
Saponins are a large group of compounds, produced mostly by plants as a side product of their metabolic activity. These compounds have attracted much attention over the years mostly because of their surface activity and antibacterial, anti-inflammatory and antifungal properties. On the other hand, most of the hitherto research has concerned the action of saponins against microbial cells as a whole. Therefore, knowing the possible interaction of saponins with biomembrane, we decided to check in-vitro the influence of saponin-rich extract of *Saponaria officinalis* on spheroplasts of two *Candida* sp. The obtained results show that 10 mg L^{-1} of extract increased the permeability of spheroplasts up to 21.76% relative to that of the control sample. Moreover, the evaluation of surface potential has revealed a decrease by almost 10 mV relative to that of the untreated samples. Such results suggest its direct correlation to integration of saponins into the biomembrane structure. The obtained results have proved the antifungal potential of saponins and their ability of permeabilization of cells. This proves the high potential of saponins use as additives to antifungal pharmaceutics, which is expected to lead to improvement of their action or reduction of required dosage.

Keywords Saponins · *Candida* · Candidiasis · Permeability · Biomembrane

Introduction

Mycosis is a worldwide problem. It is estimated that over 20–25% of the global population is affected by skin mycosis. This medical condition is mostly caused by dermatophytes from the genera *Trichophyton*, *Microsporum*, and *Epidermophyton* (Havlickova et al. 2008). Hence the name of this type of mycosis – dermatophytosis. On the other hand, the second type of mycosis - candidiasis is an infection caused by pathogenic species of *Candida* genus. This opportunistic yeast genus is responsible for superficial, as well as deep-seated mycosis (Douglas et al. 2003). According to Gawdzik et al. (2019), from among 11 000 patients from southwest Poland, mycosis was diagnosed in 1653 cases, from which 716 people were infected by yeasts, and *Candida* spp. was responsible for 67.66% of contagion. Moreover, Pfaller et al. have confirmed that invasive candidiasis is a leading cause of mycosis-associated mortality in the United States of approximately 0.4 death per 100 000 people and Brown et al. have shown that mortality related to invasive candidiasis is more than 50% (Pfaller et al. 2007; Brown et al. 2012). The main fungal pathogens that cause candidiasis are *Candida albicans*, *C. krusei, C. glabarta, C. parapsilosis*, and *C. tropicalis* (Dąbrowska et al. 2019).

Even though the *Candida* genus is an indispensable part of human flora, the candidacies affect many different types of human systems, tissues, and organs, such as oral infections, vulvovaginal candidacies, skin illnesses, bloodstream, urinary tract infections, and gastrointestinal inflammation (Vila et al. 2020; Sobel et al. 2007; Kühbacher et al. 2017; Ortega et al. 2011; Behzadi et al. 2015; Kumamoto et al. 2012). On the other hand, the global trend of increasing drug resistance of microorganisms has also affected *Candida* fungi. Increasing drug resistance includes lowering the number of substances needed for the cell wall and

✉ Adam Grzywaczyk
adam.grzywaczyk@doctorate.put.poznan.pl

Wojciech Smułek
wojciech.smulek@put.poznan.pl

Ewa Kaczorek
ewa.kaczorek@put.poznan.pl

[1] Institute of Chemical Technology and Engineering, Poznan University of Technology, Berdychowo 4, Poznan 60-695, Poland

Published online: 30 March 2024

biomembrane creation, reducing the uptake of pharmaceuticals from the environment, or gene modification (Bondaryk et al. 2013). Moreover, misuse of antifungal drugs, as well as repeated therapy may lead to increase in drug resistance (Pristov et al. 2019; Tsuzuki et al. 2007).

One possible approach to overcome this phenomenon is the use of compounds capable of interacting with a biological membrane. Saponins are an example of plant-derived biosurfactants capable of either embedding the hydrophobic part into the structure of the cell membrane, or forming holes in the structure of the cell membrane (Dawid et al. 2020). This is a diverse group of compounds that differ in the type of hydrophobic group (steroid or triterpene) and the structure of the sugar chain, which is the hydrophilic part of the saponin molecule. Moreover, these compounds can be found in many plants such as liquorice, soap tree, and soapwort (Podolak et al. 2010).

Saponaria officinalis L., commonly known as soapwort, is a plant renowned for its abundant saponin content, particularly concentrated in its root, reaching levels as high as 21% (Jurado Gonzalez et al. 2020). Indigenous to the Eurasian region, it thrives predominantly in the Mediterranean and Irano-Turanian zones, as well as across Central Europe (Jurado Gonzalez et al. 2020; Chandra et al. 2021). Its widespread presence has historically led to its holistic utilization, with various parts of the plant employed for medicinal purposes since antiquity. It has been traditionally applied in the treatment of skin ailments, such as eczema and acne, as well as for addressing rheumatism, bone deformities, respiratory issues, and liver disorders (Chandra et al. 2015). Moreover, it is recognized for its antibacterial and antifungal attributes, notably effective against *Candida* yeasts (Smułek et al. 2017; Sadowska et al. 2014).

Hence, this investigation concentrates on exploring the effects of a pure and nanofiltration-purified extract of *Saponaria officinalis* L. on *Candida albicans* and *Candida krusei* cells that have been enzymatically depleted of their cell walls, commonly referred to as spheroplasts. Although the interaction of saponins with *Candida* cells has been studied, the main concern was the presence of the cell wall, which is an important barrier between the fungal cell and the external environment (Coleman et al. 2010). In this study, knowing the properties of saponins, we decided to check the properties of the cell membrane after treatment with a saponin-rich extract, such as its permeability and adsorption capacity, which has never been described before. As we showed elsewhere, the concentration 10 mg L^{-1}*Sapindus mukorossi* saponin-rich solution, was simultaneously nontoxic to intestinal epithelial cells for which the dependence of metabolic activity on saponin concentration was determined (Grzywaczyk et al. 2023). Therefore, our previous studies led to the selection of concentrations − 5, 10, and 15 mg L^{-1}, of *Saponaria officinalis* L. both crude and purified, which may potentially have a slight impact on non-target cells including epithaphial cells, while demonstrating an effect on the permeability and adsorptive capacities of *Candida* biomembrane. The obtained results may provide important information on a possible usage of plant saponin as a drug adjuvant, cellular response to biosurfactants, and thus, constitute the next step in the research on counteracting the growing antibiotic resistance.

Materials & methods

Chemicals

All chemicals used in this study were of the highest purity grade and were purchased from Merck KGaA (Darmstadt, Germany). *Saponaria officinalis* roots were obtained from Flos (Mokrsko, Poland). Sabouraud agar dextrose 2% and Sabouraud agar glucose 4% were purchased from BTL (Łódź, Poland).

Extract preparation & nanofiltration process

The *Saponaria officinalis* extract was obtained via methanol extraction as described by Smułek et al. (2016). The plant roots were placed in a Soxhlet apparatus and subjected to methanol extraction for 6 h. After that, methanol was removed using a rotary evaporator. As a results, crude extract was obtained, marked as a SoC. In our previous research, we established the presence of Gypsogenin, Hydroxygypsogenic acid, Quillaic acid, Hederagenin, and Hydroxyhederagenin within this extract, each containing pentose or hexose sugar groups. Notably, the CMC of this extract was determined to be 1.50 g/L (Grzywaczyk et al. 2023).

Nanofiltration process was used in order to obtain a saponins-rich fraction of *Saponaria officinalis* extract. Amicon Stirred Cells (Merck Milipore, USA) equipped with 3 kDa filtration discs were used in the first step (Merck Milipore, USA), and 0.5 kDa discs were used in the next stage of the process (Sterlitech, USA).

As mentioned before, the nanofiltration process was divided into two steps. In the first step, crude extract was filtered through 3 kDa membranes, the permeate was collected and used in the second nanofiltration process. So, in the first step, a fraction with particles < 3 kDa was obtained. The second filtration was carried out using 0.5 kDa membrane and the retentate was collected. As a results, a fraction 0.5 kDa – 3.0 kDa was obtained as a rich-saponin Saponaria officinalis fraction and marked as a SoP.

Yeast strain & culture conditions

Two strains of yeast from *Candida* strain were used in the research: *Candida albicans* (Polish Collection of Microorganisms no. 2566) and *Candida krusei* (Polish Collection of Microorganisms no. 2706). The yeasts were stored, *C. krusei* on Sabouraud agar dextrose 2% and *C. albicans* on Sabouraud agar glucose 4% agar plates. For incubation, the fungal biomass was suspended in a nutrient broth until it reached the exponential growth phase. The fungal cultures prepared were then centrifuged at 4500 rcf and re-suspended in an isotonic PBS solution with a constant pH of 7.4.

To evaluate the growth curves of both strains, they were cultured with the presence of *Saponaria officinalis* L. crude and purified extracts respectively in the range of final concentration of 5.0, 6.25, 12.5, 25.0, 50.0, 62.5, 125.0, 250.0 and 500.0 mg L^{-1}.

Spheroplasts preparation

Spheroplasts were prepared as described by Stirke et al. (2019). The cells were centrifuged, suspended in lyticase pH 6.0 buffer (0.112 M of boric acid, 0.028 M of citric acid, and 0.082 M tertiary sodium phosphate) and adjusted to 1.5 OD_{600}. Then, 50 U/mL of lyticase was added and incubated for 2 h at 30 °C. After that, the cells were centrifuged and washed twice with PBS. For analysis, the spheroplasts at $OD_{600} = 1.0$ were used. The changes in structure of cells and spheroplasts were analysed with TEM microscopy. Henceforth, the spheroplasts of *C. albicans* and *C. krusei* strains will be referred to as *C.albSP* and *C.krsSP* respectively. The spheroplast were then incubated for 24 h with *Saponaria officinalis* L. crude and purified extract at concentrations of 5, 10, and 15 mg L^{-1} respectively. The positive control consisted of spheroplasts not treated with saponins, while the negative control included saponin-untreated and wall-containing cells.

Transmission electron microscopy

Morphological evaluation of the cells and their spheroplasts was made on the basis of transmission electron microscope (TEM) data, HT7700 (Hitachi, Tokyo, Japan). The cells or spheroplasts suspensions were placed on a copper grid coated with carbon film and negatively stained with 2% tungstic acid.

Cell surface properties

The surface properties were assessed using Crystal Violet assay for cell permeability determination and Congo Red assay for cells adsorption capacity evaluation. Fungal cells and the spheroplasts were prepared as described above. Then, they were resuspended in PBS buffer to obtain the $OD_{600} = 1.0$. Total membrane permeability was tested according to Devi et al. (2013) by colorimetric measurements of the rate of crystal violet absorbed by the cells/spheroplasts. Moreover, cell surface hydrophobicity was studied by measuring the adsorption of Congo red dye on the surface of microbial cells (CR assay) (Ambalam et al. 2012). Cell/spheroplasts surface zeta potential analyses were conducted as described by Smułek et al. (2016) at a constant pH of 7.4.

Cytotoxicity analysis

To evaluate fungal cells' viability, MTT assay was applied according to a modified protocol described by Oh and Hong (2022). Briefly, the test was based on the colorimetric reaction of yellow 3-(4,5-dimethylthiazol-2-yl)-2,5-diphenyltetrazolium bromide (MTT) which is transformed to its violet formazan by living cells.

Statistical analysis

The results presented in the study were calculated as an average value from at least three independent experiments. The variance analysis and t-Student test were applied to determine the statistical significance of differences between the average values. The differences were considered statistically significant at $p < 0.05$. All calculations were conducted using Excel 2019 (Microsoft Office) software.

Results & discussion

Transmission electron microscopy observation

The morphology of *Candida* cells is typical of yeast cells. After the growth in the liquid culture, the *Candida* cells may have elongated. However, the mechanism responsible for the changes in the cell shape are still unknown (Huang et al. 2008). Figure 1A presents a compact structure of a cell not subjected to enzymatic lysis of a cell wall. The visibly lighter area is most likely the vacuole (Figs. 1A), and the darker area is the cell nucleus (Fig. 1A). After the enzymatic reaction the image is changed. Major vacuoles can be noticed, i.e. the outer layer of the cells (Figs. 1A) becomes thinner, which may indicate the lack of a cell wall (Figs. 1B). Moreover, the uptake of the dye used for TEM observations increased, as the blackening of cell increased when compared to that of the control sample. In case of 5 mg L^{-1} SoC treatment (Fig. 1C), no visible changes in

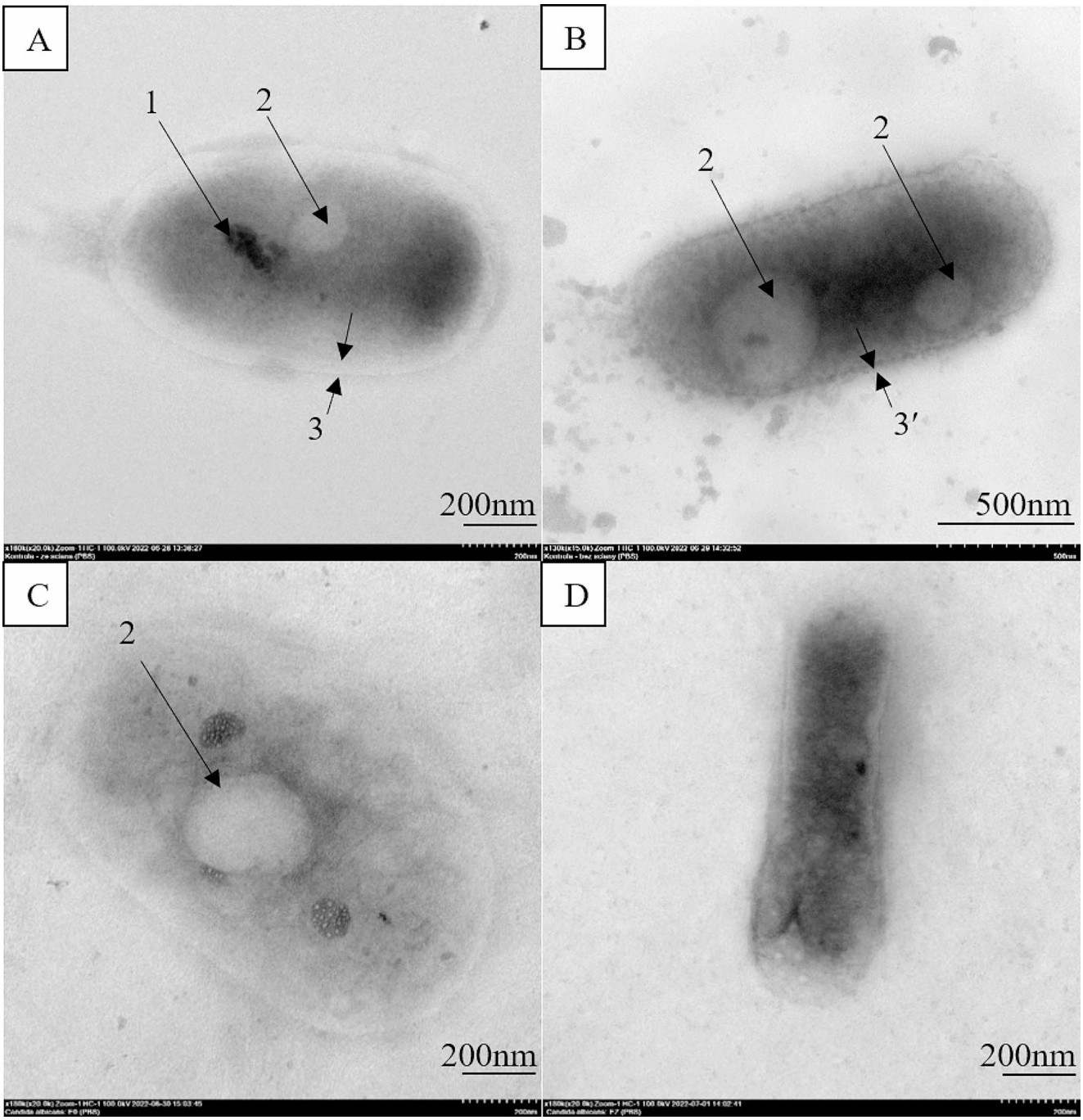

Fig. 1 TEM pictures of *Candida albicans***A** – control (untreated cells), **B** – spheroplasts, **C** – SoC treatment, **D** – SoP treatment, 1-nucelus, 2-vacuole, 3, 3' – outer cell layer

morphology of spheroplasts were observed. However, the inner part of the cell can still be visible (vacuoles, nucleus).

The morphology of *Candida krusei* cells, is similar to that obtained for *C. albicans*. In comparison to Ctrl sample, the inner part of the cell structure, to a small extent expands the outer membrane of a spheroplast, which is protected against lysis in an isotonic PBS buffer environment (Fig. 2B). The lack of cell wall does not have to be directly correlated with the cell lysis. As presented by Huang et al. (2008), the damage of *E. coli* cell wall can be compensated by cytoplasmatic bulge, without changes in the cell shape. Moreover, modification of the cell wall by bacteria may even be one of the mechanisms of their antibiotic resistance (Claessen et al. 2019). The cells of *C.krsSP* treated with 5 mg L^{-1} SoC do not show any observable structural changes. However, 5

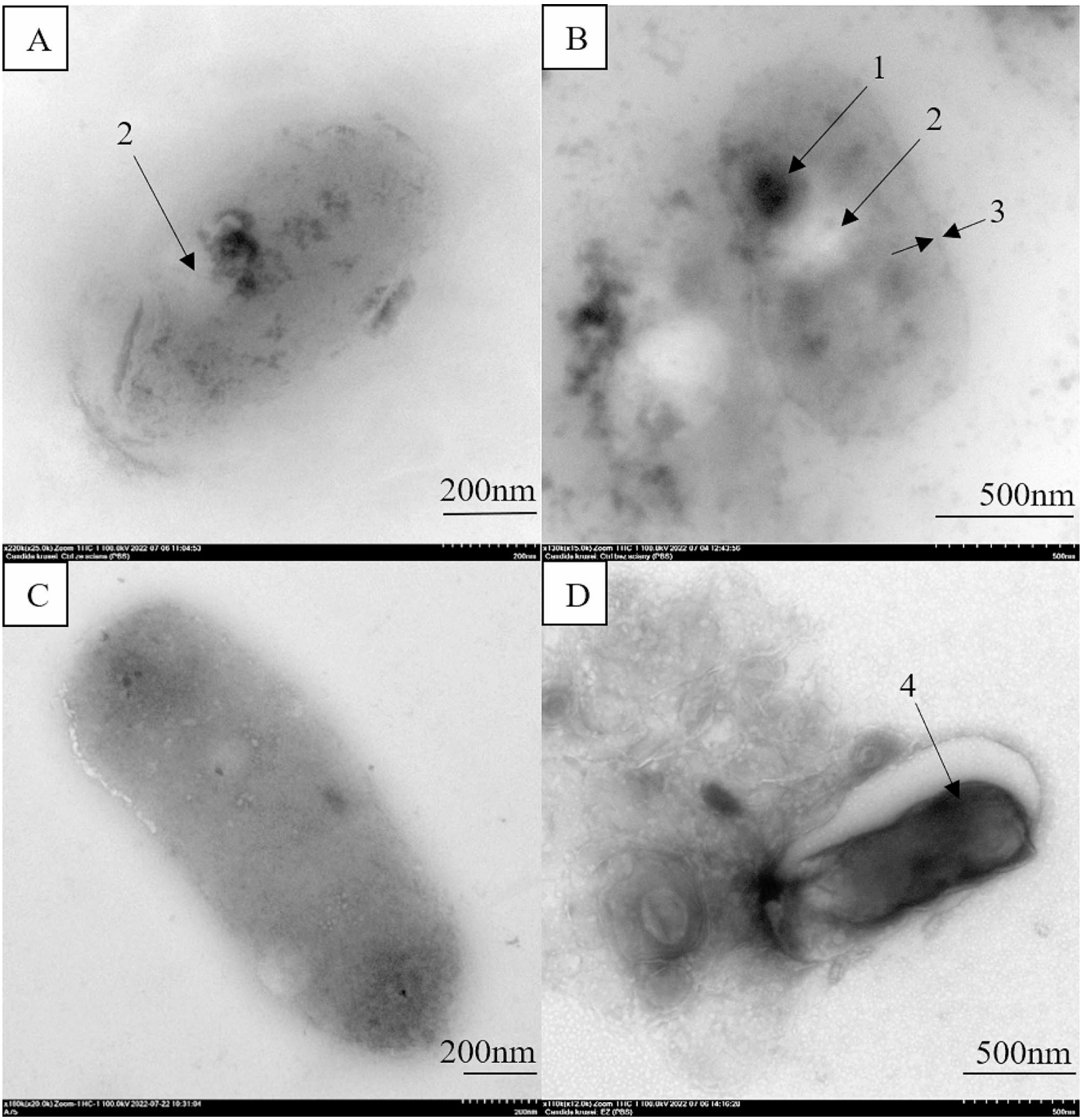

Fig. 2 TEM pictures of *Candida krusei***A** – control (untreated cells), **B** – spheroplasts, **C** – SoC treatment, **D** – SoP treatment, 1-nucelus, 2-vacuole, 3, – outer cell layer, 4 – lysed cell

mg L^{-1} of SoP caused the lysis of cells (Figs. 2D) which is evidenced by the higher uptake of the contrast dye.

As we mentioned before, saponins are able to integrate into the structure of biomembrane, but due to the possible toxic effect of saponins on human biological membranes, it is very important to use them in the right amount. The use of similar concentrations of saponins against yeasts of the *Candida* genus has been described in the existing literature. Coleman et al. (2010) used concentrations in the range of 16 and 32 µg mL^{-1} in their research, Sadowska et al. (2014) used *Medicago sativa* extract with a concentration of 500 µg mL^{-1}, while Li et al. (2020), reported the suppression of hyphae growth in the presence of saponins. During their studies, the series of concentration used was 0, 16, 32 and 64 µg mL^{-1}. They showed that the *C. albicans* hyphal growth inhibitory effect of tea saponin in the concentration

of 32 µg mL^{-1}might be rather connected to reduction of the level of cyclic adenosine monophosphate. It is worth noting that analogous changes in cell wall and cell outer membranes morphology were observed in *Pseudomonas* bacteria treated with saponins from *Sapindus mukorossi*, as reported elsewhere (Grzywaczyk et al. 2023). However, the MIC curves determined by us did not show an effect of SoC and SoP solutions, even at a concentration of 500 mg L^{-1} (see supplementary materials), on the growth of *Candida* cells.

Surface properties of spheroplasts

Cell surface properties are strictly related to the membrane and/or cell wall properties. In order to explain the activity of saponins targeted at the biomembrane, it is crucial to assess the spheroplasts surface properties. As presented in Fig. 3A., the addition of extracts in the amounts of 10 and 15 mg L^{-1} causes an increase in the uptake of Crystal Violet. Thus, we can assume, that both SoC and SoP increase the permeability of *Candida* spheroplasts. For *C.albSP*, the addition of SoC in the amount of 5, 10 and 15 mg L^{-1} caused an increase in the uptake of Crystal Violet by 12.31%, 21.76% and 16.74%, respectively. The addition of SoP in the amount of 5 mg L^{-1} caused an insignificant decrease in the CV uptake, by -3.97%, whereas its addition in the amounts of 10, and 15 mg L^{-1} caused an increase in the CV uptake by 26.10% and 16.54%, respectively. Similar observations were made for *C.krsSP*. While the addition of either SoC or SoP in the amount of 5 mg L^{-1} caused a significant decrease in permeability of about 22%, their addition in the amount of 10 and 15 mg L^{-1} caused an increase in permeability, the greatest, by 30.52%, after the addition of 15 mg L^{-1} SoC.

The well-known mechanism of saponin-biomembrane interaction involves complex formation with cholesterol or

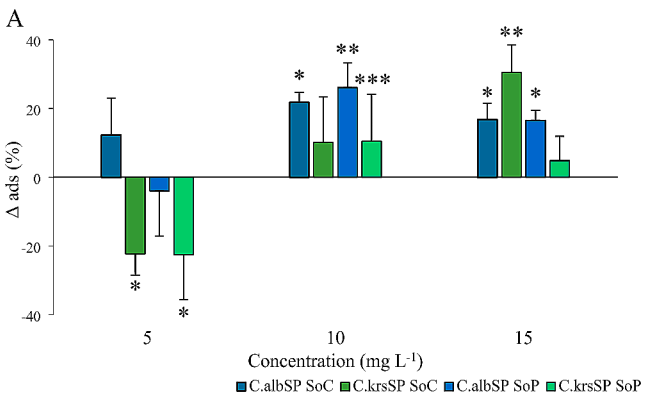

Fig. 3 Spheroplasts surface properties of *Candida albicans* and *Candida krusei***A** - spheroplasts permeability, **B** - Congo Red adsorption. The results are presented in relation to the control samples, whose permeability and adsorption, respectively, were taken as 0. Each column marked with different number of dots are significantly different ($p < 0.05$, LSD test) considering the reactions of *Candida* strains

ergosterol (De Groot et al. 2016; Akiyama et al. 1980; Story et al. 1984; Coleman et al. 2010). Sterols are vital components of eukaryotic biomembrane and they act as stiffening agents, hence, their absence can effectively disrupt the structure of the cell membrane (Doole et al. 2022). Coleman et al. (2010) have suggested, that saponins may have even higher affinity to binding to the fungal ergosterol rather than cholesterol. Increased permeability of spheroplast can be correlated to the reduction of the level of ergosterol in the biomembrane structure. As reported by Sudji et al. (2015), saponins are able to disintegrate the biomembrane through formation of complexes with cholesterol, leading to membrane leakage or even pore formation. In contrast, the results of spheroplasts' adsorption capacity may also indicate the second mechanism of saponin action on biomembrane that is integration of hydrophobic part into the structure of biomembrane (Rojewska et al. 2020). As presented in Fig. 3B, the addition of 5 mg L^{-1} SoC leads to a decrease in the adsorption capacity of *C.krsSP*. The addition of the same concentration of SoP causes a decrease in the adsorption capacity of *C.albSP.* The decrease in Congo Red adsorption is also noticeable for *C.albSP* and *C.krsSP* treated with 15 mg L^{-1} SoP. The treatment of *C.albSP*. and *C.krsSP* with SoP in the amount of 10 mg L^{-1} resulted in significant differences only for *C.albSP*. What is more, the results indicate an increase in Congo Red binding by 5.52%. A similar increase by 11.51% relative to that of the control sample was also observed for *C.krsSP* spheroplasts treated with 15 mg L^{-1} SoP. In the remaining cases, the statistical test showed no significant changes. The treatments leading to no change in Congo Red adsorption may be interpreted as connected to the aforementioned saponin-ergosterol interaction (Lorent et al. 2013). Loosening the tight structure of the cell membrane results in increased adsorption capacity of the surface of the cell membrane. The observed decrease in the adsorption capacity may be related to the incorporation of saponins in the space where cholesterol is missing. Ondevilla et al. (2021) have examined the effect of one of saponins, diosgenin (DGN). They suggested that DGN at concentrations of up to 18 mol% reproduced the functions of cholesterol i.e. acted as a stiffening agent.

The outer layers of the cell i.e. wall or biomembrane, are dynamic structures, in which many phenomena may occur. Each cell action, may eventually have impact on its composition. What is more, any unwanted change in the membrane or wall structure such as disruption or hole, may affect the zeta potential of cells (Ferreyra Maillard et al. 2021). In this study, the surface potential decreased from −5.44 to −7.38 mV after lysis of *C. krusei.* cell wall, whereas it increased from −9.36 to −8.80 mV for *C. albicans* (Table 1). However, the change in the surface potential for *C.albSP* was statistically insignificant. What is worth noting, however, is

Table 1 Zeta potential of cells and spheroplasts of *Candida albicans* and *Candida krusei*

Candida albicans cells surface potential (mV)				
Cell Ctrl	Spheroplasts Ctrl	5 mg L^{-1} SoC	10 mg L^{-1}	15 mg L^{-1}
-9.36 ± 1.54[c]	-8.80 ± 0.75[c]	-17.78 ± 2.61[a]	-17.62 ± 0.96[a]	-16.96 ± 1.56[a]
		SoP		
		-24.85 ± 2.77[b]	-24.19 ± 1.93[b]	-25.19 ± 2.16[b]
***Candida krusei*cells surface potential (mV)**				
Cell Ctrl	Spheroplasts Ctrl	5 mg L^{-1} SoC	10 mg L^{-1}	15 mg L^{-1}
-5.44 ± 1.69[e]	-7.38 ± 0.81[a]	-4.68 ± 0.31[e]	-13.72 ± 0.47[b]	-14.40 ± 0.82[c]
		SoP		
		-17.89 ± 2.35[d]	-18.43 ± 2.02[d]	-18.70 ± 1.40[d]

Values marked with the same letter do not differ significantly ($p > 0.05$)

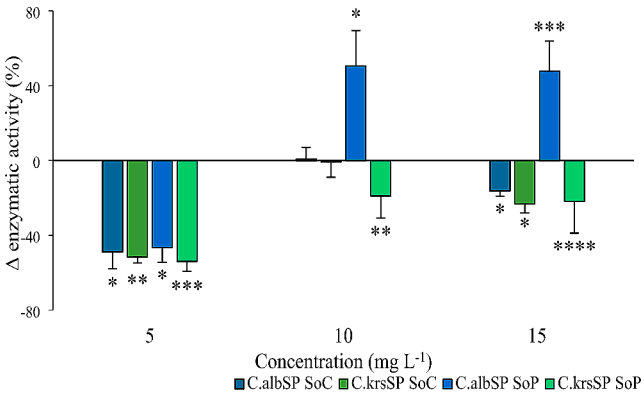

Fig. 4 Enzymatic activity of *Candida albicans* and *Candida krusei* spheroplasts. The results are presented in relation to the control samples, whose metabolic activity was taken as 0. Each column marked with different number of dots are significantly different ($p < 0.05$, LSD test) considering the reactions of *Candida* strains

a significant decrease in the value of zeta potential value after treatment of each strain with SoP or SoC. As a result of the treatment of *C.albSP* with SoC and SoP, the zeta value decreased to approx. −17 mV and −25 mV, respectively. The treatment of *C.krsSP*. with SoC and SoP resulted in a decrease in the zeta potential value to approx. −18 mV and −14 mV, respectively. Saponin integration into the biomembrane may cause such a decrease in surface potential. As observed by Lorent et al. (2013), the integration of alfa-Hederin or Hederagenin in the biomembranes caused a decrease in the DMPC multilamellar vesicles surface potential from −1.89 mV to −14.17 mV and −5.09 mV. On the other hand, Halder et al. (2015) have suggested a link between the cell permeability and zeta potential. Similarly to the results we obtained, they observed a change in the surface potential of *E. coli* and *S. aureus* cells after treatment with Polymyxin B and CTAB.

Enzymatic activity

To more deeply investigate the effect of *Saponaria officinalis* extract on *Candida* sp. spheroplasts, the metabolic activity of the cells was assessed. After treatment with 5 mg L^{-1} of SoC or SoP the metabolic activity of each strain decreased by 50% compared to Ctrl, i.e. untreated samples (Fig. 4). However, 10 mg L^{-1} of SoP caused a decrease in the metabolic activity of *C.krsSP*, but the treatment with SoP brought a high increase in that of *C.albSP*. Similar observation was made after the treatment of *C.albSP.* with 15 mg L^{-1} of SoP, which increased the *C.albSP* activity by 50% relative to the control sample.

An increase in *C.albSP*. activity as a result of treatment with 10 mg L^{-1} and 15 mg L^{-1} of SoP is most likely related to cellular response mechanisms that counteract negative phenomena resulting from a toxic environment. A similar phenomenon has been observed by Zdarta et al. (2019) who have reported that 1 g L^{-1} of a saponin-rich extract from *Hedera helix* leaves increased the metabolic activity of *Raoultella ornitinolytica* M03 by 60 ± 8%. Moreover, similarly to our results, they also observed that the application of SoP in only one concentration of 10 g L^{-1} resulted in a toxic effect. On the other hand, Tsuzuki et al. (2007), have shown the antifungal activity of *Sapindus saponaria* extract against a clinical isolate from vaginal secretions of *Candida parapsilosis* yeast with Minimal Inhibitory Concentration of 400 µg mL^{-1}. Similar observations were made by Hu et al. (2018), who reported that olean-type saponin from *Sapindus mukorossi* showed inhibitory activity against both *Trichophyton rubrum* and *Candida albicans* with MIC_{80} values of 8 mg mL^{-1}. However, the differences of enzymatic activity that occur maybe also correlated to the specificity of action of compounds present in crude and purified fraction. As we showed elsewhere, the fractions differ in terms of saponin content and composition, which is related to the porosity of the membranes used for nanofiltration (Grzywaczyk et al. 2023). Appropriate observations were made by Soberón et al. (2017), who investigated the cytotoxic effect of saponins derived from *Anagallis arvensis* L. They suggested that of the 4 compounds, triterpenoids monodesmosidic saponins: Anagallisin C, Anagallisin A, Anagallisin B, and Desglucoanagalloside A, the compound with the highest inhibitory

effect against *C. albicans* is Anagallisin C. On the other hand, in the case of our research, we focused on the use of unpurified extract and after the nanofiltration process, with an emphasis on the effect on the cell membrane, hence the answer to the question which saponin compound derived from *Saponaria officinalis* has the greatest cytotoxic effect requires further research.

Conclusions

The impacts of crude extract of *Saponaria officinalis* as well as the extract purified by nanofiltration on the biomembrane properties and permeability of spheroplast of *C. albicans* and *C. krusei* were studied. For *Candida albicans*, the crude extract showed a stronger effect of increasing the permeability of the cell membrane than the purified one. Moreover, the extract concentration of 10 mg L^{-1} turned out to be the most effective for increasing permeability. On the other hand, for *C. krusei*, the surface properties of spheroplasts subjected to the purified or crude extract were comparable. Moreover, zeta potential analysis showed a higher decrease for the spheroplasts affected by the purified *S. officinalis* extract. This may by correlated to the process of saponins binding to the cells biomembrane. The most important outcome of the study is showing a high potential of saponins used as excipients which increase the permeability of pathogenic cells. Hence, the next step of the research will be to assess the interaction of the extracts used with antifungal antibiotics.

Supplementary Information The online version contains supplementary material available at https://doi.org/10.1007/s11274-024-03961-9.

Acknowledgements This research was funded in whole by National Science Centre, Poland, grant number: 2020/39/B/NZ9/03196.

Author contributions Adam Grzywaczyk: Conceptualization, Data curation, Methodology, Formal analysis, Investigation, Writing – original draft, Visualization. Wojciech Smułek: Formal analysis Writing – original draft, Supervision. Ewa Kaczorek: Conceptualization, Supervision, Writing – review & editing, Project administration, Funding acquisition.

Data availability The datasets generated and analysed during the current study are available from the corresponding author on reasonable request.

Declarations

Competing interests The authors declare no competing interests.

References

Akiyama T, Takagi S, Sankawa U, Inari S, Hazime, Saitô (1980) Saponin-cholesterol Interaction in the multibilayers of Egg Yolk Lecithin as studied by Deuterium Nuclear magnetic resonance: Digitonin and its analogues. Biochemistry 19(9):1904–1911. https://doi.org/10.1021/bi00550a027

Ambalam P, Kondepudi KK, Nilsson I, Wadström T, Åsa L (2012) Bile stimulates cell surface hydrophobicity, Congo Red binding and biofilm formation of Lactobacillus strains. FEMS Microbiol Lett 333(1):10–19. https://doi.org/10.1111/j.1574-6968.2012.02590.x

Behzadi P, Behzadi E, Reza Ranjbar (2015) Urinary tract infections and Candida Albicans. Cent Eur J Urol 68(1):96–101. https://doi.org/10.5173/ceju.2015.01.474

Bondaryk Małgorzata, Kurzątkowski Wiesław, Staniszewska M (2013) Antifungal agents commonly used in the superficial and mucosal candidiasis treatment: Mode of Action and Resistance Development. Postepy Dermatologii i Alergologii 30(5):293–301. https://doi.org/10.5114/pdia.2013.38358

Brown GD, Denning DW, Neil AR, Gow SM, Levitz MG, Netea, White TC (2012) Hidden killers: human fungal infections. Sci Transl Med 4(165). https://doi.org/10.1126/scitranslmed.3004404

Chandra S, Rawat DS (2015) Medicinal plants of the Family Caryophyllaceae: a review of Ethno-Medicinal uses and Pharmacological properties. Integr Med Res 4(3):123–131. https://doi.org/10.1016/j.imr.2015.06.004

Chandra S, Rawat DS, and Arun Bhatt (2021) Phytochemistry and pharmacological activities of Saponaria Officinalis L.: a review. Notulae Scientia Biologicae 13(1):10809. https://doi.org/10.15835/nsb13110809

Claessen D, and Jeff Errington (2019) Cell Wall Deficiency as a coping strategy for stress. Trends Microbiol 27(12):1025–1033. https://doi.org/10.1016/j.tim.2019.07.008

Coleman JJ, Okoli I, Tegos GP, Holson EB, Wagner FF, Hamblin MR, and Eleftherios Mylonakis (2010) Characterization of Plant-Derived Saponin Natural products against Candida Albicans. ACS Chem Biol 5(3):321–332. https://doi.org/10.1021/cb900243b

Dąbrowska M, Sienkiewicz M Paweł Kwiatkowski, and Michał Dąbrowski. 2019. 'Diagnosis and treatment of Invasive Candida infections – a review article'. Ann Universitatis Mariae Curie-Sklodowska Sectio C – Biol 73 (1): 47. https://doi.org/10.17951/c.2018.73.1.47-59

Dawid C, Weber D, Musiol E, Janas V, Baur S, Lang R, and Tobias Fromme (2020) Comparative Assessment of purified saponins as Permeabilization agents during Respirometry. Biochim et Biophys Acta - Bioenergetics 1861(10). https://doi.org/10.1016/j.bbabio.2020.148251

Devi K, Pandima R, Sakthivel S, Arif Nisha N, Suganthy, Karutha Pandian S (2013) Eugenol alters the Integrity of Cell membrane and acts against the Nosocomial Pathogen Proteus Mirabilis. Arch Pharm Res 36(3):282–292. https://doi.org/10.1007/s12272-013-0028-3

Doole FT, Teshani Kumarage R, Ashkar, and Michael F Brown (2022) Cholesterol stiffening of lipid membranes. J Membr Biol 255(4):385–405. https://doi.org/10.1007/s00232-022-00263-9

Douglas L, Julia (2003) Candida Biofilms and their role in infection. Trends Microbiol 11(1):30–36. https://doi.org/10.1016/S0966-842X(02)00002-1

Ferreyra Maillard, Anike PV, Espeche JC, Maturana P, Cutro AC, and Axel Hollmann (2021) Zeta Potential beyond materials Science: applications to Bacterial systems and to the development of Novel antimicrobials. Biochim et Biophys Acta - Biomembr 1863(6):183597. https://doi.org/10.1016/j.bbamem.2021.183597

Gawdzik A, Nowogrodzka K, Hryncewicz-Gwóźdź A, Maj J, Szepietowski J, Alina Jankowska-Konsur (2019) Epidemiology

of dermatomycoses in Southwest Poland, Years 2011–2016. Postepy Dermatologii i Alergologii 36(5):604–608. https://doi.org/10.5114/ada.2018.80615

Groot C, De, Christel C, Müller-Goymann (2016) Saponin interactions with model membrane systems - Langmuir monolayer studies, hemolysis and formation of ISCOMs. Planta Med 82(18):1496–1512. https://doi.org/10.1055/s-0042-118387

Grzywaczyk A, Smułek W Agnieszka Zgoła-Grześkowiak, Ewa Kaczorek, Anna Zdziennicka, and Bronisław Jańczuk. (2023) 'Nanofiltered saponin-rich extract of Saponaria Officinalis – Adsorption and Aggregation properties of Particular fractions'. Colloids Surf a 661 (March): 130937. https://doi.org/10.1016/j.colsurfa.2023.130937

Grzywaczyk A, Smułek W, Olejnik A, Guzik U, Nowak A, and Ewa Kaczorek (2023) Co-interaction of Nitrofuran antibiotics and the saponin-rich extract on Gram-negative Bacteria and Colon epithelial cells. World J Microbiol Biotechnol 39(8):221. https://doi.org/10.1007/s11274-023-03669-2

Halder S, Yadav KK, Sarkar R, Mukherjee S, Saha P, Haldar S, Karmakar S, Sen T (2015) Alteration of Zeta Potential and membrane permeability in Bacteria: a study with Cationic agents. SpringerPlus 4(1):1–14. https://doi.org/10.1186/s40064-015-1476-7

Havlickova B, Czaika VA, and Markus Friedrich (2008) Epidemiological trends in skin Mycoses Worldwide. Mycoses 51(4):2–15. https://doi.org/10.1111/j.1439-0507.2008.01668.x

Hu Q, Chen YY, Khan QYJA, Li F, Han DF (2018) Triterpenoid Saponins from the Pulp of Sapindus Mukorossi and Their Antifungal Activities. Phytochemistry 147:1–8. https://doi.org/10.1016/j.phytochem.2017.12.004. Gui Dong Cao, and Hong Xiang Lou

Huang K, Casey R, Mukhopadhyay B, Wen Z, Gitai, and Ned S. Wingreen (2008) Cell shape and Cell-Wall Organization in Gram-negative Bacteria. Proc Natl Acad Sci USA 105(49):19282–19287. https://doi.org/10.1073/pnas.0805309105

Jurado Gonzalez, Patricia, and Pia M. Sörensen (2020) Characterization of Saponin Foam from Saponaria Officinalis for Food Applications. Food Hydrocolloids 101:105541. https://doi.org/10.1016/j.foodhyd.2019.105541

Kühbacher A, Anke Burger-Kentischer, and Steffen Rupp (2017) Interaction of Candida Species with the skin. Microorganisms 5(4):32. https://doi.org/10.3390/microorganisms5020032

Kumamoto CA (2012) Inflammation and gastrointestinal Candida Colonization. NIH Public Access Curr Opin Microbiol 14(4):386–391. https://doi.org/10.1016/j.mib.2011.07.015.Inflammation

Li Y, Shan M, Li S, Wang Y, Yang H, Chen Y, Gu B, Zhu Z (2020) Teasaponin suppresses Candida Albicans Filamentation by reducing the level of intracellular cAMP. Annals Translational Med 8(5):175–175. https://doi.org/10.21037/atm.2020.01.124

Lorent J, Le Duff CécileS, Quetin-Leclercq J, Marie Paule Mingeot-Leclercq (2013) Induction of highly curved structures in relation to membrane permeabilization and budding by the Triterpenoid Saponins, α- and δ-Hederin. J Biol Chem 288(20):14000–14017. https://doi.org/10.1074/jbc.M112.407635

Oh Y, Ji, and Jungil Hong (2022) Application of the MTT-Based colorimetric method for evaluating bacterial growth using different Solvent systems. Lwt 153:112565. https://doi.org/10.1016/j.lwt.2021.112565

Ondevilla J, Candice S, Hanashima A, Mukogawa Y, Umegawa (2021) and Michio Murata. 'Diosgenin-Induced Physicochemical Effects on Phospholipid Bilayers in Comparison with Cholesterol'. *Bioorganic and Medicinal Chemistry Letters* 36 (October 2020): 127816. https://doi.org/10.1016/j.bmcl.2021.127816

Ortega M, Marco F, Soriano A, Almela M, Martínez JA, López J, Pitart C, Mensa J (2011) Candida Species Bloodstream Infection: epidemiology and outcome in a single Institution from 1991 to 2008. J Hosp Infect 77(2):157–161. https://doi.org/10.1016/j.jhin.2010.09.026

Pfaller MA, Diekema DJ (2007) Epidemiology of invasive candidiasis: a Persistent Public Health Problem. Clin Microbiol Rev 20(1):133–163. https://doi.org/10.1128/CMR.00029-06

Podolak I, Galanty A, and Danuta Sobolewska (2010) Saponins as cytotoxic agents: a review. Phytochem Rev 9(3):425–474. https://doi.org/10.1007/s11101-010-9183-z

Pristov KE, Ghannoum MA (2019) Resistance of Candida to Azoles and Echinocandins Worldwide. Clin Microbiol Infect 25(7):792–798. https://doi.org/10.1016/j.cmi.2019.03.028

Rojewska M, Smułek W, Prochaska K, Ewa Kaczorek (2020) Combined effect of Nitrofurantoin and plant surfactant on Bacteria Phospholipid membrane. Molecules 25(11). https://doi.org/10.3390/molecules25112527

Sadowska B, Budzyńska A, Więckowska-Szakiel M, Paszkiewicz Małgorzata, Stochmal A, Moniuszko-Szajwaj B, Kowalczyk M, Różalska B (2014) New Pharmacological properties of Medicago Sativa and Saponaria Officinalis Saponin-Rich fractions addressed to Candida Albicans. J Med Microbiol 63(8):1076–1086. https://doi.org/10.1099/jmm.0.075291-0

Smułek W, Zdarta A, Łuczak M, Krawczyk P, Jesionowski T, Ewa Kaczorek (2016) Sapindus Saponins' impact on hydrocarbon biodegradation by Bacteria strains after short- and long-term contact with pollutant. Colloids Surf B 142:207–213. https://doi.org/10.1016/j.colsurfb.2016.02.049

Smułek W, Zdarta A, Pacholak A (2017) Agnieszka Zgoła-Grześkowiak, Łukasz Marczak, Maciej Jarzębski, and Ewa Kaczorek. 'Saponaria Officinalis L. Extract: Surface Active Properties and Impact on Environmental Bacterial Strains'. *Colloids and Surfaces B: Biointerfaces* 150 (February): 209–15. https://doi.org/10.1016/j.colsurfb.2016.11.035

Sobel JD (2007) Vulvovaginal Candidosis. Lancet 369(9577):1961–1971. https://doi.org/10.1016/S0140-6736(07)60917-9

Soberón JoséR, Melina A, Sgariglia AC, Pastoriza, Estela M, Soruco, Sebastián N, Jäger GR, Labadie, Diego A, Sampietro, Vattuone MA (2017) Antifungal activity and cytotoxicity of extracts and triterpenoid saponins obtained from the Aerial Parts of Anagallis Arvensis L. J Ethnopharmacol 203(May):233–240. https://doi.org/10.1016/j.jep.2017.03.056

Stirke A, Celiesiute-Germaniene R, Zimkus A, Zurauskiene N, Simonis P, Dervinis A, Ramanavicius A, Saulius Balevicius (2019) The link between yeast cell wall porosity and plasma membrane permeability after PEF Treatment. Sci Rep 9(1):1–10. https://doi.org/10.1038/s41598-019-51184-y

Story JA, LePage SL, Petro MS, West LG, Cassidy MM, Lightfoot FG, Vahouny GV (1984) Interactions of Alfalfa Plant and sprout saponins with cholesterol in Vitro and in cholesterol-Fed rats. Am J Clin Nutr 39(6):917–929. https://doi.org/10.1093/ajcn/39.6.917

Sudji I, Resmala Y, Subburaj N, Frenkel, Ana J, García-Sáez, and Michael Wink (2015) Membrane disintegration caused by the Steroid Saponin Digitonin is related to the Presence of cholesterol. Molecules 20(11):20146–20160. https://doi.org/10.3390/molecules201119682

Tsuzuki JK, Terezinha IE, Svidzinski CS, Shinobu, Luiz FA, Silva ER-F, Diógenes AG, Cortez, Izabel CP, Ferreira (2007) Antifungal activity of the extracts and saponins from Sapindus Saponaria L. Anais Da Acad Brasileira De Ciencias 79(4):577–583. https://doi.org/10.1590/s0001-37652007000400002

Vila T, Sultan AS, Daniel Montelongo-Jauregui, and Mary Ann Jabra-Rizk (2020) Oral candidiasis: a Disease of Opportunity. J Fungi 6(1):1–28. https://doi.org/10.3390/jof6010015

Zdarta A, Smułek W, Pacholak A, Kaczorek E (2019) Environmental aspects of the Use of Hedera Helix Extract in Bioremediation process. Microorganisms 7(2). https://doi.org/10.3390/microorganisms7020043

P3 Supplementary Materials

Supplementary Information

Saponaria officinalis saponins as a factor increasing permeability of *Candida* yeasts' biomembrane

Submitted to

World Journal of Microbiology and Biotechnology

by

Adam Grzywaczyk*, Wojciech Smułek, Ewa Kaczorek

Institute of Chemical Technology and Engineering, Poznan University of Technology,
Berdychowo 4, 60-695 Poznan, Poland;
e-mails: adam.grzywaczyk@doctorate.put.poznan.pl; wojciech.smulek@put.poznan.pl; ewa.kaczorek@put.poznan.pl

* corresponding author: e-mail: adam.grzywaczyk@doctorate.put.poznan.pl; phone: +48 616653686

E-Supplementary data

Growth curves

Candida albicans and *Candida krusei* fungal strains were cultured with the presence of *Saponaria officinalis* L. crude and purified by nanofiltration extract respectively in the range of final concentration of 5.0, 6.25, 12.5, 25.0, 50.0, 62.5, 125.0, 250.0 and 500.0 mg L^{-1}. 75 uL of 0.5 McFarland standards of cells in M9 salts, 25 uL of YPD medium, and 100 uL of extract in M9 salts were combined to the final volume of 200 uL. The growth curves are as follows:

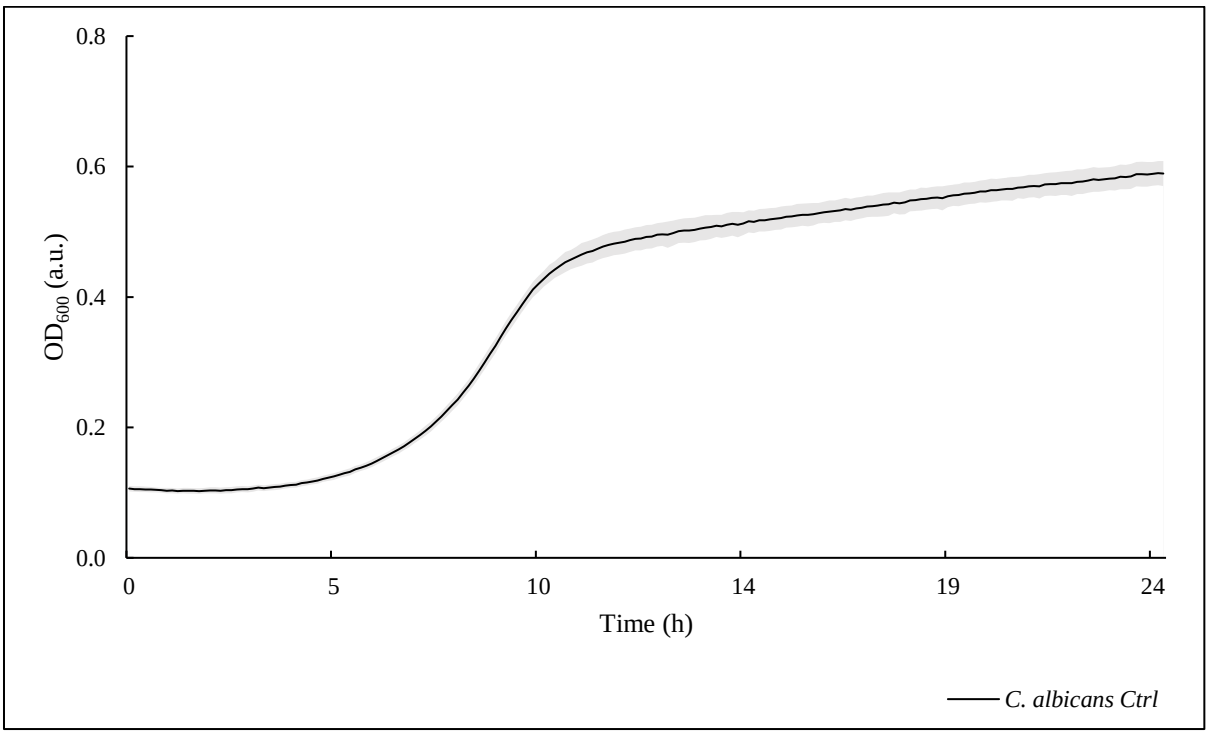

S1. Growth curve of *Candida albicans*

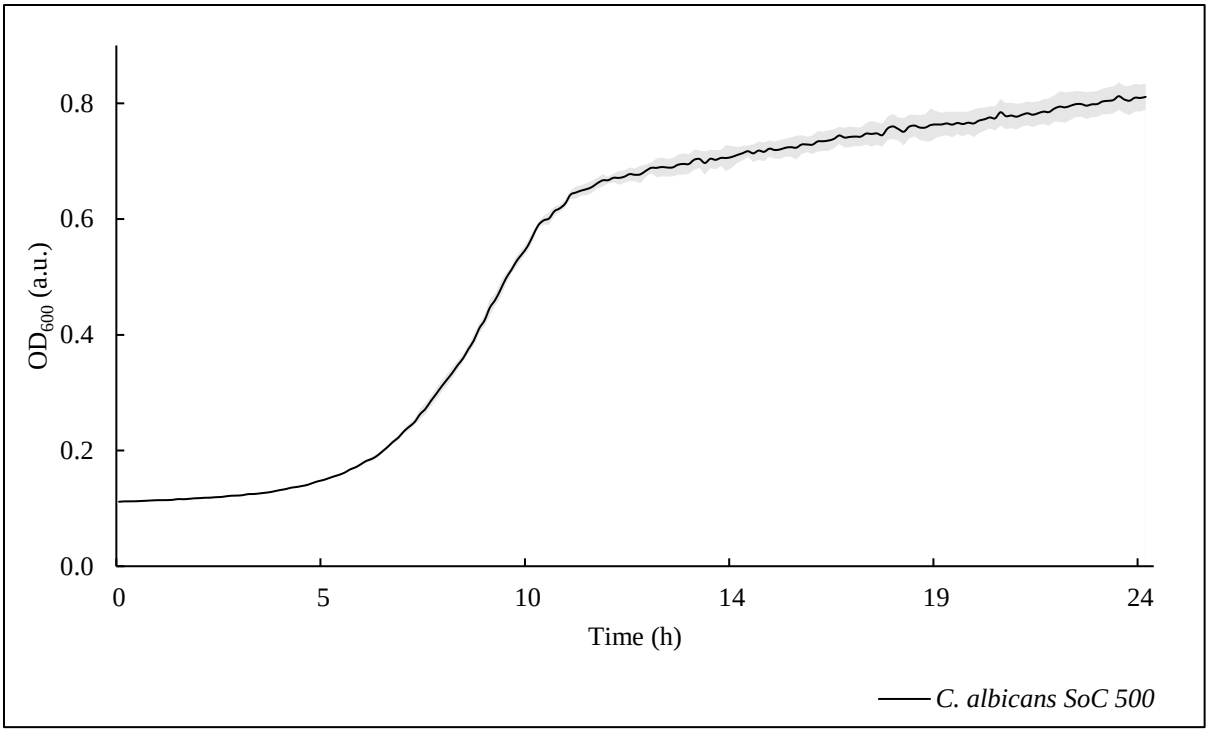

S2. Growth curve of *Candida albicans* exposed to 500 mg L^{-1} of *Saponaria officinalis* L. crude extract

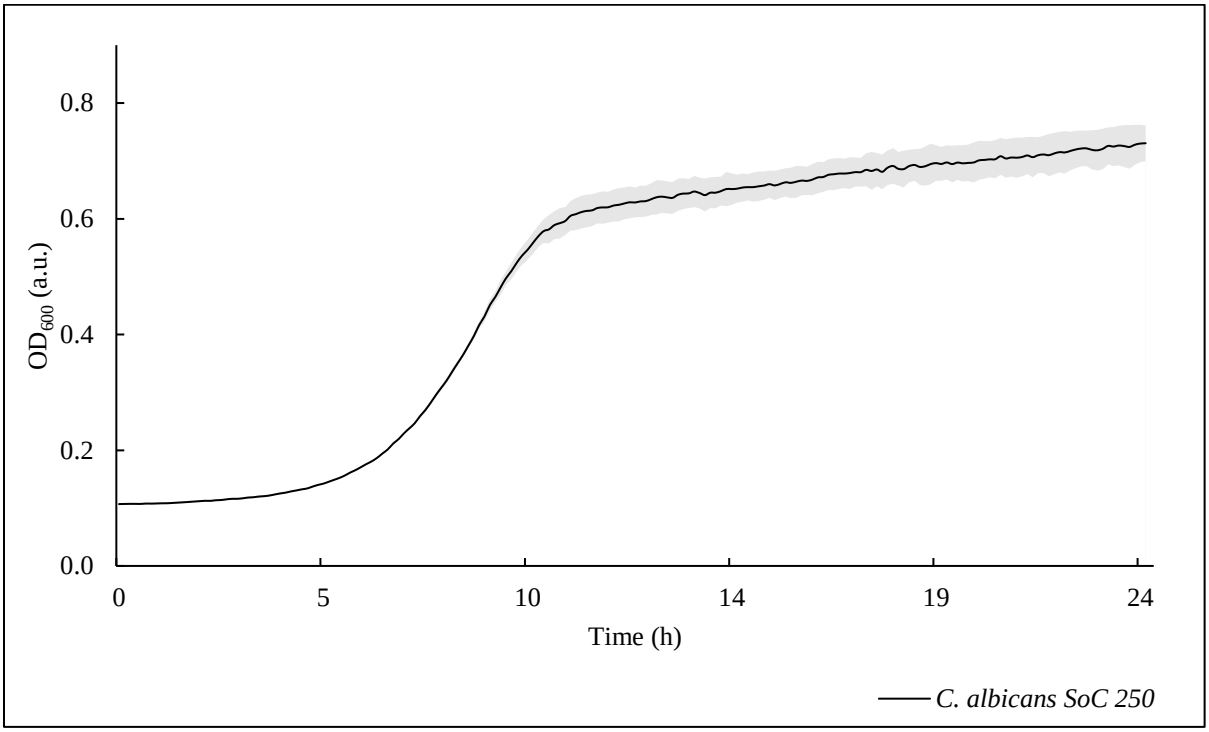

S3. Growth curve of *Candida albicans* exposed to 250 mg L^{-1} of *Saponaria officinalis* L. crude extract

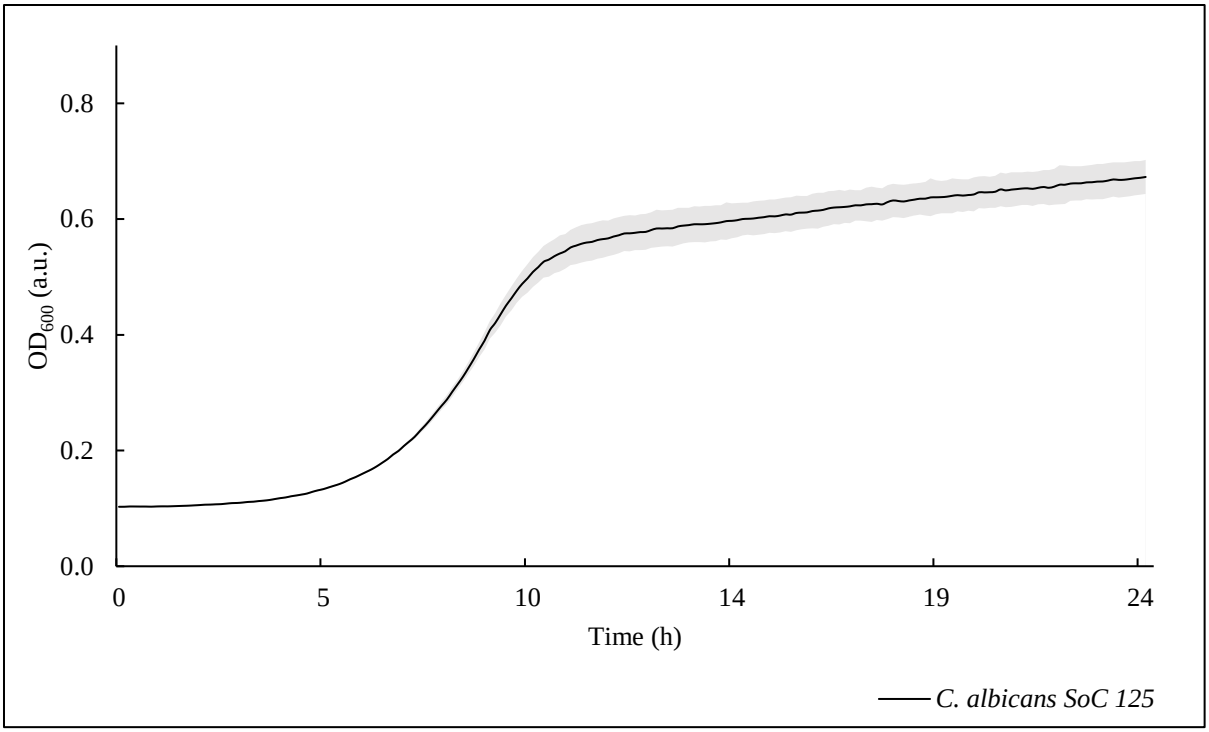

S4. Growth curve of *Candida albicans* exposed to 125 mg L^{-1} of *Saponaria officinalis* L. crude extract

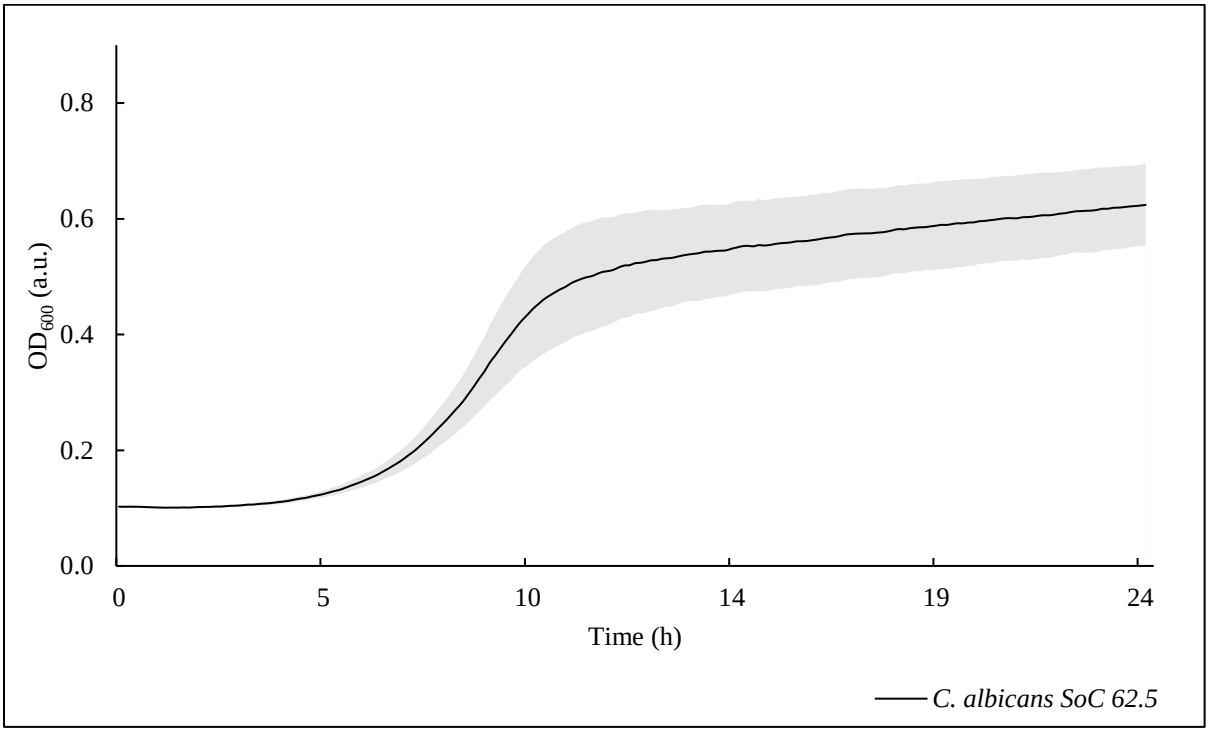

S5. Growth curve of *Candida albicans* exposed to 62.5 mg L^{-1} of *Saponaria officinalis* L. crude extract

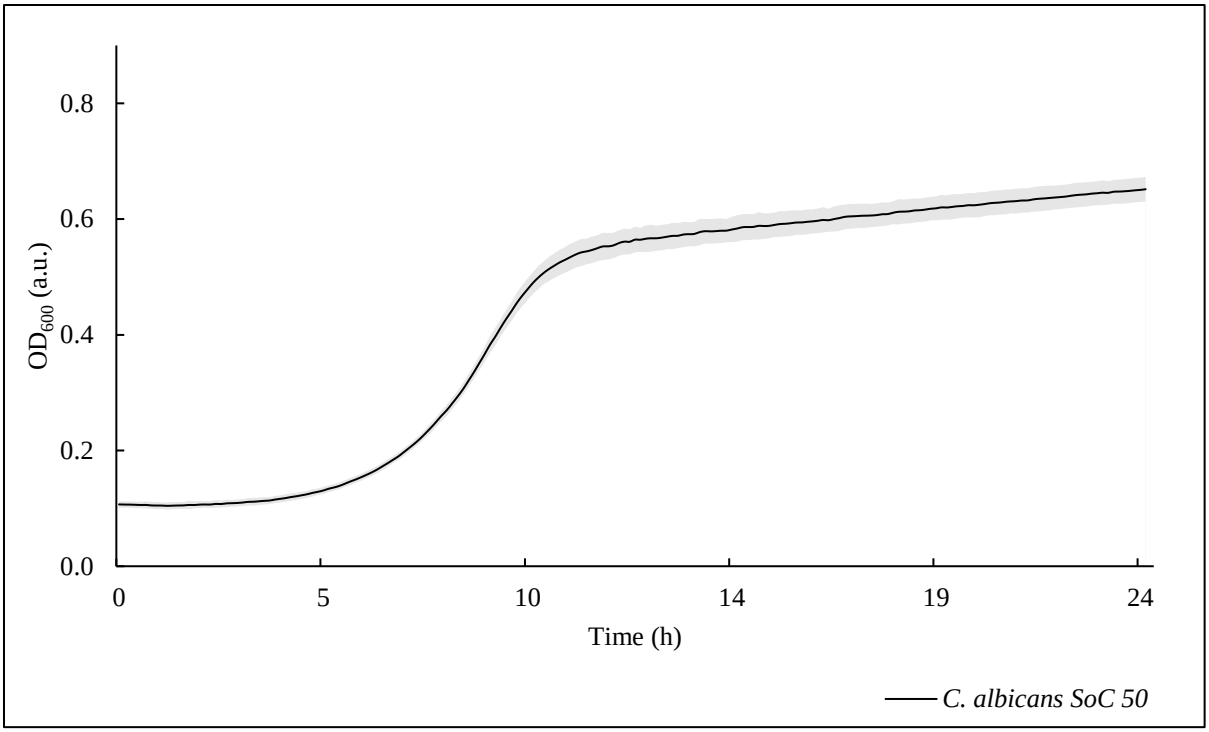

S6. Growth curve of *Candida albicans* exposed to 50 mg L^{-1} of *Saponaria officinalis* L. crude extract

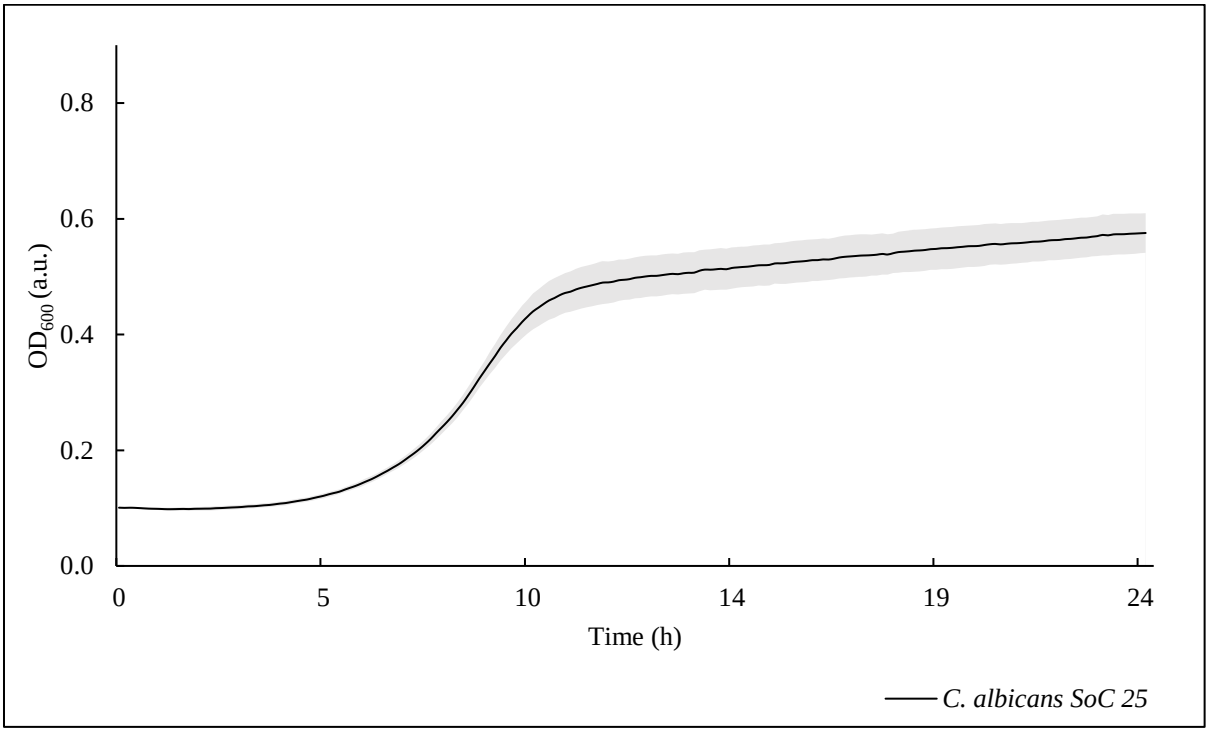

S7. Growth curve of *Candida albicans* exposed to 25 mg L^{-1} of *Saponaria officinalis* L. crude extract

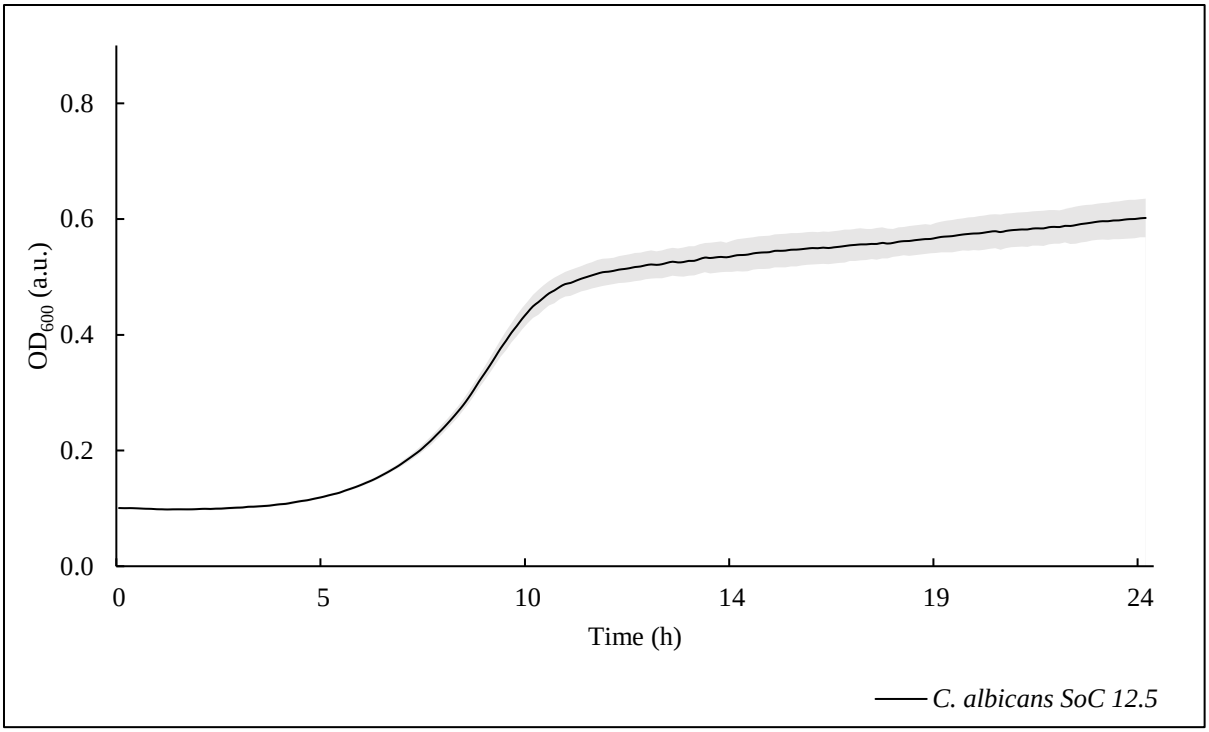

S8. Growth curve of *Candida albicans* exposed to 12.5 mg L^{-1} of *Saponaria officinalis* L. crude extract

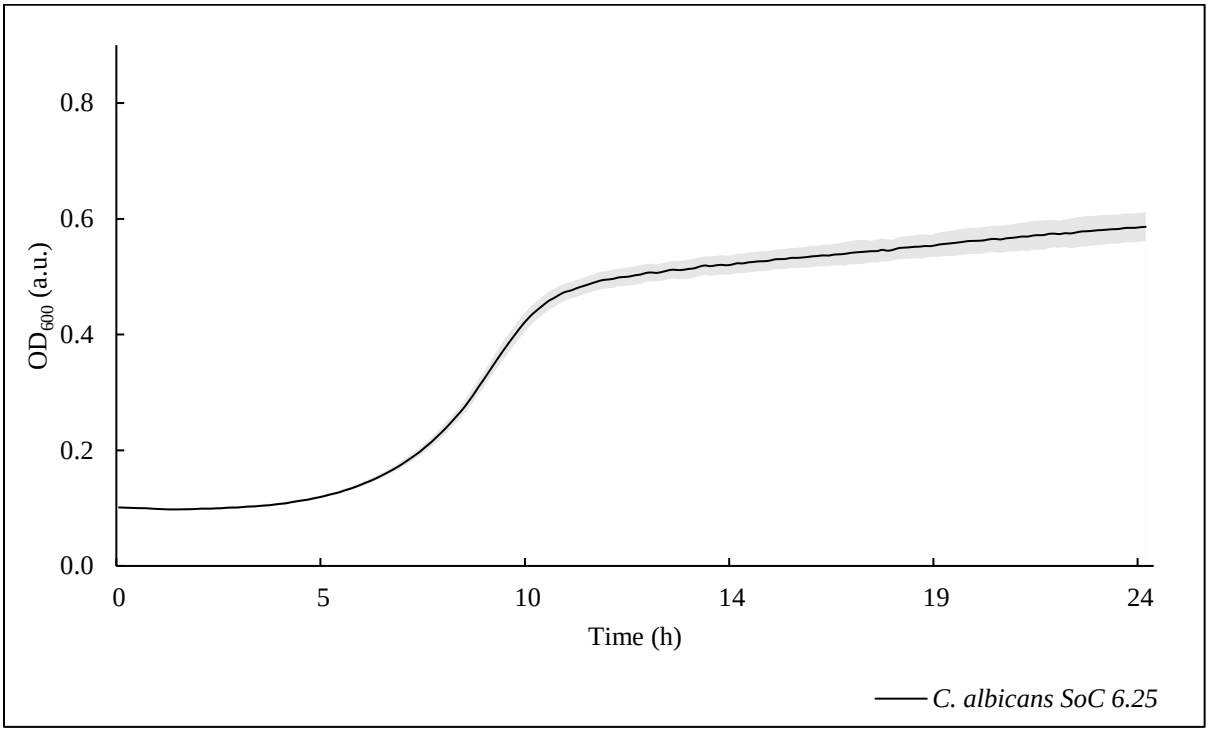

S9. Growth curve of *Candida albicans* exposed to 6.25 mg L^{-1} of *Saponaria officinalis* L. crude extract

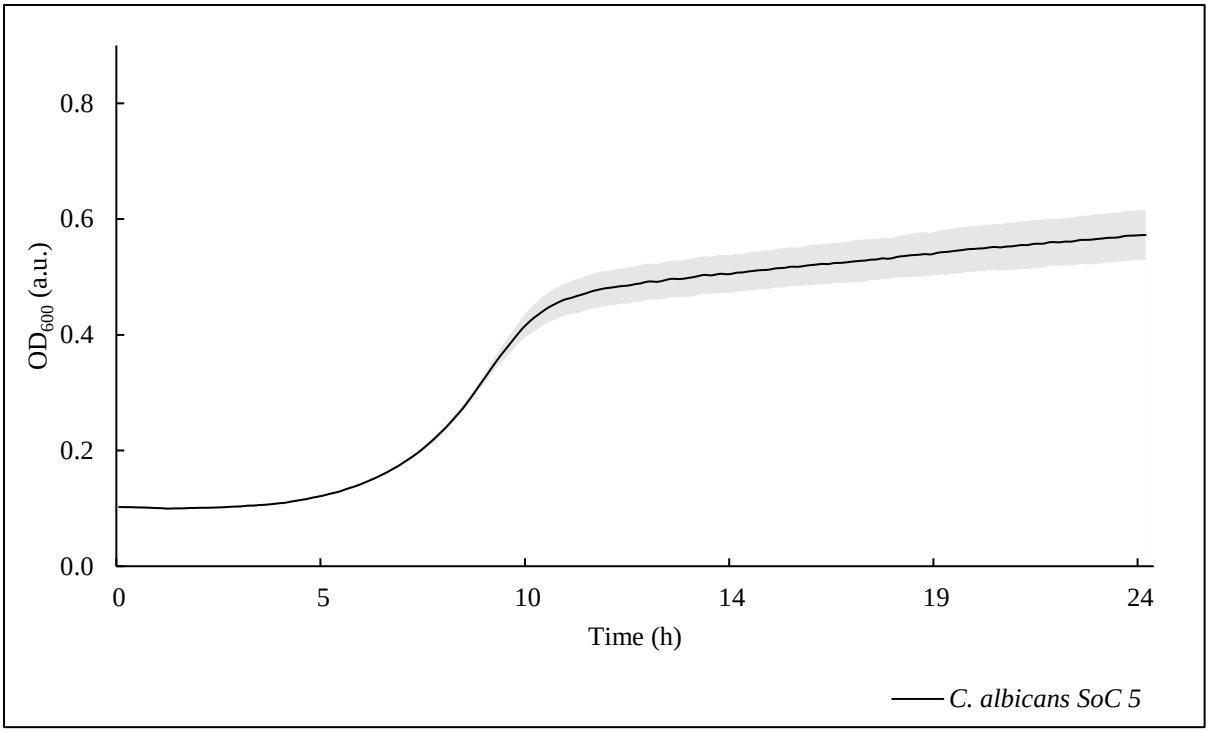

S10. Growth curve of *Candida albicans* exposed to 5 mg L^{-1} of *Saponaria officinalis* L. crude extract

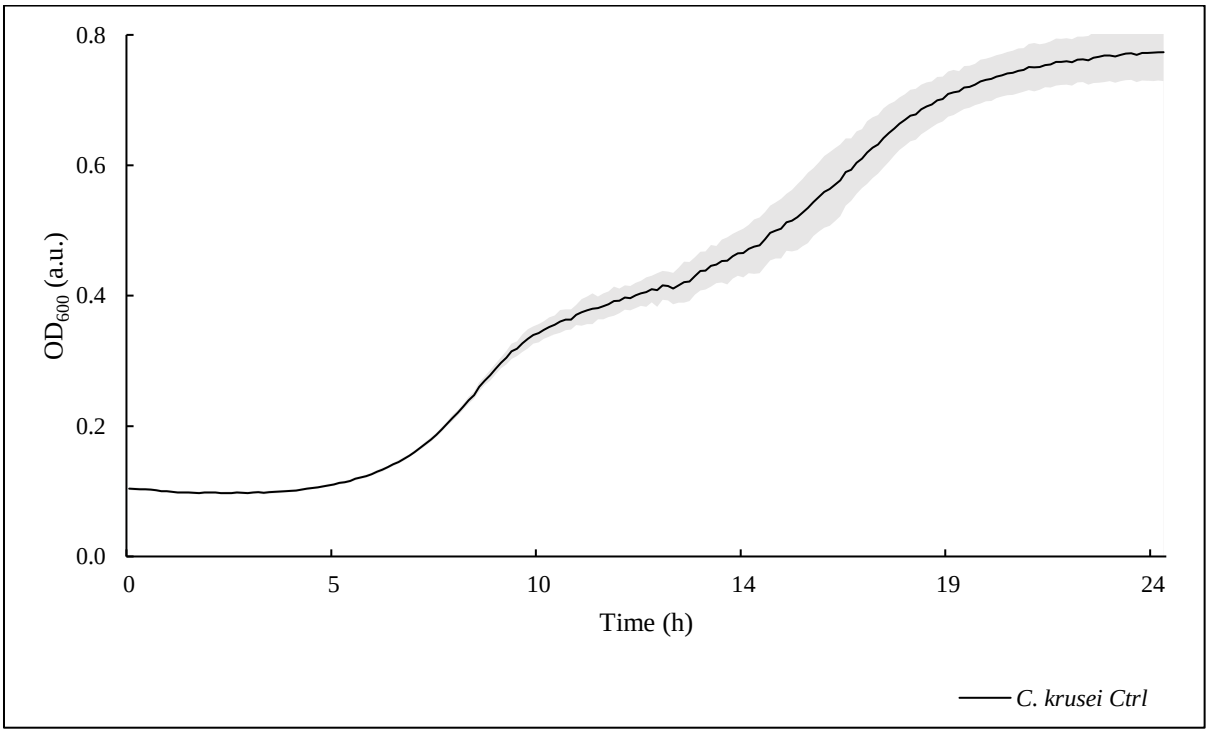

S11. Growth curve of *Candida krusei*

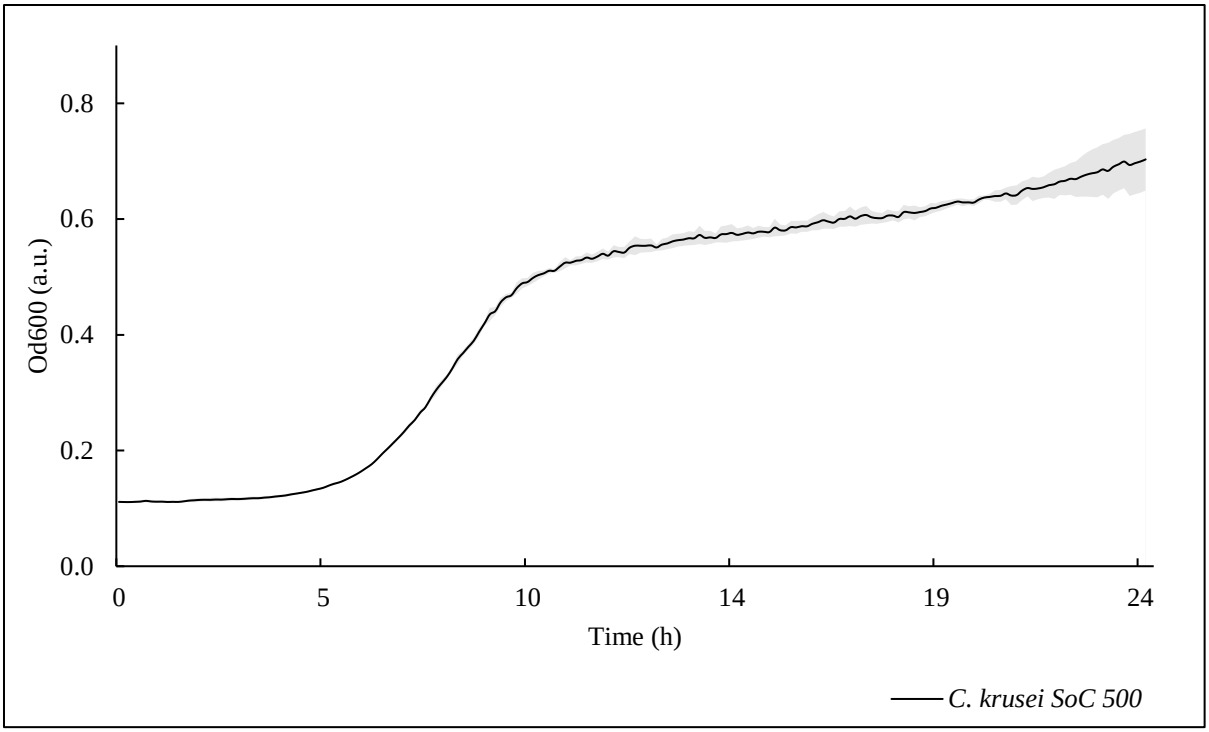

S12. Growth curve of *Candida krusei* exposed to 500 mg L^{-1} of *Saponaria officinalis* L. crude extract

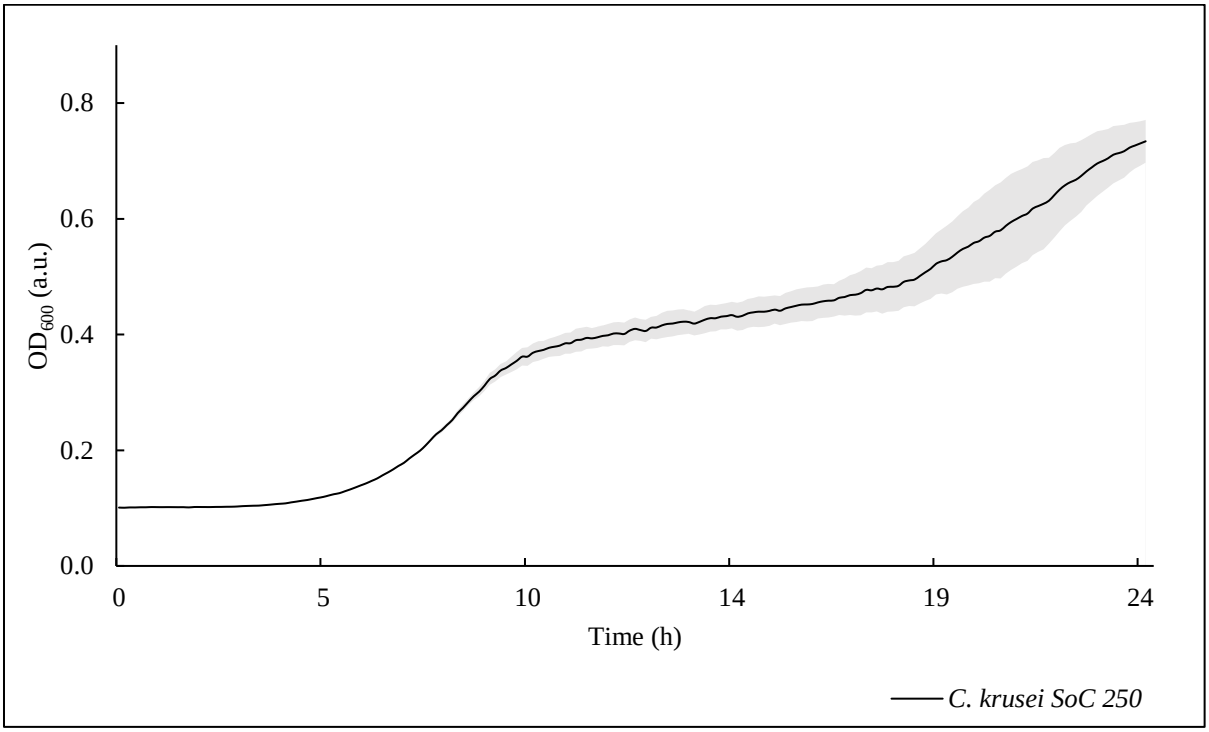

S13. Growth curve of *Candida krusei* exposed to 250 mg L^{-1} of *Saponaria officinalis* L. crude extract

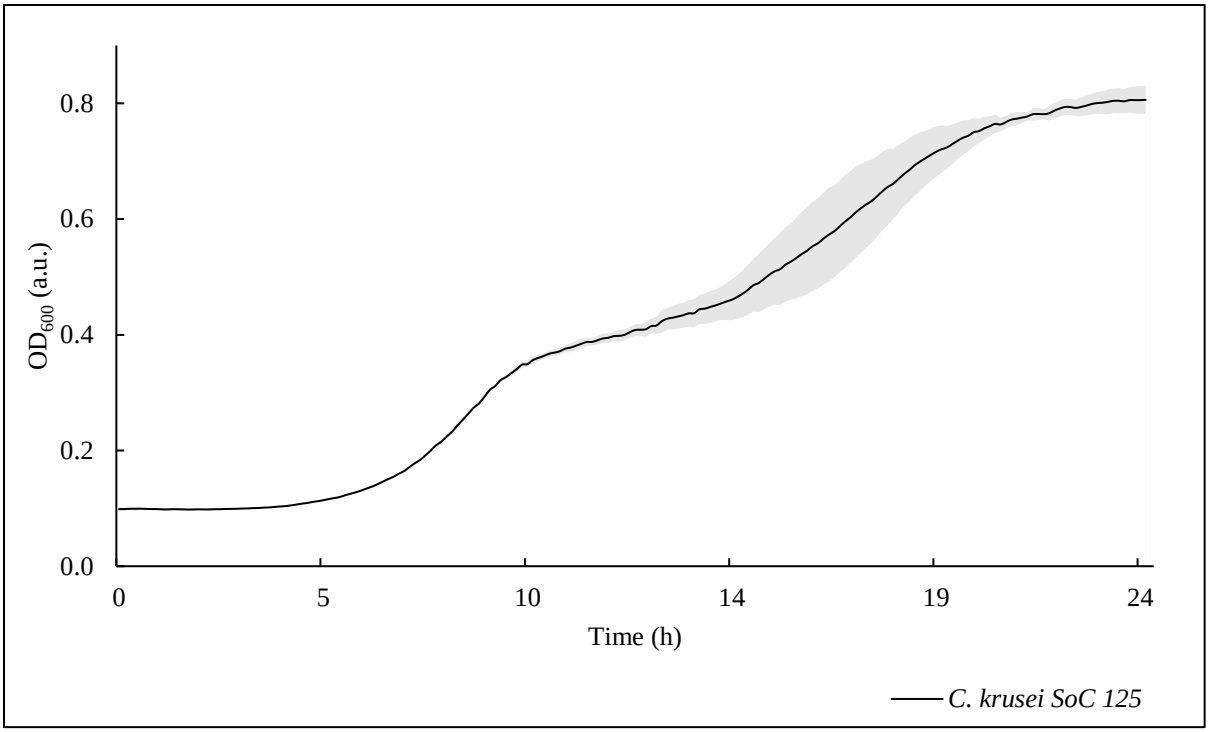

S14. Growth curve of *Candida krusei* exposed to 125 mg L^{-1} of *Saponaria officinalis* L. crude extract

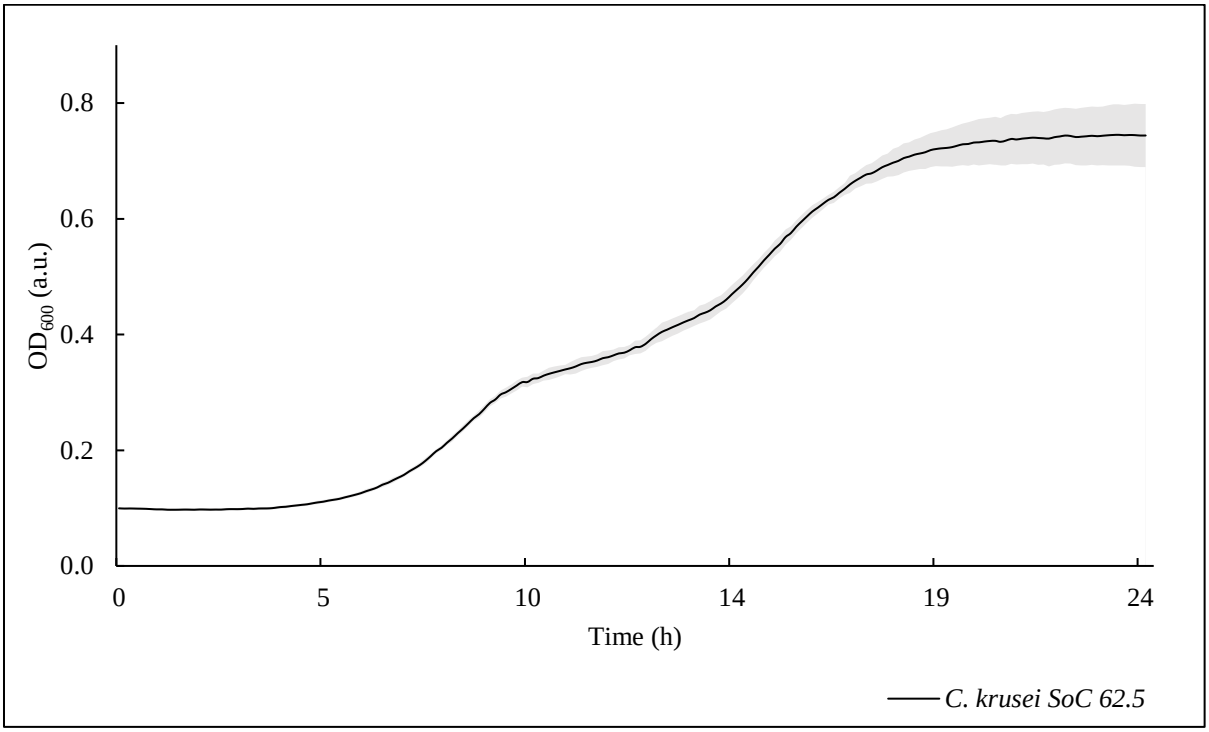

S1. Growth curve of *Candida krusei* exposed to 62.5 mg L^{-1} of *Saponaria officinalis* L. crude extract

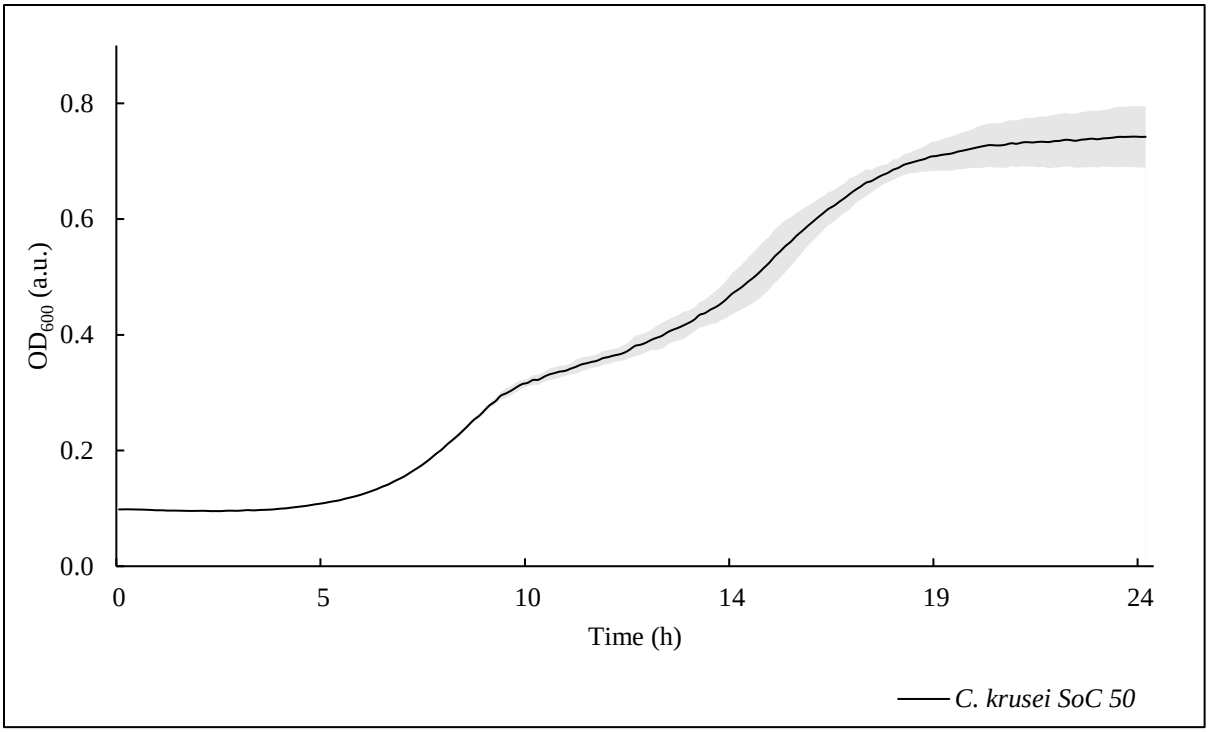

S16. Growth curve of *Candida krusei* exposed to 50 mg L^{-1} of *Saponaria officinalis* L. crude extract

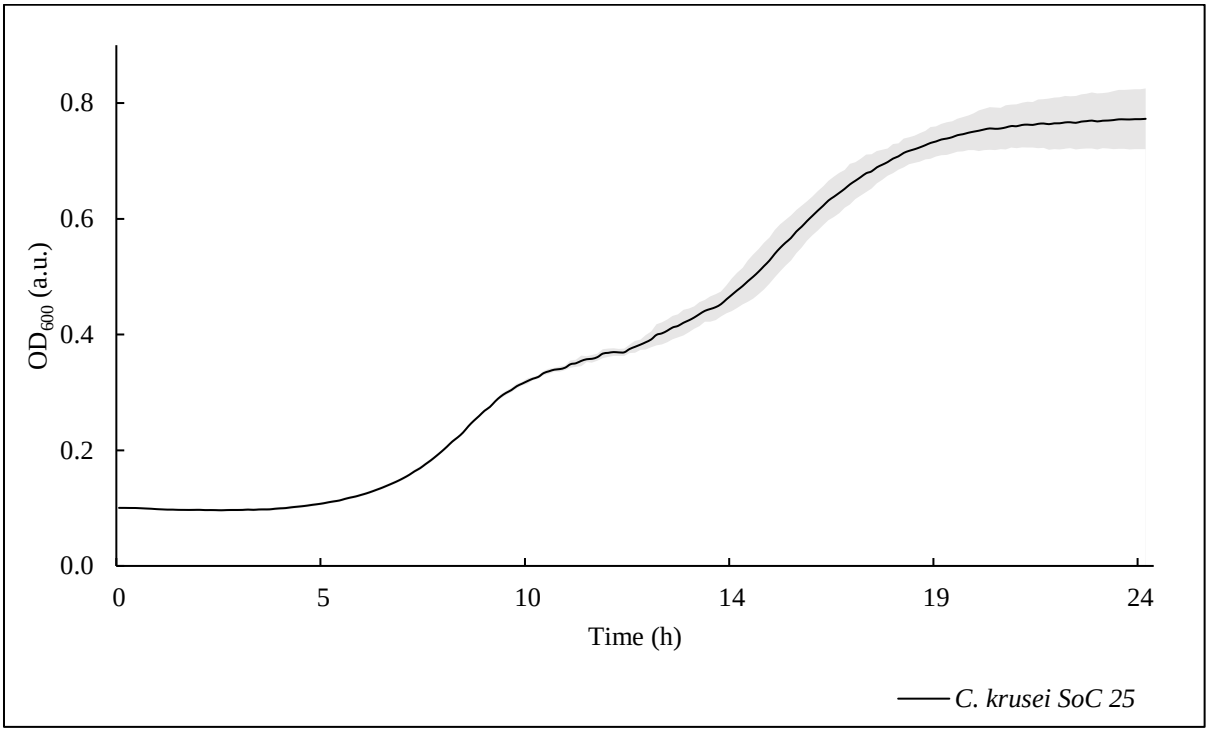

S17. Growth curve of *Candida krusei* exposed to 25 mg L^{-1} of *Saponaria officinalis* L. crude extract

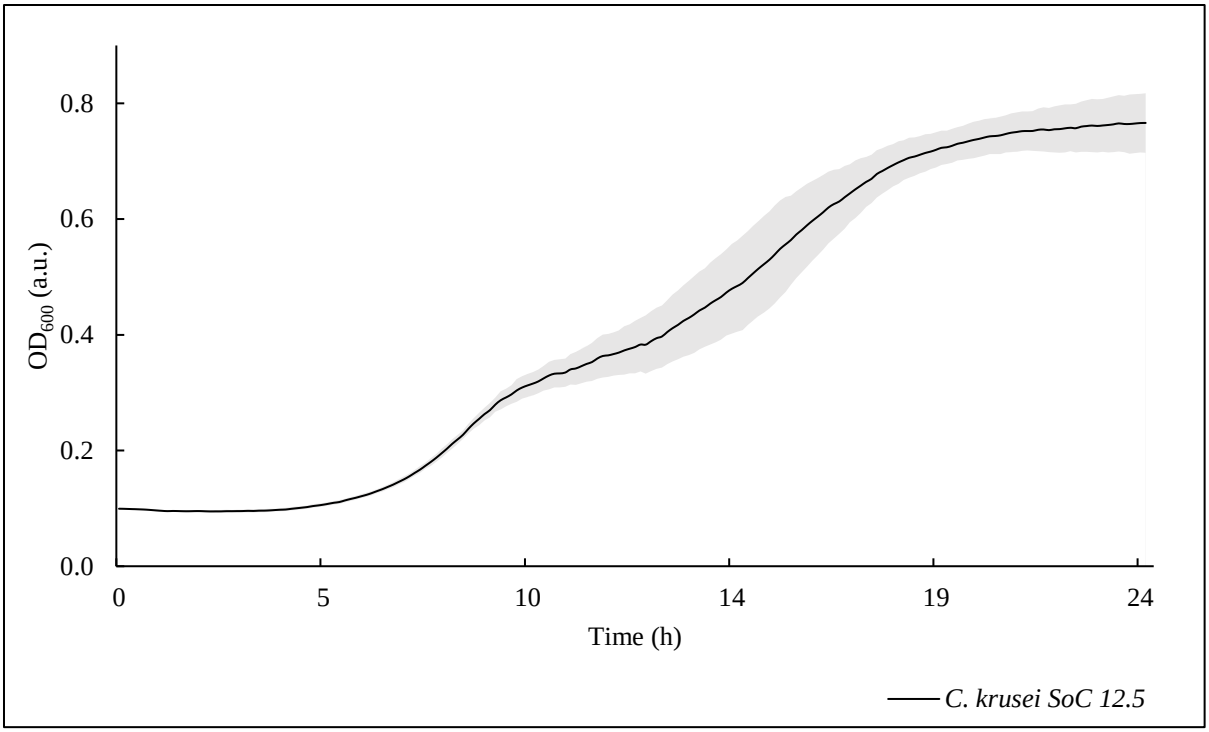

S18. Growth curve of *Candida krusei* exposed to 12.5 mg L^{-1} of *Saponaria officinalis* L. crude extract

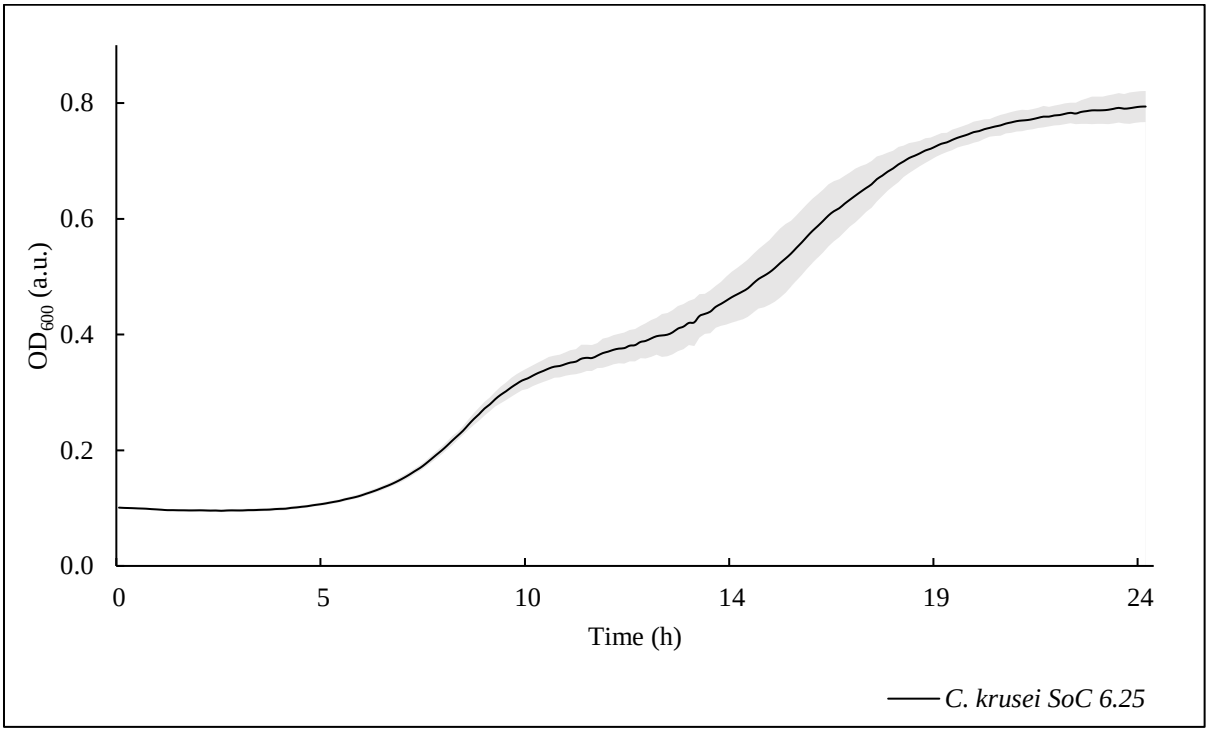

S19. Growth curve of *Candida krusei* exposed to 6.25 mg L^{-1} of *Saponaria officinalis* L. crude extract

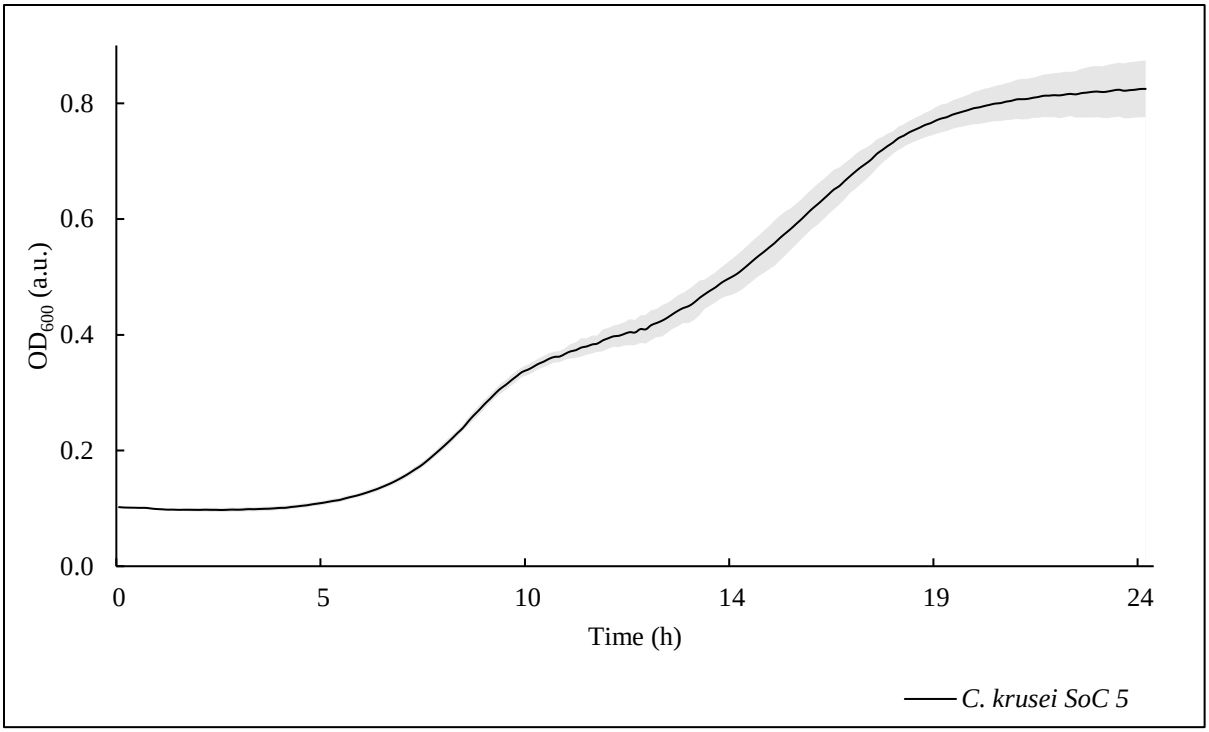

S20. Growth curve of *Candida krusei* exposed to 5 mg L^{-1} of *Saponaria officinalis* L. crude extract

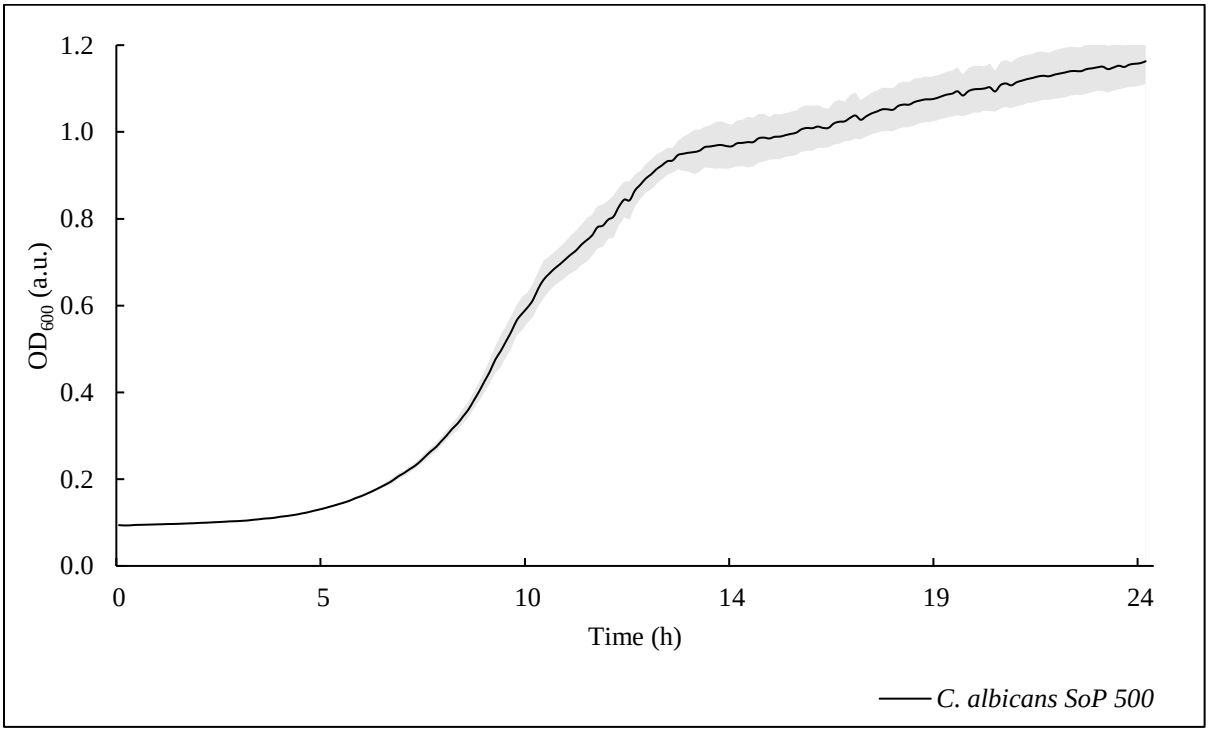

S21. Growth curve of *Candida albicans* exposed to 500 mg L^{-1} of *Saponaria officinalis* L. purified extract

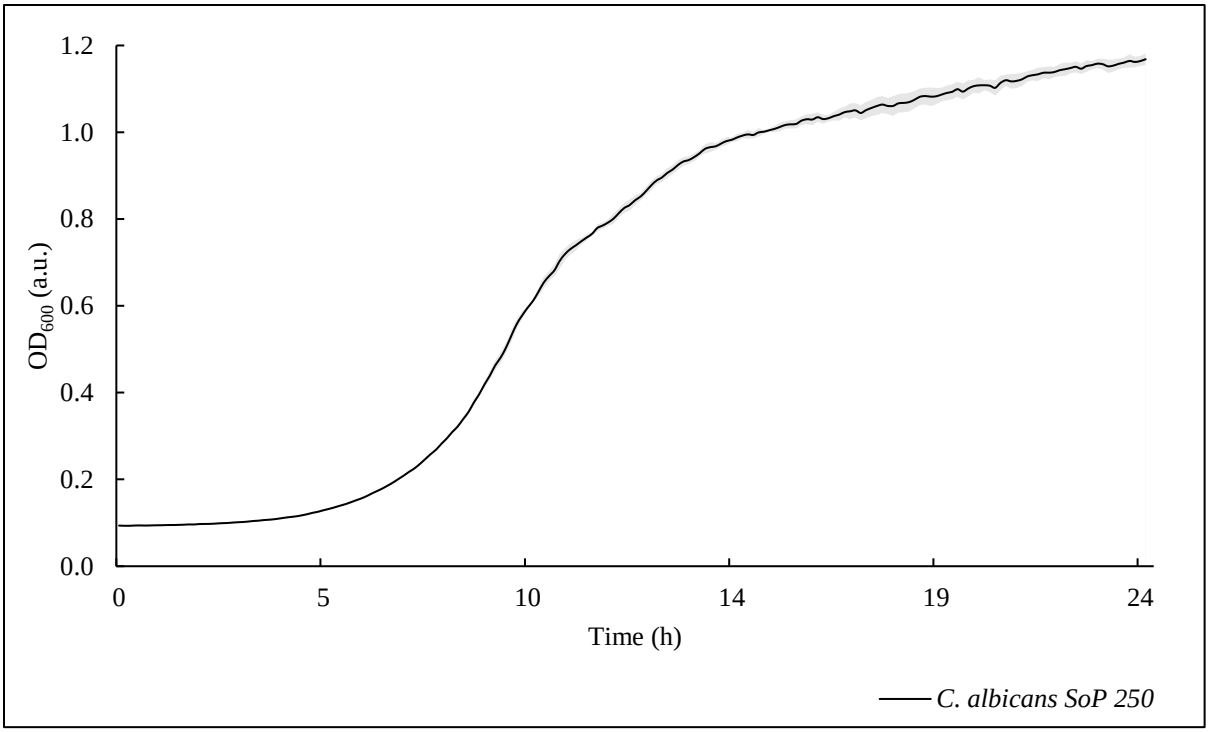

S22. Growth curve of *Candida albicans* exposed to 250 mg L^{-1} of *Saponaria officinalis* L. purified extract

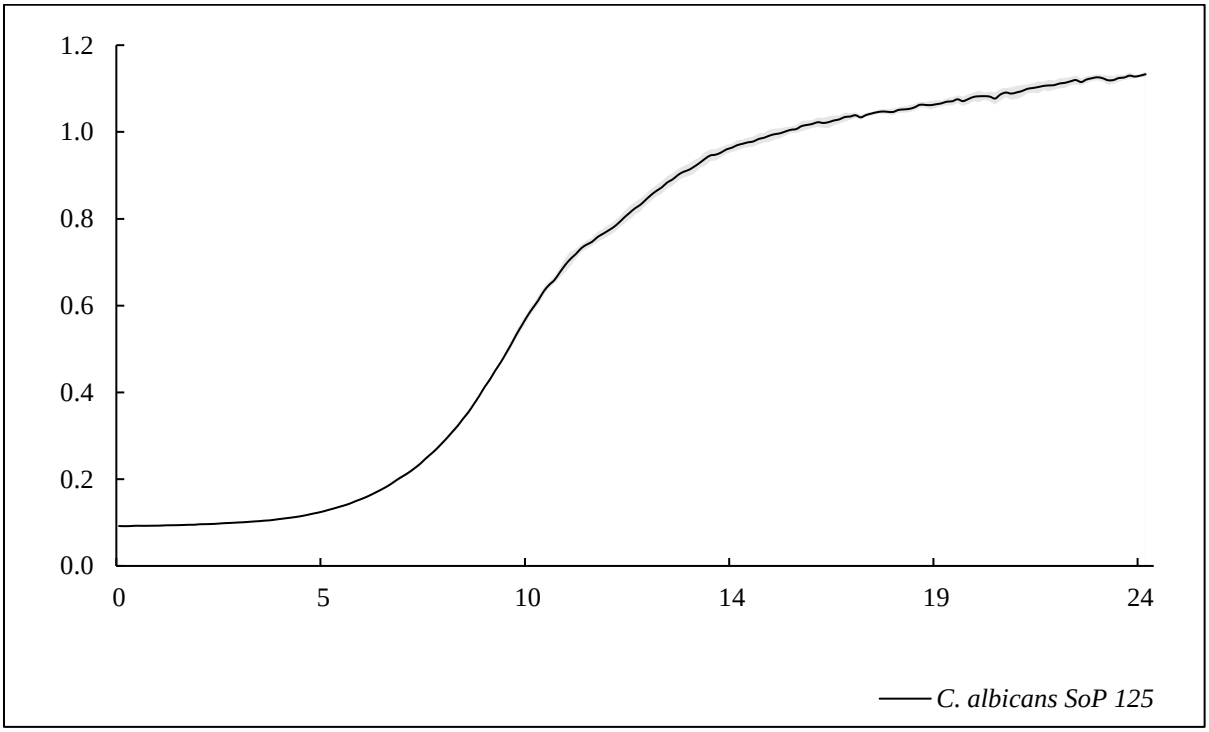

S23. Growth curve of *Candida albicans* exposed to 125 mg L^{-1} of *Saponaria officinalis* L. purified extract

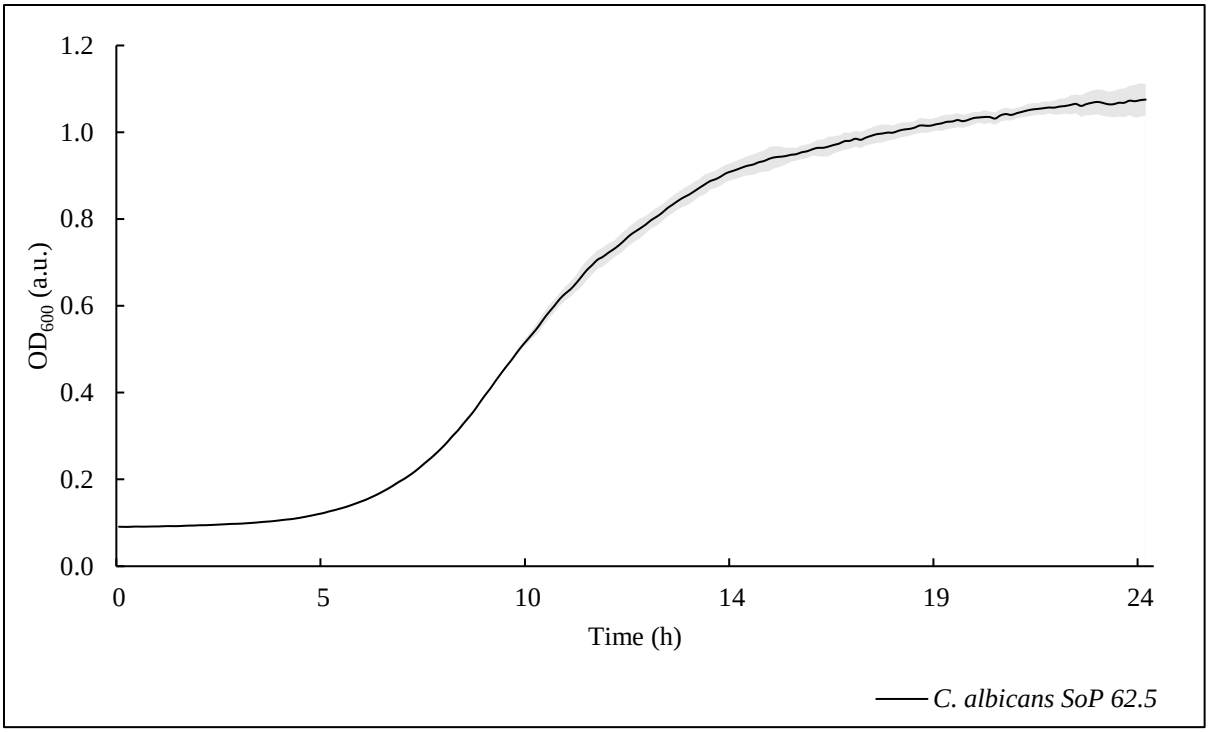

S24. Growth curve of *Candida albicans* exposed to 62.5 mg L^{-1} of *Saponaria officinalis* L. purified extract

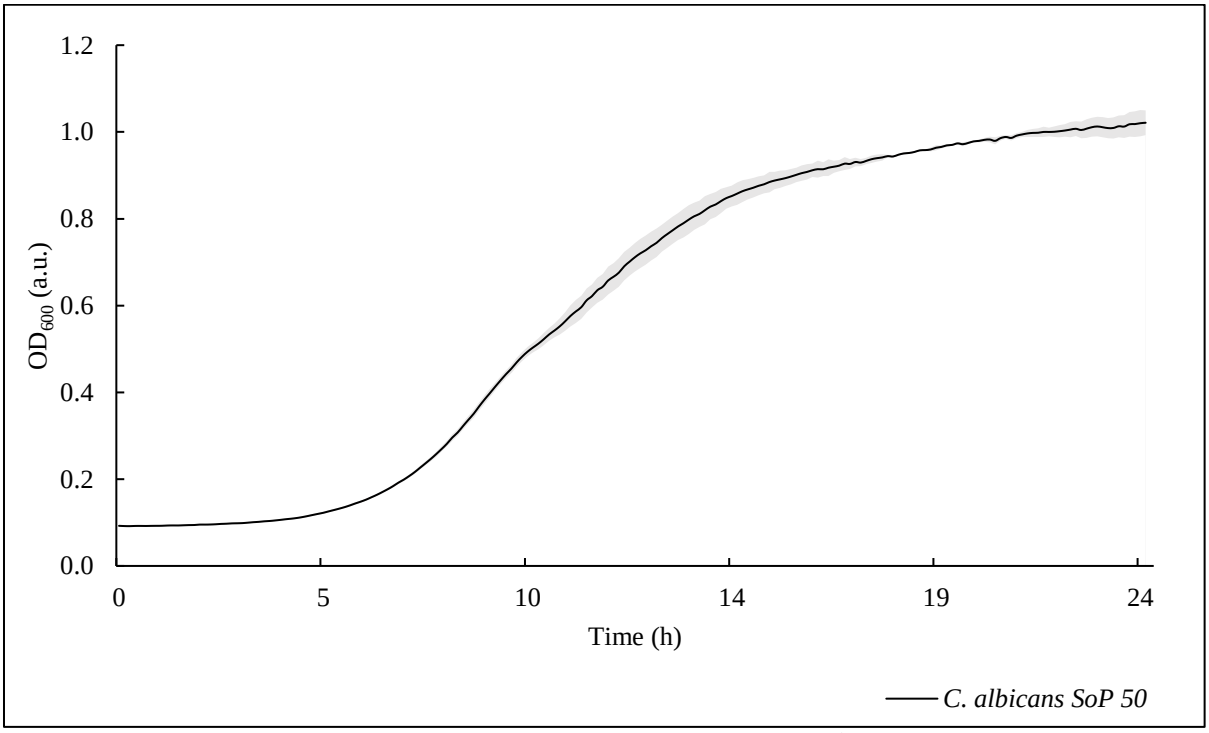

S25. Growth curve of *Candida albicans* exposed to 50 mg L^{-1} of *Saponaria officinalis* L. purified extract

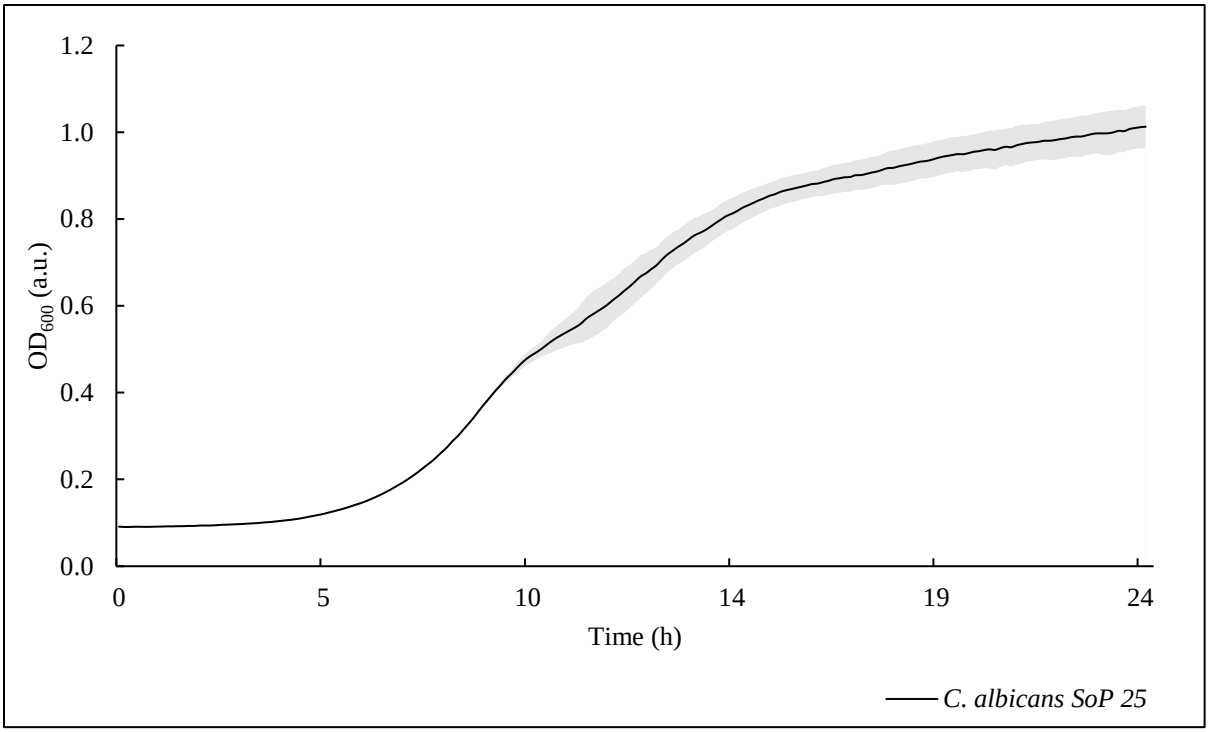

S26. Growth curve of *Candida albicans* exposed to 25 mg L^{-1} of *Saponaria officinalis* L. purified extract

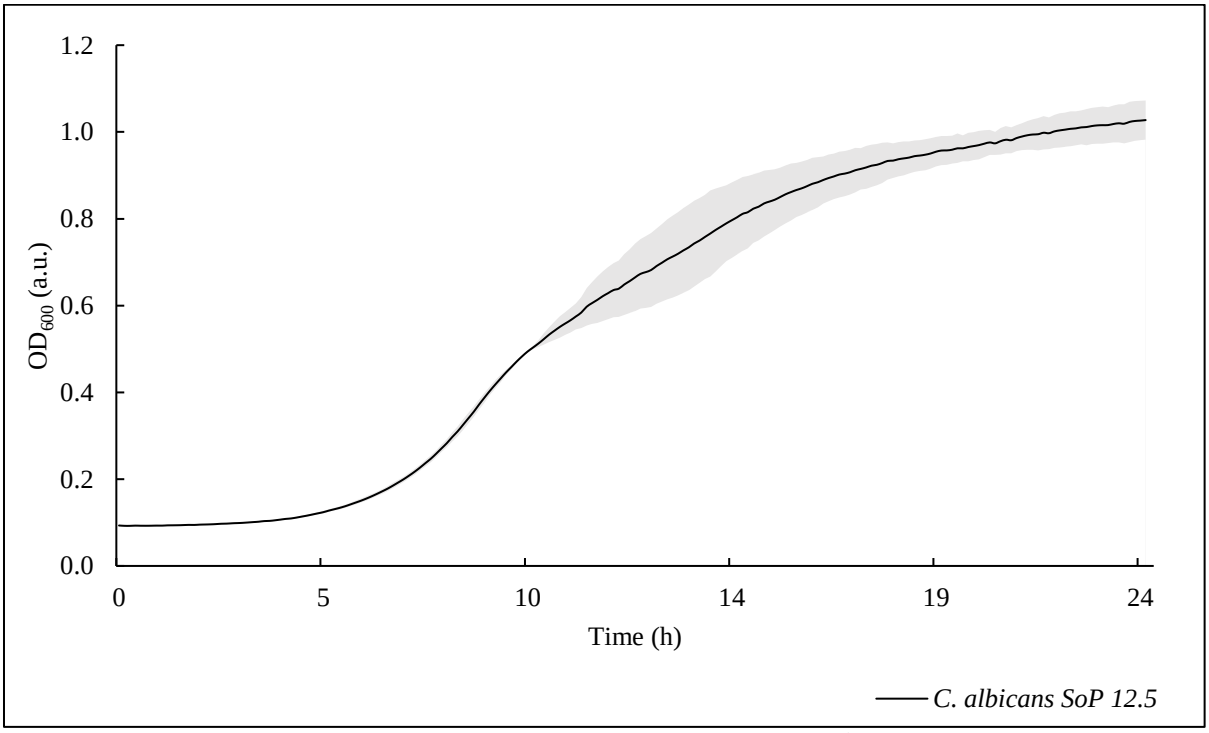

S27. Growth curve of *Candida albicans* exposed to 12.5 mg L^{-1} of *Saponaria officinalis* L. purified extract

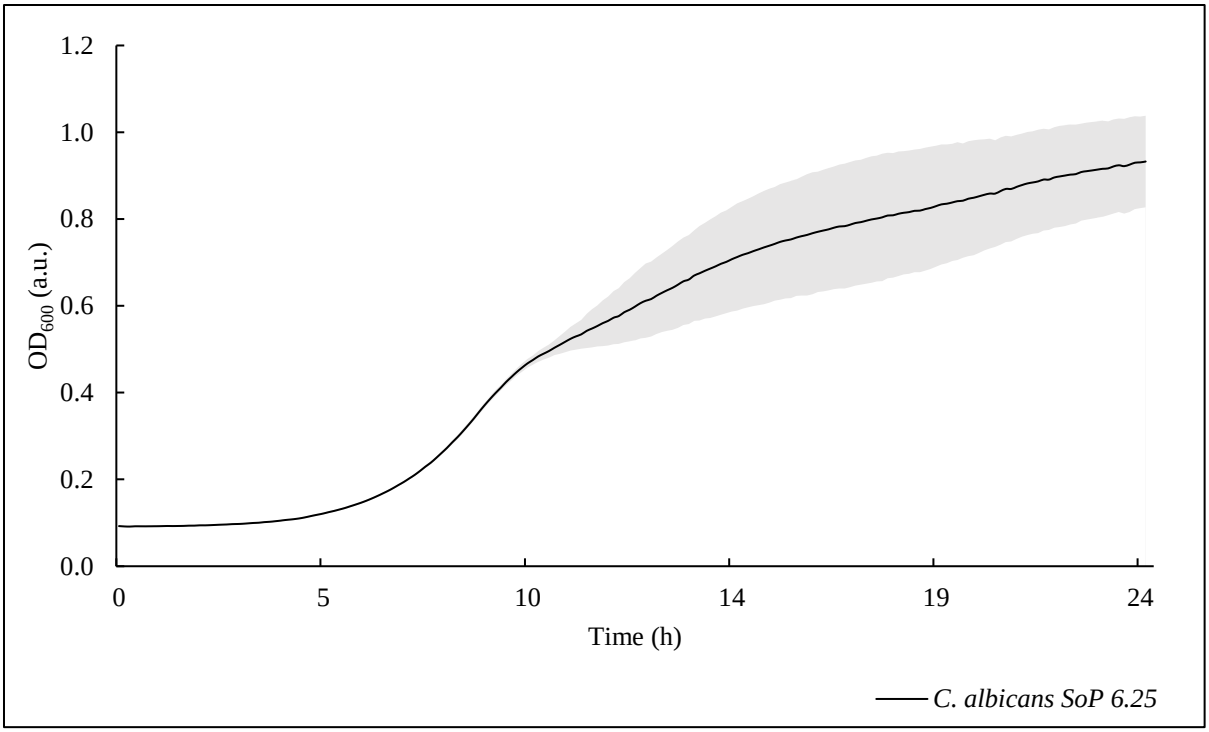

S28. Growth curve of *Candida albicans* exposed to 6.25 mg L^{-1} of *Saponaria officinalis* L. purified extract

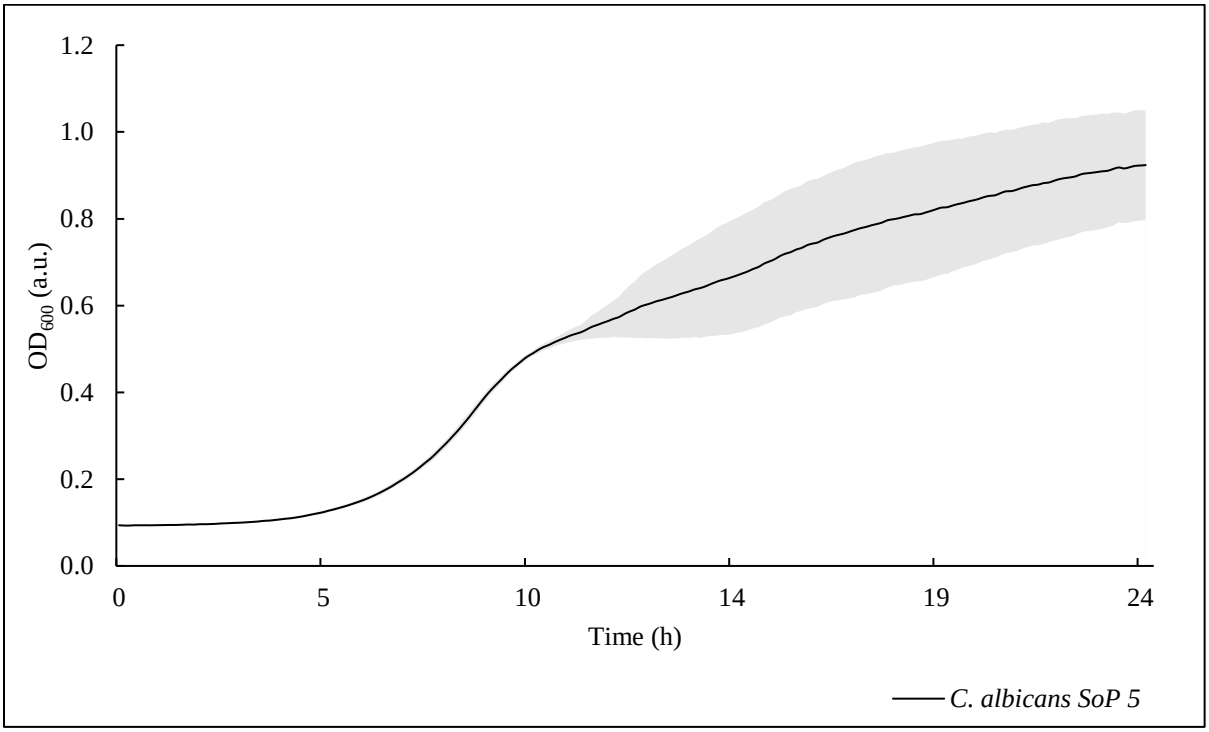

S29. Growth curve of *Candida albicans* exposed to 5 mg L^{-1} of *Saponaria officinalis* L. purified extract

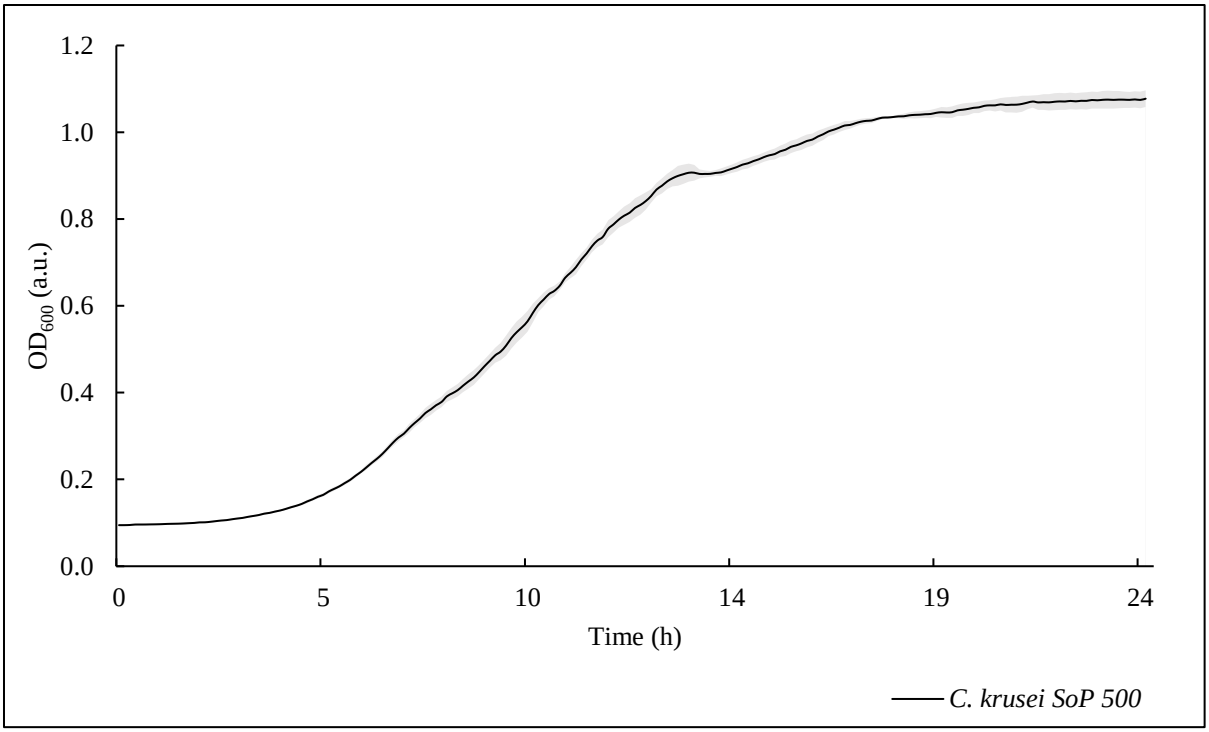

S30. Growth curve of *Candida krusei* exposed to 500 mg L^{-1} of *Saponaria officinalis* L. purified extract

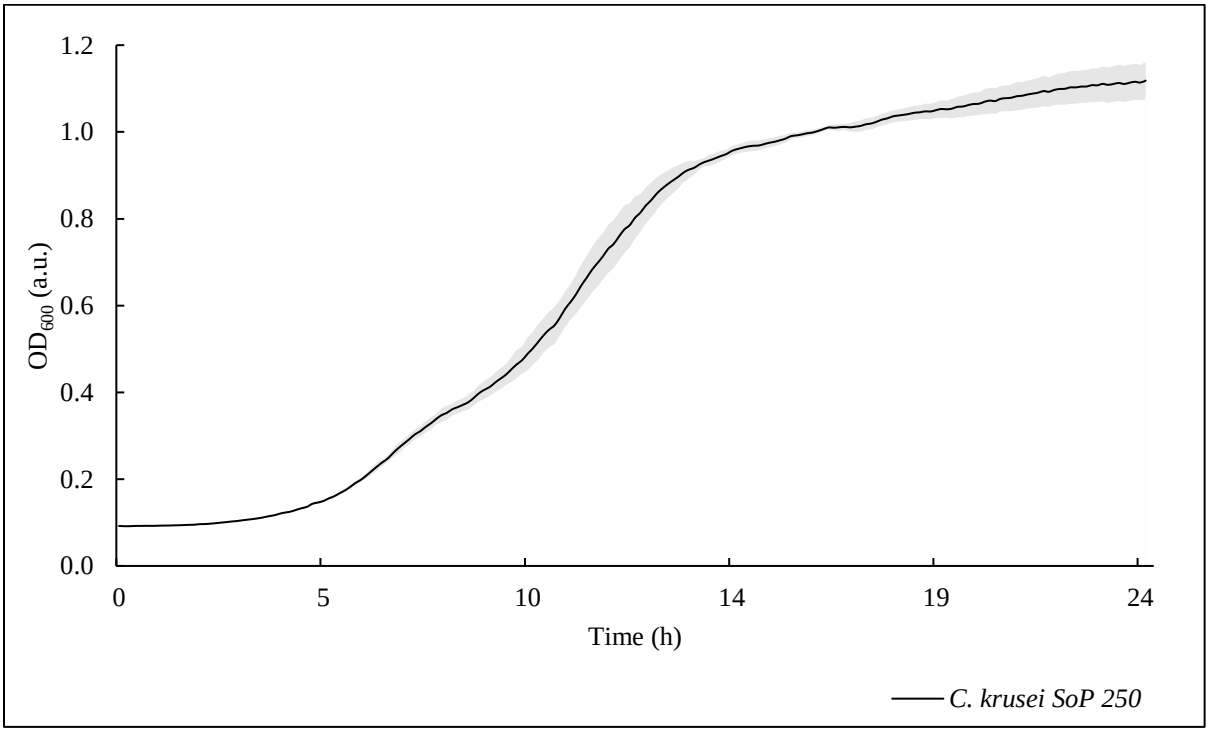

S31. Growth curve of *Candida krusei* exposed to 250 mg L^{-1} of *Saponaria officinalis* L. purified extract

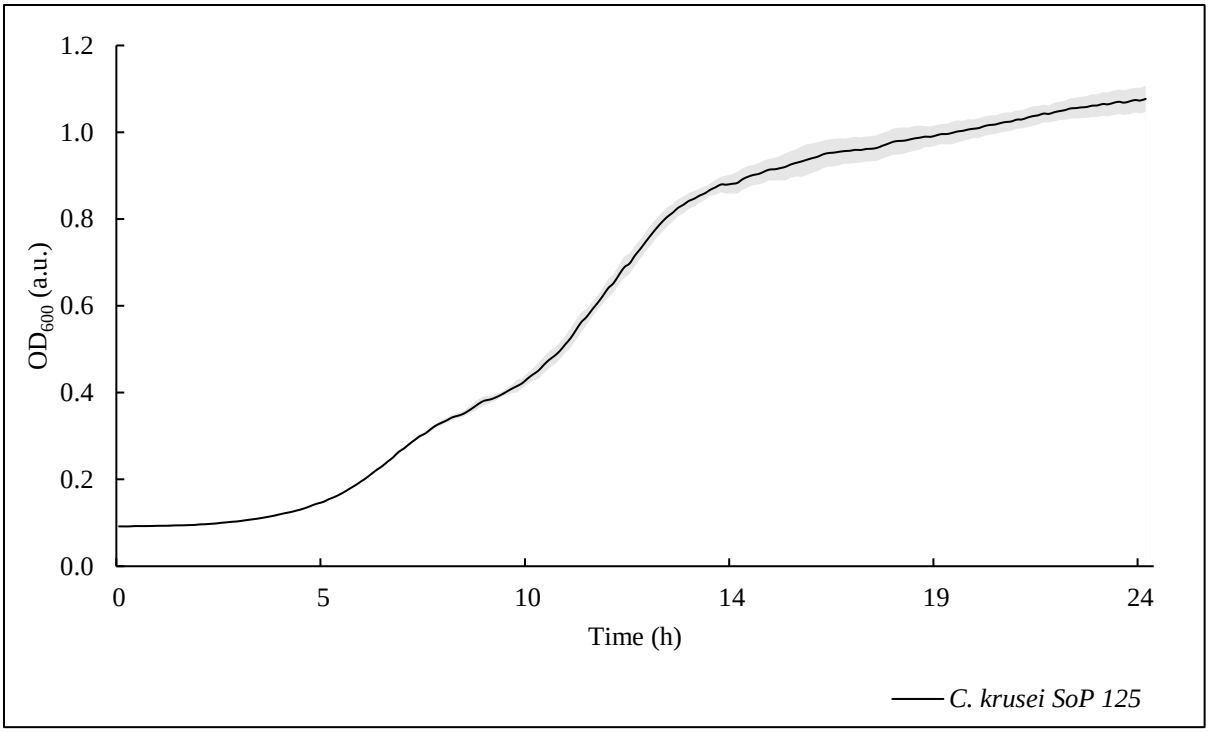

S32. Growth curve of *Candida krusei* exposed to 125 mg L^{-1} of *Saponaria officinalis* L. purified extract

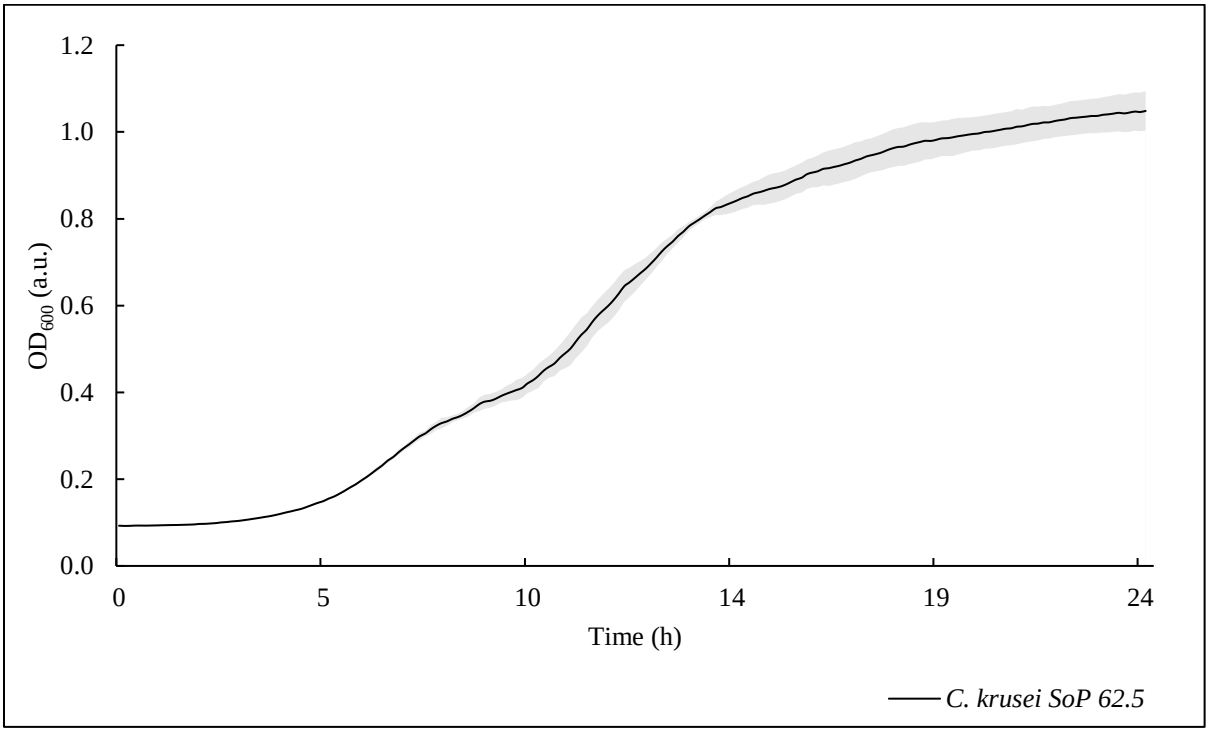

S33. Growth curve of *Candida krusei* exposed to 62.5 mg L^{-1} of *Saponaria officinalis* L. purified extract

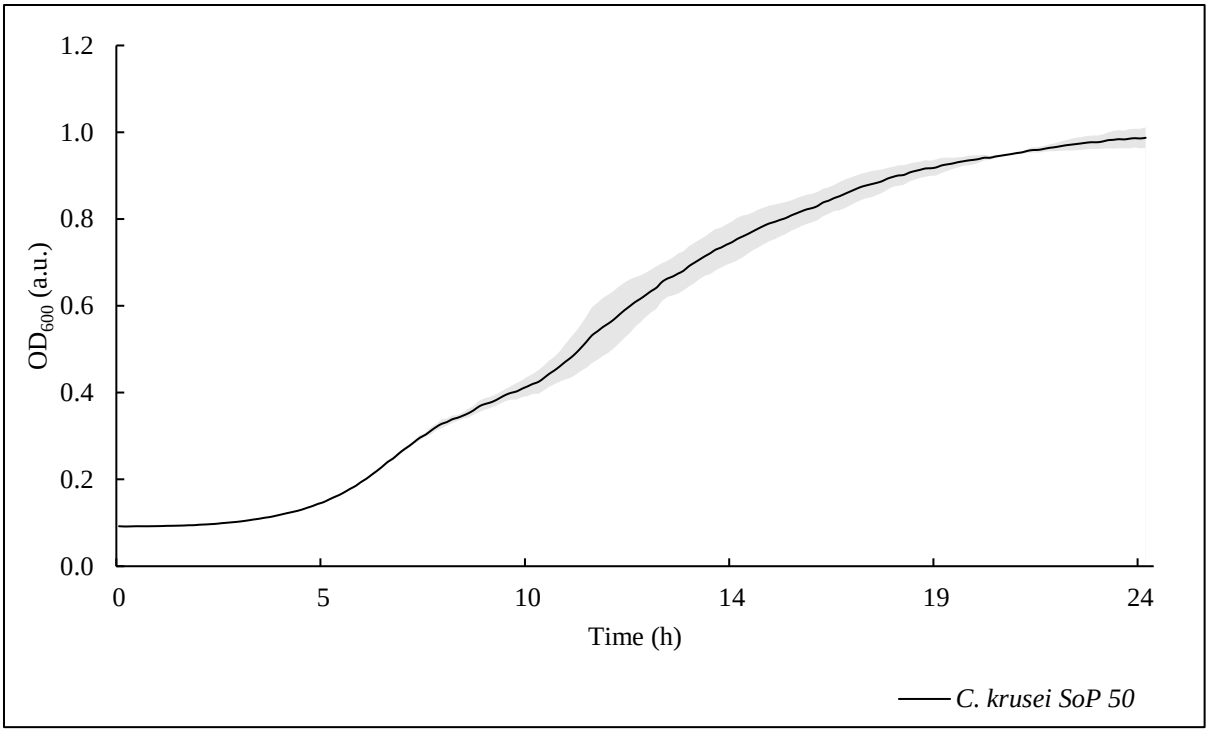

S34. Growth curve of *Candida krusei* exposed to 50 mg L^{-1} of *Saponaria officinalis* L. purified extract

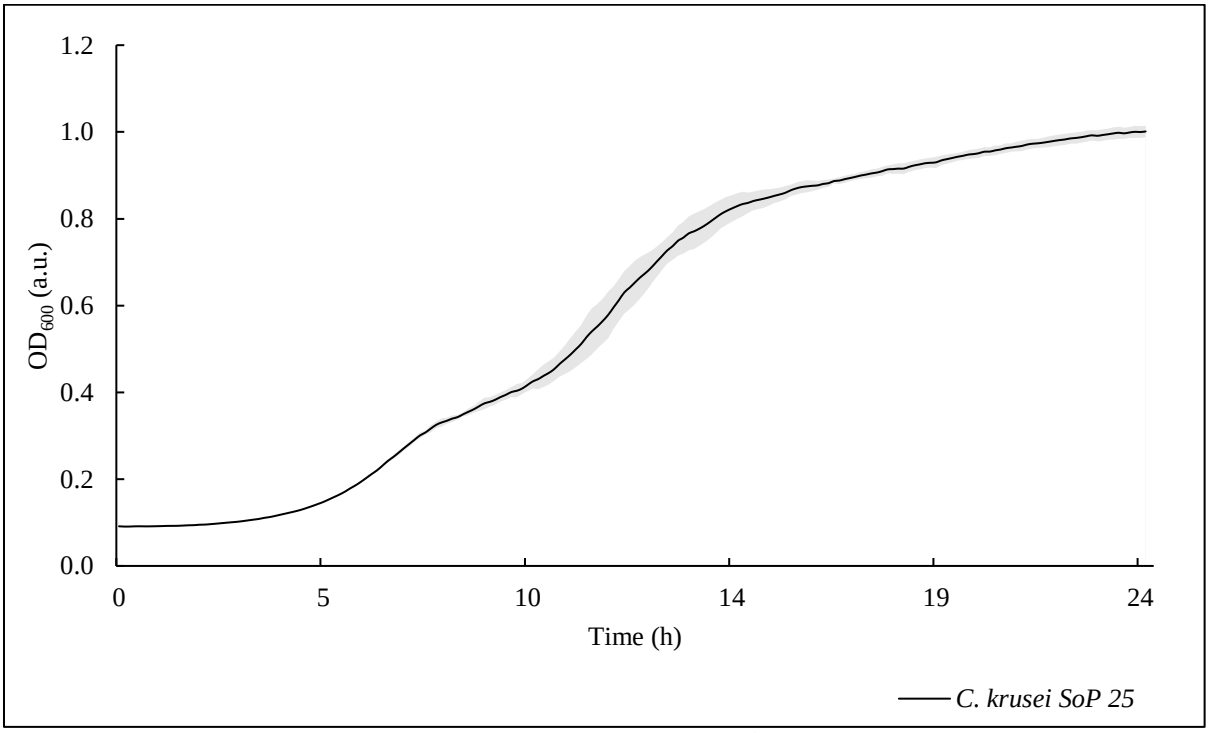

S35. Growth curve of *Candida krusei* exposed to 25 mg L^{-1} of *Saponaria officinalis* L. purified extract

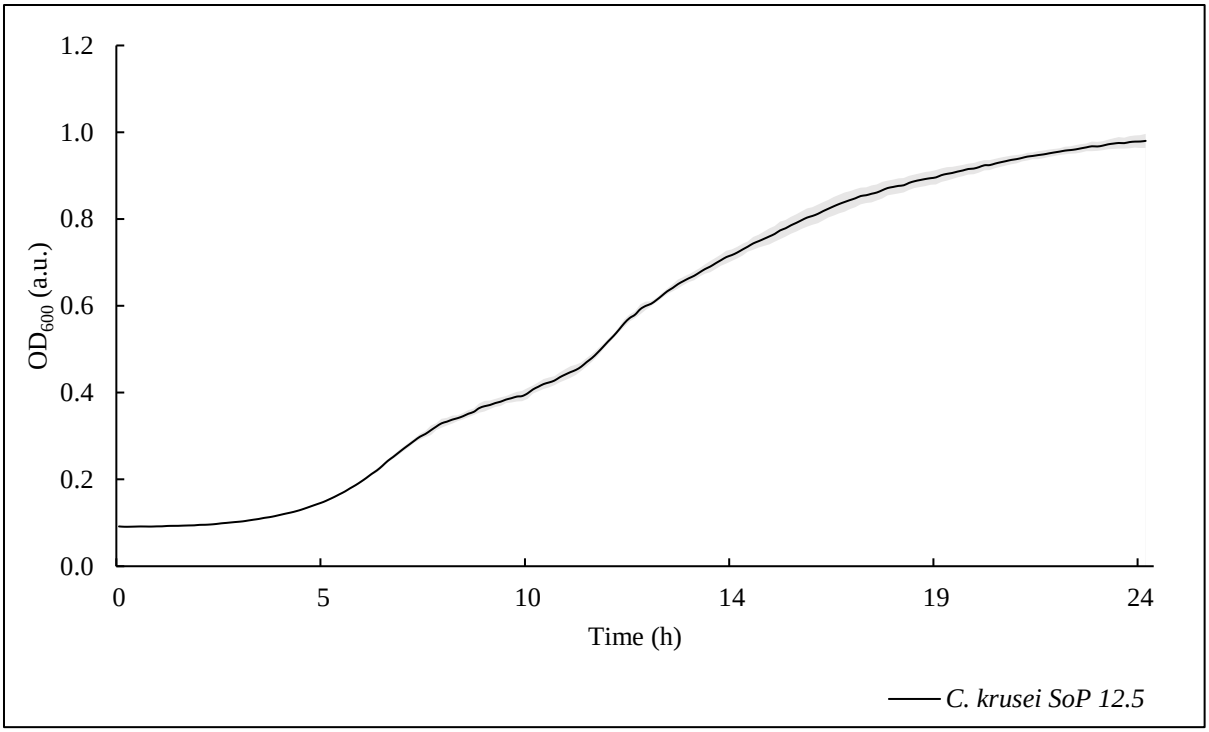

S36. Growth curve of *Candida krusei* exposed to 12.5 mg L^{-1} of *Saponaria officinalis* L. purified extract

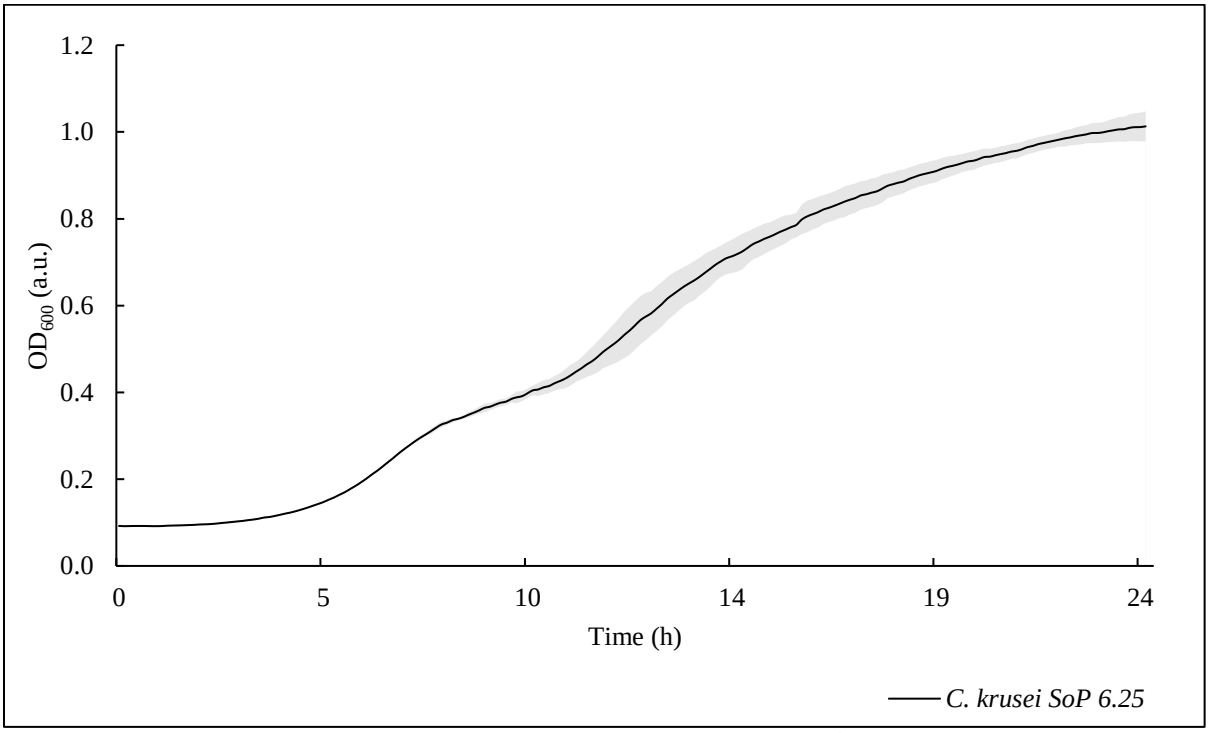

S37. Growth curve of *Candida krusei* exposed to 6.25 mg L^{-1} of *Saponaria officinalis* L. purified extract

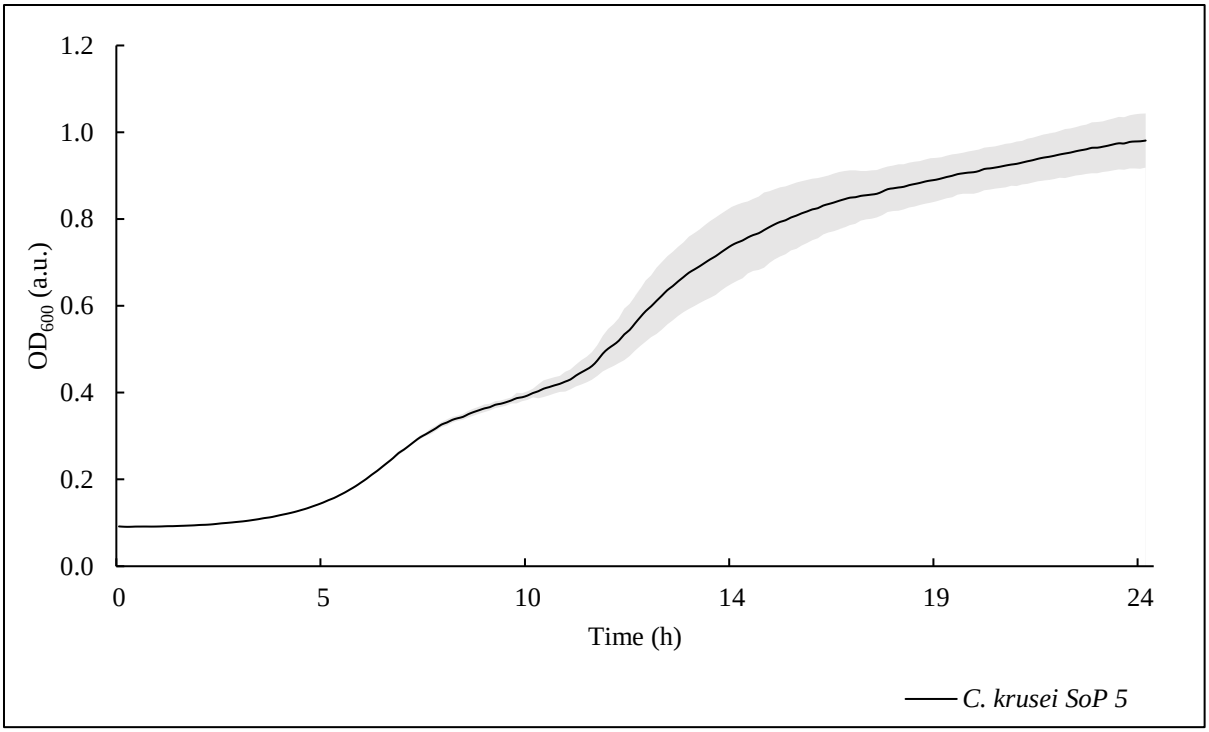

S38. Growth curve of *Candida krusei* exposed to 5 mg L^{-1} of *Saponaria officinalis* L. purified extract

Publication P4

LANGMUIR

pubs.acs.org/Langmuir Article

Glycyrrhiza glabra L. Saponins Modulate the Biophysical Properties of Bacterial Model Membranes and Affect Their Interactions with Tobramycin

Adam Grzywaczyk,* Monika Rojewska, Wojciech Smułek, Daniel A. McNaughton, Krystyna Prochaska, Philip A. Gale, and Ewa Kaczorek

Cite This: https://doi.org/10.1021/acs.langmuir.5c00927 Read Online

ABSTRACT: The global challenge of antibiotic resistance necessitates innovative approaches to improving the efficacy of existing therapeutics while mitigating their environmental impact. This study investigates the role of saponins derived from *Glycyrrhiza glabra* root extract in modulating interactions of tobramycin, a broad-spectrum aminoglycoside antibiotic, with model bacterial membranes composed of phosphatidylglycerol. Using Langmuir monolayers and vesicle models, we demonstrated that GgC saponins disrupt lipid packing, increasing membrane fluidity and altering biophysical properties. The addition of saponins at concentrations between 1.25 and 10 mg/L reduces the compressibility modulus of the lipid monolayer, with a decrease ranging from 25 to over 50%. ζ potential and dynamic light scattering analyses indicated that GgC−tobramycin interactions modify the surface charge without causing membrane lysis. These membrane changes could potentially facilitate enhanced interactions of antibiotics with bacterial cells. Importantly, these findings suggest the potential of natural surfactants such as saponins to improve antibiotic efficacy, possibly enabling reduced antibiotic dosages. This study provides insights into using saponins alongside antibiotics as a sustainable approach to addressing antibiotic resistance.

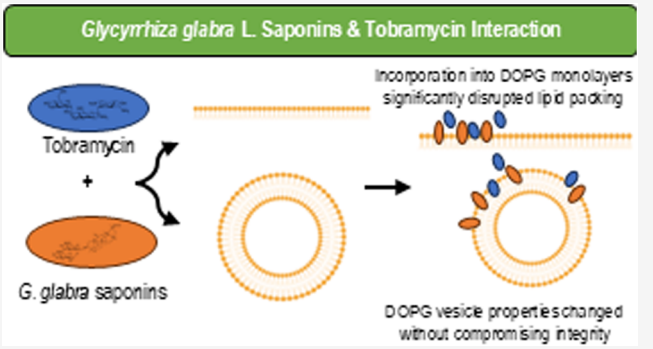

INTRODUCTION

The escalating resistance of microorganisms to antibiotics is a critical global health threat, driven largely by their overuse in human medicine and agriculture.[1,2] Overexposure accelerates the evolution of resistant bacteria, diminishing the effectiveness of the currently available antibacterial agents. With limited therapeutic options for resistant infections and a slow pace of new antibiotic development, there is an urgent need to explore alternative strategies. Addressing this global challenge requires a multifaceted approach, including improved surveillance, restricted antibiotic use, and collaborative action among national and international organizations.[1] One promising approach within the realm of chemical research is the identification of adjuvants that can enhance the efficacy of existing antibiotics, potentially overcoming resistance, broadening the antibiotic spectrum, and reducing required dosages.[3]

Aminoglycosides, including tobramycin, are potent antibiotics effective against Gram-negative bacteria, particularly in severe infections.[4] Despite declining use due to toxicity concerns, there is renewed interest in aminoglycosides to combat multidrug-resistant pathogens. Tobramycin, known for its broad-spectrum activity, is being explored as part of nanoparticle formulations that enhance efficacy and reduce side effects.[5] To enhance its efficacy, tobramycin is also often used in combination with β-lactams or other cell-wall-disrupting agents to exploit synergistic effects and mitigate resistance development.[6−8]

Saponins, natural surfactants derived from plants, present a promising approach when used in tandem with traditional antibiotics. Saponins can insert into microbial cell membranes. Notably, bacterial membranes lack cholesterol (a major target of saponins in eukaryotic cell membranes); therefore, in bacteria, saponins likely interact with other lipid constituents. This interaction disrupts the membrane structure, leading to changes in its packing.[9] By an increase in bacterial membrane fluidity, saponins may enhance membrane permeability, potentially facilitating antibiotic entry and their subsequent effects. For instance, saponins from *Sapindus mukorossi* L.

Received: February 24, 2025
Revised: April 22, 2025
Accepted: April 22, 2025

significantly increased the antibacterial activity of nitrofurantoin against *Pseudomonas aeruginosa*.[7,8] Similarly, glycyrrhizin (GC) acid enhanced the susceptibility of vancomycin-resistant enterococci to gentamicin, teicoplanin, and daptomycin.[10] Interactions between saponins and model phospholipid membranes are important in the context of biogeochemical phospholipid cycles, which govern the movement and transformation of phospholipids in the environment. In natural bacterial ecosystems, changes in the composition and structure of lipid membranes can affect key biological processes, such as organic compound degradation and nutrient exchange, meaning saponins are particularly valuable in overcoming the protective barriers that resistant bacteria often employ. Using saponins to weaken the bacteria cell membrane could reduce the required dosage of antibiotics, decreasing the risk of side effects and slowing the development of resistance. Their natural origin and potential for synergy with antibiotics make them compelling candidates in the fight against antibiotic-resistant bacteria, offering a novel approach to enhance the efficacy of existing treatments.

In light of this, our study aimed to evaluate whether *Glycyrrhiza glabra* L. root extract (GgC) affects membrane properties that could influence tobramycin interactions with a model phospholipid membrane. The transportation of drugs across cell membranes is a complex and dynamic process, and model lipid membranes are invaluable tools when examining these processes. These models mimic key features of cellular lipids, enabling researchers to elucidate the roles of lipids in cellular interactions.[11] Phospholipids are important constituents of all cell membranes. The chemical structure of individual phospholipids in the membrane is of significant importance because changes in the composition of acyl chains or headgroups affect the fluidity and stability of the bilayer and, consequently, affect the membrane's response to external stimuli.[10−12] The ability of bacteria to modify their phospholipid compositions leads to variations in the structure of their membranes. The most common phospholipids in bacterial membranes are phosphatidylglycerol (PG) and phosphatidylethanolamine (PE), which contain different polar headgroups. In our previous work, we have shown how saponins interact with model membranes composed of PE.[8,13] This study examines interactions between saponins and antibiotics using a phosphatidylglycerol (DOPG) monolayer, aiming to determine whether saponins modulate membrane properties that are potentially relevant for antibiotic transport. The choice of DOPG, which is one of the predominant phospholipids found in bacterial membranes, provides a biologically relevant system to evaluate interactions between bacterial membranes, antibiotics, and saponins under controlled experimental conditions. We envisaged that this study would provide deeper insights into the mechanisms by which saponins can enhance the efficacy of antibiotics. Improving our understanding of how saponins interact with bacterial membranes, specifically through their impact on phospholipid composition and membrane fluidity, could help identify new ways to facilitate the penetration of antibiotics into bacterial cells. Advancements in this field have the potential to overcome one of the key barriers posed by resistant bacteria: their ability to modify membrane structures to impede drug entry. Additionally, these insights could reveal how saponins may disrupt bacterial defense mechanisms or synergize with antibiotics to improve treatment outcomes.

MATERIALS AND METHODS

Chemicals and Membrane Model Structures Preparation. A chloroform of high-purity Uvasol (Merck, Warsaw, Poland) was used to prepare the Langmuir monolayer. Dulbecco's phosphate buffered saline (Merck KGaA, Darmstadt, Germany) was applied as a solvent to prepare saponin solutions or as a subphase. 8-Hydroxypyrene-1,3,6-trisulfonic acid trisodium salt (HPTS) and 5(6)-carboxyfluorescein (5(6)-CF) were obtained from Sigma-Aldrich (Merck KGaA, Darmstadt, Germany). The saponins utilized in this study were obtained through a methanolic extraction process from *G. glabra* roots, employing a Soxhlet apparatus for 6 h. *G. glabra* extract is characterized by a complex chemical composition, which includes a variety of compounds, including flavonoids and polysaccharides. The key component of this extract is glycyrrhizic acid, which can vary in content from 2 to 25%.[14] Tobramycin of 95% purity was obtained from Angene Chemical (Nanjing, Jiangsu, China).

Monolayer experiments were conducted by using the Langmuir technique. Two-dimensional (2D) models of biomembranes consist of DOPG (1,2-dioleoyl-*sn*-glycero-3-phospho-*rac*-(1-glycerol) sodium salt), 99%, from Avanti Polar Lipids (Alabaster, AL). Likewise, DOPG vesicles were prepared as liposomal bilayers (a three-dimensional membrane model—3D) via freeze−thaw and extrusion through a 200 nm porous membrane as described by Gilchrist et al.[15]

Stability Measurements and Particle Size Distribution. To assess the stability of DOPG vesicles before and after treatment with tobramycin and GgC, we employed electrophoretic light scattering (ELS) to measure the ζ potential, utilizing the Smoluchowski equation for its determination. In this procedure, GgC, tobramycin, and their combination were added to 0.01% DOPG vesicles suspended in phosphate buffer solution (pH 7.0), achieving final concentrations of 5 mg/mL for tobramycin and 10 mg/mL for GgC. Additionally, the particle size distribution and polydispersity index (PDI) of the vesicles were assessed by using dynamic light scattering (DLS). Both analyses were conducted using a Litesizer 500 instrument (Anton Paar, Graz, Austria).

HPTS and 5(6)-Carboxyfluorescein. To evaluate the potential leakage and damage to vesicles upon treatment with tobramycin and GgC, separate experiments were completed with either HPTS or 5(6)-CF dyes encapsulated within the liposomes. This was achieved by using aqueous solutions as the rehydration medium for the phospholipid film before freeze−thawing, following the method described by Gilchrist et al.[15] After the freeze−thaw process, the liposomes were extruded through a 200 nm membrane before being separated from the unencapsulated dye using Sephadex size exclusion chromatography (SEC). This was achieved using specific buffered solutions as the rehydration medium. For the HPTS assay, the internal liposome solution was 100 mM NaCl, 10 mM *N*-(2-hydroxyethyl)piperazine-*N*′-ethanesulfonic acid (HEPES), 1 mM HPTS (pH 7.2), and after SEC purification, the external buffer was 100 mM NaCl, 10 mM HEPES. For the 5(6)-carboxyfluorescein assay, the internal solution was 451 mM NaCl, 20 mM phosphate buffer (pH 7.2) with 50 mM 5(6)-carboxyfluorescein, and the external solution after SEC was 150 mM Na_2SO_4, 20 mM phosphate (pH 7.2). The liposomes, containing 0.1% of the dye, were subsequently treated with tobramycin and GgC, reaching final concentrations of 5 and 10 mg/mL, respectively. Triton-X100 was added at the end of the experiment to lyse the liposomes and determine the maximum possible fluorescence, serving as a reference for total leakage. Fluorescence emission was monitored in real-time using the GloMax Explorer System (Promega).

***π*−*A* Isotherm Measurement.** All of the experiments were performed using the KSV NIMA Langmuir film balance system (KN 0033). The surface pressure was measured using a Wilhelmy platinum plate with an accuracy of ±0.1 mN/m. The lipid monolayer (DOPG) was formed by dropping 25 μL of phospholipid solution onto a subphase interface. As the subphase, ultrapure water with a conductivity of 0.055 μS/cm and a pH of 6.7 was used (PureLab System, ELGA, Poland). The subphase was placed in a Teflon trough (KSV Nima, Helsinki, Finland) with a surface area of 238 cm^2. During

https://doi.org/10.1021/acs.langmuir.5c00927
Langmuir XXXX, XXX, XXX−XXX

the measurements, the temperature was kept constant at 25.0 ± 0.1 °C with a Julabo circulator. Before each measurement, the subphase was cleaned to a surface pressure below π = 0.35 mN/m reached at maximum compression. After spreading the phospholipid solution onto the subphase, it was followed by 15 min evaporation of the chloroform, the Langmuir monolayer was compressed at a constant barrier speed equal to 10 mm/min. One minute before the compression, the saponin solution was injected into the Langmuir trough and stirred. Saponin solution (10 mg/mL) was added in an appropriate volume to achieve the following final subphase concentrations: 1.0; 2.5; 5.0, and 10.0 mg/L. The surface pressure π (mN/m) was measured as a function of the area per DOPG molecule, A (Å^2/molec.).

A compressional modulus (C_s^{-1}) is a rheological quantity related to monolayer rigidity, and it is calculated from the π–A isotherm data using eq 1:

$$C_s^{-1} = -A \times \left(\frac{\Delta\pi}{\Delta A}\right)_T \quad (1)$$

The magnitude of this parameter provides information about the monolayer packing and the elasticity of the monolayer during compression. According to the Davies and Rideal classification,[15] the values of 12.5 < C_s^{-1} < 50 mN/m and 50 < C_s^{-1} < 250 mN/m indicate that the monolayer is formed in a liquid-expanded (LE) state and liquid-condensed (LC) state, respectively. Each experiment was repeated at least three times to ensure that the reproducibility of the curves was within ±2 Å^2.

Relaxation Measurements. To introduce additional molecules into the monolayer using a peristaltic pump, the monolayer was formed first, and then the subphase was replaced with a new solution. The exchange was performed through silicone tubing placed on a stand before the inlet and outlet hoses were inserted into the Langmuir trough on opposite sides. Both hoses were connected to the same pump head, which ensured a steady supply and the removal of liquid from the trough. All relaxation experiments described in this article were carried out with subphase exchange using a MINIPULS 3 (Gilson) peristaltic pump.

Statistical Analysis. Statistical analyses were performed using Python (v3.9) with the *statsmodels* and *seaborn* libraries. Data preparation involved simulating distributions based on the provided means and standard deviations for each treatment group. Normality was assessed using histograms and Q–Q plots, while Levene's test was applied to evaluate the homogeneity of variances. One-way analysis of variance (ANOVA) was conducted to determine the effect of the treatments. Post hoc comparisons were performed using Tukey's Honest significant difference (HSD) test to identify pairwise differences between groups.

RESULTS AND DISCUSSION

***Glycyrrhizin* Saponins and Tobramycin Effect on DOPG Vesicle.** Initial experiments focused on evaluating the effects of *G. glabra* saponins and tobramycin on DOPG vesicles in order to assess how these compounds influence vesicle stability, size distribution, and surface charge. Concentrations of 5 mg/mL for tobramycin and 10 mg/mL for GgC were chosen to align with typical therapeutic dosages, ensuring relevance to clinical applications.

The control sample, consisting of untreated DOPG liposomes, exhibited a narrow size distribution with a peak particle diameter centered around 100–120 nm (Figure 1), indicating a uniform population with minimal size variability. Treatment with GgC extract maintained the size distribution peak at 100–120 nm, similar to the control. However, a slight broadening of the distribution was observed (Figure 1), suggesting an increase in size variability among the liposomes. This implies that while GgC slightly affects the homogeneity of liposome sizes, it does not significantly alter their overall mean

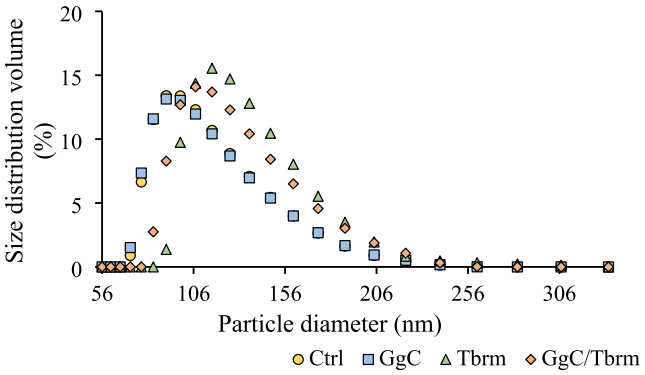

Figure 1. *G. glabra* L. root extract (GgC) and tobramycin affect the vesicle size distribution. Ctrl—untreated sample was treated with GgC (5 mg/L), Tbrm (10 mg/L) with tobramycin, GgC/Tbrm (5 mg/L) with GgC (10 mg/L) with tobramycin effect. The p-value is greater than 0.05, indicating that variances across groups are not significantly different.

size. In contrast, liposomes treated with tobramycin exhibited a peak size distribution shifted toward larger diameters (115–130 nm) compared to both the control and GgC-treated samples. The distribution also appeared broader than that of the control, indicating an increased heterogeneity. This suggests that tobramycin induces mild structural changes in the liposomes, contributing to the size variability. When GgC and tobramycin were combined, the size distribution remained centered around 100–120 nm but exhibited a more pronounced broadening and a slight shift toward larger diameters compared to the individual treatments. This broader distribution suggests an interaction between GgC and tobramycin, likely enhancing structural alterations in the liposomes and potentially leading to aggregation, or GgC may inhibit the structural alterations caused by the antibiotic. Volume-weighted size distributions are reported here to provide a representative vesicle size profile that is less biased by very large or small particles. For completeness, intensity-weighted and number-weighted distributions are included in the Supporting Information, showing similar trends. Despite these observed shifts, the polydispersity index (PDI) values (Table 1) remained low across all samples, confirming a

Table 1. Polydispersity Index (PDI) of Samples[a,b]

Ctrl	0.13 ± 0.02*
GgC	0.15 ± 0.02*
Tbrm	0.13 ± 0.03*
GgC/Tbrm	0.13 ± 0.04*

[a]Ctrl—untreated sample, GgC—5 mg/L treated, Tbrm—10 mg/L tobramycin, GgC/Tbrm 5 mg/L, GgC + 10 mg/L of tobramycin effect. [b]One-way ANOVA indicated no significant differences among the PDI (*: p > 0.05).

generally uniform size distribution under all conditions. The combination of GgC and tobramycin, however, caused subtle changes in the distribution peak and variability, indicating enhanced structural effects on the liposome population.

The ζ potential of untreated DOPG liposomes was measured at −50.0 mV, reflecting a strongly negative surface charge (Figure 2). This high level of negative charge indicates that the control DOPG liposomes have a strongly charged surface with significant electrostatic repulsion between vesicles. Upon treatment with GgC, the zeta potential showed minimal

https://doi.org/10.1021/acs.langmuir.5c00927
Langmuir XXXX, XXX, XXX−XXX

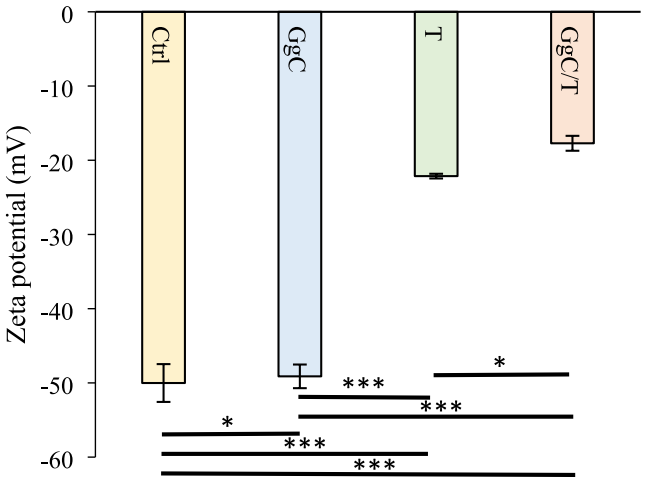

Figure 2. ζ potential of DOPG liposomes under different conditions (Ctrl: untreated control; GgC: *G. glabra* crude saponin extract at 5 mg/L; T: tobramycin at 10 mg/L; GgC/T: combination of GgC + tobramycin). Asterisks indicate statistically significant differences: *: $p < 0.05$, ***: $p < 0.001$.

influence on the stability of the liposomes (within experimental error). The marginal decrease in surface charge suggests that the electrostatic repulsion remains largely comparable to that of the untreated liposomes. In contrast, treatment with tobramycin led to a significant decrease in ζ potential, recorded at −22.1 mV. This substantial reduction in surface charge indicates that tobramycin compromises the stability of the DOPG vesicles, likely by neutralizing some of the negative charges on the liposome surface. The resulting decrease in repulsive forces increases the likelihood of liposome aggregation. When the liposomes were exposed to both GgC and tobramycin, the ζ potential further decreased to −17.7 mV. This additional reduction in surface charge, compared to that of tobramycin alone, suggests that the combination of saponin extract and tobramycin severely undermines liposome stability. The interaction between these compounds appears to further neutralize the liposome surface charge, making the liposomes even more prone to aggregation.

The stability of DOPG liposomes treated with *GgC* tobramycin and their combination was assessed using two complementary methods: the HPTS assay and the carboxyfluorescein release assay. These techniques provide a comprehensive evaluation of the liposome stability and membrane permeability. The HPTS assay monitors internal pH changes, which reflect ion leakage and membrane transport, while the carboxyfluorescein assay measures the release of an encapsulated dye, directly assessing membrane integrity. By using both methods, we can gain valuable insights into the effects of GgC, tobramycin, and their combination on the structural stability and ion permeability of the liposomal membrane. In the HPTS assay, the stability of the liposomes was tracked by measuring the internal pH changes. Before the addition of Triton-X100, liposomes treated with GgC resulted in little change in fluorescent output, indicating a minimal passage of H^+ into the membrane, and therefore preservation of integrity (Figure 3). Similarly, tobramycin-treated liposomes and liposomes exposed to the combination of GgC and tobramycin exhibited stable fluorescence, demonstrating that neither the antibiotic alone nor the combination of GgC and tobramycin destabilized the membrane. Overall, these results indicate that before the detergent lysis step, none of the treatments (GgC, tobramycin, or their combination) caused significant ion leakage or compromised the liposome membrane integrity.

The carboxyfluorescein release assay provided further confirmation of membrane stability by measuring the release of the encapsulated dye (Figure 4). As in the HPTS assay, Triton-X100 was added at the end to lyse the liposomes and establish maximum fluorescence. Liposomes treated with GgC, tobramycin, and their combination did not exhibit a change in fluorescence before Triton-X100 addition, indicating minimal dye leakage and intact membranes. Importantly, the combination of GgC and tobramycin also did not result in membrane rupture. Together, the results of the HPTS and carboxyfluorescein assays provide comprehensive evidence that DOPG liposomes remain structurally intact and stable when exposed to GgC, tobramycin, and their combination.

Impact of GgC Saponins Extract and Antibiotic on the DOPG Monolayer. The second phase of the study explored the impact of GgC and tobramycin on the DOPG monolayer, a model system mimicking bacterial membranes. Higher concentrations of both GgC and tobramycin were used in this stage to thoroughly examine their influence on the structural properties of the lipid monolayer. The goal was to assess how these compounds affect membrane packing, surface

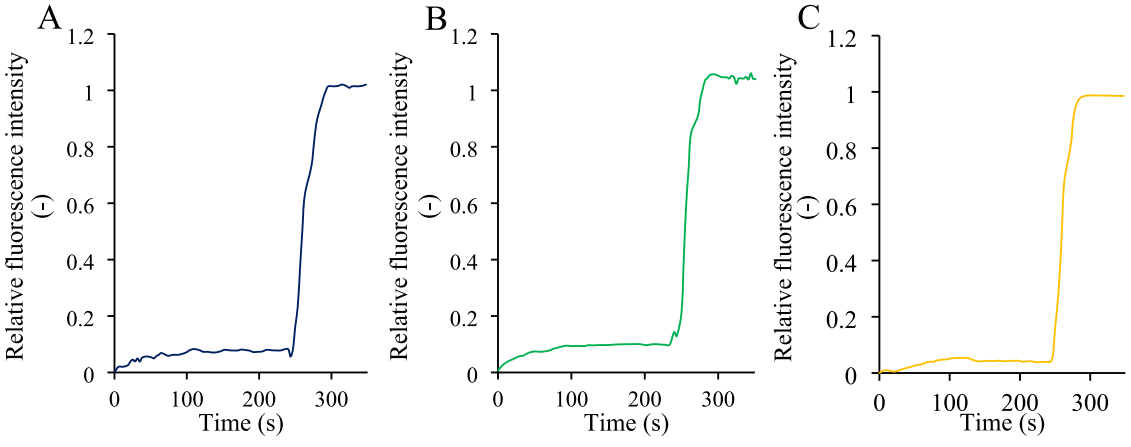

Figure 3. HPTS release assay; (A) GgC 5 mg/L treatment; (B) tobramycin 10 mg/L effect; and (C) tobramycin and *Glycyrrhiza* extract action. After 210 s, liposomes were lysed by adding a surfactant to obtain the maximum fluorescence signal.

https://doi.org/10.1021/acs.langmuir.5c00927
Langmuir XXXX, XXX, XXX−XXX

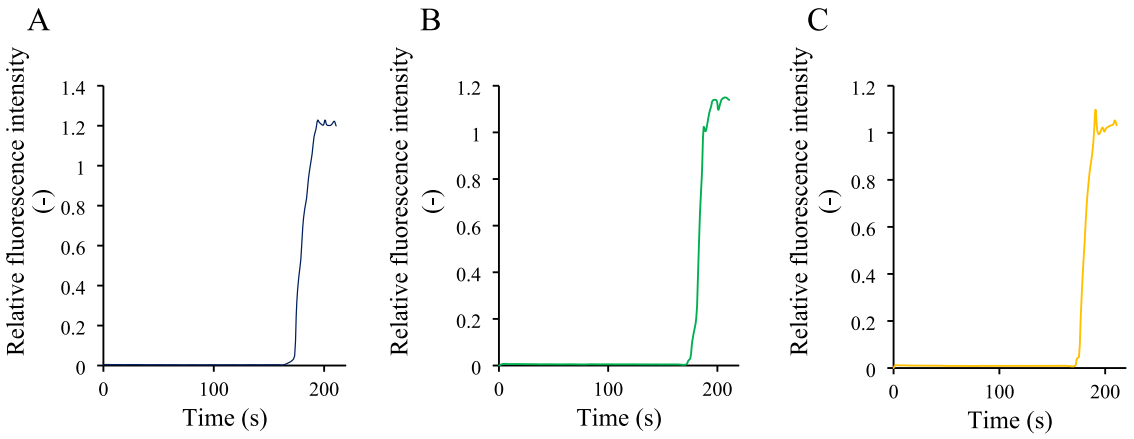

Figure 4. CF release assay: (A) GgC treatment; (B) tobramycin effect; and (C) tobramycin and *Glycyrrhiza* extract. After 175 s, the destruction of liposomes was forced by the addition of surfactant.

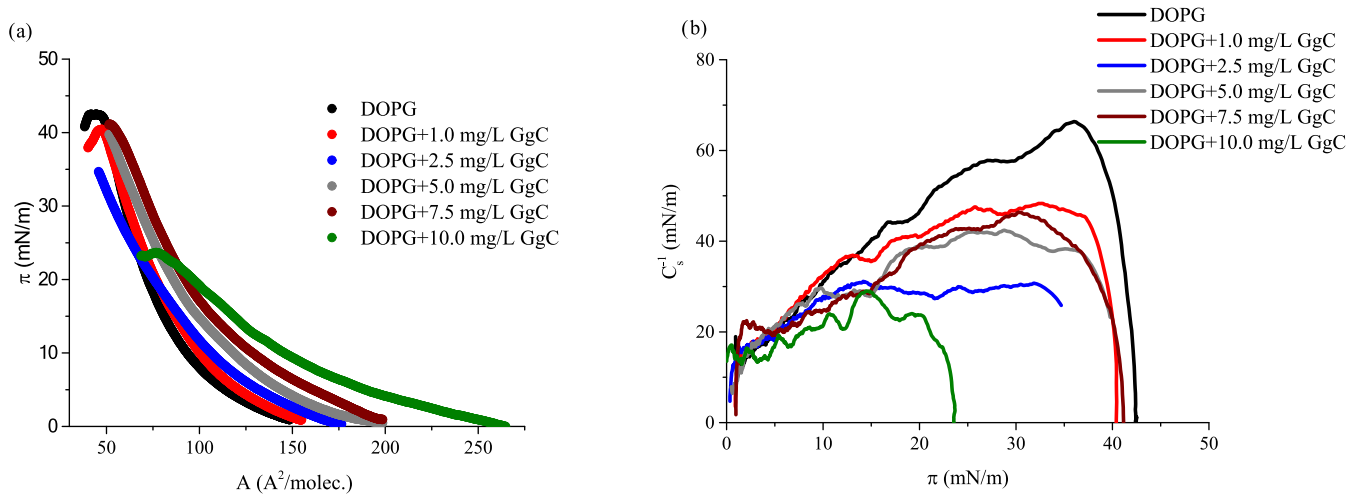

Figure 5. Surface pressure−area per molecule isotherms (π−A): (a) compression modulus−area per molecule (C_s^{-1}−π), (b) for the analyzed system: DOPG with various concentrations of the crude saponins extract GgC.

pressure, and fluidity, providing insight into their potential to enhance antibiotic penetration.

Figure 5 illustrates the surface pressure−area per molecule (π−A) isotherms obtained for the DOPG monolayer with different concentrations of saponin extract in the bulk subphase. For all analyzed systems, the π−A isotherms are shifted markedly to larger molecular areas relative to the pure DOPG monolayer. The lift-off area, $A_{\text{lift-off}}$, defines the area per molecule at which the isotherm begins to rise, indicative of the onset of intermolecular interactions. The $A_{\text{lift-off}}$ values increase with a higher concentration of saponins in the system. We have shown in our previous research[9] that expanded lipids film is caused by interactions of saponin molecules with phospholipids.

The obtained $A_{\text{lift-off}}$ values for systems DOPG + GgC are higher than those for a pure DOPG monolayer. Therefore, one can expect that saponin molecules are incorporated into the lipid structure and strongly expand the phospholipid membrane. Table 2 gives detailed information about the π−A isotherm parameters.

There is a smaller increase in the surface pressure within the monolayer compression for higher saponin concentrations in the subphase. Although the observed effects vary somewhat with concentration, at higher concentrations, a strong steric crowding effect of molecules may occur. Moreover, for some considered systems, a high extract concentration leads to the collapse of the monolayer at low surface pressure (π_{collapse}). At the collapse pressure, the Langmuir monolayer undergoes a phase transition from a two-dimensional (2D) fluid into the subphase to a three-dimensional (3D) bulk phase. The collapse or maximum surface pressure point is reached at the lower surface pressure (π_{collapse} ca. 24 mN/m) and the greater area occupied by molecules at the interface. These results suggest that a higher concentration of GgC decreases the stability of the DOPG film and enhances its structural deformation.

The π−A (surface pressure−molecular area) isotherm typically possesses distinct regions that correspond to different molecular packing arrangements in different surface pressure regimes. The run of π−A isotherm for DOPG is consistent with the literature data.[16] The DOPG monolayer with saponins forms only a liquid-expanded phase (LE) according to the estimated maximum C_s^{-1} value.[17] If the surface pressure increased, then the $C_{s,\max}^{-1}$ value also became greater and reached ca. 66 mN/m. This phenomenon is particularly visible when analyzing the behavior of lipid layers in the presence of 10 mg/L saponin extract. The collapse surface pressure value for DOPG + 10 mg/L GgC is ca. 24 mN/m. Films formed by DOPG and GgC extract molecules characterized a compres-

https://doi.org/10.1021/acs.langmuir.5c00927
Langmuir XXXX, XXX, XXX−XXX

Table 2. Characteristic Parameters of π–A Isotherms[a,b]

	$A_{lift\text{-}off}$ (Å^2/molec.)	$A_{collapse/maximum}$ (Å^2/molec.)	$\pi_{collapse/maximum}$ (mN/m)	$C_{s,max}^{-1}$ (mN/m)
DOPG	137.1	50.4	43.2	66.4
DOPG + 1.25 mg/L GgC	145.3	55.3	41.0	50.3
DOPG + 2.5 mg/L GgC	170.6	50.0	34.3	31.1
DOPG + 5.0 mg/L GgC	190.2	62.1	39.1	42.2
DOPG + 10.0 mg/L GgC	245.0	80.1	24.2	30.7

[a] $A_{lift\text{-}off}$—lift-off area of surface pressure. $A_{collapse/maximum}$—area corresponding to the monolayer collapse or maximum surface pressure, $\pi_{collapse/maximum}$—collapse pressure or maximum pressure reached by compressing [mN/m], max. C_s^{-1}—maximum value of the compression modulus [mN/m], phosphatidylglycerol (DOPG). [b] $A_{lift\text{-}off}$ values for DOPG film are ca. 137 Å^2/molec., while the addition of 10 mg/L GgC extract to subphase caused a nearly 2-fold increase compared to the $A_{lift\text{-}off}$ for DOPG monolayers only. This effect may be a consequence of the formation of aggregates, which can occupy a much larger surface area at the interface than a single phospholipid molecule. Moreover, the addition of a higher concentration of GgC extract changes the inclination angle of the π–A curve, which also confirms the interactions between saponins and phospholipid molecules.

sion modulus value lower than that for the DOPG monolayer. Generally, the obtained $C_{s,max}^{-1}$ value decreases with the rise of the extract concentration in the subphase. The formed mixed monolayers DOPG + GgC refer to the LE state. The findings demonstrate that saponins incorporated into the phospholipid monolayers cause strong fluidization. Likely, only the hydrophilic sugar part is generally submerged in the aqueous phase, while the aglycone part extends toward the air.[18] This effect was observed for other systems' lipid monolayer-saponins.[9,17] Moreover, Krochowiec et al.[19] have shown that the fluidizing effect was more significant in the case of saponins bearing a large aglycone moiety.

Based on our previous results,[12] we also state that the appropriate concentrations of saponin extract could improve the penetration of the antibiotic molecules through the lipid bilayer of the bacterial membrane. Our results allow us to assume that the concentrations of GgC saponins strongly impact the structure and packing of lipid monolayers.

In the next step, the impact of tobramycin on the surface properties of the DOPG monolayer was analyzed.

1 mL of antibiotic solution was added to the subphases, resulting in the final concentration of 5 mg/L. At the beginning of compression, the injected tobramycin does not strongly interact with the DOPG monolayers (blue line, Figure 6a). Practically, the run of π–A isotherm for pure DOPG and DOPG + tobramycin is similar. However, the C_s^{-1} parameter obtained for DOPG + tobramycin for strong compression is much lower than that for a pure DOPG monolayer. These data showed that tobramycin can alter the elastic properties of DOPG lipid monolayer by decreasing the cohesion between DOPG molecules. A similar effect was observed by Fa and co-workers[20] who studied interactions between azithromycin with 1,2-dioleoyl-*sn*-glycero-3-phosphocholine (DOPC) bilayers. The characteristic parameters of the π–A isotherms are listed in Table 3.

Table 3. Characteristic Parameters of π–A Isotherms[a]

	$A_{lift\text{-}off}$ (Å^2/molec.)	$A_{collapse/maximum}$ (Å^2/molec.)	$\pi_{collapse/maximum}$ (mN/m)	$C_{s,max}^{-1}$ (mN/m)
DOPG + tobramycin	163.1	42.3	40.2	46.8
DOPG + tobramycin + 10 mg/L GgC	200.3	72.4	35.6	45.4

[a] $A_{lift\text{-}off}$—lift-off area of surface pressure. $A_{collapse/maximum}$—area corresponding to the monolayer collapse or maximum surface pressure, $\pi_{collapse/maximum}$—collapse pressure or maximum pressure reached by compressing (mN/m), max. $C_{s,max}^{-1}$—maximum value of the compression modulus (mN/m), phosphatidylglycerol (DOPG).

A clear difference in the course of the π–A isotherm was obtained for the DOPG + tobramycin + GgC system. The presence of tobramycin and saponins in the subphase impacts

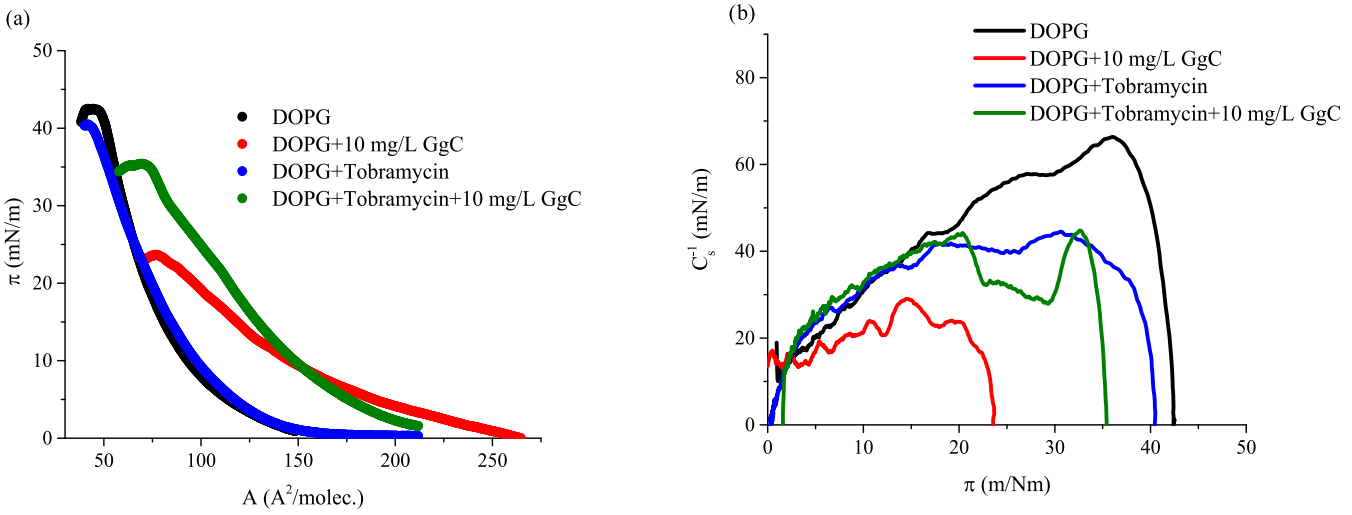

Figure 6. Surface pressure–area per molecule (π–A) isotherms: (a) compression modulus–area per molecule (C_s^{-1}–π), (b) for the analyzed systems: DOPG with the crude saponins extract GgC and antibiotic, phosphatidylglycerol (DOPG).

https://doi.org/10.1021/acs.langmuir.5c00927
Langmuir XXXX, XXX, XXX–XXX

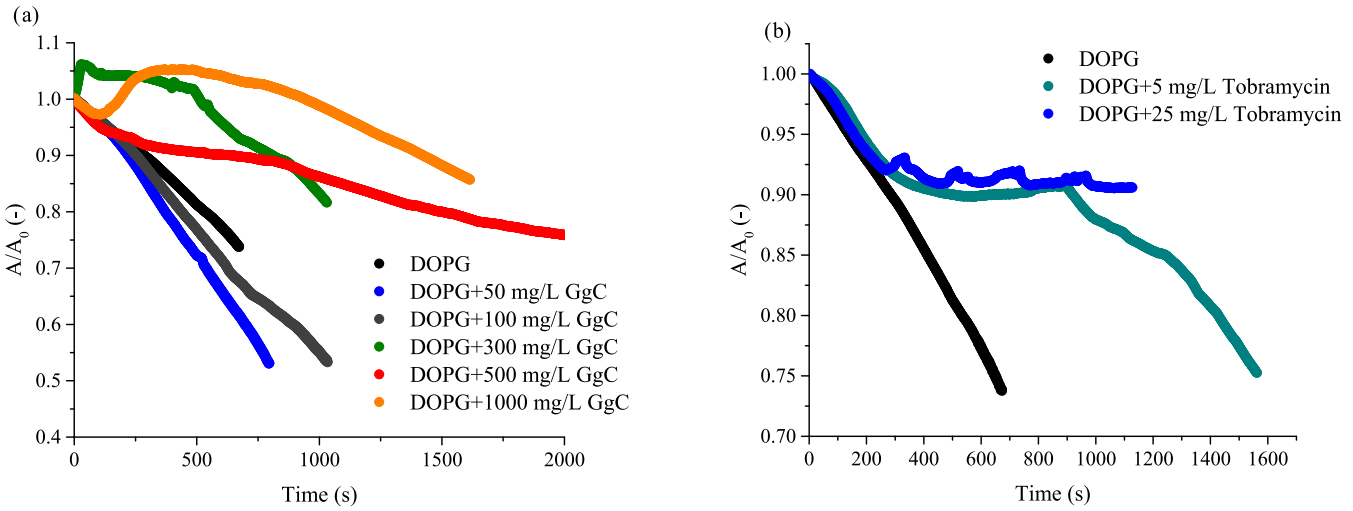

Figure 7. Relative area−time curves for the DOPG monolayer in the control sample (with buffer only) and (a) with saponins injected into the subphase in concentrations 50, 100, 300, 500, and 1000 (mg/L) and (b) with tobramycin in concentrations 5 and 25 mg/L. The plot shows the normalized area per molecule (A/A_0) as a function of time, where $A_0 = A$ (for $t = 0$), phosphatidylglycerol (DOPG).

the interactions between molecules at the interface, which is demonstrated by a greater increase in the surface pressure (π) during compression of the DOPG + tobramycin + GgC monolayer. Adding tobramycin to the subphase changes the character of interactions; the mixed monolayer of these three components is characterized by higher compressibility and elasticity. In consequence, the DOPG + tobramycin + GgC monolayer reaches higher surface pressure values than the DOPG + GgC system (Table 3). As shown in Figure 6, tobramycin molecules do not strongly interact with the DOPG monolayer; the additional compressibility in the mixed system is likely determined by interactions between the antibiotics and saponin molecules.

These studies were followed by an experiment examining the relaxation process of the DOPG monolayer in the presence of GgC extract and an antibiotic in the subphase. For this purpose, the DOPG film was compressed to the surface pressure of 30 mN/m, and after compression, the surface per molecule was estimated as A_0. At this surface pressure, the lipid packing density is similar to that of a cell membrane (pure DOPG), and the lipid monolayer mimics the outer surface of a cell membrane. By keeping the film area constant, changes in surface pressure are recorded upon addition of drugs to the subphase. Therefore, when injecting saponin extract into the subphase, a change in surface value per molecule in the DOPG monolayer ($A(t)$) is observed. The increase in ($A(t)$) compared to A_0 indicates the increase in the area per molecule caused by the incorporated saponin molecules into the phospholipid monolayer. Otherwise, if $A(t)/A_0 < 1$, there is a surface area loss in the monolayer, which could result in their desorption from the monolayer to the subphase. Consequently, the monolayer stability can be estimated as the A/A_0 parameter.

No interaction effect of saponins with the DOPG monolayer was observed for their low concentrations in the subphase, 5 or 10 mg/L. Therefore, saponin extract was added across a concentration range of 50−1000 mg/L in the subphase to determine the concentration when molecules are absorbed into the lipid monolayer. Figure 7a shows how the stability of the DOPG monolayer depends on saponin concentration and that the incorporation of saponin molecules into the DOPG film is only visible for higher concentrations of extract injected into the subphase. For concentrations greater than 300 mg/L, the relaxation curves changed the run $A/A_0 = f(t)$ in comparison to that of the pure DOPG monolayer. The addition of saponin improved the stability of the DOPG monolayer, indicating that interactions between the saponin present in the subphase and the lipid polar headgroups lead to some conformational disordering of the lipid molecules and formation of a more stable mixed monolayer.

Figure 7b shows the behavior of the DOPG monolayer in the presence of tobramycin. The injection of antibiotics into the subphase altered the relaxation behavior of the lipid film. After a maximum was reached, the normalized area $A(t)/A_0$ gradually decreased below 1.0, indicating a net loss of monolayer area over time. This could be due to a portion of the adsorbed saponin leaving the interface (desorbing) or due to molecular rearrangements that reduce the occupied area. The pure DOPG monolayer shows a significant decrease in A/A_0 after 500 s, which corresponds to a 25% decrease in area. In contrast, for the DOPG + 25 mg/L tobramycin system, only a 10% decrease in area is observed. Moreover, the higher concentration of tobramycin added resulted in the formation of a more stable mixed film.

The impact of mixtures of GgC extract and antibiotic on the model lipid membrane is shown in Figure 8. The relaxation of monolayers was registered for saponin extract at concentrations: 300 and 500 mg/L and tobramycin: 5 or 25 mg/L. A mixture of saponins and antibiotics was injected into the buffer subphase beneath the DOPG monolayer.

Generally, for all considered systems of DOPG + tobramycin + GgC, an expanding film at the interface was observed. The increasing relative area for molecules at the interface indicates that saponins and tobramycin strongly interact with the phospholipid monolayer and are incorporated into the membrane structure. The introduction of the saponin extract into the subphase results in increased membrane expansion due to its amphiphilic nature, which disrupts lipid packing and enhances lipid mobility. The surface area doubles after 15 min in a system with the addition of 500 mg/L GgC and 25 mg/L tobramycin. A similar tendency was observed for 300 mg/L GgC, but the adsorption process took more time. By

https://doi.org/10.1021/acs.langmuir.5c00927
Langmuir XXXX, XXX, XXX−XXX

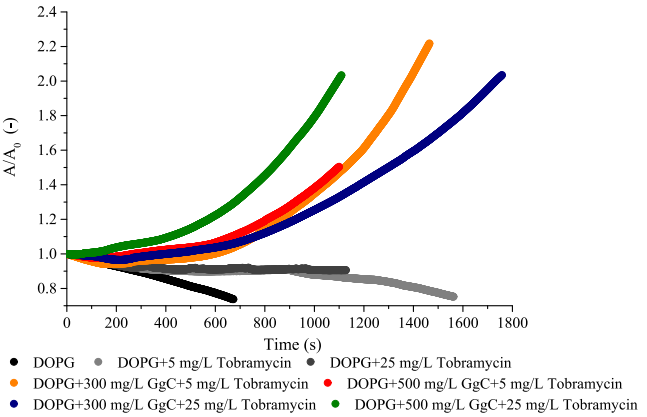

Figure 8. Relative area−time curves for the DOPG monolayer in the control sample (with buffer only) and with saponins injected into the subphase in concentrations: 300, 500 mg/L, and/or with tobramycin in concentrations: 5 and 25 mg/L. The plot shows the normalized area per molecule (A/A_0) as a function of time, where $A_0 = A$ (for t = 0), phosphatidylglycerol (DOPG).

comparing the results for the GgC + tobramycin mixture (Figure 8) with the obtained relaxation curves for component systems (Figure 7a,b), it can be concluded that the simultaneous addition of saponin and antibiotic had a more pronounced expanding effect on the DOPG film than either agent alone. This suggests a potentially cooperative interaction between GgC and tobramycin in disrupting the membrane.

The incorporation of GgC into DOPG monolayers significantly increased the molecular area per lipid, indicating that saponin inserts into the film and expands the lipid packing. Moreover, the GgC-induced reduction in the monolayer's compressional modulus (greater compressibility) and the decrease in collapse pressure point to a more fluid, less rigid film in the presence of saponin. This expansion effect, evidenced by shifts in the $\pi-A$ isotherms, aligns with previous research highlighting saponins' capacity to enhance membrane permeability and reduce lipid rigidity. Glycyrrhetinic acid (GA), the aglycon of glycyrrhizin (GC), was found to disrupt lipid raft models by reducing domain size and promoting fluid networks.[21] At higher concentrations, GgC reduced the collapse surface pressure ($\pi_{collapse}$) and compressional modulus (C_s^{-1}), confirming its membrane-destabilizing and fluidizing properties. The incorporation of GgC into DOPG monolayers at the air−liquid interface was marked by a significant shift in the $\pi-A$ isotherms toward larger molecular areas. For instance, the area per molecule increased from 137 Å^2 for pure DOPG to 245 Å^2 when 10 mg/L GgC was added, indicating disruption of lipid packing. This aligns with our previous studies demonstrating that some saponins expand lipid bilayers and reduce membrane rigidity.[9,12,18,19] Additionally, glycyrrhizin, a key bioactive component of *G. glabra*, has been shown to integrate into DOPG vesicles, modifying their structure while enhancing stability.[22] At higher GgC concentrations, the reduction in $\pi_{collapse}$ and C_s^{-1} values further validated its role in destabilizing the monolayer and promoting fluidity. These findings align with reports of saponins reducing lipid packing density to enhance membrane fluidity and disrupt structural integrity.[23,24] Tobramycin alone, however, exhibited minimal interaction with the DOPG monolayer, as evidenced by only slight reductions in the level of C_s^{-1}. This suggests weak interactions between tobramycin and the lipid layer, consistent with its known reliance on active transport mechanisms for bacterial cell penetration.[25] When combined with GgC, notable changes in the $\pi-A$ isotherms were observed, characterized by a decreased surface pressure and slightly lower monolayer compressibility, suggesting that GgC increases the membrane fluidity. Such an increased fluidity seems to facilitate interactions between tobramycin and the lipid membrane.

The combined use of saponins and antibiotics has been previously investigated, with some saponins shown to alter bacterial membrane properties.[19,26,27] ζ potential measurements revealed a progressive increase (less negative values) following treatment with GgC, tobramycin, and their combination, indicative of alterations in the liposome surface charge. Positively charged tobramycin interacts electrostatically with negatively charged phospholipid headgroups of DOPG, partially neutralizing the surface charge.[28,29] When GgC was combined with tobramycin, a more pronounced reduction in the surface charge was observed. This may result from additional interactions at the lipid−water interface facilitated by the amphiphilic nature of saponins. The hydrophilic sugar moieties of saponins could partially mask negative charges on the liposome surface, while the lipophilic aglycone regions insert into or associate with the lipid bilayer.[9] Despite these surface interactions, dynamic light scattering (DLS) data indicated no significant detrimental effect on particle size or polydispersity (PDI), suggesting that the liposome population remained uniform and stable under the studied conditions. While some reports have noted vesicle disruption and fusion in the presence of saponins,[22,23] our membrane integrity assays (HPTS and carboxyfluorescein leakage) demonstrated minimal membrane disruption, indicating vesicles remained structurally intact under the tested conditions.

Collectively, these observations demonstrate that *G. glabra* saponins modify biophysical membrane properties, potentially affecting antibiotic−membrane interactions. Although enhanced fluidity and reduced membrane rigidity suggest conditions favorable for antibiotic entry, direct evidence of increased tobramycin penetration into membranes was not obtained in this study. Further direct transport assays would be necessary to confirm such antibiotic uptake. Nonetheless, the observed biophysical membrane modulation is consistent with previous studies highlighting saponin-mediated effects that could aid antibiotic action.[10,26,28,30,31]

CONCLUSIONS

This study highlights that *G. glabra* L. saponins (GgC) modify the biophysical properties of bacterial model membranes, influencing their interaction with tobramycin. GgC incorporation into DOPG monolayers significantly disrupted lipid packing, altering membrane properties, such as molecular area and compressibility. The combination of GgC and tobramycin led to changes in the vesicle surface charge and size distribution but did not compromise membrane integrity. The combined presence of GgC and tobramycin showed an enhanced effect on the membrane fluidity (relative to each alone). These biophysical modifications suggest a potential for GgC to enhance antibiotic interactions with bacterial membranes, offering a promising strategy to address antibiotic resistance through sustainable coformulations. Further research is warranted to validate these findings across different bacterial systems and antibiotics in clinical and environmental settings.

https://doi.org/10.1021/acs.langmuir.5c00927
Langmuir XXXX, XXX, XXX−XXX

■ ASSOCIATED CONTENT

Supporting Information

The Supporting Information is available free of charge at https://pubs.acs.org/doi/10.1021/acs.langmuir.5c00927.

Dynamic light scattering (DLS) analysis presented in three distinct weighting models: number, volume, and intensity (PDF)

■ AUTHOR INFORMATION

Corresponding Author

Adam Grzywaczyk − *Institute of Chemical Technology and Engineering, Faculty of Chemical Technology, Poznan University of Technology, 60-965 Poznan, Poland;* orcid.org/0000-0002-6711-6054; Phone: +48 616653686; Email: adam.grzywaczyk@doctorate.put.poznan.pl

Authors

Monika Rojewska − *Institute of Chemical Technology and Engineering, Faculty of Chemical Technology, Poznan University of Technology, 60-965 Poznan, Poland;* orcid.org/0000-0002-8814-6711

Wojciech Smułek − *Institute of Chemical Technology and Engineering, Faculty of Chemical Technology, Poznan University of Technology, 60-965 Poznan, Poland;* orcid.org/0000-0001-5377-9933

Daniel A. McNaughton − *School of Mathematical and Physical Sciences, Faculty of Science, University of Technology Sydney, Sydney, NSW 2007, Australia; School of Chemistry, The University of Sydney, Sydney, NSW 2006, Australia*

Krystyna Prochaska − *Institute of Chemical Technology and Engineering, Faculty of Chemical Technology, Poznan University of Technology, 60-965 Poznan, Poland*

Philip A. Gale − *School of Mathematical and Physical Sciences, Faculty of Science, University of Technology Sydney, Sydney, NSW 2007, Australia; School of Chemistry, The University of Sydney, Sydney, NSW 2006, Australia*

Ewa Kaczorek − *Institute of Chemical Technology and Engineering, Faculty of Chemical Technology, Poznan University of Technology, 60-965 Poznan, Poland*

Complete contact information is available at: https://pubs.acs.org/10.1021/acs.langmuir.5c00927

Author Contributions

A.G.: Conceptualization, data curation, formal analysis, investigation, writing—original draft; M.R.: data curation, formal analysis, investigation, writing—original draft; W.S.: data curation, conceptualization, supervision, writing—original draft; D.A.M.: methodology, conceptualization, supervision, data curation, writing—original draft; P.A.G.: methodology, supervision, validation, writing—review and editing; K.P.: validation, writing—review and editing, E.K.: supervision, validation, project administration, writing—review and editing, funding acquisition, conceptualization.

Funding

This work was supported by the National Science Centre, Poland, grant number 2020/39/B/NZ9/03196.

Notes

The authors declare no competing financial interest.

■ ACKNOWLEDGMENTS

The authors thank the Polish National Agency for Academic Exchange for supporting Adam Grzywaczyk's stay at the University of Sydney within the STER Mobility II program. P.A.G. thanks the University of Technology Sydney and the University of Sydney for funding.

■ REFERENCES

(1) Salam, M. A.; Al-Amin, M. Y.; Salam, M. T.; et al. Antimicrobial Resistance: A Growing Serious Threat for Global Public Health. *Healthcare* **2023**, *11* (13), 1946.

(2) Mann, A.; Nehra, K.; Rana, J. S.; et al. Antibiotic resistance in agriculture: Perspectives on upcoming strategies to overcome upsurge in resistance. *Curr. Res. Microb. Sci.* **2021**, *2*, No. 100030.

(3) Melander, R. J.; Melander, C. The Challenge of Overcoming Antibiotic Resistance: An Adjuvant Approach? *ACS Infect. Dis.* **2017**, *3* (8), 559−563.

(4) Thy, M.; Timsit, J.-F.; De Montmollin, E. Aminoglycosides for the Treatment of Severe Infection Due to Resistant Gram-Negative Pathogens. *Antibiotics* **2023**, *12* (5), 860.

(5) Rosalia, M.; Chiesa, E.; Tottoli, E. M.; et al. Tobramycin Nanoantibiotics and Their Advantages: A Minireview. *Int. J. Mol. Sci.* **2022**, *23* (22), No. 14080.

(6) Idowu, T.; Ammeter, D.; Brizuela, M.; et al. Overcoming *β*-lactam resistance in Pseudomonas aeruginosa using non-canonical tobramycin-based antibiotic adjuvants. *Bioorg. Med. Chem. Lett.* **2020**, *30* (21), No. 127575.

(7) Díez-Aguilar, M.; Morosini, M. I.; Tedim, A. P.; et al. Antimicrobial Activity of Fosfomycin-Tobramycin Combination against Pseudomonas aeruginosa Isolates Assessed by Time-Kill Assays and Mutant Prevention Concentrations. *Antimicrob. Agents Chemother.* **2015**, *59* (10), 6039−6045.

(8) Kashyap, S.; Kaur, S.; Sharma, P.; et al. Combination of colistin and tobramycin inhibits persistence of Acinetobacter baumannii by membrane hyperpolarization and down-regulation of efflux pumps. *Microbes Infect.* **2021**, *23* (4−5), No. 104795.

(9) Rojewska, M.; Smułek, W.; Grzywaczyk, A.; et al. Study of Interactions between Saponin Biosurfactant and Model Biological Membranes: Phospholipid Monolayers and Liposomes. *Molecules* **2023**, *28* (4), 1965.

(10) Schmidt, S.; Heimesaat, M.; Fischer, A.; et al. Saponins increase susceptibility of vancomycin-resistant enterococci to antibiotic compounds. *Eur. J. Microbiol. Immunol.* **2014**, *4* (4), 204−212.

(11) Peetla, C.; Stine, A.; Labhasetwar, V. Biophysical Interactions with Model Lipid Membranes: Applications in Drug Discovery and Drug Delivery. *Mol. Pharmaceutics* **2009**, *6* (5), 1264−1276.

(12) Smułek, W.; Rojewska, M.; Pacholak, A.; et al. Co-interaction of nitrofurantoin and saponin surfactants with biomembrane leads to an increase in antibiotic's antibacterial activity. *J. Mol. Liq.* **2022**, *364*, No. 120070.

(13) Spector, A. A.; Yorek, M. A. Membrane lipid composition and cellular function. *J. Lipid Res.* **1985**, *26* (9), 1015−1035.

(14) Sweeteners: Pharmacology, Biotechnology, and Applications. In *Reference Series in Phytochemistry*; Mérillon, J.-M.; Ramawat, K. G., Eds.; Springer International Publishing: Cham, 2018.

(15) Gilchrist, A. M.; Wang, P.; Carreira-Barral, I.; et al. Supramolecular methods: the 8-hydroxypyrene-1,3,6-trisulfonic acid (HPTS) transport assay. *Supramol. Chem.* **2021**, *33* (7), 325−344.

(16) Backov, R.; Lee, C. M.; Khan, S. R.; et al. Calcium Oxalate Monohydrate Precipitation at Phosphatidylglycerol Langmuir Monolayers. *Langmuir* **2000**, *16* (14), 6013−6019.

(17) Miller, C. A.; Neogi, P. *Interfacial Phenomena: Equilibrium and Dynamic Effects*, Surfactant Science Series; CRC Press, 2008.

(18) Wojciechowski, K.; Jurek, I.; Góral, I.; et al. Surface-active extracts from plants rich in saponins − effect on lipid mono- and bilayers. *Surf. Interfaces* **2021**, *27*, No. 101486.

(19) Korchowiec, B.; Gorczyca, M.; Wojszko, K.; et al. Impact of two different saponins on the organization of model lipid membranes. *Biochim. Biophys. Acta, Biomembr.* **2015**, *1848* (10), 1963−1973.
(20) Fa, N.; Ronkart, S.; Schanck, A.; et al. Effect of the antibiotic azithromycin on thermotropic behavior of DOPC or DPPC bilayers. *Chem. Phys. Lipids* **2006**, *144* (1), 108−116.
(21) Sakamoto, S.; Uto, T.; Shoyama, Y. Effect of glycyrrhetinic acid on lipid raft model at the air/water interface. *Biochim. Biophys. Acta, Biomembr.* **2015**, *1848* (2), 434−443.
(22) Dargel, C.; Gräbitz-Bräuer, F.; Geisler, R.; et al. Stable DOPG/Glycyrrhizin vesicles with a wide range of mixing ratios: Structure and stability as seen by scattering experiments and Cryo-TEM. *Molecules* **2021**, *26* (16), 4959.
(23) Li, J.; Monje-Galvan, V. Effect of glycone diversity on the interaction of triterpenoid saponins and lipid bilayers. *ACS Appl. Bio Mater.* **2024**, *7* (2), 553−563.
(24) Sakamoto, S.; Nakahara, H.; Uto, T.; et al. Investigation of interfacial behavior of glycyrrhizin with a lipid raft model via a Langmuir monolayer study. *Biochim. Biophys. Acta, Biomembr.* **2013**, *1828* (4), 1271−1283.
(25) Yang, X.; Goswami, S.; Gorityala, B. K.; et al. A tobramycin vector enhances synergy and efficacy of efflux pump inhibitors against multidrug-resistant Gram-negative bacteria. *J. Med. Chem.* **2017**, *60* (9), 3913−3932.
(26) Tagousop, C. N.; Tamokou, J.-D.; Kengne, I. C.; et al. Antimicrobial activities of saponins from Melanthera elliptica and their synergistic effects with antibiotics against pathogenic phenotypes. *Chem. Cent. J.* **2018**, *12* (1), 97.
(27) Li, J.; Monje-Galvan, V. In vitro and in silico studies of antimicrobial saponins: A review. *Processes* **2023**, *11* (10), 2856.
(28) Himeno, H.; Shimokawa, N.; Komura, S.; et al. Charge-induced phase separation in lipid membranes. *Soft Matter* **2014**, *10* (40), 7959−7967.
(29) Alexander, A. M.; Gonda, I.; Harpur, E.; et al. Interaction of aminoglycoside antibiotics with phospholipid liposomes studied by microelectrophoresis. *J. Antibiot.* **1979**, *32* (5), 504−510.
(30) Giordani, R.; Trebaux, J.; Masi, M.; et al. Enhanced antifungal activity of ketoconazole by Euphorbia characias latex against Candida albicans. *J. Ethnopharmacol.* **2001**, *78* (1), 1−5.
(31) Tsutamoto, S.; Iwasaki, Y.; Shinohara, A.; et al. Triterpenoid saponin from Panax ginseng increases the sensitivity of methicillin-resistant Staphylococcus aureus to β-lactam and aminoglycoside antibiotics. *Microbiol. Spectrum* **2024**, *12* (6), No. e03227-23.

P4 Supplementary Materials

Supplementary Information

Glycyrrhiza glabra L. saponins modulate biophysical properties of bacterial model membranes and affect their interactions with tobramycin

Submitted to

Langmuir Journal

by

Adam Grzywaczyk [1], Monika Rojewska [1], Wojciech Smułek[1], Daniel A. McNaughton[2,3], Krystyna Prochaska [1], Philip A. Gale[2,3], Ewa Kaczorek [1]*

[1]Institute of Chemical Technology and Engineering, Faculty of Chemical Technology, Poznan University of Technology, ul. Berdychowo 4, 60-965 Poznan, Poland

[2]School of Mathematical and Physical Sciences, Faculty of Science, University of Technology Sydney, PO Box 123, Broadway, NSW, 2007, Australia

[3]School of Chemistry, The University of Sydney, NSW 2006, Australia.

Corresponding Author:

Adam Grzywaczyk Institute of Chemical Technology and Engineering, Faculty of Chemical Technology, Poznan University of Technology, ul. Berdychowo 4, 60-965 Poznan, Poland e-mail: adam.grzywaczyk@doctorate.put.poznan.pl; phone: +48 616653686

E-Supplementary data

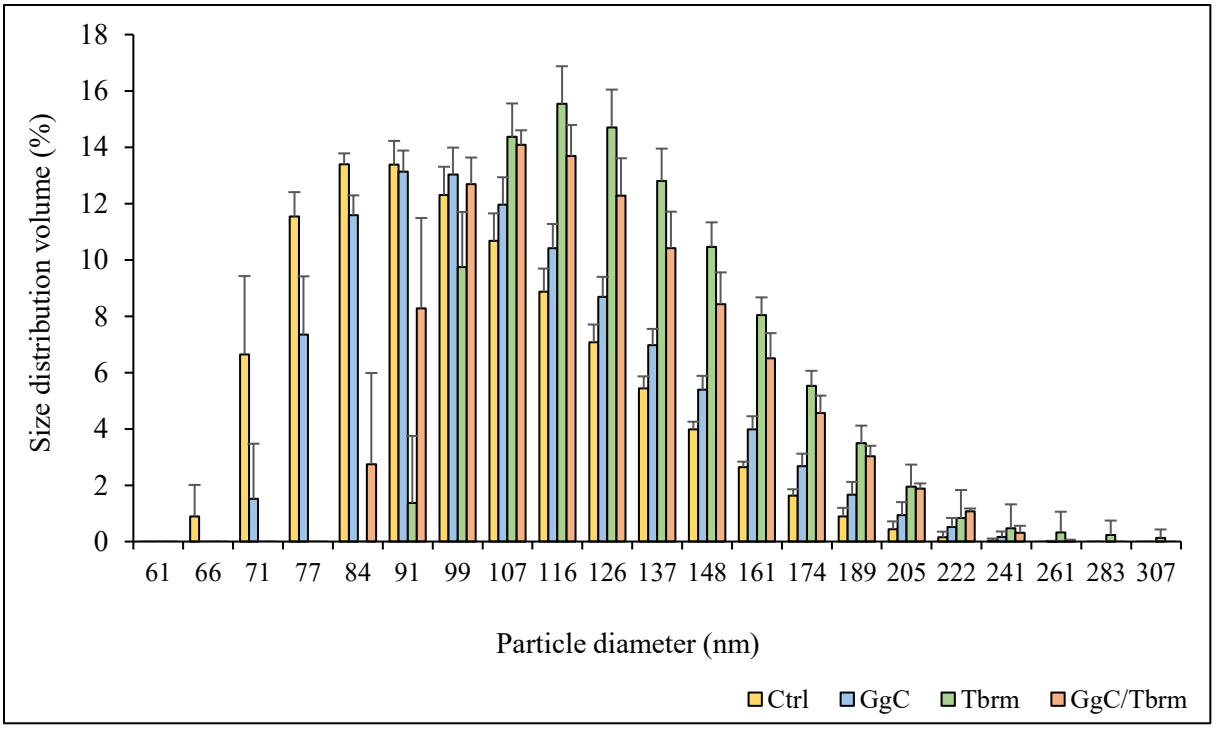

S1. Vesicle volume size distribution affected by *Glycyrrhiza glabra* L. root extract (GgC) and tobramycin. Ctrl - untreated sample, GgC - 5 mg/L treated, Tbrm - 10 mg/L Tobramycin, GgC/Tbrm 5 mg/L, GgC + 10 mg/L of Tobramycin effect

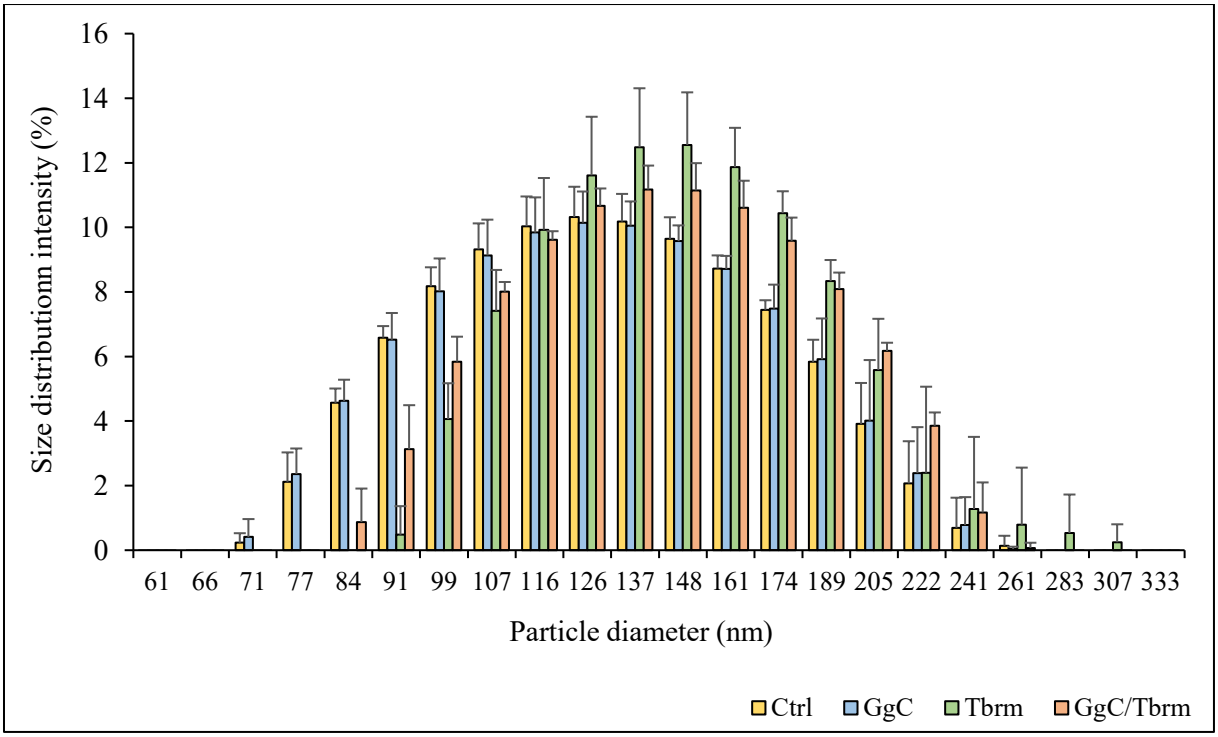

S2. Vesicle intensity size distribution affected by *Glycyrrhiza glabra* L. root extract (GgC) and tobramycin. Ctrl - untreated sample, GgC - 5 mg/L treated, Tbrm - 10 mg/L Tobramycin, GgC/Tbrm 5 mg/L, GgC + 10 mg/L of Tobramycin effect

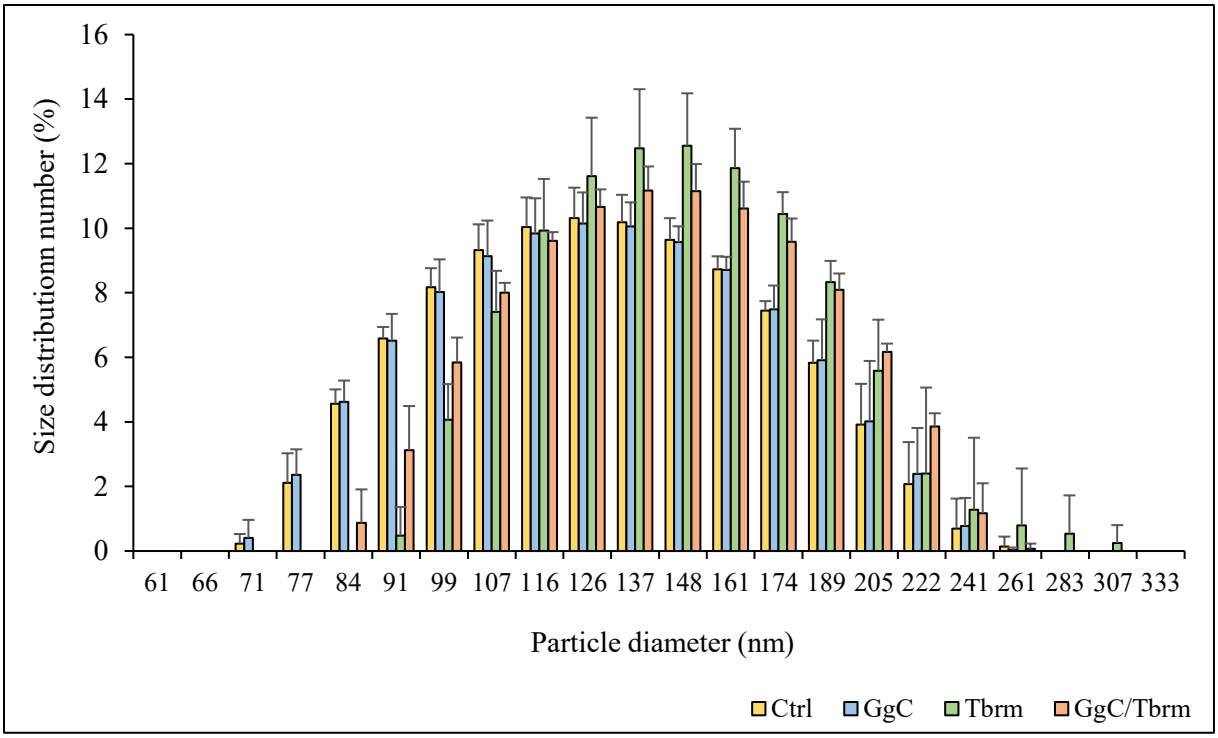

S3. Vesicle number size distribution affected by *Glycyrrhiza glabra* L. root extract (GgC) and tobramycin. Ctrl - untreated sample, GgC - 5 mg/L treated, Tbrm - 10 mg/L Tobramycin, GgC/Tbrm 5 mg/L, GgC + 10 mg/L of Tobramycin effect

Dynamic light scattering (DLS) analysis can represent particle size distribution according to three distinct weighting models: number, volume, and intensity. To facilitate clarity and comprehensive interpretation, all three distribution models are provided here, in the supplementary material. Each of these representations offers valuable insights, yet the selection of an appropriate model depends on the specific research questions or experimental requirements being addressed.

The volume-based distribution illustrates the size distribution based on the total volume occupied by particles. This distribution provides a balanced representation, moderately sensitive to both small and large particles, and thus often serves as a good general representation of sample heterogeneity. Intensity-based distribution, on the other hand, emphasises larger particles, as intensity scales strongly (proportionally to the sixth power) with particle size. Consequently, even a small number of large particles can dominate the intensity profile. This distribution is particularly useful for identifying aggregation or the presence of larger contaminants within the sample. The number-based distribution, reflects the actual numeric proportion of particles present, emphasising smaller particles, which are typically the most numerous in colloidal systems. However, this distribution can, on occasion, result in an underestimation of the significance of larger particles due to their low count.

Publication P5

World Journal of Microbiology and Biotechnology (2023) 39:221
https://doi.org/10.1007/s11274-023-03669-2

RESEARCH

Co-interaction of nitrofuran antibiotics and the saponin-rich extract on gram-negative bacteria and colon epithelial cells

Adam Grzywaczyk[1] · Wojciech Smułek[1] · Anna Olejnik[2] · Urszula Guzik[3] · Agnieszka Nowak[3] · Ewa Kaczorek[1]

Received: 3 February 2023 / Accepted: 26 May 2023

Abstract

Large-scale use of nitrofurans is associated with a number of risks related to a growing resistance to these compounds and the toxic effects following from their increasing presence in wastewater and the environment. The aim of the study was to investigate an impact of natural surfactant, saponins from *Sapindus mukorossi*, on antimicrobial properties of nitrofuran antibiotics. Measurements of bacterial metabolic activity indicated a synergistic bactericidal effect in samples with nitrofurantoin or furazolidone, to which saponins were added. Their addition led to more than 50% greater reduction in viable cells than in the samples without saponins. On the other hand, no toxic effect against human colon epithelial cell was observed. It was found that exposure to antibiotics and surfactants caused the cell membranes to be dominated by branched fatty acids. Moreover, the presence of saponins reduced the hydrophobicity of the cell surface making them almost completely hydrophilic. The results have confirmed a high affinity of saponins to the cells of *Pseudomonas* strains. Their beneficial synergistic effect on the action of antibiotics from the nitrofuran group was also demonstrated. This result opens promising prospects for the use of saponins from *S. mukorossi* as an adjuvant to reduce the emission of antibiotics into the environment.

Keywords Antibiotics · Cytotoxicity · Fatty acids · Natural surfactants · Pharmaceutics

Introduction

Nitrofurantoin (NFT), nitrofurazone (NFZ), furaltadone (FTD) and furazolidone (FZD), i.e. antibiotics from the nitrofuran group, are recognized as a group of the most popular antimicrobials all over the world. The nitrofurantoin only has been prescribed 2,957,359 times in 2019 in the USA, which is not an impressive result, but it can still be concluded that nitrofuran drugs are widely used (Nitrofurantoin Drug Usage Statistics, United States, 2013–2020, 2020). NFT has been used in the treatment of the urinary tract, while FZD has been used to treat diarrhea, cholera and bacteremic salmonellosis. In 1995, their use as a food additive for farm animals was banned due to concerns about the carcinogenicity of the drug residues and their potentially harmful effects on human health (Vass et al. 2008).

The increase in antibiotic intake is one of the main reasons for the increase in antimicrobial resistance (AMR). Increasing therapeutic doses, forced by greater drug resistance of pathogenic strains, contributes to the increasing presence of antibiotics in the environment. This phenomenon is a feedback loop, as it results in the spread of antibiotic resistance (Polianciuc et al. 2020). This process can be

✉ Ewa Kaczorek
ewa.kaczorek@put.poznan.pl

Adam Grzywaczyk
adam.grzywaczyk@doctorate.put.poznan.pl

Wojciech Smułek
wojciech.smulek@put.poznan.pl

Anna Olejnik
anna.olejnik@up.poznan.p

Urszula Guzik
urszula.guzik@us.edu.pl

Agnieszka Nowak
agnieszka.a.nowak@us.edu.pl

[1] Institute of Chemical Technology and Engineering, Poznan University of Technology, Berdychowo 4, 60-695 Poznan, Poland

[2] Department of Biotechnology and Food Microbiology, Poznań University of Life Sciences, Wojska Polskiego, 48, 60-627 Poznań, Poland

[3] Institute of Biology, Biotechnology and Environmental Protection, Faculty of Natural Science, University of Silesia in Katowice, Jagiellonska 28, 40-032 Katowice, Poland

Published online: 05 June 2023

interrupted by increasing the bioavailability of the antibiotic, allowing the use of lower doses of the antibiotic while maintaining the expected effectiveness (Price and Patel 2022). Moreover, the World Health Organization (WHO) has published a list of bacteria that are characterized by high drug resistance so that effective treatments for infections caused by them are running out (Asokan et al. 2019). At the top of the list are bacteria of the genus *Acinetobacter baumannii, Enterobacteriaceae*, and also *Pseudomonas aeruginosa* (Ropponen et al. 2021).

One of the possible methods of increasing drug bioavailability is to modify the permeability of the cell membrane with surface active properties (Smułek and Kaczorek 2022). One group of surfactants that is attracting increasing attention are saponins, natural surfactants of natural origin (Liao et al. 2021). The structure of their molecules is most likely responsible for the ability to integrate the hydrophobic part of their molecules into the structure of the cell membrane, while the hydrophilic part remains on the surface. There are also suggestions that saponin monomers can incorporate into the outer part of the membrane and increase the distance between membrane components on the surface, which leads to a positive membrane curvature and the formation of specific domains, whose size increases with time (Rojewska et al. 2023). The presence of sugar chains helps develop membrane defects and gradually increases the membrane permeability, even by creating holes in the membrane (Lorent et al. 2014; Rojewska et al. 2020).

The aim of our study was to determine the influence of the co-action of saponin-rich *Sapindus mukorossi* extract and nitrofuran antibiotics: nitrofurantoin (NFT) and furazolidone (FZD), on the cellular response of gram-negative bacteria of the *Pseudomonas* genus. *Pseudomonas aeruginosa* is outside the action spectrum of nitrofurans, and therefore, we were able to observe the properties of living cells and the effect of drug-saponin interaction on the cell membrane. The toxicity of the saponin extract on human intestinal epithelial cells was also assessed. Intestinal cells are the first barrier limiting drug penetration into the body from gastrointestinal tract. Analysis of the influence of saponins on these cells may help establish ways of reusing nitrofuran antibiotics in combination with biosurfactants. As absorption of nitrofurans by the human body is severely restricted, it is important to check saponins' toxic effects on the cells constituting the intestinal barrier in the drug absorption process (Huttner and Harbarth 2017). Although there are many studies on the modification of the permeability of model membranes as well as the bactericidal properties of the saponins themselves, there have been few reports so far on the possible synergistic effect between antibiotics and saponins (Jurek et al. 2019; Lorent et al. 2014; Rojewska et al. 2020; Sreij et al. 2018). Such an effect may contribute to achieving a desired therapeutic effect at a lower dose of the drug. Thus, in our study we focused on modifying the properties of the outer membrane of gram-negative bacteria by employing the co-interaction of the antibiotic with saponins. Using Electrophoretic light scattering and Dynamic light scattering, and analysis of Congo Red adsorption and Crystal Violet permeability, we tried to more deeply understand the possible mechanism of interaction of antibiotics and surfactants on the biological membranes. For this purpose, we also performed lipidomic analysis. The performed basic analyses of the metabolic activity of both bacterial cells and human intestinal epithelial cells provide important information about the toxicity and safety of saponins derived from *Sapindus mukkorosi,* and also indicate a possible synergistic effect between chosen antibiotics and saponins. The obtained results provide new, important information on the possible interaction of surfactants with nitrofuran antibiotics and allow a better understanding of their interference in the lipid profile of biological membranes. The use of saponins may contribute to reduction of the growing bacterial resistance to antibiotics through the use of compounds of natural origin.

Materials and methods

Chemicals

All chemicals used in the study, including two nitrofuran—NFT and FZD, were of the highest purity grade and were purchased from Merck KGaA (Darmstadt, Germany). The nutrient agar, nutrient broth and other microbiological supplements came from BTL sp. z o.o. (Łódź, Poland). *Sapindus mukorossi* nuts were obtained from Mohani (Psary, Poland). The saponins-rich extract was obtained via methanol extraction as described by Smułek et al. (2016).

Cytotoxicity analysis

The cytotoxicity of *S. mukorossi* extract combined with antibiotics was assessed using human CCD 841CoN (ATCC ®CRL-179™) cells derived from normal colon mucosa and obtained from the American Type Culture Collection (ATCC, Manassas, VA, USA). The cells were cultured in Dulbecco's Modified Eagle's Medium (Sigma-Aldrich, Poznań, Poland) supplemented with 10% fetal bovine serum (Gibco BRL, USA) and 1% nonessential amino acid solution 100 × (Sigma-Aldrich). They were grown at 37 °C in a humidified atmosphere (5% CO_2, 95% air) and subcultured twice a week after reaching ca. 80% confluence. A trypsin-EDTA solution (0.25%) was used to harvest the CCD 841CoN cells.

In the cytotoxicity experiments, the cells were grown in 96-well plates at the initial density of 1.5×10^4 cells

cm^{-2}. Twenty-four hour cell cultures were treated with *S. mukorossi* extract at concentrations ranging from 0 to 1000 µg mL^{-1} with the addition of antibiotics at a final concentration of 5 µg mL^{-1}. After 48 h of treatment, cell viability and metabolic activity were assessed using the MTT (3-(4,5-dimethylthiazol-2-yl)-2,5-diphenyltetrazolium bromide) test (Sigma-Aldrich), as described by Smulek et al. (2020). Briefly, the MTT solution was added to each well to obtain a concentration of 0.5 mg MTT mL^{-1}. The microplate was incubated at 37 °C for 3 h, and then formazan crystals were extracted with acidic isopropanol for 20 min at room temperature. Absorbance was measured at 570 and 690 nm using a Tecan M200 Infinite microplate reader (Tecan Group Ltd., Männedorf, Switzerland).

Bacteria strain and culture conditions

Three strains of bacteria of the genus *Pseudomonas* were used in the study: *Pseudomonas plecoglossicida* IsA (NCBI GenBank Accession No. KY561350), *Pseudomonas* sp. MChB (NCBI GenBank Accession No. KU563540), *Pseudomonas* sp. OS4 (NCBI GenBank Accession No. KP096512). The bacteria were stored on nutrient agar plates. For incubation, the bacterial biomass was suspended in a nutrient broth until it reached the exponential growth phase. The bacterial cultures were then centrifuged at 4500 rcf and re-suspended in a PBS (**P**hosphate-**B**uffered **S**aline) solution at a constant neutral pH.

A growth curves of pure bacteria cultures and in presence of xenobiotics are presented in Supplementary Data with additional explanation. The measurements were performed with a microplate reader (Multiskan 152 Sky, Thermo Fisher Scientific, Waltham, MA, USA) and the 96-well clear bottom sterile microplates as described by Pacholak et al. (2023) 100 µL of the prepared bacterial cultures were transferred to the microplate wells. The plates were maintained at 30 °C with pulse shaking. The OD_{600} of each well were read every 10 min for 24 h.

In order to determine the action of 5 mg L^{-1} FZD and NFT antibiotics in combination with 10 mg L^{-1} of saponins or without saponins on bacterial cells, liquid cultures were prepared. The bacteria were centrifuged from growth medium and then re-suspended in the 1 mL of described mixtures for 24 h. The control sample consisted of the bacteria suspended in the PBS solution. After 24 h, the tests described in the further experiments were carried out.

Fatty acids profile of bacterial strains

The procedure of fatty acid methyl ester extraction, analysis and identification using gas chromatography, and data interpretation were analogous to the methodology described by Nowak and Mrozik (2016). The mean fatty acid chain length was expressed by the following equation:

$$\text{Mean fatty acid chain lenght} = \sum (\%FA \times C)/100$$

where: %FA is the percentage of fatty acid, and C is the number of carbon atoms. To prevent the alterations caused by fatty acids occasionally detected, the analysis of FAMEs included only fatty acids with a content of at least 1%.

The obtained results were evaluated by analysis of variance, and statistical analyses were performed on three biological replicates of data obtained from each treatment. The statistical significance ($p < 0.05$) of differences was treated by one-way ANOVA, considering: (1) the effect of each treatment on tested bacterial strains and (2) the influence of NFT and FZD on each bacterial strain. Next, differences between particular samples were assessed by post-hoc comparison of means using the lowest significant difference (LSD) test.

Cell surface properties measurements

The above analyses were performed on cultures of bacteria suspended for 24 h in solutions containing the drug and saponins. The analysis of cell surface properties included evaluation of Congo red binding to microbial cells, according to Ambalam et al. (2012). Moreover, the cell membrane permeability test using crystal violet was performed, as well as an MTT enzymatic activity test, as described by Smulek et al. (2020). The zeta potential was calculated from the Smoluchowski equation after measurements of electrophoresis mobility using a Zetasizer Nano ZS instrument (Malvern Instruments Ltd. UK). Additionally, the cells' sizes were measured using a Mastersizer 2000 instrument (Malvern Instruments Ltd.) equipped with a Hydro 2000S unit that enables the analysis of samples in the form of a wet dispersion. The cells diameters were measured in the range of 0.02–2000 µm. For this purpose, an appropriate quantity of the material was dispersed in a water medium, and after establishing the instrument background, appropriate measurements were made. An atomic force microscope Park NX10 from Park Systems (Suwon, South Korea) was used to analyze changes in the cell topography of the bacteria as described by Pacholak et al. (2023).

Statistical analysis

The results presented in the study were calculated as an average value from at least three independent experiments. The variance analysis and t-Student test were applied to determine the statistical significance of differences between the average values. The differences were considered statistically significant at $p < 0.05$. All calculations were conducted using

Excel 2019 (Microsoft Office) software. The FAME profiles were also subjected to principal component analysis (PCA). All analyses were performed using the Statistica 13.3 PL software package.

Results and discussion

Cytotoxicity analysis

Cytotoxicity of saponins from S. *mukorossi* and nitrofuran antibiotics was determined in normal human cells to evaluate their safety in antibiotic therapy. The effect of saponins-rich plant extract on the proliferation, viability, and metabolic activity of colon epithelial CCD 841CoN cells is shown in Fig. 1.

The experiments revealed that *S. mukorossi* saponin extract at concentrations up to 10 μg mL^{-1} is not cytotoxic to the normal intestinal cells. The lowest cytotoxic dose, that is the concentration of the extract causing a decrease in cell viability by 10%, was calculated as 16.79 ± 2.87 μg mL^{-1} (Table 1). Figure 1 shows a dose–response relationship between saponin-rich extract and colon mucosa cells. Based on the experimental results and model fitting, a half maximal inhibitory concentration (IC_{50}) was determined at 32.72 ± 2.63 μg mL^{-1}. For comparison, the IC_{50} of the antibiotics were estimated to be 1.28 μg mL^{-1} and 2.92 μg mL^{-1} for FZD and NFT, respectively (Table 1). Notably, the saponin extract combined at the concentration of 10 μg mL^{-1} with the antibiotics did not significantly affect their cytotoxicity; the extract supplementation did not change the cytotoxic potential of the antibiotics at every concentration tested (Fig. 2). The obtained results indicate that the use of *S. mukorossi* saponins at non-cytotoxic doses does not cause any additional cytotoxic effect on normal human colon cells. Therefore, the concentration of saponin extract of 10 μg mL^{-1} was chosen for further experiments.

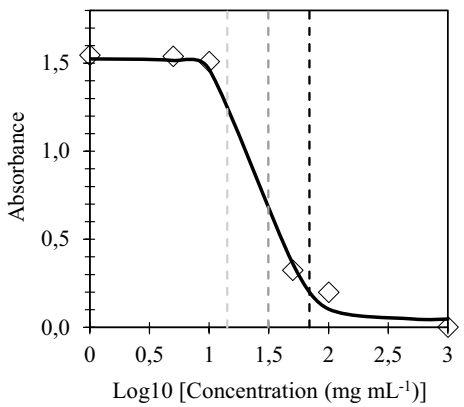

Fig. 1 Dose–response curve for normal colon CCD 841CoN cells treated with S. *mukorossi* extract at concentrations ranging from 1 to 1000 g mL^{-1}. Cell viability was measured by MTT assay. IC_{10}; IC_{50}; IC_{90}

Table 1 Cytotoxic doses expressed as inhibitory concentrations (IC) of *Sapindus mukorossi* extract and/or nitrofuran antibiotics determined in human normal colon mucosal CCD 841CoN cells. Data present first (IC_{10}), half-maximal (IC_{50}) and lethal (IC_{90}) inhibitory concentrations

Extract and/or antibiotic	IC (μg mL^{-1})		
	IC_{10}	IC_{50}	IC_{90}
S. mukorossi extract	16.79 ± 2.87	32.72 ± 2.63	64.12 ± 1.57
FZD	0.33 ± 0.06[a]	1.28 ± 0.11[b]	4.98 ± 0.29[d]
FZD *S. mukorossi* 10 μg mL^{-1}	0.27 ± 0.02[a]	1.13 ± 0.07[b]	4.22 ± 0.30[d]
NFT	1.43 ± 0.12[b]	2.92 ± 0.02[c]	6.02 ± 0.51[e]
NFT *S. mukorossi* 10 μg mL^{-1}	1.28 ± 0.12[b]	2.94 ± 0.16[c]	6.76 ± 0.17[e]

Values marked with the same letter do not differ significantly ($p > 0.05$)

As follows from peruse of literature, the results presented in our study are one of the few concerning the impact of saponin-rich extracts on unmutated human cells. The vast majority of studies reported to date have described the cytotoxicity of saponins mainly against cancer cells to assess their antitumor potential. For example, Hashemi et al. (2021) have observed that ginsenosides belonging to the saponin group have the ability to induce apoptosis and arrest the cell cycle. Moreover, gypensapogenin H derived from *Gynostemma pentaphyllum* significantly inhibited the growth of human breast cancer cells (MDA-MB-231), while exhibiting low toxicity to normal human breast epithelial MCF-10a cells (Zhang et al. 2015). Zhang et al. (2022) have reported that asiaticoside saponin at concentrations of 20, 40, and 80 μg mL^{-1} is not toxic to human retinal pigment epithelium ARPE-19 cells. Duewelhenke et al. (2007) have indicated the suppression of the proliferation of primary human osteoblasts by antibiotics fluoroquinolones, macrolides, clindamycin, chloramphenicol, rifampin, tetracycline, and linezolid at doses up to 20 or 40 μg mL^{-1}. It has been suggested that a significant problem of the group of antibiotics, such as fluoroquinolones, is that they cause mitochondrial dysfunction induced by oxidative stress in human cells (Nadanaciva et al. 2010; Xiao et al. 2019).

Bacterial cells viability

The strains utilized in this study exhibit high resistance to both antibiotics. The Minimal Inhibitory Concentration (MIC) for NFT and FZD against the IsA strain reached 100 μg mL^{-1}, while for the OS4 and MChB strains, it exceeds 200 μg mL^{-1}. Given the solubility limitations of

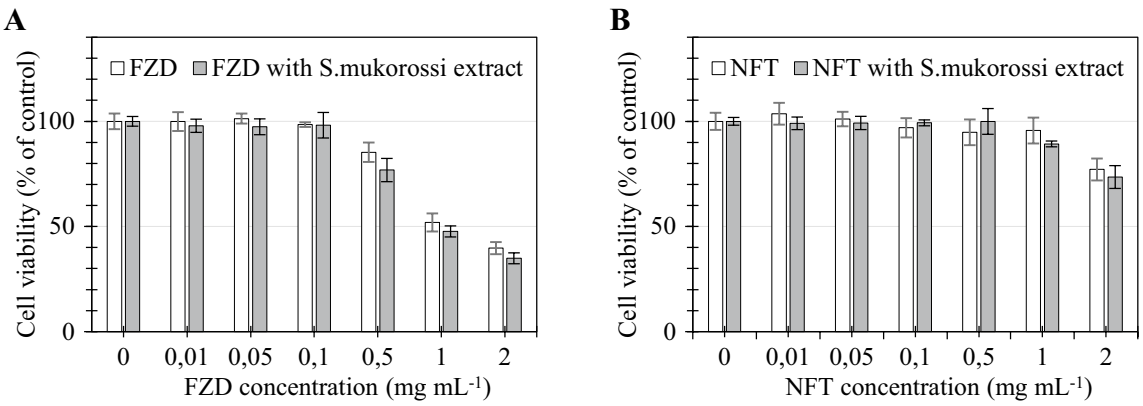

Fig. 2 Effect of FZD **A** and NFT **B** with and without *Sapindus mukorossi* extract at a concentration of 10 µg mL^{-1} on the viability of human colon mucosa CCD 841CoN cells

these antibiotics in an aqueous environment, achieving higher concentrations is not feasible. Our investigation involved the addition of *Sapindus mukorossi* extract at concentrations up to 30 µg mL^{-1}, which demonstrated no impact on bacterial growth and division (see Supplementary Data). This confirms the absence of a cytostatic effect of the extract on the selected *Pseudomonas* strains. However, in the presence of *Sapindus mukorossi* extract MIC for NFT decreased the MIC nearly 20% for all tested strains, however, for FZD no significant decrease was observed.

To investigate deeper, the saponins-antibiotics co-action, the enzymatic activity of *Pseudomonas* spp. was assessed by MTT assay (Smułek et al. 2020) and the results are presented in Fig. 3. For each tested strain, a decrease in the enzymatic activity was observed after the FZD antibiotic addition. Interestingly, a very slight increase in the activity of *Pseudomonas* sp. MChB strain exposed to NFT was observed, which may suggest no toxic effect in this case. However, the addition of saponins caused a significant decrease in the enzymatic activity relative to that of the samples without the saponins added. The highest decrease in enzymatic activity was observed for *P. plecoglossicida* IsA strain, of even up to 39% relative to that of the control sample. The addition of saponins to the NFT also caused a toxic effect (a decrease in activity of cells by 41% relative to that of the control sample) on the *Pseudomonas* sp. MChB strain, on which the drug itself did not cause such an effect. Such results may suggest the presence of a synergistic effect between nitrofuran antibiotics and saponins, which enhance the toxic effect of the antibiotic. Moreover, pure saponins also caused a decrease in the metabolic activity of *P. plecoglossicida* IsA strain of up to 52% compared to that of the control. Both phenomena may be related to the formation of holes and the incorporation of saponins into the outer cell membrane, which is the first barrier between the bacterial cell and the environment. Zaynab et al. (2021) have suggested that saponins have a toxic effect on both gram-positive and gram-negative bacteria as well as fungi. The results obtained in our study correlate well with those obtained by Khan et al. (2018). The saponins obtained from green tea seeds show antibacterial activity against *Escherichia coli*, *Salmonella* spp., and *Staphylococcus aureus*. For most of the tested strains, a decrease in OD_{600} to a value close to 0 was observed for the saponin concentration equal to the minimal inhibitory concentration, as well as a decrease in OD_{600} with increasing concentration of saponins. On the other hand, Zdarta et al. (2019) have observed no toxic effect of saponins derived from *Hedera helix*, and even their stimulating effect towards *Raoultella ornithinolytica* and *Achromobacter calcoaceticus*. A fairly large variety of saponins, as well as the presence of a sugar part in the molecule, which can be used as an alternative carbon source for bacteria, determine the possibility of obtaining different results of toxicity assessment for different bacteria strains.

Regarding cell morphology (refer to AFM images in Supplementary Data) of the control samples, a regular structure without defects and uniformity in all directions can be observed. The dimensions of the cells for all strains are approximately 2 µm in length. Notably, exposure to NFT resulted in distinct changes such as visible furrows and irregularities, particularly prominent in the IsA and OS4 strains, and to a lesser extent in MChB. The addition of saponins does not appear to have a significant impact on cell topography, as the effects are primarily attributed to NFT itself. These changes may indicate cellular damage caused by the antibiotic; however, complete cell lysis is not evident, as supported by the obtained growth curves that indicate no cytostatic effect. Similar observations were made by Pacholak et al. (2023), who found that *Stenotrophomonas acidaminiphila* N0B, *Pseudomonas*

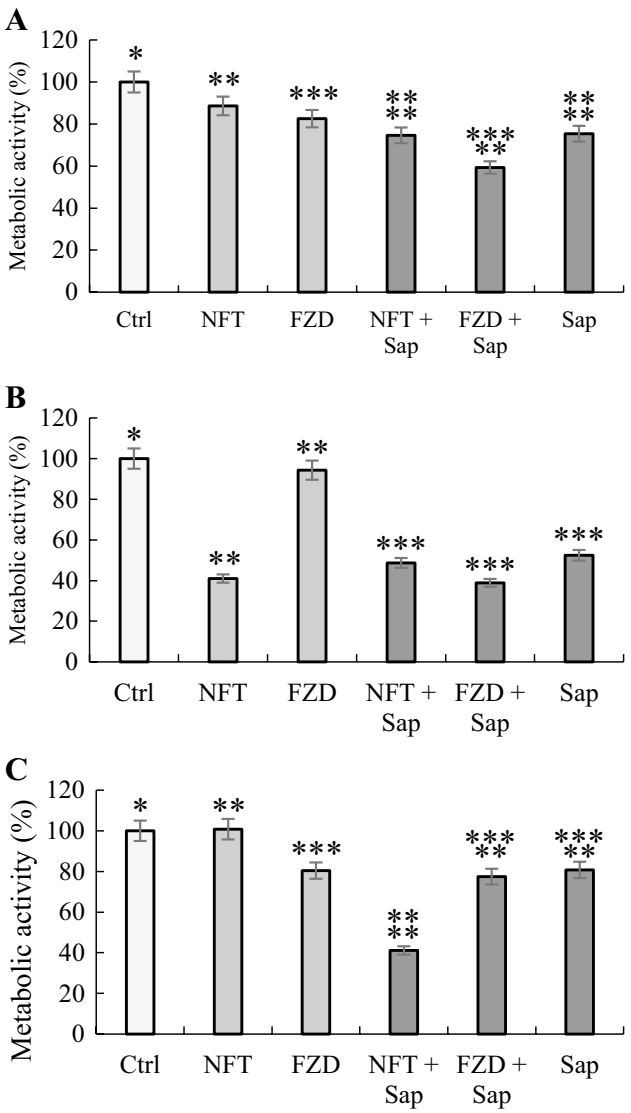

Fig. 3 Relative cell metabolic activity of *Pseudomonas* strains in response to different antibiotics and/or *S. mukorossi* extracts; A—*Pseudomonas* sp. OS4, B—*Pseudomonas plecoglossicida* IsA, C—*Pseudomonas* sp. MChB, Ctrl—control culture (without antibiotics and plant saponins), NFT—nitrofurantoin at 5 mg L^{-1}, FZD—furazolidone at 5 mg L^{-1}, Sap – *Sapindus mukorossi* plant saponins at 10 mg L^{-1}

indoloxydans WB, and *Serratia marcescens* ODW152 exhibit discernible alterations in cell structure after prolonged exposure to nitrofurantoin, with greater severity observed after 28 days.

Bacterial fatty acid profile

Because the study focuses on bacterial cells membrane and wall properties, the first step of the study was to determine the profile of membrane fatty acids (FA) and the reaction of the strains to the contact with antibiotics. Figure 4 and Table 2 present the share of particular groups of FA in the membranes. In *Pseudomonas plecoglossicida* IsA strain, the straight-chain and saturated FA dominated. The branched FA had the relatively smallest share in the total amount of FA. In the case of two other strains, *Pseudomonas* sp. MChB *Pseudomonas* sp. OS4, the branched FA accounted for over 90% and 50% of total FA, respectively. In contrast to IsA and OS4 in whose cell membranes hydroxy and cyclopropane FA can be found, the FA profile of *P.* MChB cell membrane is limited only to unsaturated and 12:0 aldehyde (Fig. 5).

It should be emphasized that the addition of saponins significantly changed the membrane fatty acid profile for IsA and OS4 strains, but had rather limited influence on MChB strain membrane. After the addition of saponin, the percentage of branched fatty acids in OS4 strain membrane increased from 56 to 94% for Sap/FZD and to 97% for Sap and Sap/NFT, whereas the share of unbranched fatty acids decreased from 35 to 3.06% and 6.75% for Sap/NFT and Sap/FZD, respectively. For MChB strain cell membrane a small fluctuation can be noticed for unsaturated acids after treatment with saponins—the share of unsaturated acids increased from 0.79 to 2.29% for Sap/FZD and 2.9% for Sap and Sap/NFT, at the expanse of branched and straight chain fatty acids. Nonetheless, the share of unsaturated FA was about 95% for each sample of MChB strain. The IsA strain cell membrane has the most complex composition with 45% straight-chain, 10.5% hydroxylated, 11% cyclopropane, 5.5% branched, 8.5% 12:0 aldehyde, and 27.5% unsaturated FAs. In this case, the addition of pure saponin did not change the membrane FA profile. Interestingly, the synergistic effect between saponin and FZD/NFT might occur, and as a result, only in this combination, the branched FA share increased from 5.5% to 18.30% and 16.74% for Sap/NFT and Sap/FZD, respectively. What should also be noted, after Sap/FZD treatment the share of straight chain FA increased to 48%. This also confirmed that bacteria modify their cells biomembrane in response to a toxic environment.

The modulation of the length, branching, and saturation of the FA acyl chains is one of the main bacteria mechanisms in response to stress conditions. The increased amount of unsaturated and branched FA increase membrane fluidity and enhance the diffusion processes through it (Willdigg and Helmann 2021). Such a change can be noticed for IsA and OS4 strains after treatment with saponins. Górny et al. (2019) have studied the interaction of naproxen with *Bacillus thuringiensis* B1 and observed, after contact with the pharmaceutic, a decrease in the content of unsaturated FA, which were replaced by hydroxy FA. Similarly, Pacholak et al. (2021) have found for *Pseudomonas hibiscicola* strain FZD2 that after its contact with NFT and furazolidone, the proportion of branched FA increased at the expense of unsaturated and straight-chain FA. Hence, the results obtained in our study indicate that the tested *Pseudomonas* strains

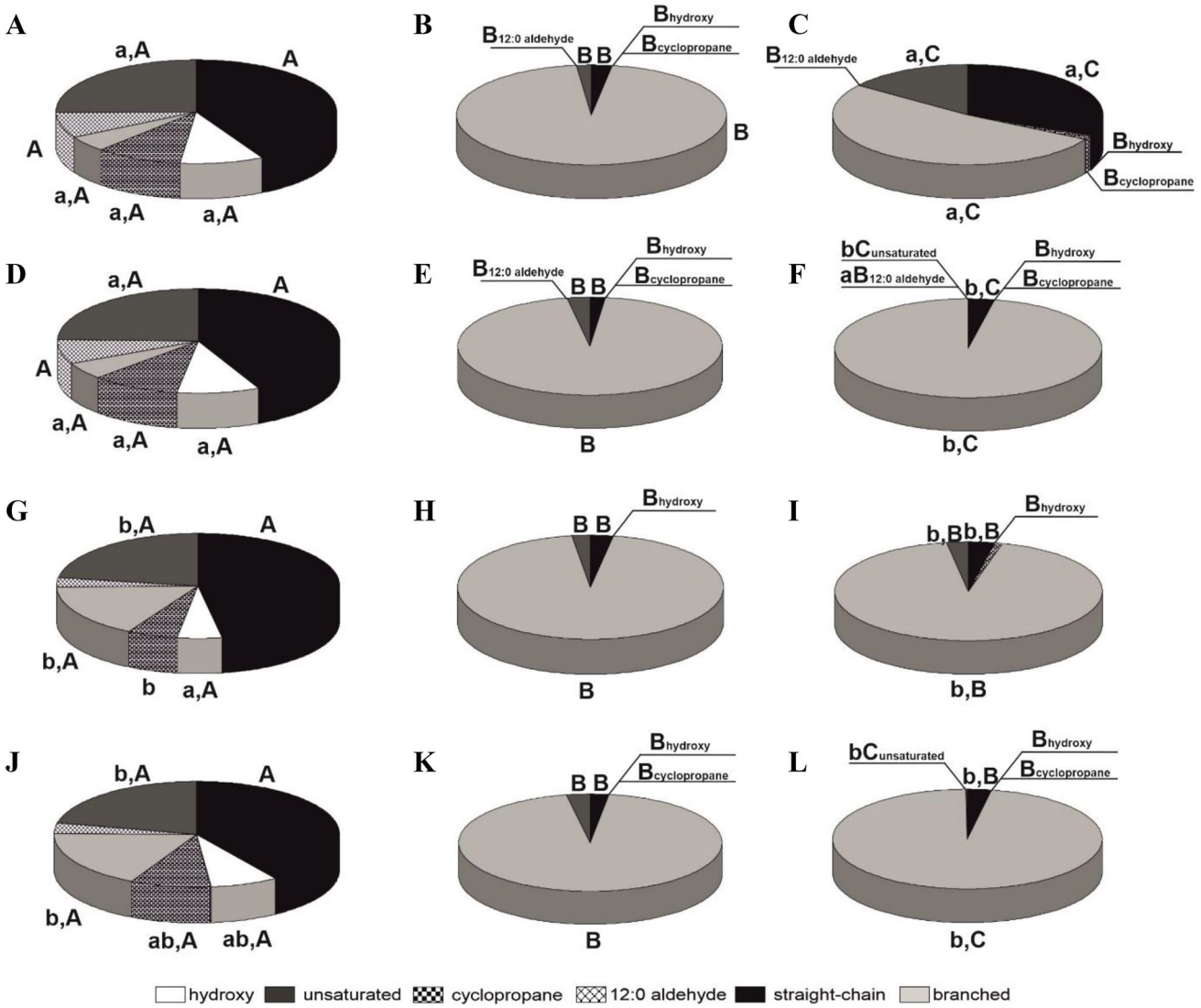

Fig. 4 Proportions of fatty acids in IsA (**A**, **D**, **G**, **J**), MChB (**B**, **E**, **H**, **K**), and OS4 (**C**, **F**, **I**, **L**) growing on nutrient broth (**A**, **B**, **C**), and nutrient broth supplemented with Sap (**D**, **E**, **F**), nutrient broth supplemented with Sap and FZD (**G**, **H**, **I**), and nutrient broth supplemented with Sap and NFT (**J**, **K**, **L**). The class of hydroxyl fatty acids contains additionally the branched hydroxyl fatty acids. In each column, samples with the same bacterial strain but with different treatments (with or without Sap, NFT and FZD) with different lowercase are significantly different ($p < 0.05$, LSD test). It means that lowercase indicates differences in FAME profiles within the same bacterial strain. Results without any lowercase are statistically equal at a significance level $p < 0.05$. The means with the same treatment with a different capital letter are significantly different ($p < 0.05$, LSD test) considering the effect of treatment (addition of NFT, FZD, or without additional carbon source) between tested bacterial strains. It means that one test was done for control samples (**A**, **B**, **C**), the second for samples with Sap (**D**, **E**, **F**), the third for samples with Sap and furazolidon (**G**, **H**, **I**)), and fourth for samples with Sap and NFT (**J**, **K**, **L**)

appeared to be relatively resistant to the antibiotics studied, from among which particularly strongly resistant to NFT. This antibiotic seemed to have no significant effect on the cell membrane. What is more, no changes in FA profile after exposed to saponins were observed. Moreover, in *P. plecoglossicida* IsA cell membranes the share of straight-chain FA increased in response to the toxic environment.

Cell membrane permeability

Low permeability of the bacteria cell membrane is one of the key factors limiting the effectiveness of antibiotics. Lowering the membrane permeability is also one of the possible mechanisms of cellular response to stressful conditions. The cell membrane permeability was assessed

Table 2 Mean fatty acid chain length and ratio of saturated to unsaturated fatty acids of tested bacterial strains in response to different antibiotics and/or *S. mukorossi* extracts: a) *Pseudomonas plecoglossicida* IsA, b) *Pseudomonas* sp. OS4, c) *Pseudomonas* sp. MChB

Treatment	Ctrl	Sap	Sap/NFT	Sap/FZD
Strain	*Pseudomonas plecoglossicida* IsA			
Mean fatty acid chain length	16.92 ± 0.06	17.40 ± 0.78	16.14 ± 0.52	15.93 ± 0.61[a]
Sat./Unsat. ratio	2.96 ± 0.17	3.08 ± 10.89	3.63 ± 0.07[a]	3.43 ± 0.07[a,b]
Strain	*Pseudomonas* sp. MChB			
Treatment	Ctrl	Sap	Sap/NFT	Sap/FZD
Mean fatty acid chain length	15.72 ± 0.01[a]	15.70 ± 0.01[a,b]	15.68 ± 0.00[c]	15.75 ± 0.02[a,d]
Sat./Unsat. ratio	55.14 ± 6.54	34.55 ± 0.56[a]	32.98 ± 0.91	49.54 ± 26.40[a]
Strain	*Pseudomonas* sp. OS4			
Treatment	Ctrl	Sap	Sap/NFT	Sap/FZD
Mean fatty acid chain length	15.67 ± 0.53	15.74 ± 0.00	15.73 ± 0.01	15.95 ± 0.028[a]
Sat./Unsat. ratio	5.97 ± 2.08	0.00 ± 0.00[a]	0.00 ± 0.00[a]	43.64 ± 24.11[b]

In each table row, the means with different lowercases are significantly different ($p < 0.05$, LSD test) considering the effect of treatment (Sap, Sap/NFT, Sap/FZD) on bacterial strain. In each column, the means with the same treatment marked with different letters are significantly different ($p < 0.05$, LSD test) considering the reactions of bacterial strains. It means that one test was done for Control samples, the second for Sap, third for NFT samples, and the fouth for FZD samples

using the absorption of crystal violet by bacterial cells, on a scale where 100% meant complete dye absorption, 0% meant no crystal violet absorption and thus, a complete stop of the transport process through the cell membrane. The effect of reducing the permeability of the cell membrane can be observed when treated with pure antibiotic solutions without the addition of saponins (Table 3). The greatest decrease in the dye absorption was obtained for the *Pseudomonas* sp. OS4 strain—from 59.9 to 36.2% for FZD. A subtle increase in cell membrane permeability was obtained for the *P. pleocglossicida* IsA strain from 65.6 to 66.4%. Such a small increase is within the limit of the measurement error and may indicate practically no effect. A significant increase in the permeability for each of the tested strains was observed after adding the extract of *S. mukorossi*. In the case of the *P. plecoglossicida* IsA strain, the obtained results suggested an increase in the permeability of the cell membrane by about 20–25 percentage points as compared to the control sample. Comparing the results for pure antibiotics, the addition of saponins increased the permeability by 23 percentage points for *P. plecoglossicida* IsA exposed to FZD or FZD and *S. mukorossi* extract, and even by 53 percentage points for the *Pseudomonas* sp. MChB strain and the NFT drug. Knudsen et al. (2008) have come to similar conclusions. In their study they observed that the presence of soyabean saponins increase the intestinal epithelial permeability as determined by both reduced transepithelial resistance and increased apparent permeability of [^{14}C] mannitol (Knudsen et al. 2008). The increase in permeability may be related, as suggested by Jacob et al. (1991) and Zheng and Gallot (2021), to the ability of saponins to solubilize cholesterol, thereby creating tears without disturbing the remaining structure of the biomembrane. Sudji et al. (2015) on the other hand, have suggested that it is the presence of cholesterol in the cell membrane that determines the action of saponins. The absence of cholesterol in the cell membrane means that saponins do not have the effect of increasing the membrane permeability (Sudji et al. 2015).

Cell surface properties

Zeta potential may be one of many determinants of cell behavior in stress conditions. Both antibiotics, NFT and FZD, cause an increase in electrokinetic potential accumulated on the surface of bacterial cells (Table 3). Only for *Pseudomonas* sp. MChB with FZD added a slight decrease, from − 16.2 to − 16.6 mV, in zeta potential was observed. In the case of treatment with pure antibiotics, the zeta potential changes slightly fluctuated by approx. 1–2 mV; the addition of saponins from *Sapindus mukorossi* caused a significant decrease in the zeta potential of bacterial cells. For each of the tested strains, there was a twofold decrease in the value of the zeta potential. Saponin molecules accumulated on the cell surface, embedding themselves in the outer cell membrane, may be responsible for such a large decrease. Amphiphilic saponin molecules can be incorporated into biological membranes by their hydrophobic (aglycon) part, while the glyconic part remains outside the outer membrane region, thus causing a decrease in the stability of the colloidal

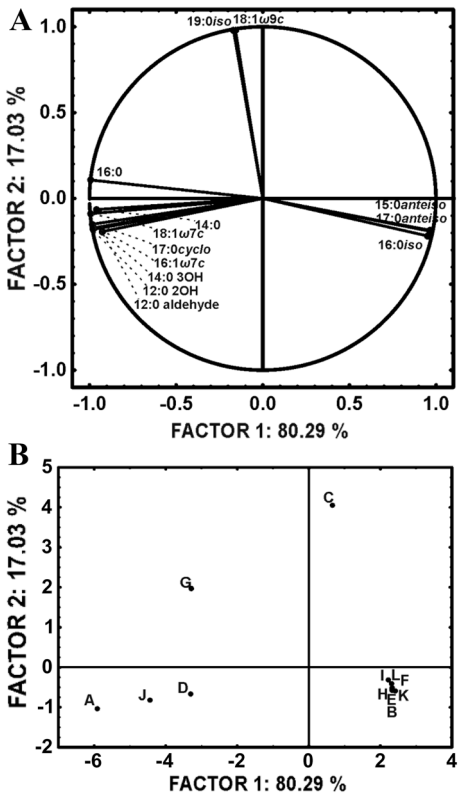

Fig. 5 PCA analysis of fatty acids profile of bacterial strains in response to different antibiotics and/or *S. mukorossi* extracts. The test systems are marked with capital letters: A – IsA strain growing on nutrient broth; B—MChB strain growing on nutrient broth; C – OS4 strain growing on nutrient broth; D—IsA strain growing on nutrient broth supplemented with Sap; E—MChB strain growing on nutrient broth supplemented with Sap; F – OS4 strain growing on nutrient broth supplemented with Sap; G—IsA strain growing on nutrient broth supplemented with Sap and FZD; H—MChB strain growing on nutrient broth supplemented with Sap and FZD; I – OS4 strain growing on nutrient broth supplemented with Sap and FZD; J—IsA strain growing on nutrient broth supplemented with Sap and NFT; K—MChB strain growing on nutrient broth supplemented with Sap and NFT; L—OS4 strain growing on nutrient broth supplemented with Sap and NFT

solution of bacterial cells, which causes a decrease in zeta potential (Lorent et al. 2014; Rojewska et al. 2020). Similar observations have been were made by Muniyan et al. (2017).

The Congo red adsorption test permitted evaluation of the cell adhesivity (Table 3). Comparing the results obtained for the cells treated with NFT, even 72.03% of the dye was adsorbed on cells of MChB strain. The lowest cell adhesivity value was obtained for the OS.4 strain with NFT—51.44%. It is worth noting that in the case of this series of tests, the cell adhesivity value does not drop below 50%, which proves that the dye is incorporated into the structure of bacterial cells membrane (Smułek et al. 2020). The addition of the extract caused a significant drop in the Congo Red adsorption, even below 2%. The highest value of Congo Red adsorption, of almost 30%, was obtained for the samples of MChB strain exposed to saponins only. As noted by Rojewska et al. (2020), the decrease in the Congo Red adsorption due to the presence of saponins is most likely related to the incorporation of biosurfactant molecules into the structure of the cell membrane. This results in a restriction of the space for the incorporation of the dye molecules (Rojewska et al. 2020).

Conclusions

The results obtained in our study provide a broad perspective on the effects of nitrofuran derivatives and saponins from *Sapindus mukorossi* on the living cells. The aim of the experiments carried out was to check the possibility of enhancement of the effect of antibiotics through the supporting activity of natural surfactants on the bacterial membrane. As found, the synergistic effect was particularly evident in the systems containing both FZD and saponins, leading to a pronounced reduction in the metabolic activity of cells of s *Pseudomonas* sp. OS4 and *P. plecoglossicida* IsA strains. On the other hand, the strongest biocidal effect on *Pseudomonas* sp. MChB was observed in the samples with NFT and saponins. At the same time, the tested compounds were found to affect the fatty acid profile in the cell membranes in different ways. The cell membrane of *Pseudomonas* sp. MChB strain did not show significant modifications as a result of a contact with antibiotics and saponins, but in the cell membranes of *Pseudomonas* OS4 strain after exposition to antibiotics and surfactants were found to show dominant presence of branched fatty acids. The proportion of branched-chain fatty acids also increased significantly in the *P. plecoglossicida* IsA skeleton. The changes were evident at the level of cell surface properties. The saponins very strongly reduced the hydrophobicity of the cell surface and decreased its zeta potential. This result may indicate strong adsorption of saponins on the cell surface. In view of potential use of saponins as an antibiotic adjuvants in pharmaceutical preparations, the toxicity of antibiotics and/or saponins to colon epithelial cells was also investigated, which permitted determination of a safe dose of saponins from *S. mukorossi* at which they are not toxic and do not increase the toxicity of antibiotics. The results

Table 3 Cell membrane permeability and cell surface properties of tested strains after exposure to antibiotics and/or *S. mukorossi* extract; A – *Pseudomonas* sp. OS4, B – *Pseudomonas plecoglossicida* IsA, C – *Pseudomonas* sp. MChB, Ctrl – control culture (without antibiotics and plant saponins), NFT – nitrofurantoin at 5 mg L^{-1}, FZD – furazolidone at 5 mg L^{-1}, Sap – *Sapindus mukorossi* plant saponins at 10 mg L^{-1}

	Pseudomonas sp. OS.4	*Pseudomonas plecoglossicida* IsA	*Pseudomonas* sp. MChB
Cell membrane permeability [%]			
Ctrl	58.9 ± 2.9^{a}	65.6 ± 3.3^{a}	58.5 ± 2.9^{a}
NFT	44.3 ± 2.2^{b}	45.4 ± 2.3^{b}	34.6 ± 1.7^{b}
FZD	36.2 ± 1.8^{c}	66.4 ± 3.3^{a}	49.6 ± 2.5^{c}
NFT + Sap	84.1 ± 4.2^{d}	84.1 ± 4.2^{c}	86.4 ± 4.3^{d}
FZD + Sap	87.8 ± 4.4^{d}	89.5 ± 4.5^{c}	87.5 ± 4.4^{d}
Sap	84.6 ± 4.2^{d}	90.3 ± 4.5^{c}	87.0 ± 4.4^{d}
Cell surface adhesivity [%]			
Ctrl	64.9 ± 3.2^{a}	71.4 ± 3.6^{a}	71.2 ± 3.6^{a}
NFT	51.4 ± 2.6^{b}	68.3 ± 3.4^{a}	72.0 ± 3.6^{a}
FZD	62.3 ± 3.1^{a}	69.7 ± 3.4^{a}	65.3 ± 3.3^{a}
NFT + Sap	$< 2.0^{c}$	34.3 ± 1.7^{b}	$< 2.0^{b}$
FZD + Sap	$< 2.0^{c}$	15.0 ± 0.7^{c}	6.0 ± 0.3^{c}
Sap	$< 2.0^{c}$	24.8 ± 1.2^{d}	29.9 ± 1.5^{d}
Zeta potential [mV]			
Ctrl	-10.1 ± 0.5^{a}	-12.3 ± 0.6^{a}	-14.5 ± 0.7^{a}
NFT	-9.8 ± 0.5^{a}	-9.7 ± 0.5^{b}	-13.6 ± 0.7^{a}
FZD	-9.5 ± 0.5^{a}	-8.8 ± 0.4^{b}	-14.8 ± 0.7^{a}
NFT + Sap	-36.1 ± 1.8^{b}	-27.2 ± 1.4^{c}	-32.3 ± 1.6^{b}
FZD + Sap	-33.8 ± 1.7^{b}	-24.9 ± 1.2^{c}	-32.6 ± 1.6^{b}
Sap	-17.7 ± 0.9^{c}	-16.2 ± 0.8^{d}	-17.6 ± 0.9^{c}

In each column, the means with the same treatment marked with different letters are significantly different ($p < 0.05$, LSD test) considering the reactions of bacterial strains

obtained represent significant scientific novelty and provide a basis for further research into the use of saponins for supporting the effects of antibiotics.

Supplementary Information The online version contains supplementary material available at https://doi.org/10.1007/s11274-023-03669-2.

Acknowledgements This study was funded by National Science Centre, Poland (grant No. 2017/27/B/NZ9/01603).

Author contributions Adam Grzywaczyk: Methodology; Formal analysis, Investigation; Writing - Original Draft, VisualizationWojciech Smułek: Writing - Original Draft, Supervision, Conceptualization, Formal analysis; Data curationAnna Olejnik: Formal analysis; Investigation; Methodology; Writing - Review & Editing;Urszula Guzik: Formal analysis; Investigation; Methodology; Writing - Review & EditingAgnieszka Nowak: Formal analysis; Investigation; Methodology; Writing - Review & EditingEwa Kaczorek: Conceptualization; Writing - Review & Editing; Supervision; Project administration; Funding Acquisition

Data availability Data will be made available on request.

Declarations

Competing interests The authors declare no competing interests.

References

Ambalam P, Kondepudi KK, Nilsson I, Wadström T, Ljungh Å (2012) Bile stimulates cell surface hydrophobicity, Congo red binding and biofilm formation of *Lactobacillus* strains. FEMS Microbiol Lett 333:10–19

Asokan GV, Ramadhan T, Ahmed E, Sanad H (2019) WHO global priority pathogens list a bibliometric analysis of medline- pubmed for knowledge mobilization to infection prevention and control practices in Bahrain. Oman Med J 34(3):184–193

Duewelhenke N, Krut O, Eysel P (2007) Influence on mitochondria and cytotoxicity of different antibiotics administered in high concentrations on primary human osteoblasts and cell lines. Antimicrob Agents Ch 51:54–63

Górny D, Guzik U, Hupert-Kocurek K, Wojcieszyńska D (2019) Naproxen ecotoxicity and biodegradation by *Bacillus thuringiensis* B1(2015b) strain. Ecotoxicol Environ Saf 167:505–512

Hashemi F, Zarrabi A, Zabolian A, Saleki H et al (2021) Novel strategy in breast cancer therapy: revealing the bright side of Ginsenosides. CMP 14:1093–1111

Huttner A, Harbarth S (2017) Miscellaneous Agents Infectious Diseases, vol 2, 4th edn. Elsevier, Amsterdam

Jurek I, Góral I, Gęsiński K, Wojciechowski K (2019) Effect of saponins from quinoa on a skin-mimetic lipid monolayer containing cholesterol. Steroids 147:52–57

Khan MI, Ahhmed A, Shin JH et al (2018) Green tea seed isolated saponins exerts antibacterial effects against various strains of gram positive and gram negative bacteria, a comprehensive study in vitro and in vivo. Evid Based Complementary Altern Med. https://doi.org/10.1155/2018/3486106

Knudsen D, Jutfelt F, Sundh H et al (2008) Dietary soya saponins increase gut permeability and play a key role in the onset of soyabean-induced enteritis in Atlantic salmon (*Salmo salar* L.). Br J Nutr 100:120–129

Liao Y, Li Z, Zhou Q, Sheng M et al (2021) Saponin surfactants used in drug delivery systems: A new application for natural medicine components. Int J Pharm 603:120709

Lorent J, Lins L, Domenech Ò et al (2014) Domain formation and permeabilization induced by the saponin α-hederin and its aglycone hederagenin in a cholesterol-containing bilayer. Langmuir 30:4556–4569

Muniyan A, Ravi K, Mohan U, Panchamoorthy R (2017) Characterization and in vitro antibacterial activity of saponin-conjugated silver nanoparticles against bacteria that cause burn wound infection. World J Microbiol Biotechnol 33(7):147

Nadanaciva S, Dillman K, Gebhard DF, Shrikhande A, Will Y (2010) High-content screening for compounds that affect mtDNA-encoded protein levels in eukaryotic cells. J Biomol Screen 15:937–948

Nitrofurantoin Drug Usage Statistics, United States, (2013–2020). https://clincalc.com/DrugStats/Drugs/Nitrofurantoin.

Nowak A, Mrozik A (2016) Facilitation of co-metabolic transformation and degradation of monochlorophenols by *Pseudomonas* sp. CF600 and changes in its fatty acid composition. Water Air Soil Pollut 227:83

Pacholak A, Burlaga N, Guzik U, Kaczorek E (2021) Investigation of the bacterial cell envelope nanomechanical properties after long-term exposure to nitrofurans. J Hazard Mater 407:124352

Pacholak A, Juzwa W, Zgoła-Grześkowiak A, Kaczorek E (2023) Multi-faceted analysis of bacterial transformation of nitrofurantoin. Sci Total Environ 874:162422

Polianciuc SI, Gurzău AE, Kiss B, Ștefan MG, Loghin F (2020) Antibiotics in the environment: causes and consequences. Med Pharm Rep 93(3):231–240

Price G, Patel DA (2022) Drug bioavailability, StatPearls [Internet]. StatPearls Publishing, Treasure Island (FL)

Rojewska M, Smułek W, Prochaska K, Kaczorek E (2020) Combined effect of nitrofurantoin and plant surfactant on bacteria phospholipid membrane. Molecules 25(11):2527

Rojewska M, Smułek W, Grzywaczyk A et al (2023) Study of Interactions between Saponin Biosurfactant and Model Biological Membranes: Phospholipid Monolayers and Liposomes. Molecules 28:1965

Ropponen HK, Richter R, Hirsch AKH, Lehr CM (2021) Mastering the gram-negative bacterial barrier – Chemical approaches to increase bacterial bioavailability of antibiotics. Adv Drug Deliv Rev 172:339–360

Smułek W, Kaczorek E (2022) Factors Influencing the Bioavailability of Organic Molecules to Bacterial Cells—A Mini-Review. Molecules 27(19):6579

Smułek W, Zdarta A, Łuczak M et al (2016) Sapindus saponins' impact on hydrocarbon biodegradation by bacteria strains after short- and long-term contact with pollutant. Colloids Surf B Biointerfaces 142:207–213

Smułek W, Zdarta A, Grzywaczyk A et al (2020) Evaluation of the physico-chemical properties of hydrocarbons-exposed bacterial biomass. Colloids Surf B Biointerfaces 196:111310

Sreij R, Prévost S, Dargel C et al (2018) Interaction of the saponin Aescin with Ibuprofen in DMPC model membranes. Mol Pharm 15:4446–4461

Sudji IR, Subburaj Y, Frenkel N et al (2015) Membrane disintegration caused by the steroid saponin digitonin is related to the presence of cholesterol. Molecules 20:20146–20160

Vass M, Hruska K, Franek M (2008) Nitrofuran antibiotics: A review on the application, prohibition and residual analysis. Vet Med 53:469–500

Willdigg JR, Helmann JD (2021) Mini Review: Bacterial membrane composition and its modulation in response to stress. Front Mol Biosci 8:1–11

Xiao Y, Xiong T, Meng X, Yu D, Xiao Z, Song L (2019) Different influences on mitochondrial function, oxidative stress and cytotoxicity of antibiotics on primary human neuron and cell lines. J Biochem Mol Toxicol 33:1–7

Zaynab M, Sharif Y, Abbas S al. (2021) Saponin toxicity as key player in plant defense against pathogens Toxicon 19321–19327. https://doi.org/10.1016/j.toxicon.2021.01.009

Zdarta A, Smułek W, Pacholak A, Kaczorek E (2019) Environmental aspects of the use of Hedera helix extract in bioremediation process. Microorganisms 7(2):43. https://doi.org/10.3390/microorganisms7020043

Zhang XS, Cao JQ, Zhao C, Wang XDe, Wu XJ, Zhao YQ, (2015) Novel dammarane-type triterpenes isolated from hydrolyzate of total Gynostemma pentaphyllum saponins. Bioorganic Med Chem Lett 25:3095–3099

Zhang Y, Meng X, Liu K (2022) The modulation of cAMP/PKA pathway by asiaticoside ameliorates high glucose-induced inflammation and apoptosis of retinal pigment epithelial cells. J Bioenerg Biomembr 54:9–16

Zheng X, Gallot G (2021) Dynamics of cell membrane permeabilization by saponins using terahertz attenuated total reflection. Optics InfoBase Conference Papers Doi 10(1117/12):2615463

P5 Supplementary material

Supplementary Information

Co-interaction of nitrofuran antibiotics and the saponin-rich extract on Gram-negative bacteria and colon epithelial cells

Submitted to

World Journal of Microbiology and Biotechnology

by

Adam Grzywaczyk[1], Wojciech Smułek[1], Anna Olejnik[2], Urszula Guzik[3], Agnieszka Nowak[3], Ewa Kaczorek[1]*

[1] *Institute of Chemical Technology and Engineering, Poznan University of Technology, Berdychowo 4, 60-695 Poznan, Poland; e-mails: adam.grzywaczyk@doctorate.put.poznan.pl; wojciech.smulek@put.poznan.pl; ewa.kaczorek@put.poznan.pl*

[2] *Department of Biotechnology and Food Microbiology, Poznań University of Life Sciences, Wojska Polskiego 48, 60-627 Poznań, Poland; e-mail: anna.olejnik@up.poznan.pl*

[3] *Institute of Biology, Biotechnology and Environmental Protection, Faculty of Natural Science, University of Silesia in Katowice, Jagiellonska 28, 40-032 Katowice, Poland; e-mails: urszula.guzik@us.edu.pl; agnieszka.a.nowak@us.edu.pl*

*Corresponding author:
e-mail: ewa.kaczorek@put.poznan.pl, tel. +48 (61) 6652601

E-Supplementary data

Growth curves

Each bacteria strain was cultured with the presence of antibiotic in the concentration range of 0.01, 0.02, 0.05, 0.1, 0.2, 0.5, 1.0, 2.0, 5.0, 10, 20, 25, 50, 75, 100, 125, 150, 175 and 200 µg mL^{-1} of nitrofurantoin or furazolidone respectively. To 75 µg mL^{-1} of antibiotics for *P. plecoglossicida* IsA and 200 µg mL^{-1} for *Pseudomonas* sp. OS4 and MChB, *Sapindus mukorossi* extract in athe range of 30, 20, 10 and 5 µg mL^{-1} was added. Selected curves are presented.

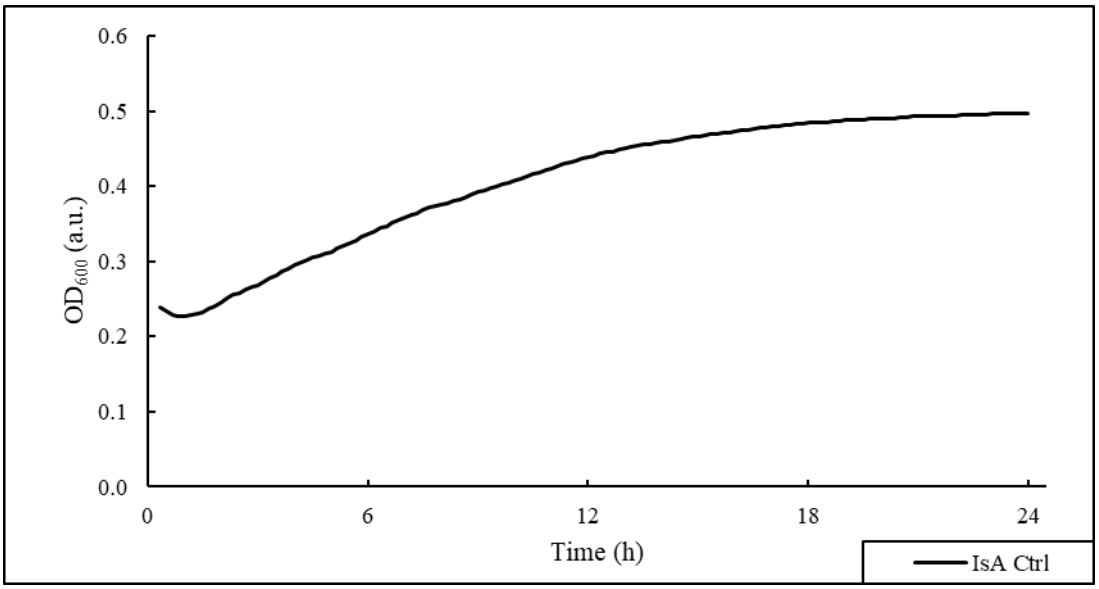

S1. Growth curve of *Pseudomonas plecoglossicida* IsA

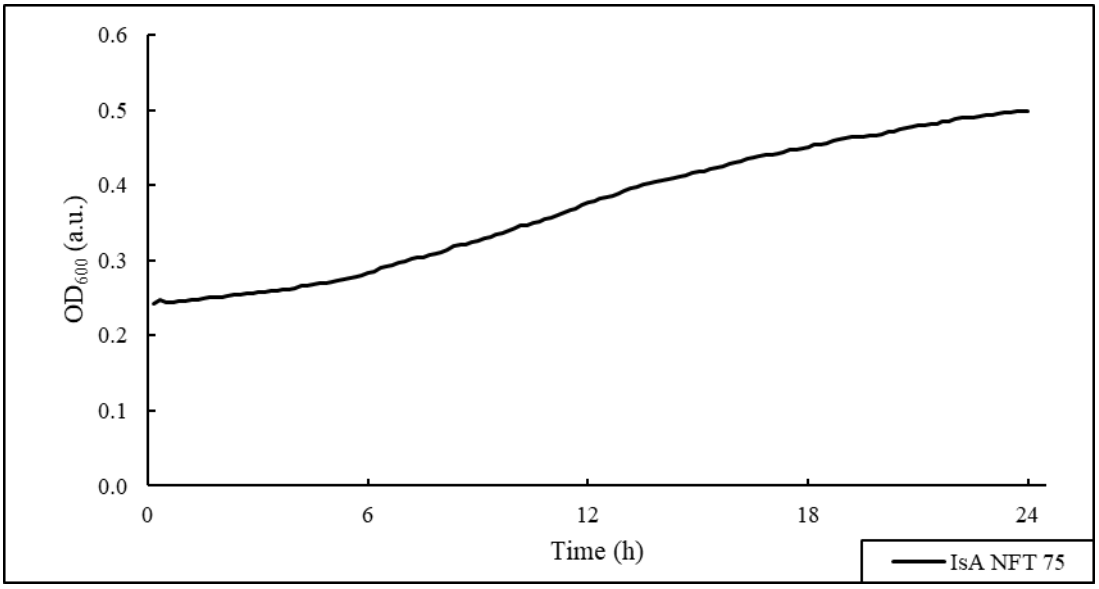

S2. Growth curve of *Pseudomonas plecoglossicida* IsA exposed to 75 µg mL^{-1} of nitrofurantoin

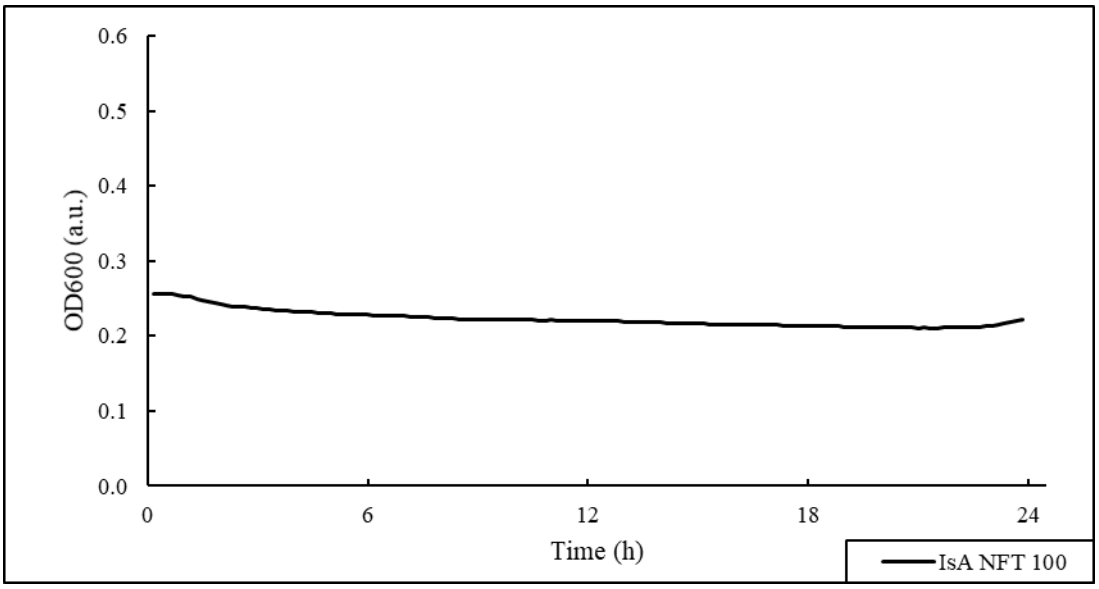

S3. Growth curve of *Pseudomonas plecoglossicida* IsA exposed to 100 µg mL^{-1} of nitrofurantoin

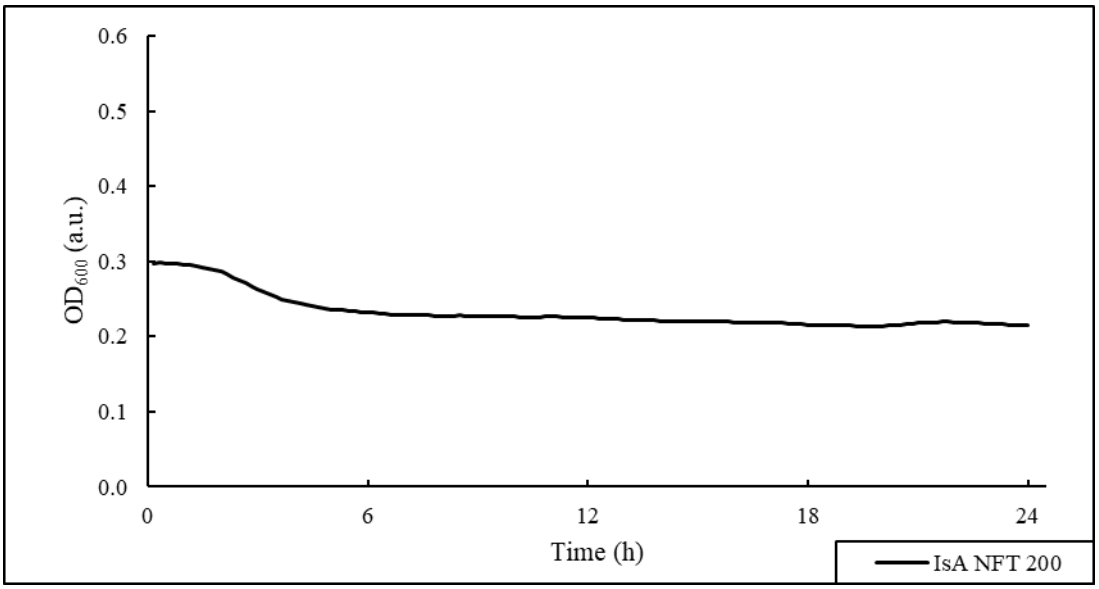

S4. Growth curve of *Pseudomonas plecoglossicida* IsA exposed to 200 µg mL^{-1} of nitrofurantoin

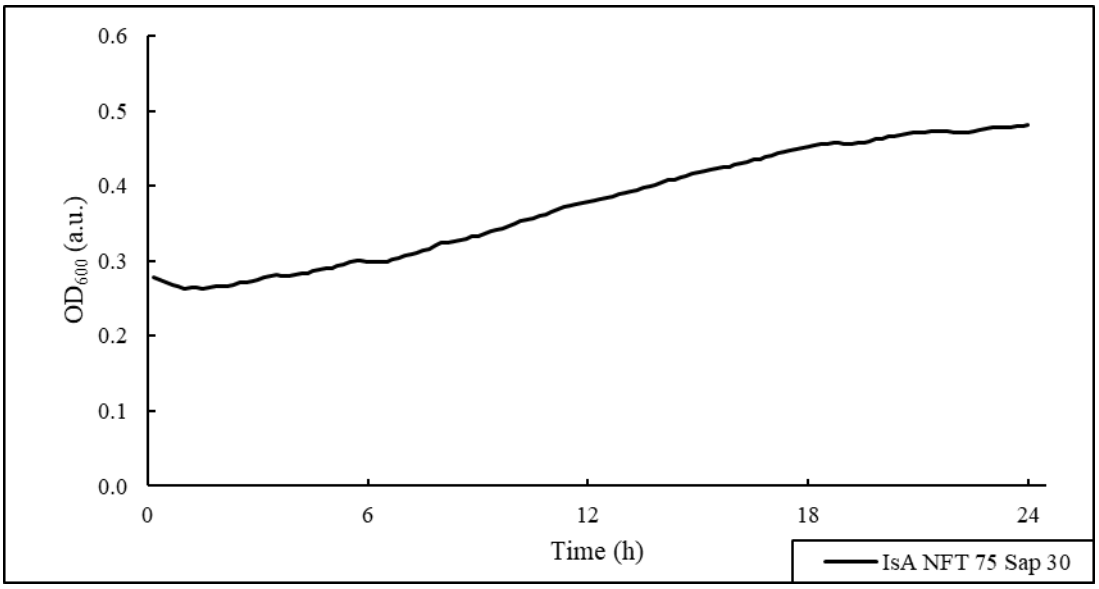

S5. Growth curve of *Pseudomonas plecoglossicida* IsA exposed to 75 µg mL^{-1} of nitrofurantoin and 30 µg mL^{-1} of *Sapindus mukorossi*

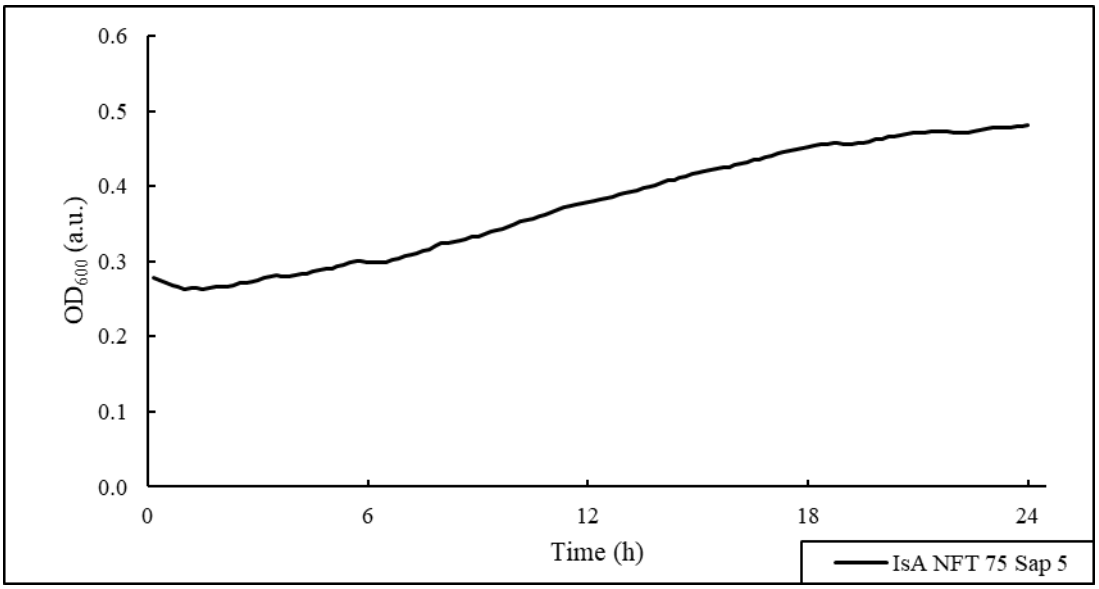

S6. Growth curve of *Pseudomonas plecoglossicida* IsA exposed to 75 µg mL^{-1} of nitrofurantoin and 5 µg mL^{-1} of *Sapindus mukorossi*

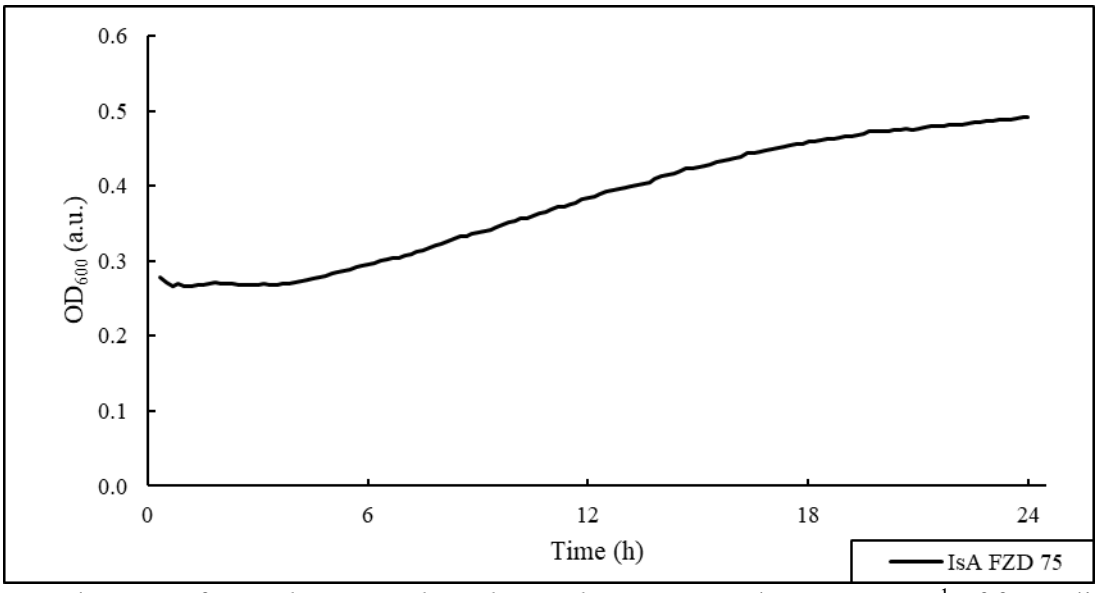

S7. Growth curve of *Pseudomonas plecoglossicida* IsA exposed to 75 µg mL^{-1} of furazolidone

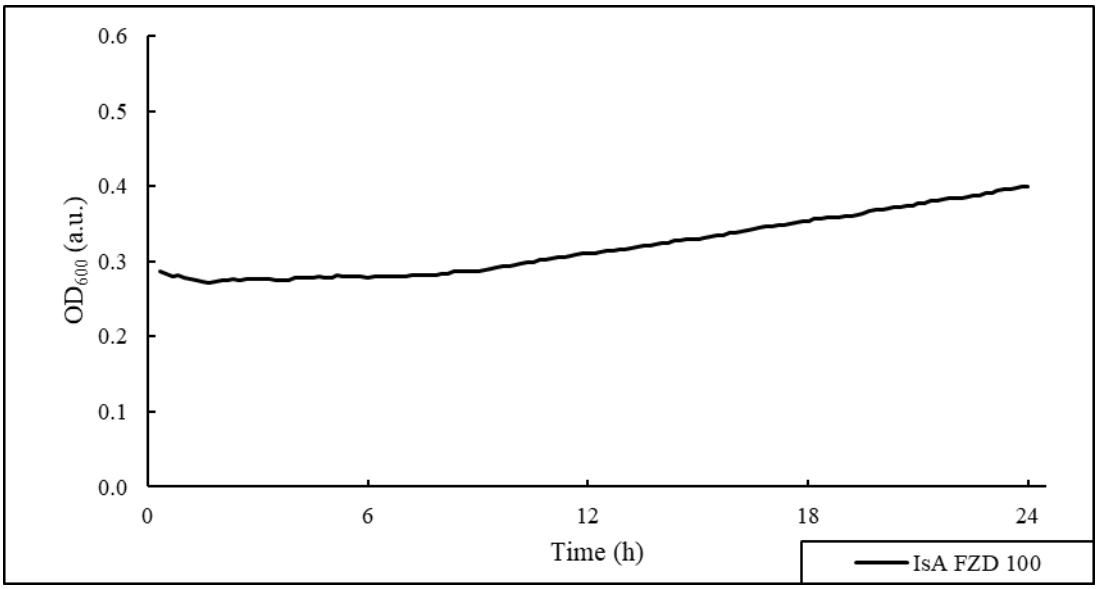

S8. Growth curve of *Pseudomonas plecoglossicida* IsA exposed to 100 µg mL^{-1} of furazolidone

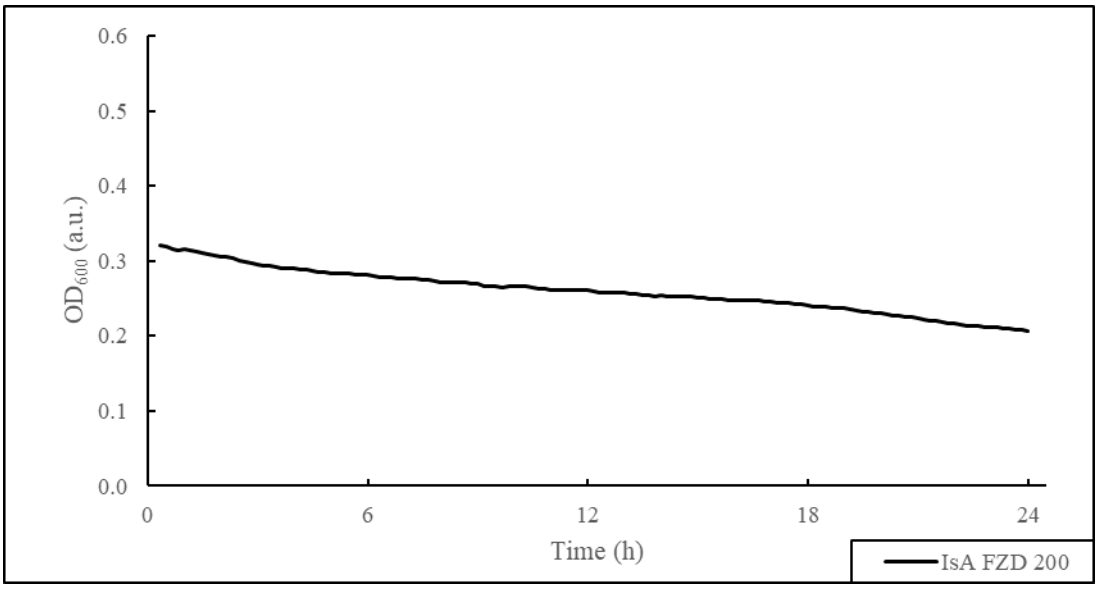

S9. Growth curve of *Pseudomonas plecoglossicida* IsA exposed to 200 µg mL^{-1} of furazolidone

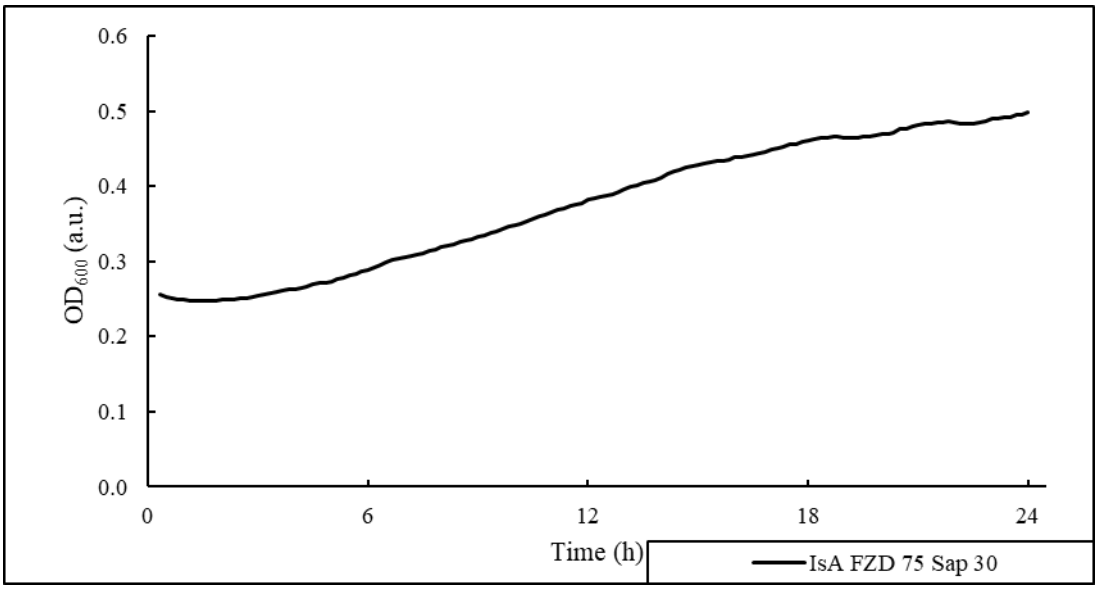

S10. Growth curve of *Pseudomonas plecoglossicida* IsA exposed to 75 µg mL^{-1} of furazolidone and 30 µg mL^{-1} of *Sapindus mukorossi*

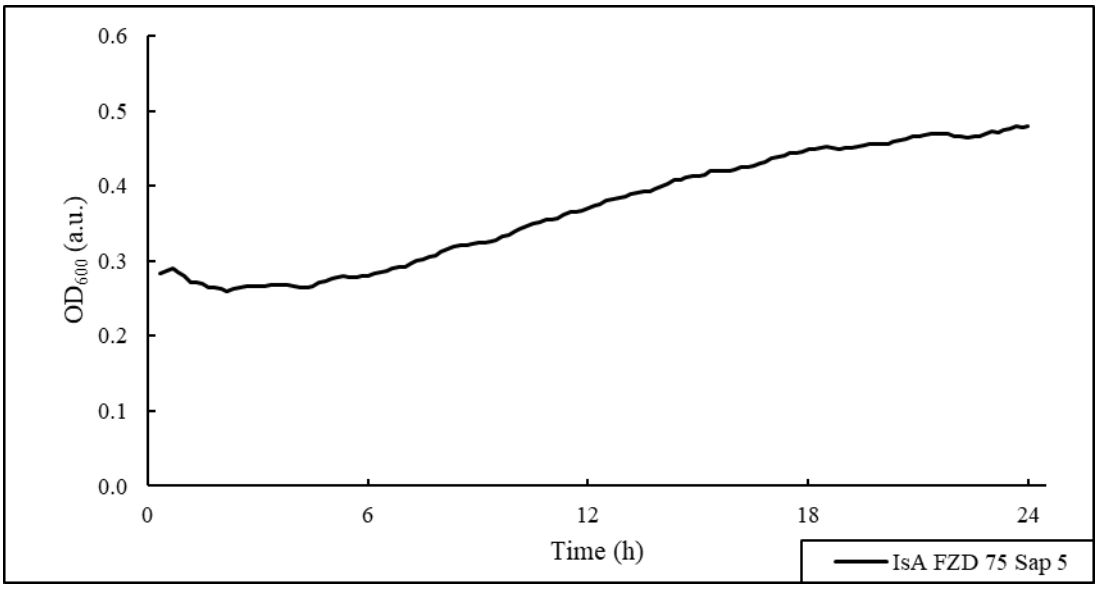

S11. Growth curve of *Pseudomonas plecoglossicida* IsA exposed to 75 µg mL^{-1} of furazolidone and 5 µg mL^{-1} of *Sapindus mukorossi*

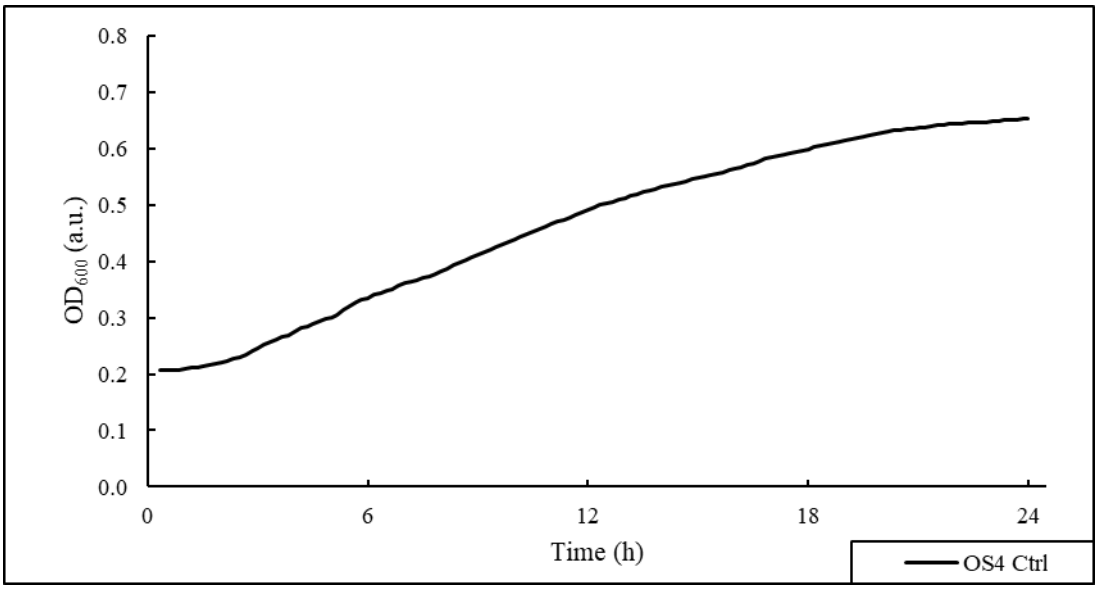

S12. Growth curve of *Pseudomonas sp.* OS4

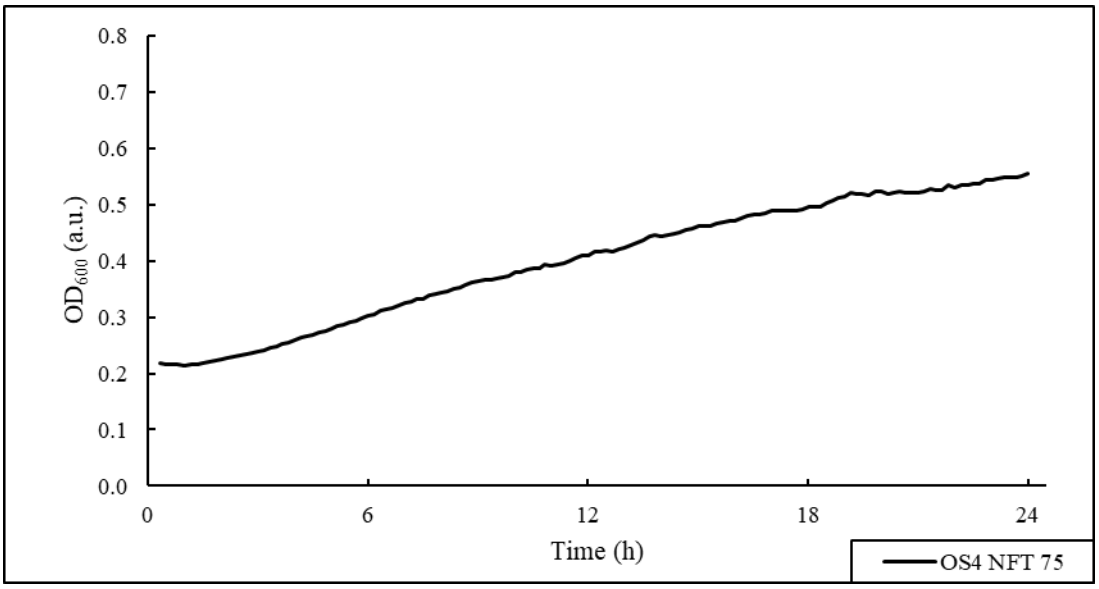

S13. Growth curve of *Pseudomonas sp.* OS4 exposed to 75 µg mL^{-1} of nitrofurantoin

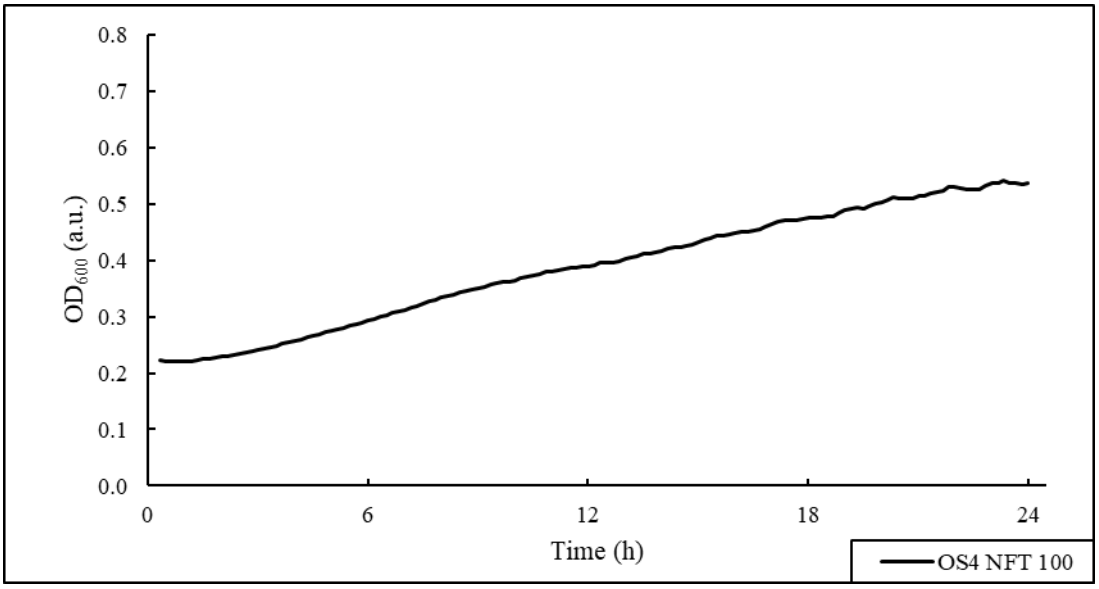

S14. Growth curve of *Pseudomonas sp.* OS4 exposed to 100 µg mL^{-1} of nitrofurantoin

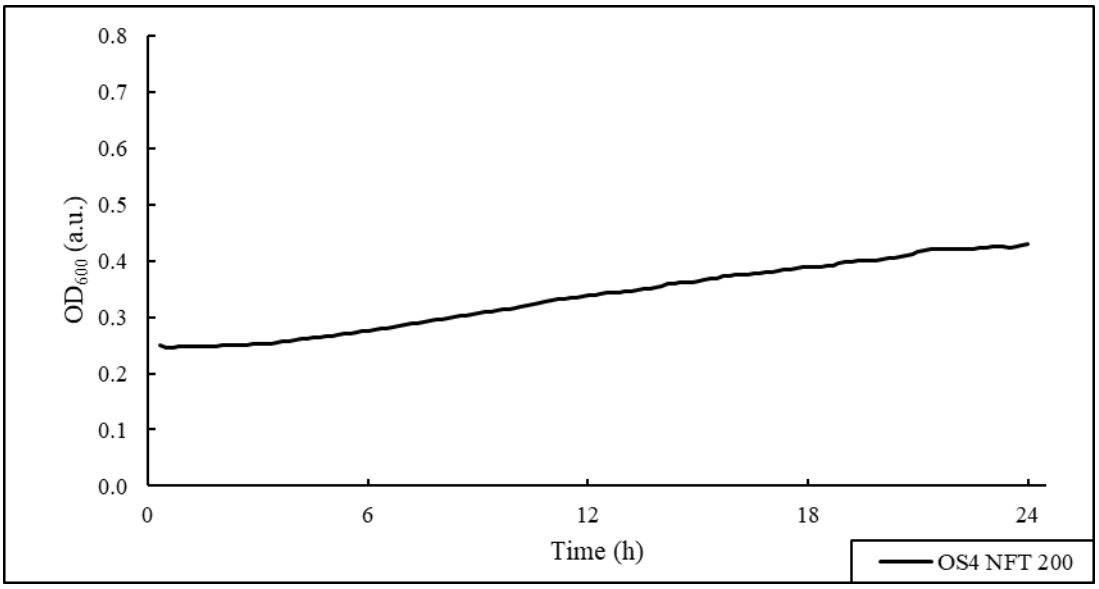

S15. Growth curve of *Pseudomonas sp.* OS4 exposed to 200 µg mL^{-1} of nitrofurantoin

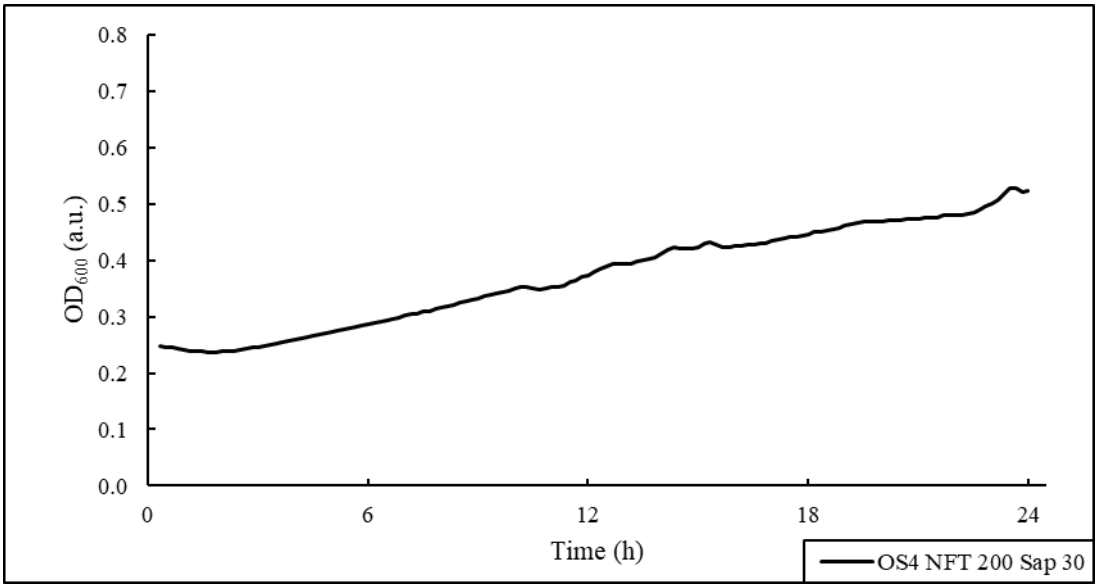

S16. Growth curve of *Pseudomonas sp.* OS4 exposed to 200 µg mL^{-1} of nitrofurantoin and 30 µg mL^{-1} of *Sapindus mukorossi*

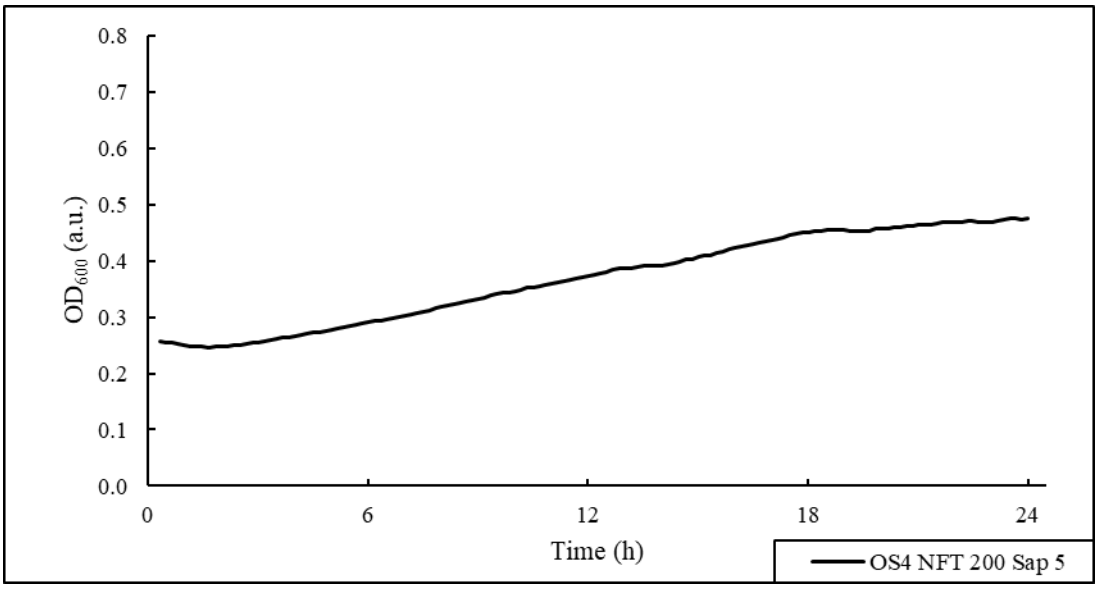

S16. Growth curve of *Pseudomonas sp.* OS4 exposed to 200 µg mL^{-1} of nitrofurantoin and 5 µg mL^{-1} of *Sapindus mukorossi*

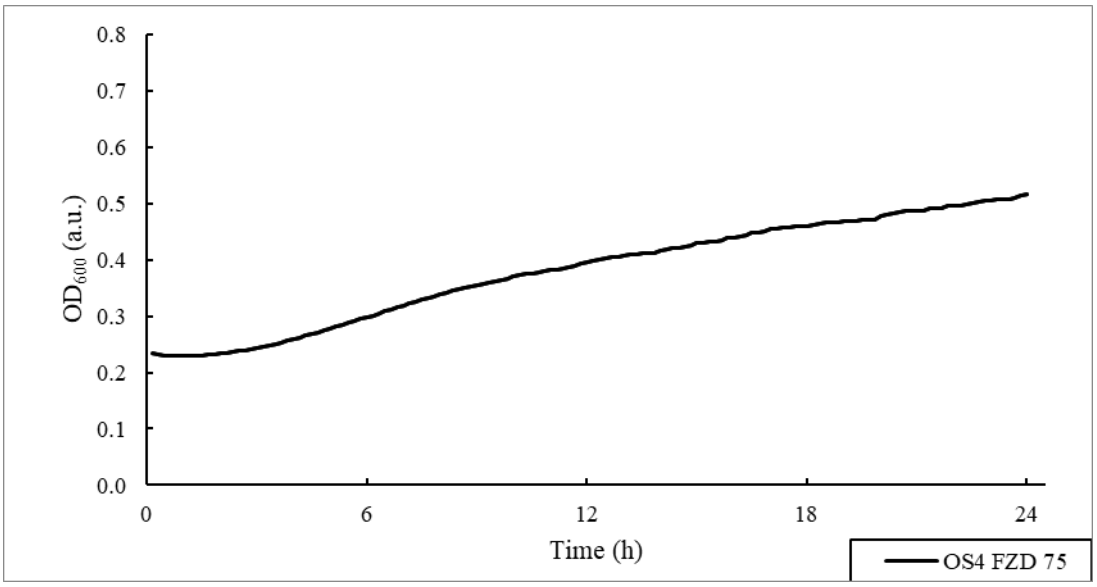

S17. Growth curve of *Pseudomonas sp.* OS4 exposed to 75 µg mL^{-1} of furazolidone

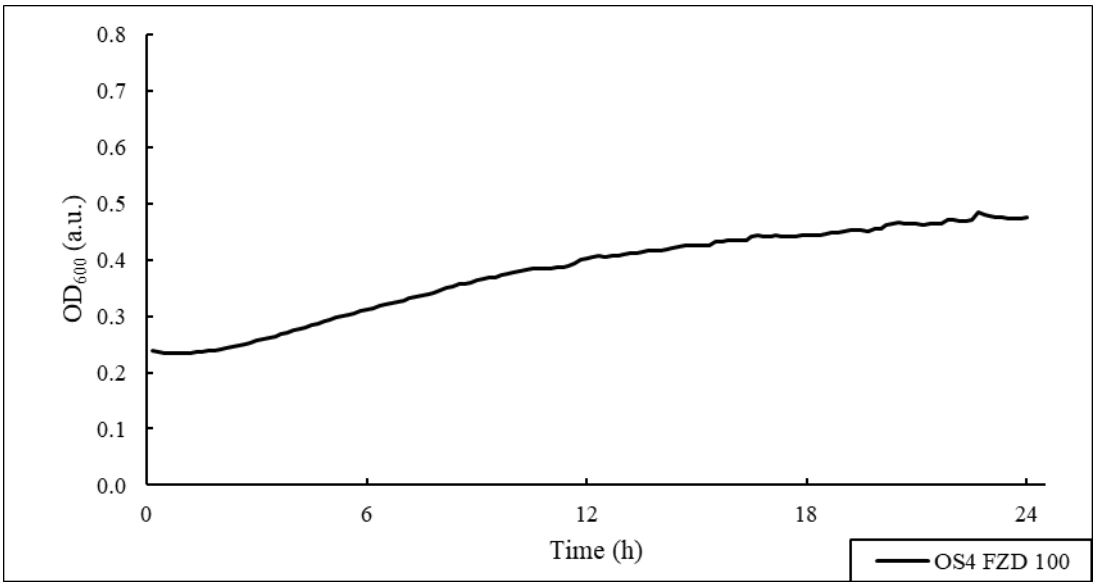

S18. Growth curve of *Pseudomonas sp.* OS4 exposed to 100 µg mL^{-1} of furazolidone

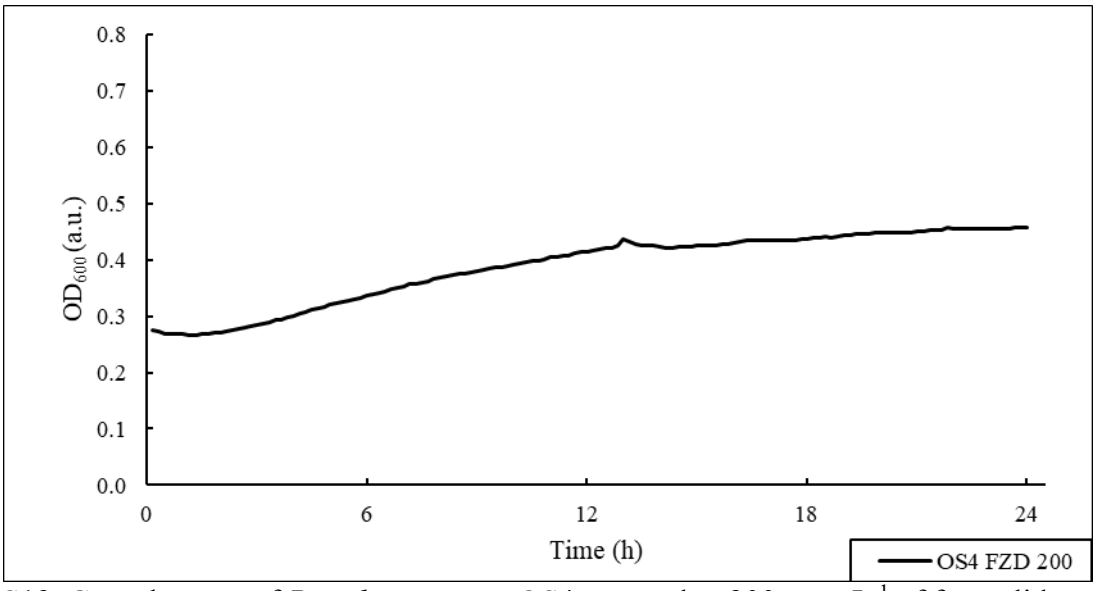

S19. Growth curve of *Pseudomonas sp.* OS4 exposed to 200 µg mL^{-1} of furazolidone

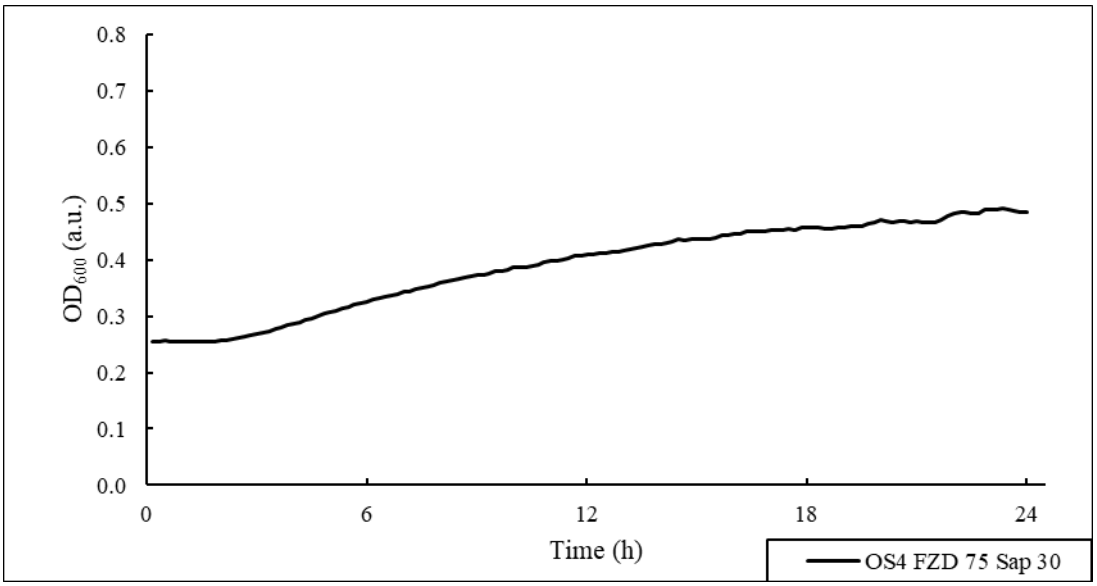

S20. Growth curve of *Pseudomonas sp.* OS4 exposed to 200 µg mL^{-1} of furazolidone and 30 µg mL^{-1} of *Sapindus mukorossi*

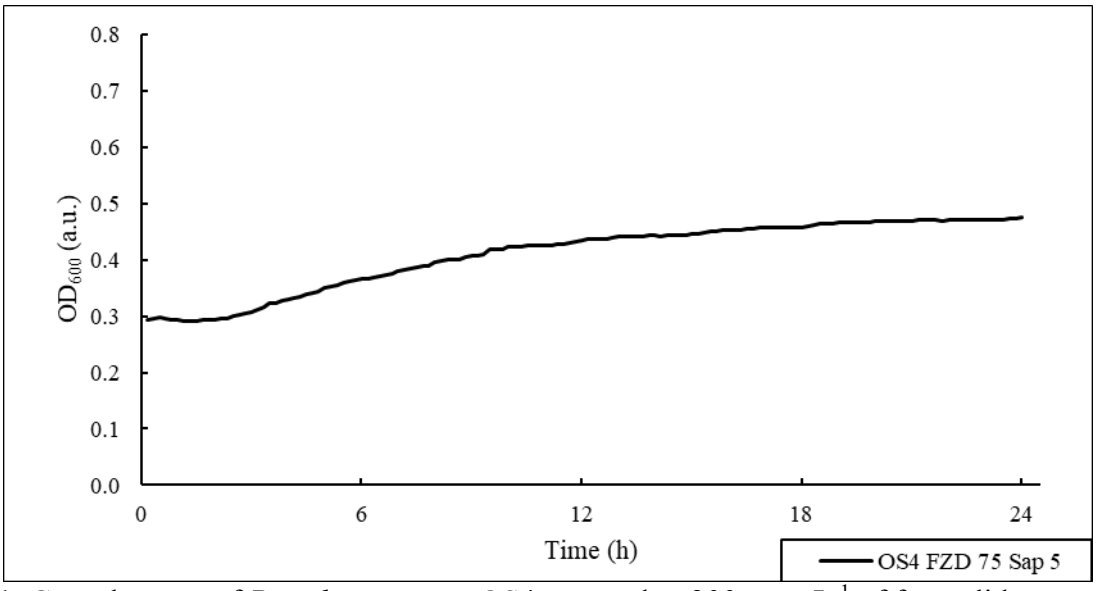

S21. Growth curve of *Pseudomonas sp.* OS4 exposed to 200 µg mL^{-1} of furazolidone and 5 µg mL^{-1} of *Sapindus mukorossi*

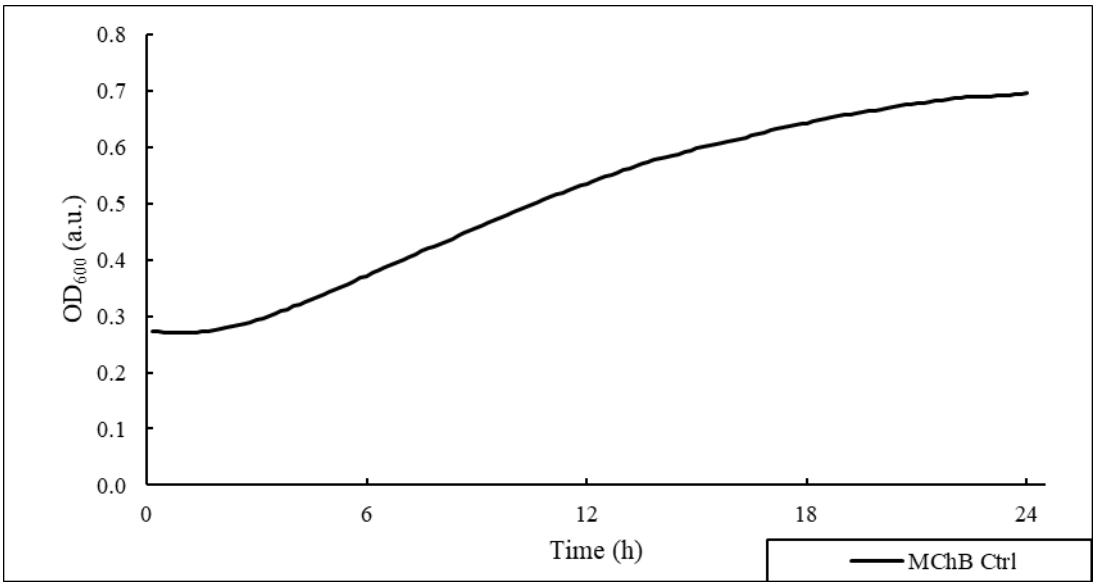

S22. Growth curve of *Pseudomonas sp.* MChB

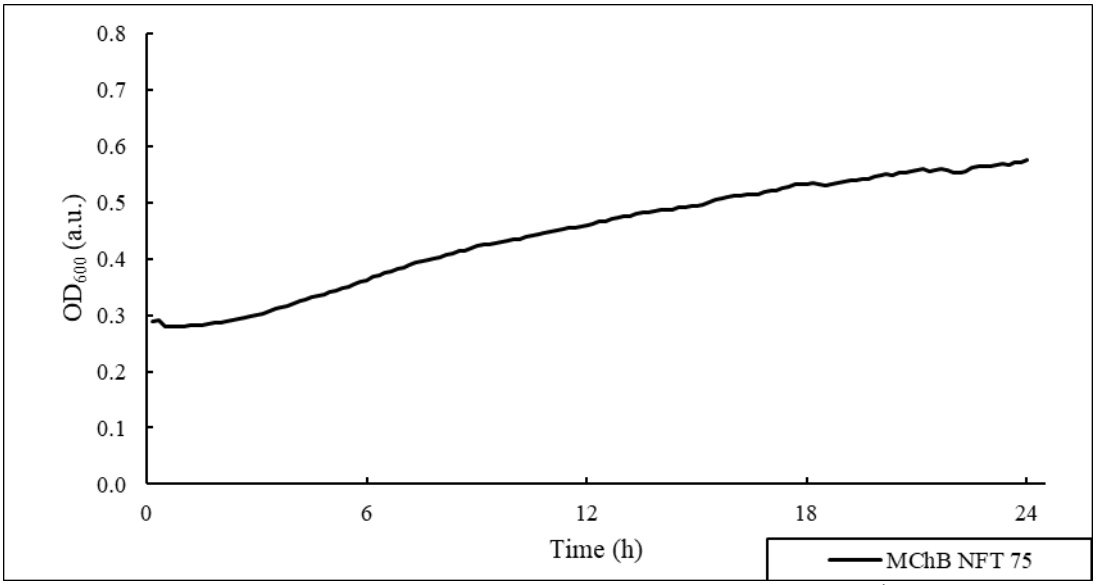

S23. Growth curve of *Pseudomonas sp.* MChB exposed to 75 µg mL^{-1} of nitrofurantoin

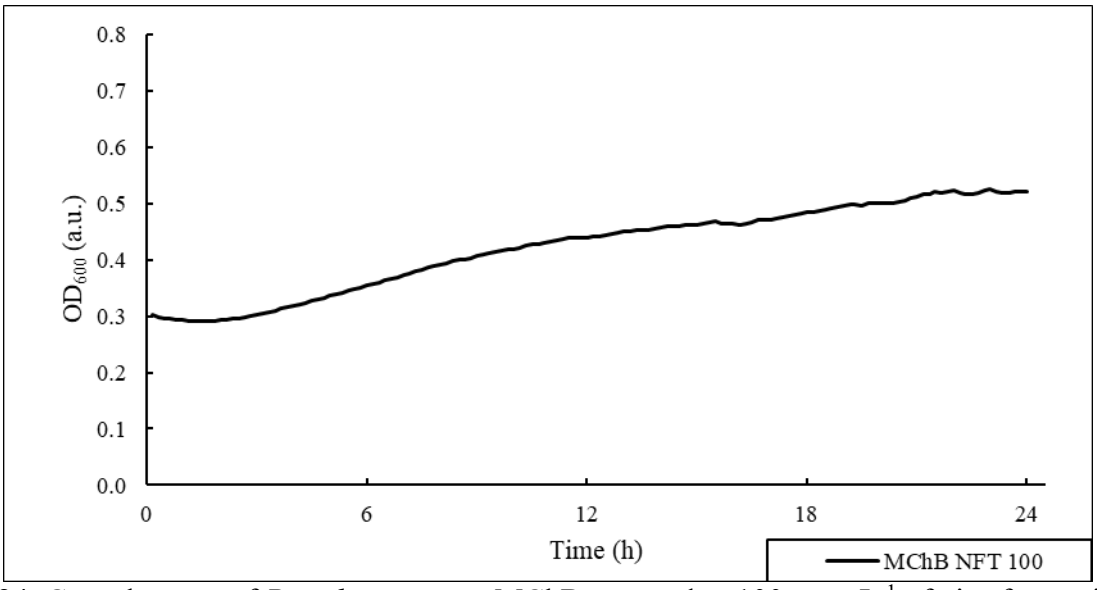

S24. Growth curve of *Pseudomonas sp.* MChB exposed to 100 µg mL^{-1} of nitrofurantoin

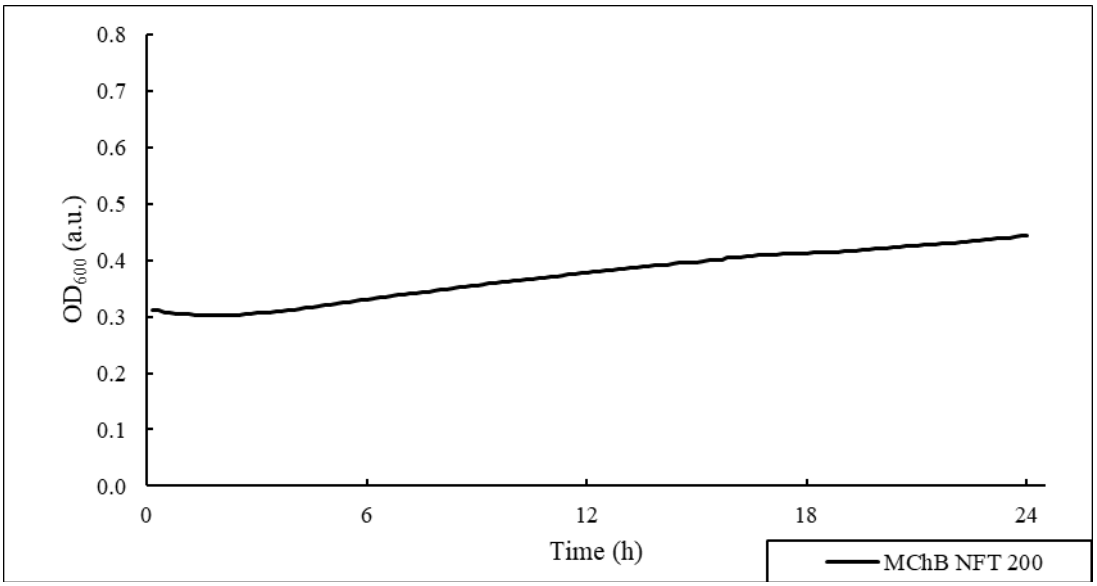

S25. Growth curve of *Pseudomonas sp.* MChB exposed to 200 µg mL^{-1} of nitrofurantoin

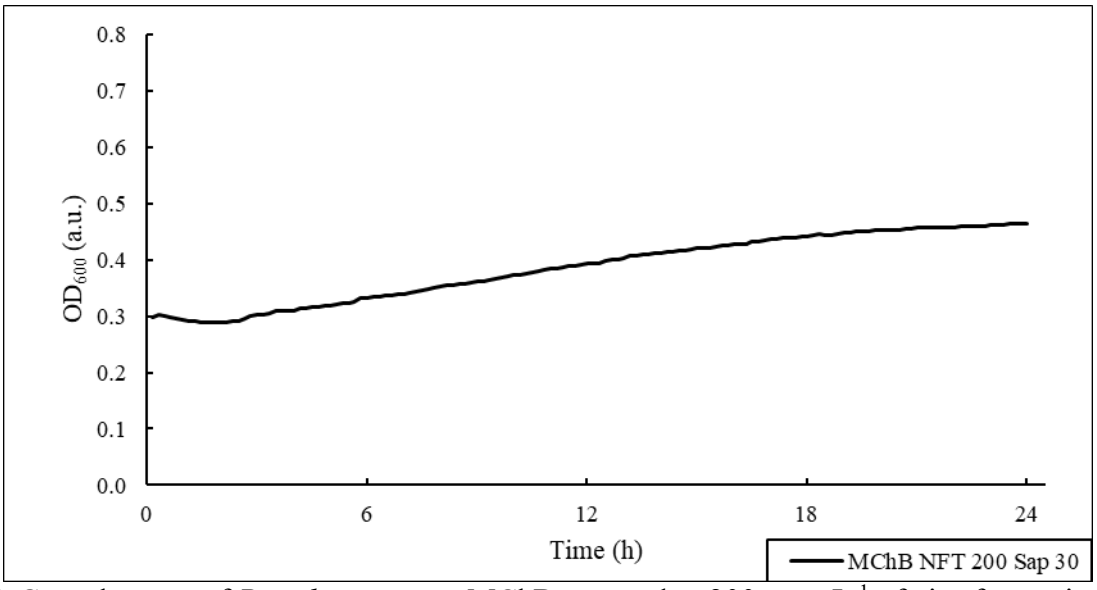

S26. Growth curve of *Pseudomonas sp.* MChB exposed to 200 µg mL^{-1} of nitrofurantoin and 30 µg mL^{-1} of *Sapindus mukorossi*

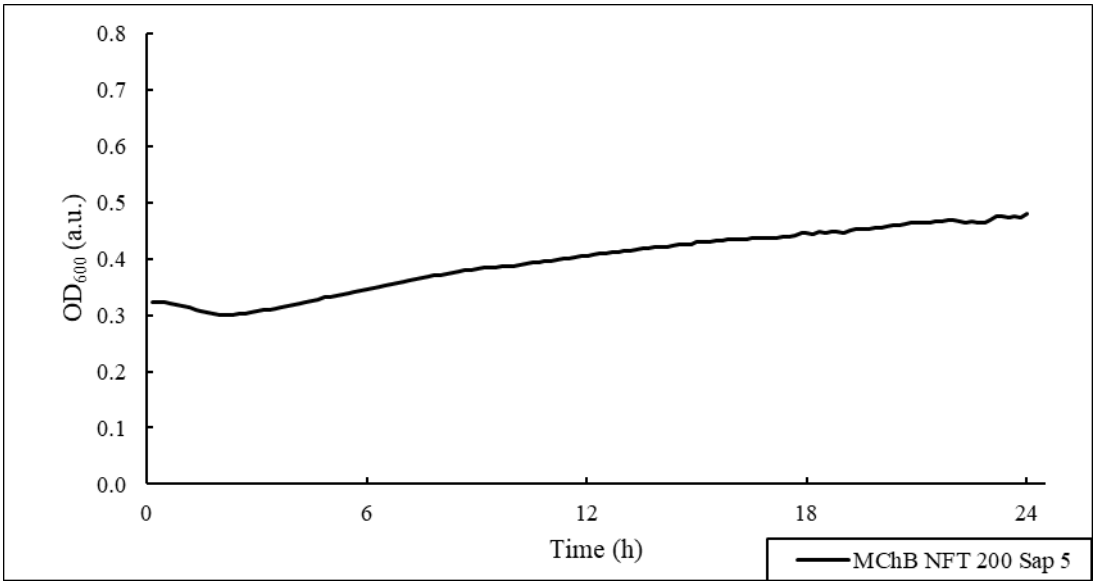

S27. Growth curve of *Pseudomonas sp.* MChB exposed to 200 µg mL^{-1} of nitrofurantoin and 5 µg mL^{-1} of *Sapindus mukorossi*

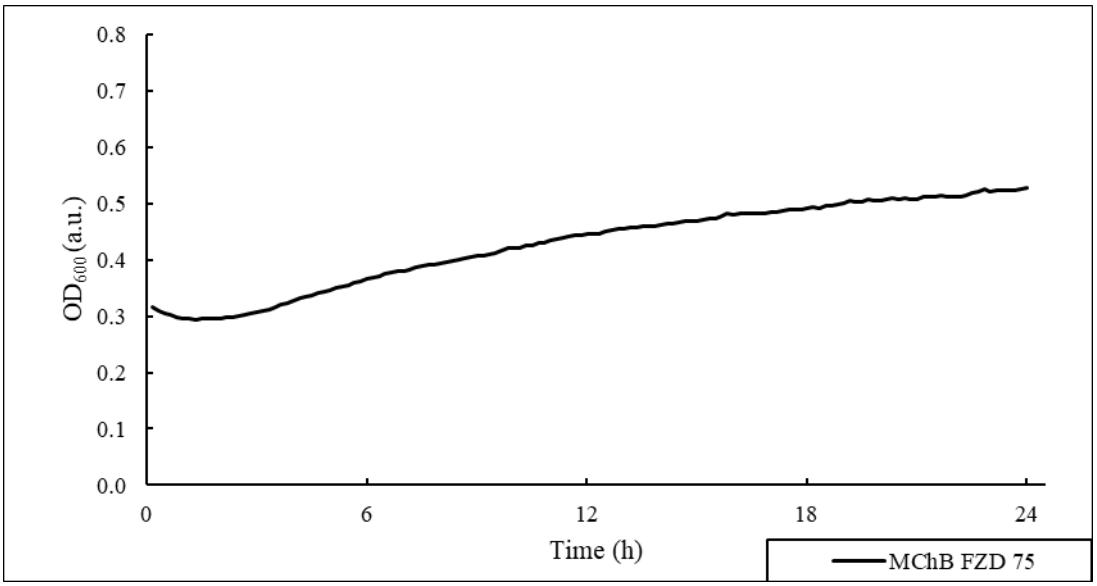

S28. Growth curve of *Pseudomonas sp.* MChB exposed to 75 µg mL^{-1} of furazolidone

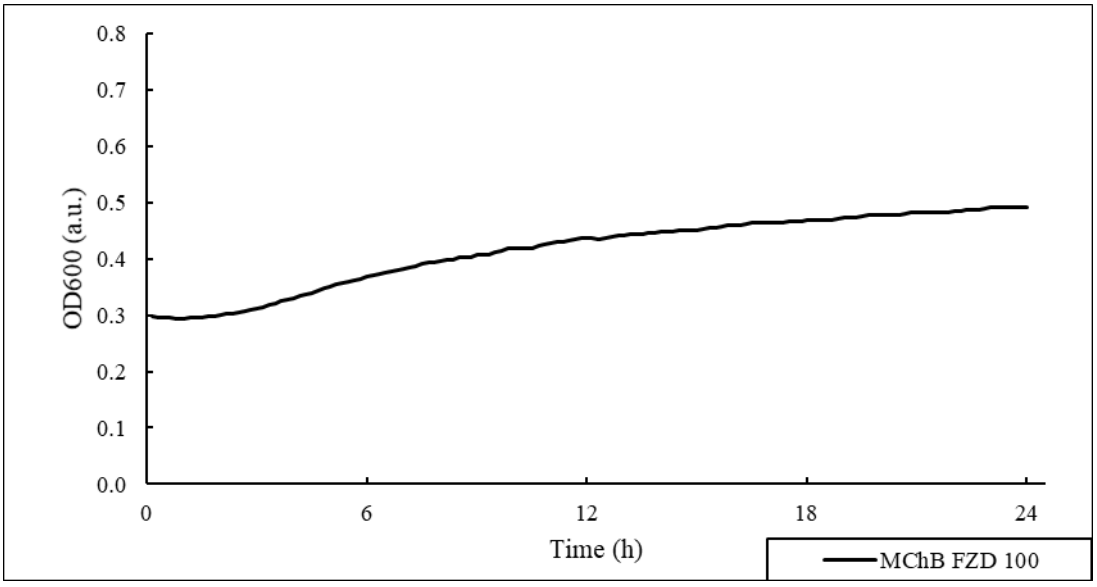

S29. Growth curve of *Pseudomonas sp.* MChB exposed to 100 µg mL^{-1} of furazolidone

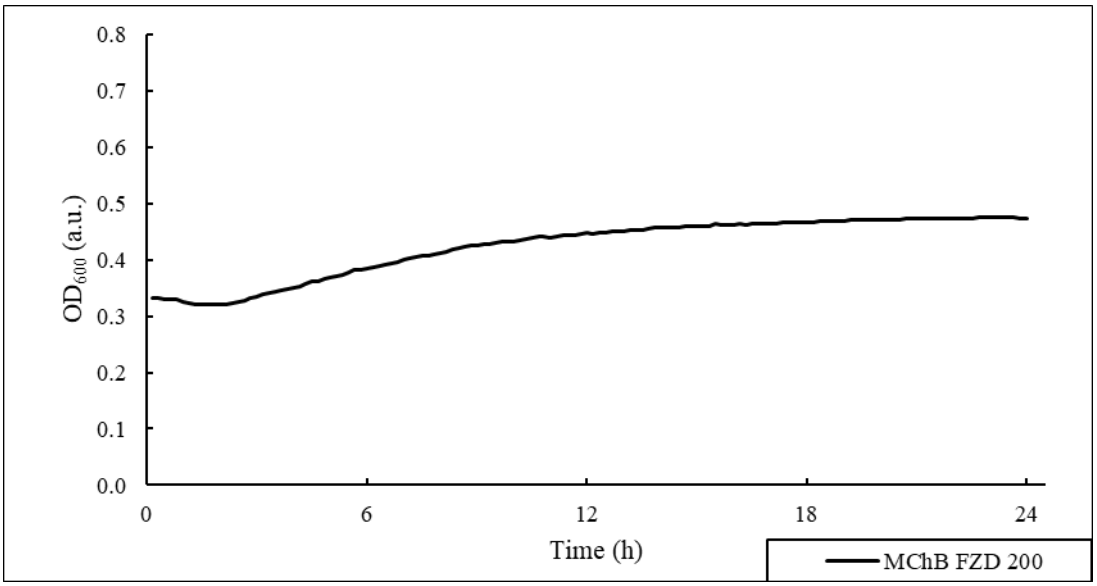

S32. Growth curve of *Pseudomonas sp.* MChB exposed to 200 µg mL^{-1} of furazolidone

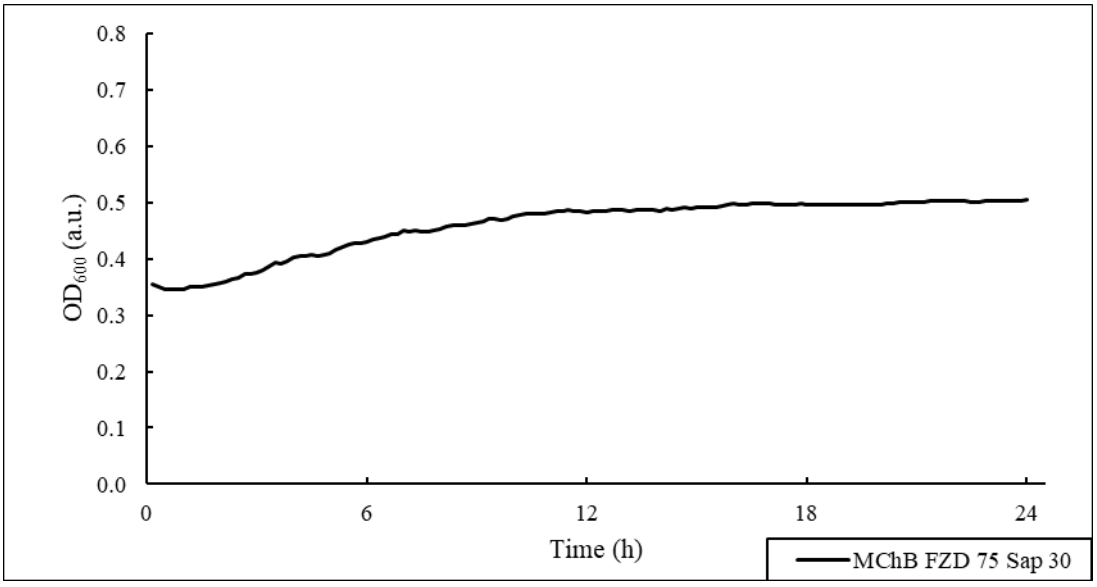

S33. Growth curve of *Pseudomonas sp.* MChB exposed to 200 µg mL^{-1} of furazolidone and 30 µg mL^{-1} of *Sapindus mukorossi*

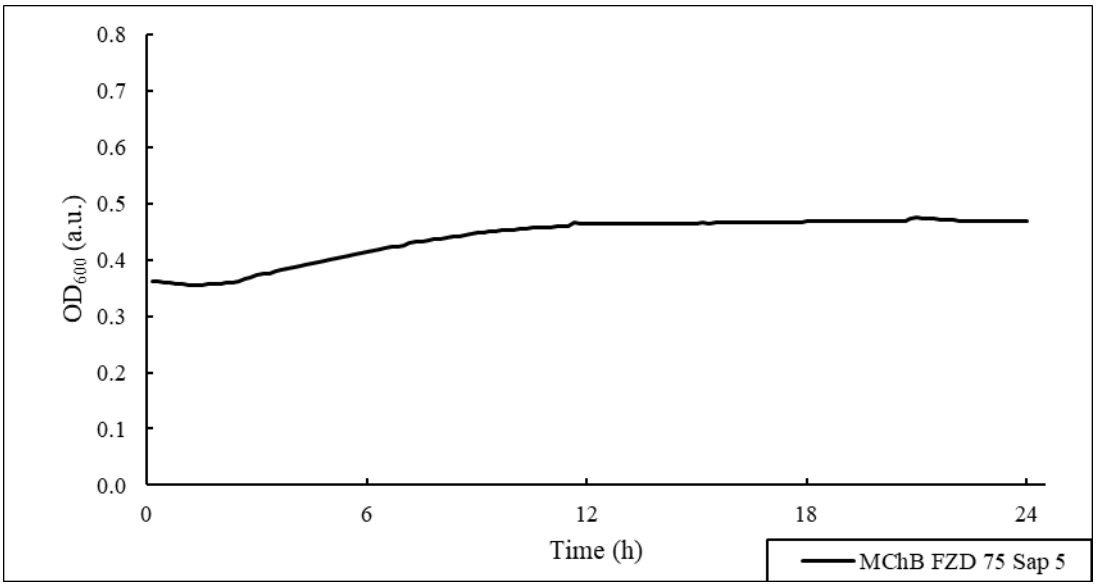

S34. Growth curve of *Pseudomonas sp.* MChB exposed to 200 µg mL^{-1} of furazolidone and 5 µg mL^{-1} of *Sapindus mukorossi*

Cell topography

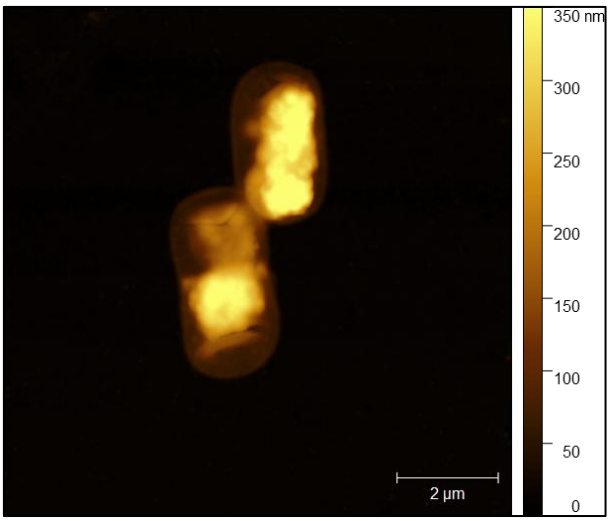

S35. Surface two-dimensional height images illustrating the *Pseudomonas plecoglossicida* IsA topography, Control sample

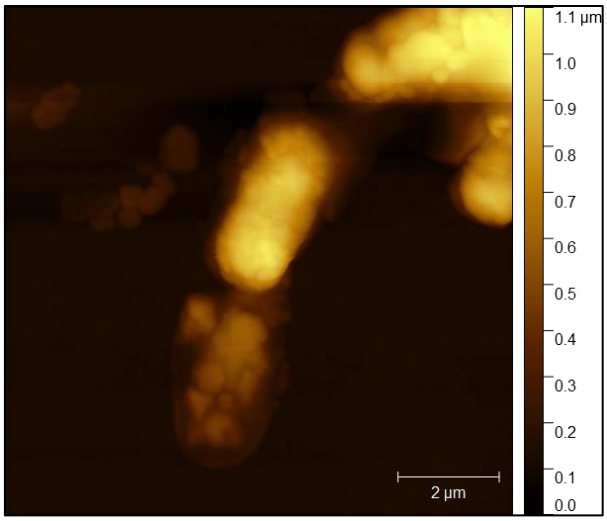

S36. Surface two-dimensional height images illustrating the *Pseudomonas plecoglossicida* IsA topography, Exposed to 5 µg mL^{-1} of NFT

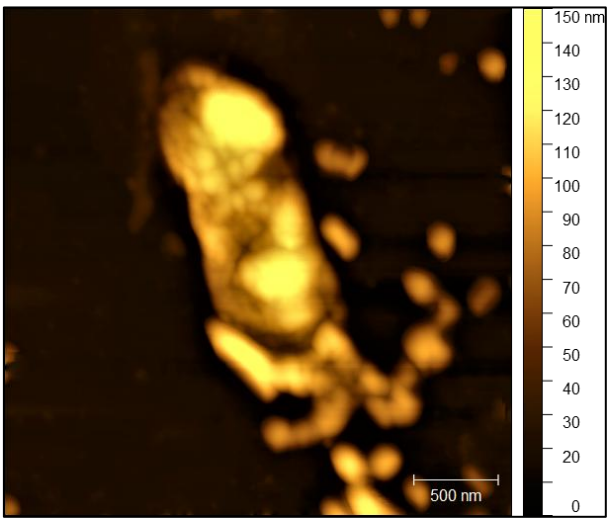

S37. Surface two-dimensional height images illustrating the *Pseudomonas plecoglossicida* IsA topography, Exposed to 5 µg mL^{-1} of NFT and 10 µg mL^{-1} of saponins

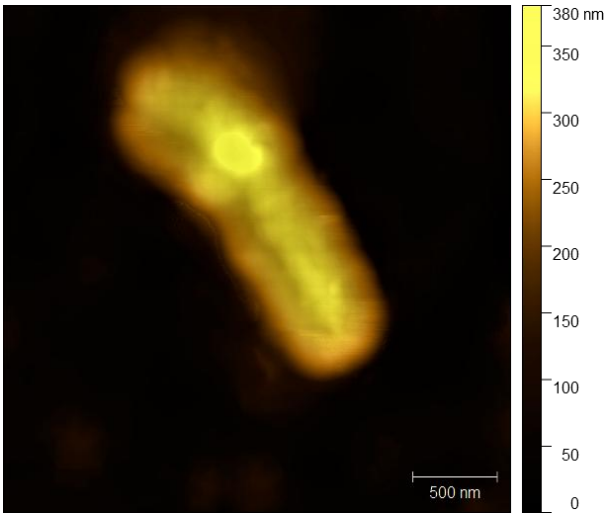

S38. Surface two-dimensional height images illustrating the *Pseudomonas sp.* OS4 topography, Control sample

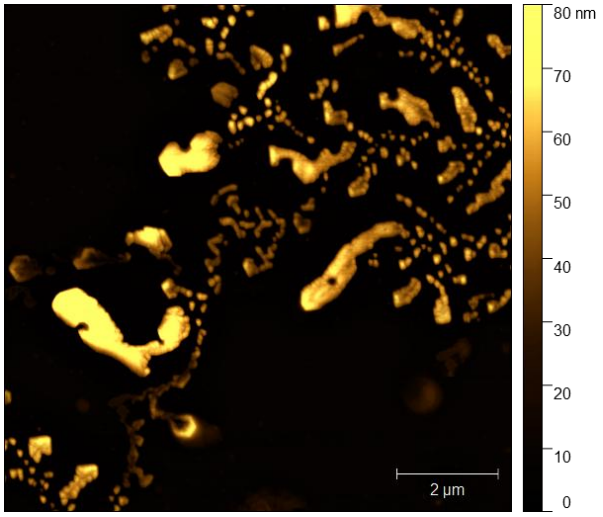

S39. Surface two-dimensional height images illustrating the *Pseudomonas sp.* OS4 topography, Exposed to 5 µg mL^{-1} of NFT

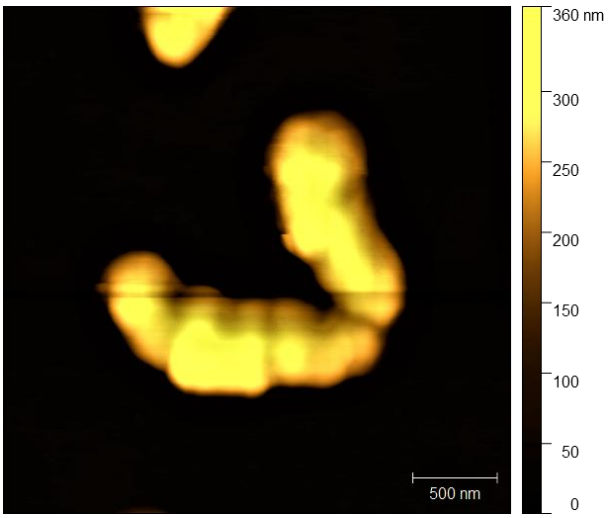

S40. Surface two-dimensional height images illustrating the *Pseudomonas sp.* OS4 topography, Exposed to 5 µg mL^{-1} of NFT and 10 µg mL^{-1} of saponins

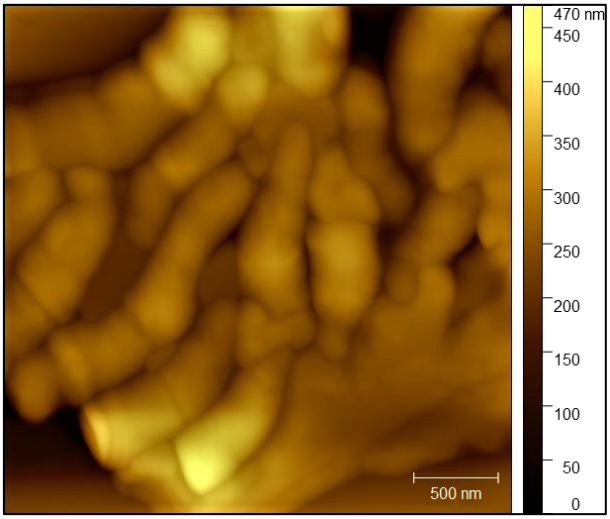

S41. Surface two-dimensional height images illustrating the *Pseudomonas sp.* MChB topography, Control sample

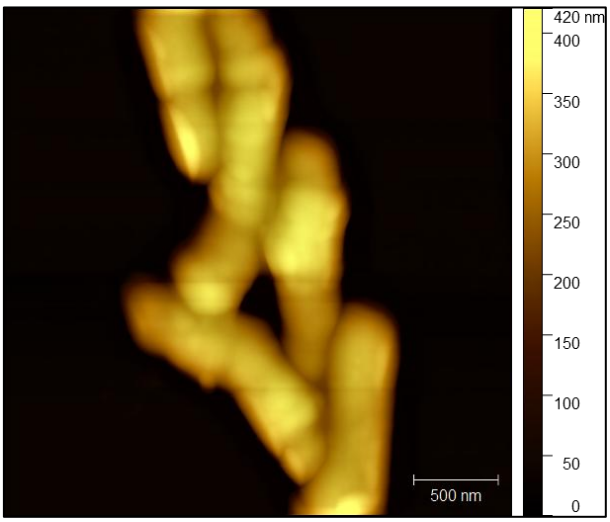

S42. Surface two-dimensional height images illustrating the *Pseudomonas sp.* MChB topography, Exposed to 5 µg mL^{-1} of NFT

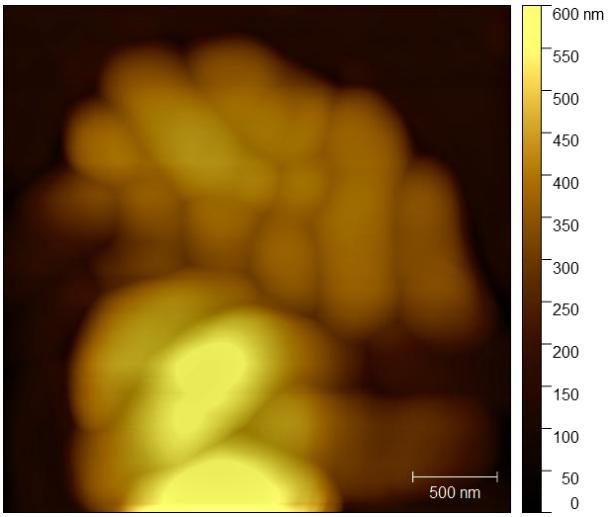

S43. Surface two-dimensional height images illustrating the *Pseudomonas sp.* MChB topography, Exposed to 5 µg mL^{-1} of NFT and 10 µg mL^{-1} of saponins

Author's contribution

P1:

- conceptualizing the research,
- conducting a literature review,
- drafting the manuscript,
- contributing to the editing of the manuscript and preparing responses to reviewers
- preparation of material for testing, including extraction and nanofiltration
- conducting a GC-MS analysis
- conducting particle size distribution analysis
- particle size distribution, GC-MS and LC-MS data interpretation and visualization

P2:

- conceptualizing the research,
- conducting a literature review,
- drafting the manuscript,
- contributing to the editing of the manuscript and preparing responses to reviewers
- preparation of material for testing, including extraction and nanofiltration
- carrying out all analyses on 3D model vesicles, including Dynamic Light Scattering, Electrophoretic Light Scattering, Fourier Transform Infrared Spectroscopy and data interpretation
- statistical analysis of the tests carried out

P3:

- conceptualizing the research,
- conducting a literature review,
- drafting the manuscript,
- contributing to the editing of the manuscript and preparing responses to reviewers
- preparation of material for testing including extraction and nanofiltration
- *Candida* cell preparation for testing
- spheroplasts preparation
- performance of all analyses, excluding TEM microscopy
- statistical analysis of the tests
- all data interpretation and visualization
- corresponding author

P4:

- conceptualizing the research,
- conducting a literature review,
- drafting the manuscript,
- contributing to the editing of the manuscript and preparing responses to reviewers
- preparation of material for testing, including extraction
- carrying out all analyses on 3D model vesicles, including Dynamic Light Scattering, Electrophoretic Light Scattering, HPTS, and 5(6)-CF analysis
- statistical analysis of the tests carried out
- visualization of the tests carried out
- corresponding author

P5:

- conceptualizing the research,
- conducting a literature review,
- drafting the manuscript,
- contributing to the editing of the manuscript and preparing responses to reviewers
- preparation of material for testing, including extraction
- preparation of material for fatty acid profile analysis
- bacterial cell preparation
- carrying out all analyses on bacteria, including cell membrane permeability (Crystal Violet and MTT analysis), Electrophoretic Light Scattering,
- statistical analysis of the tests carried out
- visualization of the tests carried out

All authors' contributions

The declarations and contributions of all other co-authors of the publications included in the publication cycle of this dissertation are given below. The Table shows all co-authors and their contributions to the individual publications included in this PhD thesis.

Authors	P1	P2	P3	P4	P5
Philip A. Gale				•	
Urszula Guzik					•
Bronisław Jańczuk	•				
Ewa Kaczorek	•	•	•	•	•
Daniel A. McNaughton				•	
Agnieszka Nowak					•
Anna Olejnik					•
Krystyna Prochaska		•		•	
Monika Rojewska		•		•	
Wojciech Smułek	•	•	•	•	•
Anna Zdziennicka	•				
Agnieszka Zgoła-Grześkowiak	•				

UTS UNIVERSITY OF TECHNOLOGY SYDNEY

Professor Philip A. Gale MA DPhil DSc
Deputy Dean
Faculty of Science
15 Broadway, Ultimo NSW 2007

T: +61 2 9514 5469
M: +61 (0) 458 705 193
philip.gale@uts.edu.au

PO Box 123
Broadway
NSW 2007 Australia
www.uts.edu.au

UTS CRICOS PROVIDER CODE 00099F

22nd July, 2025

Declarationon the individual percentage and substantive contribution of the co-author

As co-author of the publication mentioned:

P4: *Glycyrrhiza glabra L. saponins modulate the biophysical properties of bacterial model membranes and affect their interactions with tobramycin* Adam Grzywaczyk, Monika Rojewska, Wojciech Smułek, Daniel A. McNaughton, Krystyna Prochaska, Philip A. Gale, Ewa Kaczorek Langmuir 41(18), 11701-11710 (2025) DOI: 10.1021/acs.langmuir.5c00927

I declare that my contribution included:

HPTS & 5(6)-CF analysis methodology, contribution to manuscript review

Philip A. Gale
Professor of Chemistry and Deputy Dean of Science
University of Technology Sydney
Email: philip.gale@uts.edu.au

UNIWERSYTET ŚLĄSKI
W KATOWICACH

Katowice; 22.07.2025

dr hab. Urszula Guzik, Ph.D.
Associate Professor
Institute of Biology, Biotechnology and Environmental Protection
University of Silesia in Katowice
Jagiellonska 28, 40-032 Katowice, Poland
e-mail: urszula.guzik@us.edu.pl

Declaration

on the individual percentage and substantive contribution of the co-author

As co-author of the publication mentioned:

P5. Co-interaction of nitrofuran antibiotics and the saponin-rich extract on gram-negative bacteria and colon epithelial cells Adam Grzywaczyk, Wojciech Smułek, Anna Olejnik, Urszula Guzik, Agnieszka Nowak, Ewa Kaczorek World Journal of Microbiology and Biotechnology 39:221 (2023) DOI: 10.1007/s11274-023-03669-2

I declare that my contribution included:

Research on bacterial fatty acid profile determination using Gas Chromatography Mass Spectrometry, manuscript review.

UNIWERSYTET MARII CURIE-SKŁODOWSKIEJ W LUBLINIE
Wydział Chemii, Instytut Nauk Chemicznych,
Katedra Zjawisk Międzyfazowych

prof. dr hab. Bronisław Jańczuk

Declaration
on the individual percentage and substantive contribution of the co-author

As co-author of the publication mentioned:

P1. *Nanofiltered saponin-rich extract of Saponaria officinalis – Adsorption and aggregation properties of particular fractions* Adam Grzywaczyk, Wojciech Smułek, Agnieszka Zgoła-Grześkowiak, Ewa Kaczorek*, Anna Zdziennicka, Bronisław Jańczuk Colloids and Surfaces A: Physicochemical and Engineering Aspects, 661 (2023) 130937 DOI: 10.1016/j.colsurfa.2023.130937

I declare that my contribution included:

Research on surface tension analysis, determination of concentration of the surfactants in the monolayer at the water-air interface, contribution to manuscript preparation, and reviewing.

23.07.2025 Prof. Dr. hab. Bronisław Jańczuk

184 Pl. M. Curie-Skłodowskiej ..... 20-031 Lublin, www.umcs.pl
tel.: +48 81 537 56-70
e-mail:anna.zdziennicka@mail.umcs.pl

NIP: 712-010-36-92
REGON: 000001353

POLITECHNIKA POZNAŃSKA

prof. dr hab. inż. Ewa Kaczorek

WYDZIAŁ TECHNOLOGII CHEMICZNEJ
Instytut Technologii i Inżynierii Chemicznej
ul. Berdychowo 4, 60-965 Poznań, tel.: +48 61 665 2601
e-mail: ewa.kaczorek@put.poznan.pl, www.fct.put.poznan.pl

Declaration
on the individual percentage and substantive contribution of the co-author

As co-author of the publication mentioned:

P1. *Nanofiltered saponin-rich extract of Saponaria officinalis – Adsorption and aggregation properties of particular fractions* Adam Grzywaczyk, Wojciech Smułek, Agnieszka Zgoła-Grześkowiak, Ewa Kaczorek, Anna Zdziennicka, Bronisław Jańczuk Journal: Colloids and Surfaces A: Physicochemical and Engineering Aspects, 661 (2023) 130937 DOI: 10.1016/j.colsurfa.2023.130937

P2. *Study of Interactions between Saponin Biosurfactant and Model Biological Membranes: Phospholipid Monolayers and Liposomes*, Monika Rojewska, Wojciech Smułek, Adam Grzywaczyk, Ewa Kaczorek, Krystyna Prochaska Journal: Molecules 28(4), 1965 (2023) DOI: 10.3390/molecules28041965

P3. *Saponaria officinalis saponins as a factor increasing permeability of Candida yeasts' biomembrane* Adam Grzywaczyk, Wojciech Smułek, Ewa Kaczorek World Journal of Microbiology and Biotechnology 40:152 (2024) DOI: 10.1007/s11274-024-03961-9

P4: *Glycyrrhiza glabra L. saponins modulate the biophysical properties of bacterial model membranes and affect their interactions with tobramycin* Adam Grzywaczyk, Monika Rojewska, Wojciech Smułek, Daniel A. McNaughton, Krystyna Prochaska, Philip A. Gale, Ewa Kaczorek Langmuir 41(18), 11701-11710 (2025) DOI: 10.1021/acs.langmuir.5c00927

P5. *Co-interaction of nitrofuran antibiotics and the saponin-rich extract on gram-negative bacteria and colon epithelial cells* Adam Grzywaczyk, Wojciech Smułek, Anna Olejnik, Urszula Guzik, Agnieszka Nowak, Ewa Kaczorek World Journal of Microbiology and Biotechnology 39:221 (2023) DOI: 10.1007/s11274-023-03669-2

I declare that my contribution included:

P1, P5: Conceptualization, Manuscript review, Project supervision, Research and project funding, contribution to preparation of responses to reviewers, Corresponding author, preparation of responses to reviewers
P2-P4: Conceptualization, Manuscript review, Project supervision, Research and project funding, contribution to preparation of responses to reviewers

E. Kaczorek

UTS UNIVERSITY OF TECHNOLOGY SYDNEY

Professor Philip A. Gale MA DPhil DSc
Deputy Dean
Faculty of Science
15 Broadway, Ultimo NSW 2007

T: +61 2 9514 5469
M: +61 (0) 458 705 193
philip.gale@uts.edu.au

PO Box 123
Broadway
NSW 2007 Australia
www.uts.edu.au

UTS CRICOS PROVIDER CODE 00099F

22 July 2025

Declaration on the individual percentage and substantive contribution of the co-author

As co-author of the publication mentioned:

P4: *Glycyrrhiza glabra L. saponins modulate the biophysical properties of bacterial model membranes and affect their interactions with tobramycin* Adam Grzywaczyk, Monika Rojewska, Wojciech Smułek, Daniel A. McNaughton, Krystyna Prochaska, Philip A. Gale, Ewa Kaczorek Langmuir 41(18), 11701-11710 (2025) DOI: 10.1021/acs.langmuir.5c00927

I declare that my contribution included:

HPTS & 5(6)-CF analysis methodology and interpretation, contribution to manuscript preparation and review.

Daniel McNaughton
Research Fellow in Medicinal Chemistry
Monash Institute of Pharmaceutical Sciences

Daniel.mcnaughton@monash.edu

UNIWERSYTET ŚLĄSKI
W KATOWICACH

Katowice, 04.08.2025

Declaration

on the individual percentage and substantive contribution of the co-author

As co-author of the publication mentioned:

P5. *Co-interaction of nitrofuran antibiotics and the saponin-rich extract on gram-negative bacteria and colon epithelial cells* Adam Grzywaczyk, Wojciech Smułek, Anna Olejnik, Urszula Guzik, Agnieszka Nowak, Ewa Kaczorek World Journal of Microbiology and Biotechnology 39:221 (2023) DOI: 10.1007/s11274-023-03669-2

I declare that my contribution included:

Research on bacterial fatty acid profile determination using Gas Chromatography Mass Spectrometry method, manuscript review

Agnieszka Nowak

University of Silesia in Katowice
Faculty of Natural Science
Institute Biology, Biotechnology and Environmental Protection
Jagiellońska 28, 40-032 Katowice, Poland

Uniwersytet Przyrodniczy w Poznaniu

Poznań University of Life Sciences

FACULTY OF FOOD SCIENCE AND NUTRITION

dr hab. inż. Anna Olejnik, prof. UPP
Department of Biotechnology and Food Microbiology
Wojska Polskiego 48 Str.
60-627 Poznań

Declaration
on the individual percentage and substantive contribution of the co-author

As co-author of the publication mentioned:

P5. Co-interaction of nitrofuran antibiotics and the saponin-rich extract on gram-negative bacteria and colon epithelial cells Adam Grzywaczyk, Wojciech Smułek, Anna Olejnik, Urszula Guzik, Agnieszka Nowak, Ewa Kaczorek World Journal of Microbiology and Biotechnology 39:221 (2023) DOI: 10.1007/s11274-023-03669-2

I declare that my contribution included:

Cytotoxicity analysis of colon epithelial CCD 841CoN cells exposed to *Sapindus mukorossi* extract and antibiotics, manuscript review.

Anna Olejnik

Anna Olejnik

POLITECHNIKA POZNAŃSKA

Prof. dr hab. inż. Krystyna Prochaska
WYDZIAŁ TECHNOLOGII CHEMICZNEJ
Instytut Technologii i Inżynierii Chemicznej
ul. Berdychowo 4, 60-965 Poznań
tel.: +48 (61) 665 36 01
e-mail: krystyna.prochaska@put.poznan.pl

Poznań, July 24, 2025

Declaration on substantive contribution of the co-author

As co-author of the publication mentioned:

P2. *Study of Interactions between Saponin Biosurfactant and Model Biological Membranes: Phospholipid Monolayers and Liposomes*, Monika Rojewska, Wojciech Smułek, Adam Grzywaczyk, Ewa Kaczorek, Krystyna Prochaska Molecules 28(4), 1965 (2023) DOI: 10.3390/molecules28041965

P4: Glycyrrhiza glabra L. saponins modulate the biophysical properties of bacterial model membranes and affect their interactions with tobramycin Adam Grzywaczyk, Monika Rojewska, Wojciech Smułek, Daniel A. McNaughton, Krystyna Prochaska, Philip A. Gale, Ewa Kaczorek Langmuir 41(18), 11701-11710 (2025) DOI: 10.1021/acs.langmuir.5c00927

I declare that my contribution included:

P2: analysis: The Surface Pressure-Area and Surface Potential-Area Isotherms, Brewster Angle Microscopy Images, Relaxation/Penetration Studies, elaboration of results, contribution to the preparation of the manuscript, contribution to the response to reviewers

P4: analysis: π−A Isotherm Measurement, Relaxation Measurements, elaboration of results, contribution to the preparation of the manuscript, contribution to the response to reviewers

POLITECHNIKA POZNAŃSKA

Dr inż. Monika Rojewska
WYDZIAŁ TECHNOLOGII CHEMICZNEJ
Instytut Technologii I Inżynierii Chemicznej
ul. Berdychowo 4, 60-965 Poznań
tel.: +48 665 37 72
e-mail: monika.rojewska@put.poznan.pl

Poznań, 10.09.2025

Declaration on substantive contribution of the co-author

As co-author of the publication mentioned:

P2. *Study of Interactions between Saponin Biosurfactant and Model Biological Membranes: Phospholipid Monolayers and Liposomes*, Monika Rojewska, Wojciech Smułek, Adam Grzywaczyk, Ewa Kaczorek, Krystyna Prochaska Molecules 28(4), 1965 (2023) DOI: 10.3390/molecules28041965

P4: Glycyrrhiza glabra L. saponins modulate the biophysical properties of bacterial model membranes and affect their interactions with tobramycin Adam Grzywaczyk, Monika Rojewska, Wojciech Smułek, Daniel A. McNaughton, Krystyna Prochaska, Philip A. Gale, Ewa Kaczorek Langmuir 41(18), 11701-11710 (2025) DOI: 10.1021/acs.langmuir.5c00927

I declare that my contribution included:

P2: analysis: The Surface Pressure-Area and Surface Potential-Area Isotherms, Brewster Angle Microscopy Images, Relaxation/Penetration Studies, elaboration of results, contribution to the preparation of the manuscript, contribution to the response to reviewers

P4: analysis: π–A Isotherm Measurement, Relaxation Measurements, elaboration of results, contribution to the preparation of the manuscript, contribution to the response to reviewers

Monika Rojewska

POLITECHNIKA POZNAŃSKA

dr hab. inż. Wojciech Smułek
WYDZIAŁ TECHNOLOGII CHEMICZNEJ
Instytut Technologii i Inżynierii Chemicznej
ul. Berdychowo 4, 60-965 Poznań, tel. +48 61 665 3671, fax +48 61 665 3649
e-mail: wojciech.smulek@put.poznan.pl

Poznań, 22.09.2025

Declaration

on the individual percentage and substantive contribution of the co-author

As co-author of the publication mentioned:

P1. *Nanofiltered saponin-rich extract of Saponaria officinalis – Adsorption and aggregation properties of particular fractions* Adam Grzywaczyk, Wojciech Smułek, Agnieszka Zgoła-Grześkowiak, Ewa Kaczorek, Anna Zdziennicka, Bronisław Jańczuk Journal: Colloids and Surfaces A: Physicochemical and Engineering Aspects, 661 (2023) 130937 DOI: 10.1016/j.colsurfa.2023.130937

P2. *Study of Interactions between Saponin Biosurfactant and Model Biological Membranes: Phospholipid Monolayers and Liposomes*, Monika Rojewska, Wojciech Smułek, Adam Grzywaczyk, Ewa Kaczorek, Krystyna Prochaska Journal: Molecules 28(4), 1965 (2023) DOI: 10.3390/molecules28041965

P3. *Saponaria officinalis saponins as a factor increasing permeability of Candida yeasts' biomembrane* Adam Grzywaczyk, Wojciech Smułek, Ewa Kaczorek World Journal of Microbiology and Biotechnology 40:152 (2024) DOI: 10.1007/s11274-024-03961-9

P4: *Glycyrrhiza glabra L. saponins modulate the biophysical properties of bacterial model membranes and affect their interactions with tobramycin* Adam Grzywaczyk, Monika Rojewska, Wojciech Smułek, Daniel A. McNaughton, Krystyna Prochaska, Philip A. Gale, Ewa Kaczorek Langmuir 41(18), 11701-11710 (2025) DOI: 10.1021/acs.langmuir.5c00927

P5. *Co-interaction of nitrofuran antibiotics and the saponin-rich extract on gram-negative bacteria and colon epithelial cells* Adam Grzywaczyk, Wojciech Smułek, Anna Olejnik, Urszula Guzik, Agnieszka Nowak, Ewa Kaczorek World Journal of Microbiology and Biotechnology 39:221 (2023) DOI: 10.1007/s11274-023-03669-2

I declare that my contribution included:

P1-P5: Conceptualization, Microbial analysis methodology, Contribution to manuscript preparation and review, assistance with interpretation of results and preparation of responses to reviewers.

Wojciech Smułek

UNIWERSYTET MARII CURIE-SKŁODOWSKIEJ W LUBLINIE
Wydział Chemii, Instytut Nauk Chemicznych,
Katedra Zjawisk Międzyfazowych

prof. dr hab. Anna Zdziennicka

DECLARATION

on the individual percentage and substantive contribution of the co-author

As co-author of the publication mentioned:

P1. *Nanofiltered saponin-rich extract of Saponaria officinalis – Adsorption and aggregation properties of particular fractions* Adam Grzywaczyk, Wojciech Smułek, Agnieszka Zgoła-Grześkowiak, Ewa Kaczorek, Anna Zdziennicka, Bronisław Jańczuk Colloids and Surfaces A: Physicochemical and Engineering Aspects, 661 (2023) 130937 DOI: 10.1016/j.colsurfa.2023.130937

I declare that my contribution included:

Research on surface tension analysis, determination of concentration of the surfactants in the monolayer at the water-air interface, contribution to manuscript preparation and reviewing.

Anna Zdziennicka

POLITECHNIKA POZNAŃSKA

dr hab. inż. Agnieszka Zgoła-Grześkowiak, prof. PP
WYDZIAŁ TECHNOLOGII CHEMICZNEJ
ul. Berdychowo 4, 60-965 Poznań, tel. +48 61 665 2351, -2352, fax +48 61 665 2852
e-mail: office_dctf@put.poznan.pl, www.fct.put.poznan.pl

Poznan, 22.07.2025

Author contribution statement

As co-author of the publication mentioned:

P1. Nanofiltered saponin-rich extract of Saponaria officinalis – Adsorption and aggregation properties of particular fractions Adam Grzywaczyk, Wojciech Smułek, Agnieszka Zgoła-Grześkowiak, Ewa Kaczorek, Anna Zdziennicka, Bronisław Jańczuk Colloids and Surfaces A: Physicochemical and Engineering Aspects, 661 (2023) 130937 DOI: 10.1016/j.colsurfa.2023.130937

I declare that my contribution included:

Research on analysis of the qualitative composition of the Saponaria officinalis fractions using Liquid Chromatography Mass Spectrometry method, contribution to manuscript preparation and reviewing

A. Zgoła-G

Agnieszka Zgoła-Grześkowiak